UNIVERSITÀ DEGLI STUDI DI TRIESTE

XXVIII CICLO DEL DOTTORATO DI RICERCA IN

SCIENZE E TECNOLOGIE CHIMICHE E FARMACEUTICHE

Exploring drug molecular effects in cancer disease models

Settore scientifico-disciplinare: ING-IND/24

DOTTORANDA
FEDERICA TONON

COORDINATORE
PROF. MAURO STENER

SUPERVISORE DI TESI
PROF. MARIO GRASSI

CO-SUPERVISORE DI TESI
PROF. GABRIELE GRASSI

ANNO ACCADEMICO 2014 / 2015

To my family

TABLE OF CONTENTS

Riassunto

Il tumore primitivo del fegato è il quinto tipo di tumore più diffuso al mondo e rappresenta la terza causa di morte cancro-correlata, con approssimativamente 600.000 morti all'anno[1]. Il più rappresentato tumore primitivo del fegato è l'epatocarcinoma (EC)[2], che comprende circa l'85% dei casi di carcinoma primitivo del fegato[1]. L'EC è un tumore con prognosi particolarmente infausta e con alto tasso di mortalità [3]. Queste caratteristiche sono in parte dovute al fatto che l'EC è spesso asintomatico nei suoi stadi iniziali e i sintomi iniziano a comparire quando ormai il tumore si trova in stadi avanzati. In questi casi, la maggior parte dei pazienti non sono più candidabili alla resezione chirurgica o al trapianto di fegato[4] e l'unico approccio terapeutico possibile è l'assunzione di terapia sistemica che tuttavia non garantisce un significativo miglioramento sia dell'*outcome* che della prognosi [5]. Attualmente, l'unico trattamento sistemico approvato dalla FDA per il trattamento di EC è *Sorafenib*, un inibitore di recettori ad attività tirosin-chinasica, che tuttavia garantisce un modesto miglioramento della sopravvivenza dei pazienti[4]. Inoltre, non è infrequente che pazienti sottoposti a trattamento con *Sorafenib* sviluppino resistenza al trattamento farmacologico, che può essere associata sia ad eterogeneità genetica sia all'attivazione di *pathways* compensatorie[6].

La scarsa varietà di trattamenti terapeutici disponibili attualmente per EC, ha spinto la comunità scientifica a sviluppare nuovi approcci terapeutici nel tentativo di migliorare l'*outcome* di pazienti affetti da questo tipo di tumore. 5-azacitidina, un farmaco ad azione de-metilante, potrebbe rappresentare una buona strategia terapeutica per i pazienti con EC poiché è noto che la metilazione aberrante gioca un ruolo di rilievo nell'epatocarcinogenesi. Infatti, in EC risultano ipermetilate [7,8],e quindi inattivate, le regioni promotrici di numerosi geni ad azione oncosopressiva, il cui numero aumenta progressivamente con l'aggravarsi della patologia[8]. E' quindi evidente come il trattamento con farmaci ad azione de-metilante, quali 5-azacitidina, potrebbe indurre la riattivazione di geni oncosopressori silenziati e quindi promuovere l'eradicazione del tumore. Inoltre, 5-azacitidina è un farmaco commerciale che è già stato approvato dalla FDA per il trattamento delle sindromi mielodisplastiche e per le leucemie mieloidi acute e croniche[9].

In questa tesi abbiamo valutato gli effetti del trattamento con 5-azacitidina su linee cellulari di EC e su un modello *xenograft* murino di EC. Da un punto di vista fenotipico, i nostri dati indicano che 5-azacitidina esercita un potente effetto inibitorio sulla vitalità e proliferazione cellulare. Inoltre il trattamento farmacologico ripetuto induce un arresto delle cellule in fase G1/G0 e G2/M del ciclo cellulare nonché una significativa alterazione della

struttura citoscheletrica. Queste evidenze sembrano compatibili con il fenomeno noto come *Catastrofe Mitotica,* una morte cellulare caratterizzata dalla comparsa di mitosi aberrante. Gli effetti del trattamento con 5-azacitidina risultano meno significativi in una linea di epatociti umani immortalizzati (IHH) e in epatociti umani ottenuti del differenziamento di cellule staminali embrionali, che sono stati utilizzati come cellule epatiche normali di controllo. Queste osservazioni sembrano suggerire che 5-azacitidina potrebbe avere un effetto predominante sulle cellule tumorali epatiche rispetto alle cellule sane, preservando quindi le generali funzionalità epatiche. Infine, abbiamo osservato che il trattamento con 5-azacitidina compromette significativamente la migrazione delle cellule tumorali. Tutte queste osservazioni avvalorano l'efficacia di 5-azacitidina nei modelli *in vitro* di EC.

Da un punto di vista molecolare, in questo lavoro ci siamo focalizzati sullo studio degli effetti di 5-azacitdina sulla pathway miR 139-5p/ROCK2/MMP2. Il microRNA 139-5p ha una funzione molto rilevante in EC in quanto la riduzione della sua espressione è stata chiaramente associata a prognosi infausta e a caratteristiche tumorali metastatiche [10]. Il miR 139-5p regola negativamente la proteina ROCK2, una serin-treonin chinasi i cui livelli sono direttamente correlati alla prognosi in EC. Inoltre, ROCK2 aumenta i livelli di MMP2, un enzima regolatore della migrazione cellulare, anch'esso inversamente correlato alla prognosi in EC[11]. I dati presentati in questa tesi indicano che il trattamento con 5-azacitidina promuove l'espressione del miRNA 139-5p, che induce la riduzione proteica di ROCK2. Ridotti livelli di ROCK2 si traducono in una diminuzione dei livelli proteici di MMP2 che, non più stabilizzata da ROCK2 stesso, subisce probabilmente degradazione proteolitica ad opera del proteasoma. Queste osservazioni risultano in linea con il potente effetto anti-migratorio osservato in seguito al trattamento con 5-azacitidina. Inoltre, poiché ROCK2 controlla l'espressione di molteplici proteine coinvolte nella transizione G2/M del ciclo cellulare, è plausibile che la riduzione della sua espressione sia in parte responsabile dell'accumulo cellulare in fase G2/M che osserviamo in seguito al trattamento con il farmaco. Gli effetti molecolari osservati in seguito al trattamento con 5-azacitidina nei nostri modelli cellulari di EC sono stati, infine, confermati anche su un modello *xenograft* di EC in topo. 5-azacitidina non solo riduce la crescita tumorale ma aumenta significativamente la sopravvivenza degli animali trattati rispetto agli animali di controllo.

I dati presentati in questa tesi, associati alla nota importanza della *pathway* miR 139-5p/ROCK2/MMP2 in EC, suggeriscono che 5-azacitidina possa essere effettivamente una buona alternativa terapeutica in pazienti con EC avanzato.

Abstract

Primary liver cancer (PLC) is the fifth most common cancer in the world and the third leading cause of cancer-related deaths worldwide, with approximately 600.000 deaths annually[1]. HCC is the most represented liver primary cancer[2], which accounts for approximately 85% of all PLC [1]. HCC has in general a poor prognosis [3] since it is typically asymptomatic in its early stages and when symptoms occur the cancer is already in advanced stages. In these cases, most patients are not candidates for either surgery or transplant [4] and they are eligible for drug systemic treatments only. However, drug treatments are poorly effective[5]. Currently the only FDA-approved systemic treatment for HCC [4] is an oral multi-kinase inhibitor called *Sorafenib*. It is used for the treatment of asymptomatic HCC patients with well-preserved liver functions who cannot receive curative treatment, such as hepatic resection or liver transplantation, and patients with advanced HCC [4]. Whereas *Sorafenib* improves the median overall survival, this improvement is limited to about three months. Moreover, it is common that patients develop drug-resistance to *Sorafenib* treatment. The main resistance mechanism could be associated both with the genetic heterogeneity and with the activation of compensatory pathways, including PI3K/AKT and JAK/STAT signaling pathways[6].

The few pharmacological treatments currently available for HCC, has led the scientific community to develop novel therapeutic approaches. 5-azacytidine, a drug with hypomethylating property, could be an alternative treatment for HCC because aberrant hyper methylation plays a key role in hepato-carcinogenesis. In fact, it is widely known that promoter regions of important tumor suppressor genes are frequently hyper methylated in HCC[7,8] and the number of methylated genes gradually increase with the progression of cancer stage[8]. Thus, the treatment with de-methylating agents could, in principle, promote the re-expression of silenced tumor suppressor genes, favoring tumor cell death. So far, US FDA has approved 5-azacytide for the treatment of myelodysplastic syndrome and acute and chronic myeloid leukemia[9].

In this thesis we have evaluated the effects of 5-azacytidine in cultured HCC cell lines and in a subcutaneous xenograft mouse model of HCC. From the phenotypic point of view, our data indicate that 5-azacytine exerts a powerful inhibitory effect on cell viability, promotes cell cycle arrest in G0/G1 and G2/M phases and alters the cell cytoskeleton. Notably, the G2/M block seems to be compatible with the so-called *Mitotic catastrophe,* a recently discovered phenomenon, characterized by the occurrence of aberrant mitosis. Notably, the above effects are significantly less evident if not absent in Immortalized Human

Hepatocytes (IHH) and human hepatocyte-like cells, which have been undertaken as "control normal" liver cells. This observation anticipates that *in vivo* 5-azacytidine may affect predominantly the tumor cells compared to the normal liver cells thus preserving the liver functions. Finally, 5-azacytidine determines a significant inhibition of cell migration. Taken together these observations point towards the effectiveness of 5-azacytidine in HCC.

From the molecular point of view, we observed that 5-azacytidine has pleiotropic effects. In this work, we focused on the 5-azacytidine mediated targeting of the miR139-5p/ROCK2/MMP2 pathway. miR 139-5p is relevant for HCC as its downregulation in HCC patients is associated with poor prognosis and features of metastatic tumors [10]. miRNA 139-5p negatively regulates ROCK2, a kinase whose level directly correlates to HCC progression. Finally, ROCK2 increases the levels of the metallo-proteinase MMP2, an enzyme required for cell migration whose expression level inversely correlates with HCC prognosis [11]. Our data indicate that 5-azacytidine can increase the expression of miR139-5p thus inducing the reduction of ROCK2 levels, which in turn cannot stabilize MMP2 thus resulting in a reduction in MMP2 levels and activity. These observations are in line with the anti-migratory effects we observed for 5-azacytidine. Moreover, as ROCK2 controls many proteins involved in the G2/M transition, it is feasible that its reduction can account for the G2/M block we observed. The effect of 5-azacytidine on the miR139-5p/ROCK2/MMP2 pathway have been studied in cultured cells and confirmed in a xenograft subcutaneous mouse model of HCC. Notably, in this model not only 5-azacytidine reduced tumor, it also improved animal survival.

Our data, together with the relevance of miR 139-5p/ROCK2/MMP2 pathway in HCC patients, suggest that 5-azacytidine have the potential to be of great therapeutic value in HCC.

List of Abbreviations:

AFB1 = Aflotoxin B1
AMPK = AMP-activated protein kinase
ANG2 = Angiopoietin 2
APC = Adenomatous Polyposis Coli
AP-1 = Activator Protein 1
API-5 = Apoptosis inhibitor-5
ARID1A = AT-rich interactive domain-containing protein 1A
ARID2 = AT-rich interactive domain-containing protein 2
ATF3 = Activating Transcription Factor 3
ATF4 = Activating Transcription Factor 4
ATM = Ataxia Telangiectasia Mutated
ATR = Ataxia Telangiectasia And Rad3-Related Protein
BRG1 = Brahma-related gene-1
BRM = Brama
BUB3 = Budding Uninhibited By Benzimidazoles 3
Cdc 20 = Cell division cycle 25
Cdc 25 = Cell division cycle 25
CDH1 = Cadherin 1
CDKN1B = Cyclin-Dependent Kinase inhibitor 1B
CDKN1C = Cyclin-Dependent Kinase inhibitor 1C
CDKN2A = Cyclin-Dependent Kinase inhibitor 2A
CDKN2B = Cyclin-Dependent Kinase inhibitor 2B
CDK1 = Cyclin-dependent kinase 1
CDK4 = Cyclin-dependent kinase 4
CDK6 = Cyclin-dependent kinase 6
C/EBP-α = CCAAT-Enhancer-Binding Proteins- α
CHD1L = Chromodomain Helicase DNA Binding Protein 1-Like
CHK1 = Cell Cycle Checkpoint Kinase 1
CHK2 = Cell Cycle Checkpoint Kinase 2
CTGF = Connective Tissue Growth Factor
CycA = Cyclin A
DDIT3 = DNA damage-inducible transcript 3
DDIT4 = DNA damage-inducible transcript 4
DGCR8 = DiGeorge syndrome Chromosomal Region 8
DNMT = DNA Methyltransferase
DNMT1 = DNA MethylTransferase-1
DNMT3A = DNA MethylTransferase-3A
DNMT3B = DNA MethylTransferase-3B
DLC1 = Deleted in liver cancer 1
EGFR = Endothelial Growth Factor Receptor
EMT = Epithelial-Mesenchymal Transition
ERK1 = Extracellular-signal-Regulated Kinase-1
ERK2 = Extracellular-signal-Regulated Kinase-2
FDA = Food and Drug Administration
FoxM1 = Forkhead Box M1
GSK-3β = Glycogen Synthase Kinase-3 beta
HAT = Histone Acetyltransferase
HDAC = Histone Deacetylase
HGF = Hepatocyte Growth Factor
HGFR = Hepatocyte Growth Factor Receptor

HIF-1α = Hypoxia Inducible Factor 1α
HMT = Histone Methyltransferase
HNF-1α = Hepatocyte Nuclear Factor-1α
HNF-3β = Hepatocyte Nuclear Factor-3β
HNF-4α = Hepatocyte Nuclear Factor-4α
HNF-6 = Hepatocyte Nuclear Factor-6
hTERT = Human Telomerase Reverse Transcriptase
ICAM-1 = Intercellular Adhesion Molecule 1
IGF_R = Insulin-like Growth Factor Receptor
IGF_{R1} = Insulin-like Growth Factor Receptor 1
IL-1 = Interleukin 1
IL-6 = Interleukin 6
IL-8 = Interleukin 8
INO80 Family = Inositol requiring 80 Family
ISWI family = Imitation SWI family
ITACs = IFN-gamma-inducible T cells alpha chemo-attractant
JAK = Janus kinase
JNK = Jun N-terminal kinase
KLF17 = Kruppel-Like Factor 17
LN-5 = Laminin-5
MACF1 = Microtubule-Actin Crosslinking Factor 1
MAD2 = Mitotic Arrest Deficient 2
MAEL = Maelstrom
MAP3K = MAP kinase kinase kinase
MAPK1 = Mitogen-Activated Protein Kinase 1
MCP-1 = Macrophage Chemotactic Protein-1
MHC = Major Histocompatibility Complex
MIP-1α = Macrophage Inflammatory Protein α
MK2 = Mitogen-Activated Protein Kinase-Activated Protein Kinase 2
MMP2 = Matrix Metalloproteinase 2
MMP9 = Matrix Metalloproteinase 9
NF-κB = Nuclear Factor kappa-light-chain-enhancer of activated B cells
NuRD/CHD Family = Nucleosome Remodeling and Deacetylation/Chromodomain Helicase, DNA binding Family
mTOR = mammalian Target Of Rapamycin
OSGIN1 = Oxidative Stress-Induced Growth Inhibitor 1
PCAF = P300/CBP-associated factor
PDCD4 = Programmed Cell Death 4
PECAM-1 = Platelet endothelial cell adhesion molecule-1
PTCH = Patched
PTK2 = Protein Tyrosine Kinase 2
PDGFR = Platelet Derived Growth Factor Receptor
PI3K = PhosphatIdylinositol 3-Kinase
PTEN = Phosphatase and TENsin homolog
p38 MAPK = P38 mitogen-activated protein kinases
RAC1 = Ras-Related C3 Botulinum Toxin Substrate 1
Rb (pRb) = Retinoblastoma
Rb1 = Retinoblastoma 1
RIZ1 = Rb-interacting zinc finger 1
RNAi = RNA interference
ROCK1 = Rho-associated coiled kinase 1

ROCK2 = Rho-associated coiled kinase 2
SGK3 = Serum/Glucocorticoid Regulated Kinase
S.H.A.R.P. = Sorafenib Hepatocellular Carcinoma Assessment Randomized Protocol
siRNAs = small interfering RNAs
SMAD 2 = Small Mother Against Decapentaplegic 2
SMAD 3 = Small Mother Against Decapentaplegic 3
SMO = Smoothened
SOCS-1 = Suppressor of Cytokine Signaling-1
SWI/SNF Family = Switching defective/Sucrose non-fermenting Family
TAT = Tyrosine AminoTransferase
TGF-β = Transforming growth factor-β
TNF-α = Tumour Necrosis Factor α
TPM4 = Tropomyosin 4
TP53 = Tumor Protein 53
TRAIL = TNF-Related Apoptosis-Inducing Ligand
TRAP1 = TNF Receptor-Associated Protein 1
TSC1 = Tuberous Sclerosis 1
TSC2 = Tuberous Sclerosis 2
UBR1 = ubiquitin-protein ligase E3
VCAM-1 = Vascular cell adhesion protein 1
VEGF = Vascular Endothelial Growth Factor

1. Introduction

1.1 The physiology of liver

The liver is the largest solid organ in the body and it can weigh up to 1.5 kg in adults. Liver is located in the upper-right abdomen, just under the rib cage and below the diaphragm. The liver performs many important functions in the body[12]:

- *It filters blood removing and excreting body wastes and hormones as well as drugs and foreign substances;* these substances enter the blood either through metabolism production or from the outside as drugs or toxic compounds. Enzymes located in the liver change toxins so they can be easily excreted in urine.
- *It synthesizes plasma proteins including those necessary for blood coagulation;* liver produces most of the 12 clotting factors. Other plasma proteins synthesized by the liver include albumin, which contributes to osmotic pressure, fibrinogen, which is the key component of the clotting process, and globulins, which transport substances such as cholesterol and iron.
- *It produces immune factors and removes bacteria;* producing proteins associated with inflammation process and immune cell activities, the liver helps the body fight infections.
- *It produces bile*, which is made up of bile salts, cholesterol, bilirubin, electrolytes and water. Bile helps the small intestine digest and absorb fats, cholesterol and some vitamins.
- *It synthesises bilirubin*, which is a yellow-red substance formed by haemoglobin when red blood cells break down. The iron derived from the haemoglobin is stored in the liver or used by the bone marrow to produce new red blood cells.
- *It stores vitamins, minerals and sugars;* the liver stores glucose as glycogen reserve, which can be used if the body needs energy. It stores also fats, iron, copper and different kinds of vitamins including vitamins A, D, K and B12.

1.2 The pathophysiology of liver inflammation and damage

From a microscopic point of view, in the liver there are different kinds of cell populations. Hepatocytes are the most represented population, making up about 70-80% of the liver mass. These cells are involved in hormones and proteins synthesis and storage, carbohydrates transformation, cholesterol and bile salts formation and detoxification of

exogenous and endogenous substances[13]. Hepatocytes have an average life of about 5 months and have the ability to regenerate. These cells are organised into plates separated by vascular channels called *sinusoids* (Fig. 1. 1).

The second type of liver cell population is the *hepatic stellate cells*, also known as *pericytes* which are found in the *perisinusoidal space* of the liver (*space of Disse)*. Stellate cells, representing about 5-8% of the total number of liver cells, are the major cell type involved in fibrosis in response to liver damage[14]. In the normal liver these cells are described as being in a quiescent state and able to store vitamin A. But when the liver is damaged, quiescent stellate cells change into an activated state and produce extracellular matrix and collagen[14]. Hepatic stellate cells might also play a role during liver inflammation and hepatic injury by producing several cytokines and chemokine and modulating the recruitment and migration of mononuclear cells within the *perisinusoidal space* of diseased liver[15] (Fig. 1.1).

Sinusoids display a discontinuous, fenestrated endothelial cell lining, which is separated from hepatocytes by the *space of Disse*. Under normal conditions, the hepatic sinusoidal endothelial cells express low levels of MCP-1, IL-8 and MIP-1 α, which are factors involved in the routine leukocyte recirculating and immunological surveillance[13]. During inflammation, the normal hepatic endothelium changes its chemokines expression profile, producing high levels of *ITACs*. Similarly, the pattern of adhesion molecules also changes in the endothelial cells, which express high levels of ICAM-1 and VCAM-1 proteins and low levels of PECAM-1[13] (Fig. 1.1).

The last cell population located in the liver is represented by the *Kupffer cells*, specialized macrophages that form the major part of the *reticuloendothelial system*. Under physiological conditions, the red blood cell is broken down by the phagocytic action of *Kupffer* cells and the haemoglobin molecule is split. Whereas the globin chains are reutilized, the *heme* is broken down into iron, which is reused, and protoporphyrin IX which is converted into bilirubin. Bilirubin is then conjugated with glucuronic acid within hepatocytes and secreted into bile[13].

During liver injury, the *Kupffer* cells get activated and start to secrete a large number of chemical mediators such as cytokines (IL-1, IL-6. IL-8, TNF- α) and chemokines (C-X-C chemokines: MIP-1, IP-109; C-C chemokines: MIP-1α, MCP-1) which can induce liver injury either by acting directly on the liver cells or via chemo-attraction of extra-hepatic cells (neutrophils and lymphocytes). Under inflammatory conditions, also *Kupffer* cells change the expression pattern of their adhesion molecules, producing more ICAM-1 than in physiological conditions.[13] (Fig. 1.1).

A) Sinusoidal structure in normal liver

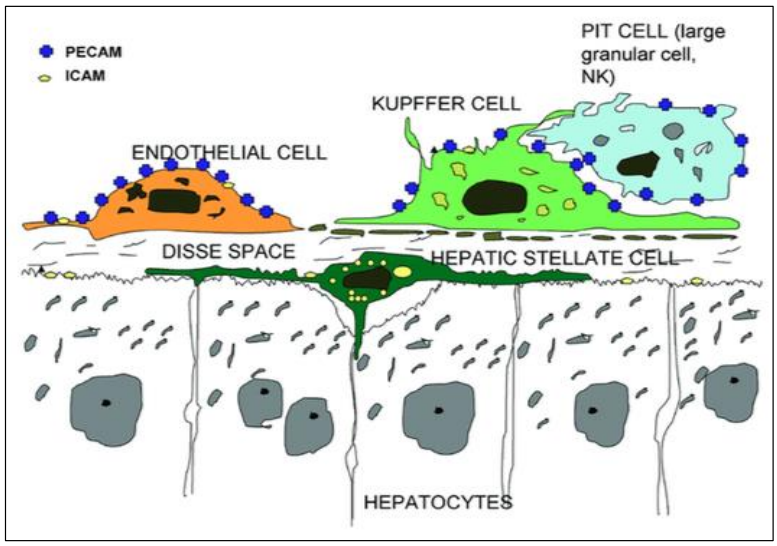

B) Liver inflammation

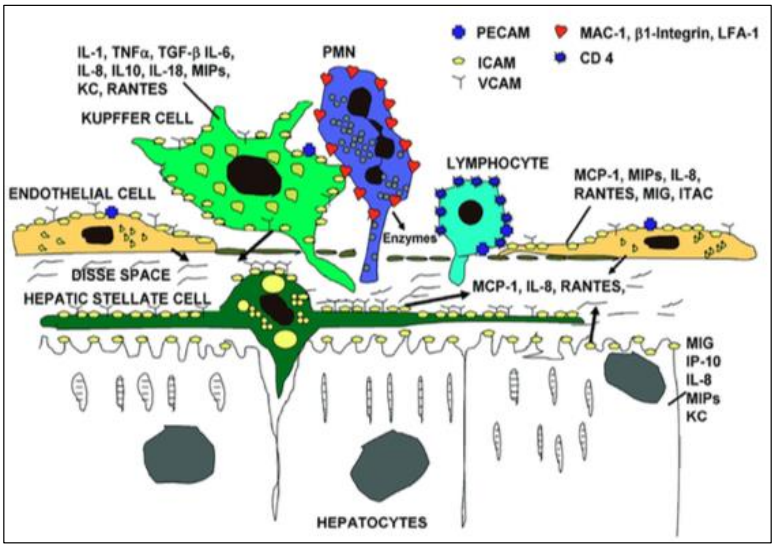

Fig. 1.1 – Scheme of sinusoidal structure in normal liver (A) and in liver inflammation (B). The hepatocellular stress induced by infection or hepatic toxins may lead to activation of *Kupffer cells* which release pro-inflammatory cytokines. They induce an increased expression of cell adhesion molecules (ICAM-1, VCAM-1) on the sinusoidal endothelial cells and a down-regulation of platelet endothelial cell adhesion molecules (PECAM-1). These molecules allow the recruitment of inflammation cells toward hepatocytes[13].

Persistent inflammation is known to promote cells malignancy. Primary liver cancer, mostly *hepatocellular carcinoma* (HCC), is a clear example of inflammation-related cancer as more than 90 % of HCCs arise in the context of hepatic injury and inflammation[16].

1.3 Hepatocellular carcinoma

1.3.1 Epidemiology

Primary liver cancer (PLC) is the fifth most common cancer in the world and the third leading cause cancer-related deaths worldwide, with approximately 600.000 deaths annually [1]. HCC is the most represented liver primary cancer [2], which accounts for approximately 85% of all PLC[1]. Cholangiocarcinoma (CCA), a malignant tumor arising from cholangiocytes in the biliary epithelium, is the second most common variant of liver cancer and accounts for about 15% of PLC[1].

HCC has several peculiar epidemiologic features including dynamic temporal trends, variation among geographic regions, ethnic groups and between men and women. For example, males have generally higher liver cancer rate than females with an average male: female ratios between 2:1 and 4:1[17].

The estimated incidence of new cases of HCC is about 500.000-1.00.000 per year even if an important difference has been noted between countries[2] (Fig. 1.2).

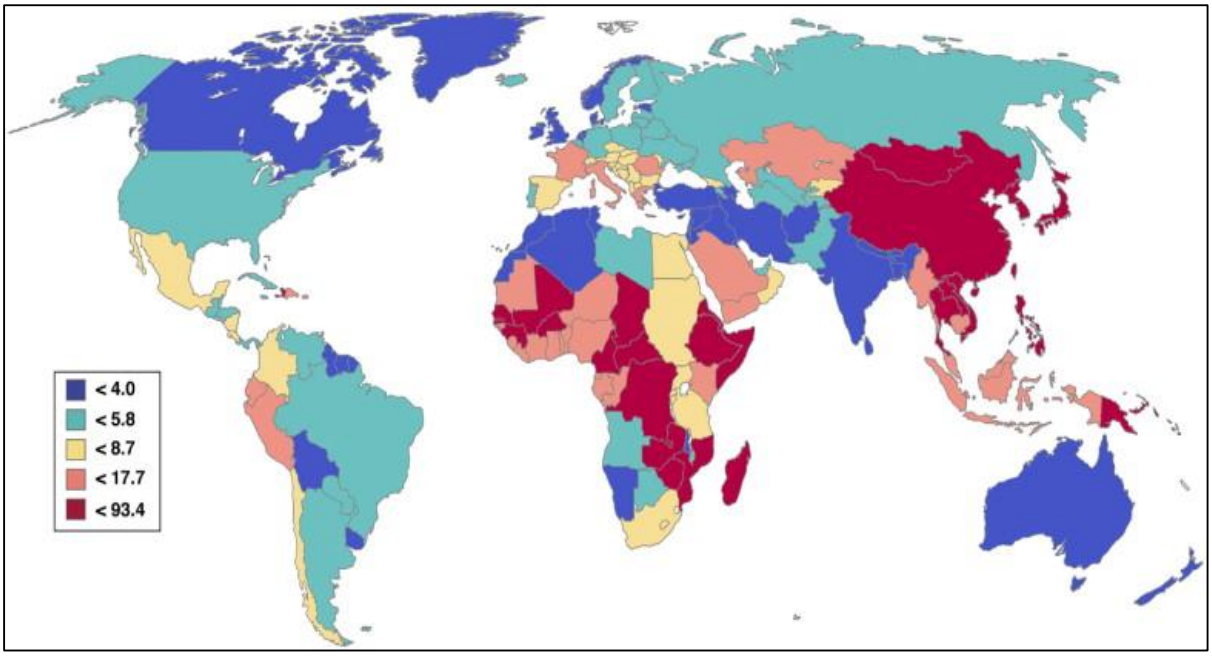

Fig. 1.2 – Age-standardized incidence rates of liver cancer in male per 100.000 population[6].

As shown in Fig. 1.2, most cases of HCC occur in Asia where several regions have a very high incidence. Although the incidence of HCC in developed countries is relatively low, it is rising annually [18]. For example in the United States there has been an increase of about 80% in the annual incidence of HCC from 1.4/100.000 (cases/inhabitants) per year in the eighties to 2.4/100.000 per year in the nineties[2]. Other developed countries have noted similar

increasing trends, for example Italy but also United Kingdom and Canada. This increase is related to migration flow from parts of the world with high prevalence, such as sub-Saharan Africa and Asia, being associated with a parallel increase in hospitalization and mortality for HCC[19].

The incidence of HCC increases with age reaching its highest prevalence among those subjects aged over 65 years [20]. Although in developed countries the HCC onset is rare before 50 years old, a shift in incidence towards younger persons has been noted in the nineties[2].

1.3.2 Risk factors

Certainly the major risk factors for the development of HCC are chronic liver inflammations and cirrhosis, which represent the underlying condition of HCC in about 80-90% of all detected cases. The development of HCC often follows viral infections (hepatitis B and hepatitis C), toxic agents (alcohol and aflatoxin), metabolic disease (diabetes and non-alcoholic fatty liver disease, hemochromatosis), and immune-related disease (primary biliary cirrhosis and autoimmune hepatitis)[20].

1.3.2.1 Hepatitis C Virus

Hepatitis C virus (HCV), belonging to the *Flaviviridae* virus family, owns a strong hepatic tropism[21]. It is a small single strand-RNA (ssRNA) virus with spherical shape that encodes structural (core, E1, E2) and non-structural proteins (p7, NS2, NS3, NS4A, NS4B, NS5A and NS5B)[22].

The viral particle is formed by a nucleus capsid comprising the core proteins and viral genome, and an envelope consisting of the glycoproteins E1 and E2. Following viral infection, the cellular expression of the nucleus capsid core protein localizes in the cytosol, lipid droplets, endoplasmic reticulum/Golgi apparatus, mitochondria and nuclei, and has been suggested to affect a variety of cellular functions [23]. The envelope glycoproteins (E1 and E2) are involved in both interactions with host cells and viral entry. NS3 is a serine protease with helicase activity that cleaves downstream NS proteins together with NS4A. NS4B is a component of the *membrane-associated cytoplasmic HCV replication complex*. NS5A is an indispensable factor in the HCV replication complex and virion assembly. NS5B, an RNA-dependent RNA polymerase, synthesizes viral ss-RNA. Because HCV is not able to stably integrate into the host genome, it requires continuous replication for its viability[23].

HCV is the most important risk factor for HCC in developed countries and epidemiological studies have shown that up to 70% of patients with HCC have anti-HCV antibody in the serum [2]. HCV infection increases HCC risk by promoting fibrosis and cirrhosis[17] and in fact liver cancer has a higher prevalence in patients with HCV-associated cirrhosis compared to non-viral chronic liver disease[2]. The prevalence of HCV infection changes considerably by geographical region: African and Asian countries report a higher HCV infection prevalence rate than North America and Europe[2]. The risk of developing HCC in HCV-infected patients depends on the severity of the underlying liver disease. Up to 80% of HCV-infected individuals fail to eliminate the virus acutely and progress to chronic HCV infection in which continuous inflammation and hepatocyte regeneration can lead to chromosomal damage and possibly initiate hepatic carcinogenesis[24]. The rate of fibrotic progression following HCV infection is markedly variable and depends on the age of the patients at the time of infection, sex and HCV genotype.

Chronic hepatitis C is more aggressive in HIV-infected patients leading to cirrhosis and liver damage in a shorter time period. Co-infection with HIV is a frequent occurrence because the two virus share the same routes of transmission. Recently, it has been shown that in HIV-HCV co-infected patients, HCC develops more rapidly than into only HCV patients [25].

Because the HCV is a completely cytoplasmic-replicating virus, the main hypothesis for HCV carcinogenesis is that it occurs via indirect pathways through the effects of chronic inflammation and hepatocellular injury. Several studies based on cell culture systems and animal models have reported that HCV proteins are correlated with HCC development. The HCV core protein is involved in viral particle assembly and generation of complete virions. However, the core protein is also involved in cell signaling, transcription activation, apoptosis, lipid metabolism and transformation [26]. In transgenic mice models, the HCV core protein has been shown to induce HCC through different mechanisms included the induction of oxidative stress and the production of reactive oxygen species. The oxidative stress may decrease metabolic processes within the mitochondria, with a decline in microsomal triglyceride transfer protein activity, resulting in the development of steatosis[27]. The HCV core protein has also been shown to interfere with several cellular regulatory pathways involved in cellular proliferation, cell cycle control and tumor formation[26]. The HCV core protein can bind to p53 and pRb tumor suppressor proteins modulating the expression of p21/Waf, which is involved in cell cycle control, and interacts with cytoplasmic signal transduction molecules to regulate transcription[28] (Fig. 1.3).

Apart from the core proteins, other HCV proteins have also been shown to contribute to hepato-carcinogenesis. For example, the E2 protein can bind CD81 receptor and inhibit T and NT cells and this immunity modulation promotes infected cell survival and proliferation. The HCV NS3 protein is a multifunctional protein with protease, RNA helicase and NTPase activity. NS3 can promote hepato-carcinogenesis by its interaction with p21 and p53. HCV-NS5A, a membrane-associated protein, is involved in the replication of the HCV genome. NS5A is located into cytoplasm and it is bound to membranes. However, the truncated form of HCV-NS5A can move into the nucleus to act as a transcriptional activator, promoting the suppression of the host immune response and the inhibition of apoptosis[29] (Fig. 1.3).

In the last five years new powerful drugs has been developed for the treatment of chronic HCV infections. Multiple direct-acting antivirals (DAAs) are molecules that target specific nonstructural viral proteins resulting in the disruption of viral replication and infection. There are four classes of DAAs which are defined by their mechanism of action and therapeutic targets: nonstructural proteins 3/4A (NS3/4A) protease inhibitors (PIs), NS5B nucleoside polymerase inhibitors (NPIs), NS5B non-nucleoside polymerase inhibitors (NNPIs), and NS5A inhibitors[30].

Nonstructural proteins 3/4A (NS3/4A) protease inhibitors (PIs) are inhibitors of the NS3/4A serine proteases, which are involved in the post-translational processing, and replication of HCV. The PIs act by blocking the NS3 catalytic site or the NS3/NS4A interaction[31]. It has been developed a first-generation of protease inhibitors, such as *Boceprevir* and *Telaprevir*, which had many side effects, in particular anemia and cutaneous rash. Moreover, their use has been significantly restricted due to a large number of drug-drug interactions with compounds that are commonly used for human immunodeficiency virus infection (HIV), immunosuppression, hyperlipidemia, and pulmonary hypertension. The second-generation of protease inhibitors, such as *Semeprevir*, offers several benefits over earlier protease inhibitors, including fewer drug-drug interactions, improved dosing schedules, and less frequent and severe side effects.

The NS5B nucleoside polymerase inhibitors (NPIs) target the catalytic site of NS5B and result in chain termination during the viral RNA replication. This class of inhibitors has high efficacy across all six genotypes and a very high barrier to resistance. Another potential advantage of NPIs is that the NS5B active site is relatively intolerant to amino acid substitutions. As a result, active site NS5B mutations that confer resistance to NPIs are more likely to also impair RNA polymerase activity compared with mutations in NNPI allosteric binding pockets, thus rendering the mutant virus less adapted compared with wild-type virus.

One of the most important NPIs is *Sofosbuvir,* formerly known as GS-7977, a uridine nucleotide analogue that inhibits the highly conserve active site of the HCV-specific NS5B polymerase preventing viral replication. In 2013 it has revolutionized the treatment of hepatitis C virus (HCV) infection by leading to high rates of *sustained virological response* (SVR) with few side effects [32]. The pangenotypic antiviral efficacy of *Sofosbuvir* supports the continued investigation of *Sofosbuvir* alone or in combination with other direct-acting antiviral agents in various populations of patients with HCV infection (Early Patterns of *Sofosbuvir* Utilization by State Medicaid Programs). Actually the drug is still very expensive and only patients with particular physio-pathological features can access to the treatment.

The non-nucleoside polymerase inhibitors (NNPIs) act as allosteric inhibitor of NS5B RNA polymerase targeting four allosteric sites which are *thumb domains 1* and *2* and *palm domains 1* and *2*. NNPIs are less potent and more genotype specific (all NNPIs in clinical development have been optimized for genotype 1). Moreover, they have from low to moderate barrier to resistance and variable toxicity profiles [33]. Consequently, this class of drug has been studied primarily as an adjunct to more potent compounds with higher barriers to resistance.

The NS5A inhibitors, such as *Ledipasvir*, *Ombitasvir* and *Daclatasvir*, target the viral NS5A protein which plays a role in both HCV replication and assembly[34]. However, the precise molecular mechanisms by which NS5A accomplishes these functions are uncertain. Thus, the exact mechanism of action of HCV-NS5A inhibitors is unclear. This class of agents are generally quite potent and are effective across all genotypes, but they have a low barrier to resistance and variable toxicity profiles[35].

Through the emerging use of DAAs for the treatment of chronic HCV infections, it is expected to reduce HCV-related HCC. However, HCV eradication doesn't eliminate the risk to develop HCC, especially when patients already have advanced liver fibrosis[23].

1.3.2.2 Hepatitis B Virus

Hepatitis B virus (HBV) belongs to the *Hepadnaviridae* virus family. It is a small partially double strand-DNA (dsDNA) virus that has an envelope and a strong hepatic tropism. An estimated 350 million persons worldwide are chronically infected with HBV. Of these, up to 40% will develop cirrhosis and HCC [36]. The annual risk for chronic HBV carriers is less than 1% but is higher in those patients with concurrent cirrhosis (2-3%)[37]. Approximately 70–80% of HBV-related HCC occurs in cirrhotic livers, whereas the remainder of the HCC occurs in the absence of underlying cirrhosis. The increased HCC risk

associated with HBV infection particularly applies to areas where HBV is endemic such as Asia. In these areas, it is usually transmitted from mother to newborn and up to 90% of infected individuals follows a chronic course of the disease [17]. This pattern changed in areas with low HCC incidence rate, where HBV is acquired in adulthood through sexual transmission with more than 90% of acute infections resolving spontaneously[17].

HBV can induce HCC development via indirect or direct pathways. In the former, HBV incites chronic injury to the hepatocytes, with continuous necro-inflammation and regeneration activities that leads to increasing hepatocyte turnover . This condition promotes accumulation of potential critical mutations in the hepatocyte genome, with subsequent malignant transformation and clonal expansion, leading to HCC [36]. In addition, HBV has been shown to be an oncogenic virus. Because HBV contains partially ds-DNA, it can directly cause HCC by integrating its DNA into the host genome even if its integration into DNA host is not required for its replication. It is important to underline that HBV integration can also be found in non-HCC tissue. Integration is usually multiple in different random sites and it can occur also during the early stages of infection. HBV integration can have several mutagenic consequences, including large inverted duplications, deletions, amplifications and translocation, resulting in chromosomal instability [38]. When these genetic alterations confer a selective growth advantage to the infected cells, malignant transformation occurs. Usually HBV integrates into genes that are involved in cell proliferation and differentiation, such as hTERT, MAPK1, CycA and TRAP1 [39]. The direct pathway used by HBV to promote HCC development includes HBx gene that is the most commonly integrated gene (Fig. 1.3). Over 95% of patients with HBV-related cirrhosis and dysplasia are positive for HBx, which is expressed in 70% of patients with HBV-related HCC. The exact mechanism by which HBx can induce HCC development remains to be fully elucidated. It is known that HBx is a transcription activator through its interaction with a wide range of both viral and host regulatory elements[40] such as MHC, EGFR, c-MYC, c-JUN, c-FOS, TP53, AP-1, NF-κB and SP1[36]. Through its effects on these regulatory elements, HBx can interfere with hepatocytes DNA repair system and with several elements which control cell proliferation and death.

Other HBV gene elements integrating into the host genome have been associated to hepato-carcinogenesis. These include the truncated Pre-S2/S gene, which encodes both a group of transcriptional activators proteins (PreS2) and the envelope proteins (LHBs, MHBs and SHBs)[41] (Fig. 1.3). The PreS2 transcriptional activators undergo phosphorylation by protein kinase C, with subsequent activation of the AP-1 and NF-jB proteins, causing an increase in hepatocyte proliferation. In addition, the overproduction of envelope proteins may

lead to their accumulation into the cytoplasm of hepatocytes, causing cellular stress and the predisposition to undergo malignant transformation[42].

Another HBV protein, known as the HBV spliced protein, is expressed in chronic hepatitis B infection. It has been suggested that this spliced protein can induce apoptosis and also promote liver fibrosis and hepato-carcinogenesis modulating TGF-β signalling[36] (Fig. 1.3).

However, the currently available antiviral therapy and vaccination for HBV appear to be effective in lowering the risk of HCC development and given the high mortality rate HCC-related, prevention is extremely important. In addition, screening programs for high-risk individuals increase the opportunity of timelier treatment, with improved long-term survival[36].

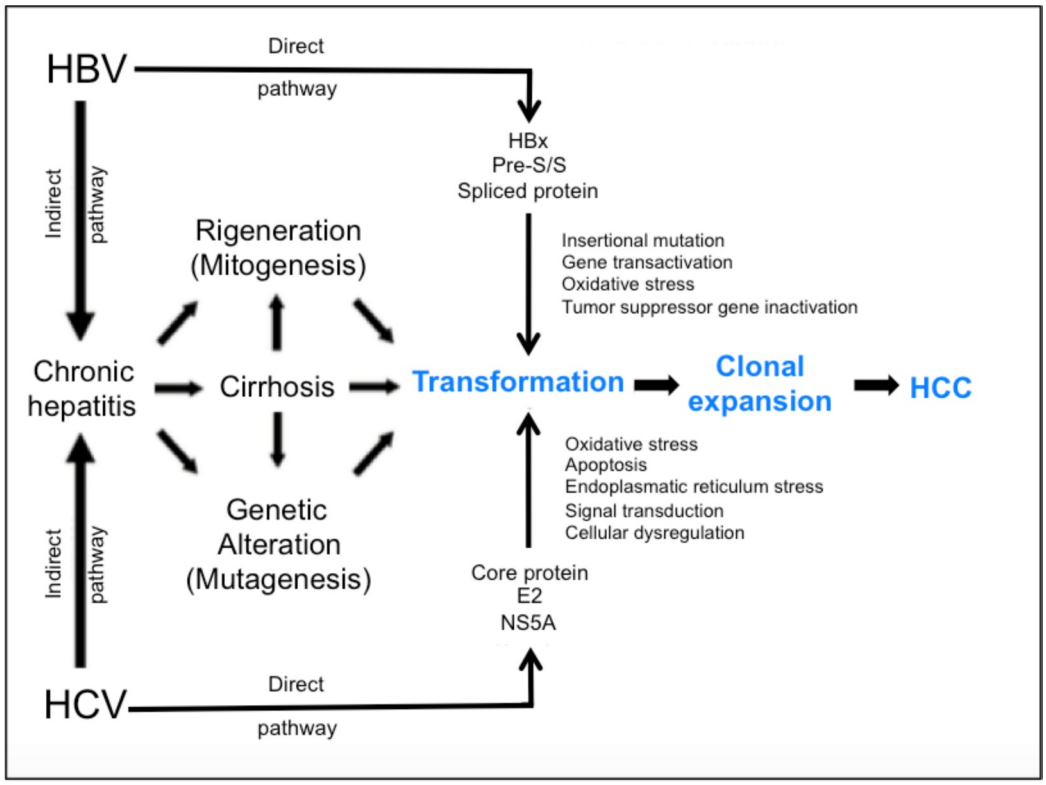

Fig. 1.3 - Proposed mechanisms of hepato-carcinogenesis related to HBV and HCV infections[26].

1.3.2.3 Diabetes mellitus

An American population-based study has found that diabetes is an independent risk factor for the development of HCC. In fact, in the paper, Davila et al. has shown that about 60% of the patients with HCC are not diagnosed with chronic HCV-related or HBV-related hepatitis, alcoholic liver or other known causes of chronic liver disease and 47% of these

patients have diabetes which is higher than those whit other risk factors (41%)[43]. These observations suggest that diabetes may be responsible for a considerable proportion of patients with idiopathic HCC[43]. An increased risk to develop HCC among patients with diabetes alone is also reported in a Danish population-based study. In this study, a threefold increased risk of HCC among patients hospitalized with diabetes was observed. Moreover, in a Swedish study, a fourfold risk in the presence of hepatitis and cirrhosis [43]. Diabetes has been implicated as risk factor for the development of *non-alcoholic fatty liver disease* (NAFLD), including its most severe form *non-alcoholic steatohepatitis* (NASH), which has been identified as a cause of HCC[43].

1.3.2.4 Diet and obesity

Many epidemiological studies have observed the relationship between diet and the risk to develop HCC. Even if the results are somewhat conflicting, an inverse relationship seems to exist between eating habits and HCC. For example, different studies demonstrate that meat and animal protein consumption is associated with increased risk of HCC, instead coffee drinking seems to reduce the development of HCC. This favorable effect of coffee drinking is established in many studies that have considered both populations where coffee is widely consumed and other where coffee intake is less frequent[44,45]. Some compounds in coffee, including *diterpenes*, *cafestrol* and *kahweol* may act as HCC blocking agents via the modulation of multiple enzymes involved in carcinogenic detoxification[46] and the modification of the xenotoxic metabolism via the induction of glutathione-S-transferase and the inhibition of N-acetyltransferase[47].

Moreover, heavy alcohol intake defined as ingestion of more than 70g/day of alcohol for prolonged period is a well-known HCC risk factor. Even if it is not clear whether risk of HCC development is significantly altered in individuals with moderate alcohol intake, it is known that heavy alcohol intake is strongly associated with the development of cirrhosis, which can be a favorable condition to liver carcinogenesis[17].

In a large prospective cohort study of more than 900.000 individuals in the United States followed up for 16 years, HCC mortality rates are 5 times higher among men with the greatest body mass index (BMI included between 35 to 40) compared with those with a normal body mass index[17]. Two other population-based cohort studies find high HCC risk in obese men and women compared with those with a normal BMI [48,49]. A complication strongly associated with obesity is insulin resistance, which significantly contributes to the development of hepatic steatosis. Increased level of steatosis has been associated with more

severe inflammatory activity and fibrosis and some studies suggest that the increase of steatosis itself may be an indicator of fibrosis progression [50]. Moreover, liver disease occurs more frequently in patients with more severe metabolic alterations and with insulin resistance showing an increase in disease progression[51].

1.3.2.5 Toxic Exposures

Among the toxic compounds associated with the increase of HCC risk there is *Aflatoxin*, a mycotoxin produced by *Aspergillus fungus*. This fungus mainly grows on foodstuffs, such as corn, stored in warm conditions. Animal tests show that *Aflatoxin* is a powerful hepatocarcinogen and for this reason the *International Agency of Research on Cancer* has classified it as carcinogenic compound [17]. Once ingested, *Aflatoxin* is metabolized to an active intermediate, which can bind DNA causing its damage such as a characteristic mutation in p53 tumor-suppressor gene [52]. This mutation has been observed in 30%-60% of HCC associated with exposure to *Aflatoxin*. The interaction between *Aflatoxin* exposure and chronic HBV infection is shown in a Chinese study where the authors have discovered that individuals who both excrete *Aflatoxin* metabolites and are HBV carriers have a dramatic increase in HCC risk[53]. In most areas where *Aflatoxin* exposure is high, chronic HBV infection also is prevalent. Thus, in addition to HBV vaccination, as the major preventive action, persons already chronically infected could benefit by eliminating *Aflatoxin* exposure[17].

Another environmental factor hypothesized to increase the risk of HCC is pesticides, which are considered to be possible epigenetic carcinogens through several mechanisms such as spontaneous genetic changes, cytotoxicity, oxidative stress, and inhibition of apoptosis and suppression of intracellular communication[54]. A case-control study of HCC in HBV and/or HCV infected patients suggests that pesticides have an additive effect on the risk to develop HCC amongst individuals that use organophosphate compounds or carbamate while working[54].

1.3.2.6 Nonalchoholic fatty liver disease

Nonalcholic fatty liver disease (NAFLD) refers to the accumulation of hepatic steatosis not due to excess alcohol consumption. The prevalence of NAFLD is up to 30% in developed countries and nearly 10% in developing nations, making NAFLD the most common liver condition in the world[55]. NAFLD includes a clinic pathologic spectrum of diseases, ranging from isolated hepatic steatosis to nonalcoholic steatohepatitis (NASH), which is the more aggressive form of fatty liver disease. HASH can progress to cirrhosis and

its associated complications, including hepatic failure and HCC [56]. NASH may account for a large proportion of idiopathic or cryptogenic cirrhosis (CC), which predisposes these patients to the development of HCC[57].

NASH has been proposed as a probable cause of idiopathic or cryptic cirrhosis (CC) even though most of the histologic hallmarks of NASH are not present in CC [57,58]. Multiple retrospective studies have been performed evaluating HCC in the setting of CC, which support the idea that NASH accounts for a large proportion of CC and can progress to HCC [57]. In 2002, Bugianesi et al. reviewed 641 patients with HCC[58] showing that 6.9% of the 641 patients developed HCC in the setting of CC, and these patients were compared to patients with HCC from HCV-related cirrhosis, hepatitis B virus (HBV)-related cirrhosis, and alcoholic cirrhosis[57,58]. Analysis from this comparison confirmed that features associated with NASH, including obesity, diabetes, dyslipidemia, elevated glucose, and insulin resistance, were all significantly associated with CC [57,58] Another review of 100 patients with HCC found a highest prevalence of 29% with underlying CC [59]. This study confirms the significant association of obesity, diabetes, and hypertriglyceridemia with CC when compared to other causes of liver disease[59]. In this review, 20% of patients in the cryptogenic liver disease group had evidence of NASH on liver biopsies prior to developing HCC, whereas half of the patients with CC had prior NASH or suspected NAFLD. The authors concluded that NAFLD was the underlying liver disease in 13% of the patients with HCC[59].

1.3.2.7 Hemochromatosis

Hemochromatosis is a common inherited disorder especially of Caucasian peoples where the incidence of expressed disease is 1 in 400[60]. The gene responsible of the hemochromatosis (HFE) has been identified on the short arm of chromosome 6[61], 80% to 90% of patients are homozygous for the C282Y mutation [62]. Major complications of genetic hemochromatosis (GH) are cirrhosis and HCC, which can accounts for 45% of deaths in people with hemochromatosis[63]. The risk for HCC development in patients with HH was estimated to be over 200-fold increased in several Australians [64] and German [65] studies based on the evidence that the incidence of HCC in the analyzed cohorts was approximately 8%–10%. A subsequent Danish study, involving a cohort of 93 patients, also showed a strong relationship between hemochromatosis and HCC, with the incidence of HCC identified to be 93-folds increased[66]. Furthermore, the mortality risk associated with HCC in the setting of hemochromatosis was estimated to be 8%, owing to the lack of any treatment options for this disease. Moreover, HCC has been identified as the leading cause of premature mortality in

hemochromatosis. In his study, Neadeau et al. showed that in a cohort of 251 patients with phenotypically defined hemochromatosis and cirrhosis, long-term survival was significantly lower than in age- and sex-matched population controls, and the increased risk for premature mortality was primarily related to HCC[67].

1.3.3 Hepatocarcinogenesis

1.3.3.1 Precursor lesions in the evolution of HCC

The molecular mechanisms of HCC are still very intricate. Cancer cells have defects in regulatory genes that are associated with normal cells proliferation and homeostasis due to a progressive accumulation of mutations[68]. The alterations in cells physiology that promote malignant growth are mainly the activation of growth signals (oncogenes), the inactivation of growth-inhibitory signals (tumor suppressor genes), the escape from apoptosis, limitless replicative potential and neo-angiogenesis[69]. All these modifications induce the malignant transformation of liver parenchymal cells followed by vascular invasion and metastasis [70] (Fig. 1.4).

Either directly or indirectly, the most common liver carcinogens, such as HBV, HCV, alcohol, AFB1, promote DNA damage in hepatocytes, impair repair through chronic inflammation and incite intensive regeneration and fibrogenesis[71]. Several morphologically distinct lesions, called *pre-neoplastic lesions*, precede HCC onset. These include *dysplastic foci* and *dysplastic nodules*[70]. *Dysplastic foci* are small groups of altered hepatocytes that may consist of both large and small cell types [72]. A focus of small cell dysplasia (SCD) is defined as a group of hepatocytes with decreased cytoplasmic volume, nuclear polymorphism and increased nucleocytoplasmic ratio [72]. Large cell dysplastic foci (LCD) are defined as a group of hepatocytes characterized by nuclear and cellular enlargement, normal nucleocytoplasmic ratio, nuclear polymorphism, with multi-nucleation and prominent nucleoli [72]. SCD is a highly proliferative lesion that has morphological and histological features similar to HCC. The prevalence of SCD is higher in cirrhotic liver with HCC than those without [73]. Foci of SCD also contain chromosomal losses and gains, which are also present in HCC but not in the surrounding cirrhotic parenchyma. For these reasons, SCD is considered to be early precursor injures associated with HCC [70]. However, it is also known that only a small amount of SCD will eventually evolve into HCC and LCD foci are more prevalent in cirrhotic livers with HCC than without [74]. Because LCD contains aberrant and increased DNA, this supports the idea that such foci may also be direct precursor injuries of HCC [70]. Conversely, the presence of features such as the normal nucleocytoplasmic ratio, low proliferative index, high apoptotic

activity, absence of histological continuum with HCC and lack of genetic aberrations seem to argue against this hypothesis.

The development of HCC in a cirrhotic contest is often preceded and accompanied by macroscopically nodular injuries showing atypical morphological features. Some of these nodules may contain malignant foci; moreover histological observations suggest a role of dysplastic nodules as immediate precursors of HCC. They are classified as low grade (LGD) or high grade (HGD) by morphological criteria[70]. HGD frequently owns vascular and metastatic profiles, which partially resemble those of adjacent HCC tissue[70].

Hepato-carcinogenesis is considered a multistep process involving progressive gene mutations, which regulate proliferation and apoptosis in the hepatocytes subjected to continuous inflammatory and regenerative stimuli [68]. For example, mutations that occur very frequently are the inactivating modifications in TP53, Rb and IGF_{R1} genes whereas c-myc and cyclin D are often overexpressed (Fig. 1.4) [75]. Loss of heterozygosity (LOH) involving multiple chromosomes in single tumors also strongly suggests multistep carcinogenesis[76].

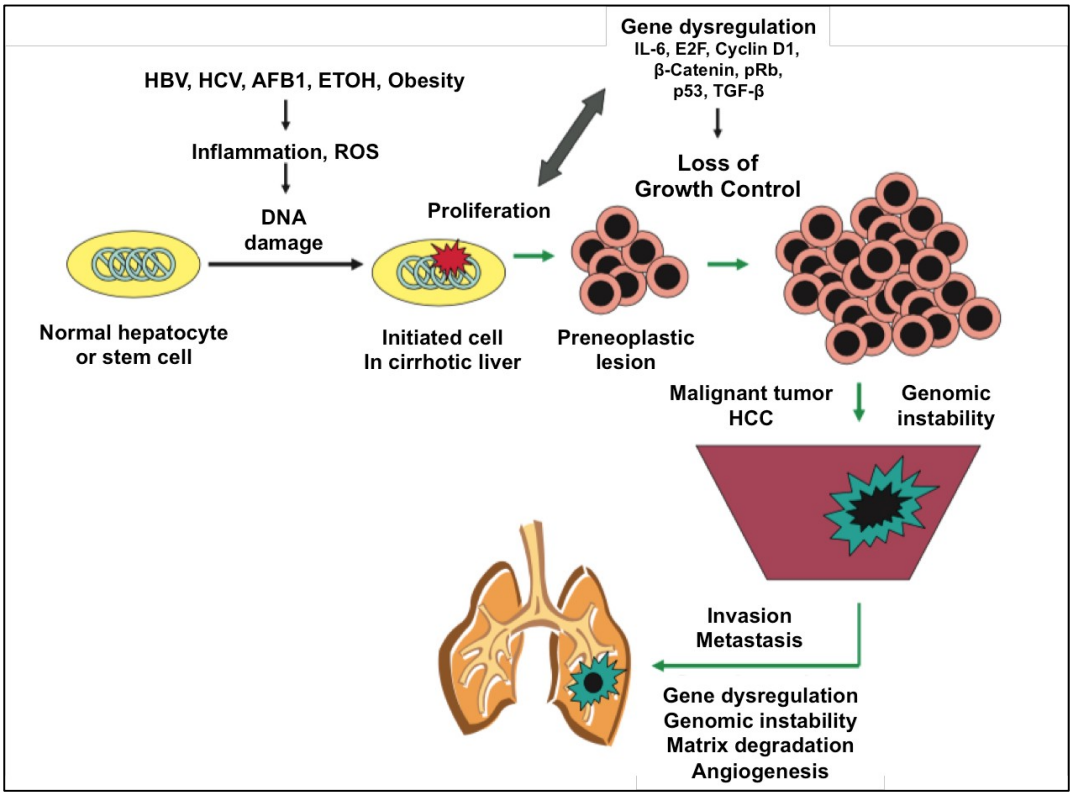

Fig. 1.4 – Pathogenic mechanisms in hepatocarcinogenesis. AFB1, aflotoxin B1; ETHO, alchol; HCC, heptocarcinoma; HBV, hepatitis B virus; HCV, hepatitis C virus; ROS, reactive oxygen species[60].

1.3.3.2 Chromosomal Instability in HCC

Chromosomal instability is the most common genetic modification in HCC. It could be induced by either error during mitosis or alterations in DNA replication and repair [77]. The chromosome modifications observed in HCC can be the gain and loss of whole chromosome arms or just amplification and deletion of small chromosomal fragments. According to the genomic hybridization data, chromosome 1q and 8q are frequently amplified, whereas chromosome 1p, 4q, 6q, 9p, 16p, 16q, and 17p are mainly lost in HCC[78]. The presence of chromosomal alterations in pre-neoplastic liver tissues indicated that chromosome instability may occur in the early stage of HCC, and accumulates during tumor progression[79].

Amplification of chromosome 1q is one of the most frequently observed chromosome abnormalities in HCC and its amplification is found in more than 50% of HCC patients. On chromosome 1 is localized the well characterized oncogene CHD1L[80], which has several oncogenic roles such as inhibiting cell apoptosis, regulating cell mitosis, and promoting cell *epithelial-to-mesenchymal* (EMT) transition during hepato-carcinogenesis [77]. CHD1L can also regulate TP53 stability, probably through the interaction with SCYLIBP1, which modulates the degradation of TP53. A recent study has showed that Adenovirus-mediated silencing of CHD1L could inhibit HCC tumorigenesis in xenograft mouse model suggesting CHD1L as a potential therapeutic target in HCC treatment[81]. In addition to chromosome 1q21, a study published in 2013 indicated a novel potential oncogene MAEL at 1q24, which could induce EMT and promote stem properties of HCC cells[82].

Chromosome 8q is another highly amplified chromosome arm in HCC and well-known oncogene-linked to HCC development, such as c-Myc and PTK2, which are located in the 8q24 region[83,84]. In addition to 8q24, the chromosomal region proximal to the centromere is also frequently amplified in HCC [85] and here the serine/threonine kinase SGK3 is found to be frequently amplified[86].

Chromosome segmental loss is also frequently observed in HCC and the minimal region of 1p35-36 is deleted in more than 50% of HCC patients. Several tumor suppressors including 14-3-3σ and RIZ1 are located in this region [87]. Loss of the short arm of chromosome 8 has been recurrently observed in HCC and in fact the minimal region of 8p21-22 is frequently deleted in HCC. DLC-1, which is located in this region [88], has found to be frequently down-expressed in HCC tissues, due to allele loss and promoter hypermethylation[89]. The restoration of DLC-1 expression in hepatoma cells could induce apoptosis in tumor cells and inhibition of cell growth[90].

Chromosome 16q is another region with frequent deletion in HCC. Two genes that are located on 16q22 region are CDH1, a tumor suppressor gene that inhibits cell proliferation and metastasis[91] and the TAT gene, which might contribute to the pathogenesis of HCC [92]. In a recent study focused on a cohort of HCC patient, a significant allele-specific imbalance was identified in the 16q23 due to LOH. The affected gene OSGIN1 can directly induce apoptosis in HCC cells and significantly contribute to the progression of HCC[93].

Another frequently lost region in HCC is the 17p13.1, where the well-known tumor suppressor TP53 is mapped. The 17p13 region is characterized by DNA hypermethylation; moreover, loss of 17p13.1 was closely associated with TP53 mutations[94].

1.3.3.3 Genetic alterations: balance between oncogenes and tumor suppressor genes

An important contributing factor associated with the development of a tumor is the balance between the activation of oncogenes and the inactivation of the tumor suppressor genes. Oncogenes usually promote cells proliferation, prevent apoptosis, inhibit differentiation[95] and in the healthy cells they are expressed at very low levels or not expressed at all. However, environmental factors such as ionizing radiations, physical damage and chemical mutagen compounds can produce genetic mutations, which occur in these genes promoting the activation from the proto-oncogene into oncogenes[95]. In HCC, N-Ras and Hepatitis b virus X (HBx) protein are the most common proto-oncogenes[96]. The strong correlation between HBV infection and HCC has already been described. The oncogenic function of HBx protein is well-known and is due to its multifunctional activities on cellular signaling pathways, transcriptional regulations, cell cycle progress, DNA repair, cell death and genetic stability[97]. HBx is often expressed from integrated fragments of the HBV genome in HCC tissue; notably, mice expressing HBx protein in their liver either develop HCC spontaneously or show more susceptibility to hepatocarcinogenesis [95]. HBx can interact with a lot of signaling pathways, which are associated with cellular proliferation and survival such as RAS/RAF/MAPK, MEKK1/JNK and PI3K/AKT/mTOR but can also modulate apoptosis and immune response interacting with host factors.

Tumor suppressor genes are usually expressed in normal cells and regulate cellular proliferation and differentiation. These genes can inhibit cell cycle progression, induce terminal differentiation and cell death and promote genome integrity. The TP53, Rb, CDK1NA and pTEN genes are the most common tumor suppressor genes [98]. The formation of malignant cancer is a multi-step process involving oncogenes activation and tumor suppressor

genes inactivation. It is known that these genes play an important role both in initiation and in development of the tumor. For example *BTG2*, is an anti-proliferative gene that encodes a protein of 158 amino acids. The protein contains the response element for the wild-type form of TP53 which is required for its activation [99]. BTG2 is connected up-stream with TP53 and down-stream with proteins, with anti-proliferative properties. Notably, BTG2 is expressed at low levels in different type of tumors. Previous data have shown that BTG2 expression was significantly increased in early liver cancer stage whereas its level was dramatically decreased in advanced HCC[100]. Of course the functions of many oncogenes and tumor suppressor genes are still unknown and the balanced expression of these genes is considered to be the main regulator of homeostasis. Once this balance is lost, cancer formation may occur[95].

1.3.3.4 Aberrant activation of molecular signaling pathways

Several molecular alterations have been observed in HCC and their accumulation has been thought to play an important role in the development of HCC [101,102]. Specifically, those alterations involve VEGF-mediated angiogenesis, proteins regulating the G1/S restriction point, Wnt/β-Catenin, PI3K/AKT/mTOR, AMPK and c-MET pathways.

VEGF-mediated angiogenesis pathway

Genetic instability and DNA mutations of cancer cells represent therapeutic targets of most novel drugs. Despite this, anti-angiogenetic drugs target normal endothelial cells which are less susceptible to acquired drug resistances. The rationale is that the targeting of endothelial cells can down regulate tumor angiogenesis thus limiting tumor development. Thus, angiogenesis inhibitors are emerging as anti-cancer drugs both in mono-therapy and in combination therapy. Recently, the role of angiogenesis in the progression of hepatocarcinogenesis from pre-malignant liver injury has prompted researchers to study VEGF in the natural history of HCC [103]. Several studies suggested that VEGF is frequently over-expressed in HCC and its tissue expression level increases according with the stepwise development of the tumor [101]. In HCC, hypoxia probably increases VEGF expression through the expression of HIF-1α[104]. Furthermore, VEGF is able to promote vascular permeability and stimulate proliferation of endothelial cells specifically through tyrosine kinase receptors[101]. On cancer cells both VEGF and Ang-2 are expressed and Ang-2 enhances vascular remodeling preventing vascular stability thus allowing VEGF to stimulate endothelial cells[101].

Proteins involved in the G1/S restriction point

It is known that signaling pathways involved in the regulation of the G1/S restriction point are frequently disrupted in HCC. The proteins that are mainly de-regulated during hepatocarcinogenesis are E2F proteins [105] and Cyclin D1, whose expression is also promoted by β-Catenin activation[70]. E2F proteins are central regulators of G1/S progression and consist of a family of transcription factors, which can act both as pro-proliferative and as inhibitory members[70]. Genes associated with proliferation are normally transcriptionally repressed in quiescent cells and during G1 phase as a result of anti-proliferative proteins expression including E2F4, E2F5, pRB, p130 and chromatin remodeling proteins [106]. During G1/S transition, cyclin D1, CDK4, CDK6, cyclin E and the dimers CDK2 sequentially phosphorylate pRb and p130 leading to the dissolution of the inhibitory complex[106]. This event enables the transcription of E2F target genes. Interestingly, amongst the early genes to be activated are those encoding the activators E2F1, E2F2 and E2F3 themselves, which then positively regulate downstream genes encoding proteins involved in DNA synthesis, in mitotic spindle assembly and in mitotic checkpoint functionality[70].

Increased expression levels of E2F have been found to be crucial in hepatocarcinogenesis[107]. In transgenic mice where E2F1 is overexpressed, the hepatocyte proliferation is highest in the early stages of hepatocarcinogenesis, whereas c-myc/TGFα transgenic mice show a rapid development of HCC associated with high expression levels of both E2F1 and E2F2[107].

The earliest cyclin-CDK complex activated during G1 phase progression is cyclin D1-CDK4/6 complex and the cell cycle progression through the G1/S phase transition depends on cyclin D1 expression[70]. In hepatocytes, its overexpression induces replication whereas in regenerating liver cyclin D1 promotes growth through metabolic signals, which induce the exit of hepatocytes from G1/S phase[108]. Cyclin D1 expression is increased in HCC and correlates with advanced tumor stage and progression [70]. Cyclin D1 transient overexpression in murine hepatocytes causes chromosomal instability, centrosome amplification and mitotic spindle abnormalities[109]. It is also known that an exaggerate expression of cylin D1, both in human and in murine models, is associated with amplification of its gene due to chromosomal aberrations[109]. These findings suggest that the overexpression of cyclin D1 is likely to be a late event in hepatocarcinogenesis rather than in tumor initiation[70].

Mutations in the pocket protein pRb have been frequently found in HCC [70]. pRb may promote long-term silencing of proliferative genes in those cells that are terminally quiescent[110]. Because hepatocytes preserve the ability to rapidly re-enter the cell cycle in

response to liver injury, it is probably that the pRb family members, p130 e p107, are responsible for the repression of cell cycle-associated genes[70]. The observation that pRb is preserved in those HCC patients where cyclin D1 is overexpressed, supports the idea that inactivation of other pocket proteins may be responsible of growth deregulation in some liver cancer cases[109].

WNT/β-catenin signaling pathway

Wnt/β-Catenin signaling pathway is composed of the Wnt protein, Wnt protein ligands, also known as Frizzled receptors, and related regulator proteins such as GSK-3β and β-catenin[101]. The canonical Wnt pathway occurs as a cascade of events beginning with the translocation of β-catenin from the cell membrane into the nucleus, where β-catenin acts as a co-activator of the TCF/LEF transcription factors family. Here,β-catenin can regulate the expression of specific target genes including c-myc, cyclin D1 and Survivin[70].

In normal cells, β-catenin is associated with *adherens junctions* of cellular membrane, linking E-cadherin to the actin cytoskeleton[111]. In the extracellular environment, the signaling cascade is normally activated when enough Wnt ligand stimulates the release of the signaling message through the trans-membrane receptor Frizzled. Activated Frizzled receptor signals to β-catenin to escape from the E-cadherin complex, avoiding its phosphorylation by a degradation complex made up of GSK-3β, a serin-threonin kinase, and scaffolds protein including ANIX and APC[111]. Normally, when Wnt pathway is not activated, cytoplasmatic β-catenin is phosphorylated and ubiquitinated to be sent to proteosomal degradation[70]. However, mutation in these proteins may allow β-catenin to translocate into the nucleus to promote constitutively the transcription of its target genes[112] (Fig. 1.5).

Nuclear localization of β-catenin is considered a precursor of its oncogenicity[112]. Most mutations in the Wnt pathway lead to cancer formation: some of these mutations can inactivate the function of APC or stabilize β-catenin by changing its binding site to the scaffold proteins, therefore allowing its translocation into the nucleus and escaping degradation by the proteasome[112]. Furthermore, Wnt signaling intermediates have been shown to be up-regulated in HCC, with more than 10 studies demonstrating β-catenin mutations[70]. Mutations of β-catenin described in HCC are located in exon 3 of its gene CTNNB1, which represents the phosphorylation site for GSK-3β. Calvisi et al. reported that transgenic c-myc mice developed liver cancer associated with mutations in β-catenin, suggesting that the activation of β-catenin may increase tumor growth and metastasis[113]. Also HBV and HCV

infection can induce high β-catenin levels promoting the occurrence of HCC[114]. Axin mutations and deletions have also been described in HCC [70] whereas Freezed receptor 7 has been found to be overexpressed in up to 90% of HCC [115]. Even if 20-40% of HCC cases have shown abnormal cytoplasmic and β-catenin nuclear accumulation by immunohistochemical staining, not all studies promote a strong correlation between high nuclear β-catenin level and expression of its transcriptional targets. This implicates that probably the expression of these target genes is regulated by alternative signaling mechanisms[70].

Ras/Raf/MAPK signaling pathway

Among the studied signaling pathways involved in the onset of HCC, the Ras/Raf/MAPK may be one of the most critical pathways. Signals from membrane-bound tyrosine kinase receptors, such as EGFR, IGFR, c-Met and PDGFR are transduced to the nucleus through Ras/Raf/MAPK pathway to regulate different cellular functions including cell growth, differentiation, survival and ultimately cancer[116] (Fig. 1.5). The overexpression of Ras/Raf/MAPK signaling correlates with advanced HCC stage. The mechanisms promoting the activity of this pathway include aberrant up-stream signals (EGFR signaling and IGF signaling), inactivation of Raf kinase inhibitor protein and induction by hepatitis viral proteins, such as HBx protein and the hepatitis C core proteins[117]. In the last years many drugs blocking Ras/Raf/MAPK signaling were investigated, such as *Sorafenib*, which is the only multi-tyrosine kinase inhibitor approved by FDA for the treatment of un-resectable HCC [101].

PI3K/AKT/mTOR signaling pathway

PI3K/AKT/mTOR pathway plays a key role in cell regulation because it is involved in many cellular processes including cell division, cell growth and programmed cell death[118]. PI3K/AKT/mTOR pathway can be triggered by a lot of different stimuli, such as activated tyrosine kinase growth factor receptors, G-protein-coupled receptors and oncogenes as Ras [119]. PI3K activation promotes the phosphorylation and activation of AKT, localizing it in the plasma membrane. AKT can have many downstream effects such as activating CREB[120], inhibiting p27, activating mTOR, which, in turn, can affect the transcription of p70 and 4EBP1[121] (Fig. 1.5).

It is known that PI3K/AKT/mTOR pathway is activated in 30-50% of HCC whereas in normal liver tissue this pathway is negatively regulated by the tumor suppressor phosphatase PTEN, which dephosphorylates PI3K[95]. In HCC, anomalies in PTEN function may lead to over-activation of the PI3K/AKT/mTOR pathway. Notably, PTEN is down regulated in

nearly half of all HCC, resulting in the constitutive activation of the PI3K/AKT/mTOR pathway[95]. A tissue microarray analysis performed using HCC samples reveals that the loss of PTEN and the up regulation of AKT and m-TOR are correlated with tumor grade, metastasis formation, vascular invasion TNM stage and MMP2 and MMP9 up regulation[122].

The mTOR complex is an important therapeutic target because it represents an intracellular key protein for a number of cellular signaling pathways. The inhibition of mTOR can prevent aberrant proliferation, tumor angiogenesis and abnormal cellular metabolism, thus validating the idea that mTOR can be a potential therapeutic target [123]. Several studies have shown that selective mTOR inhibition can lead to AKT activation, which is mediated by IGF_{R1} pathway[101]. Activation of AKT can limit the anti-tumor activity of mTOR inhibitors thus leading to the development of resistance. This pathways is activated in a subset of HCC patients and the use of *Rapalogs*, a class of first generation mTOR inhibitors, has been shown to inhibit tumor growth both in HCC cell lines and in experimental animal models[124].

Hedgehog signaling pathway

The *Hedgehog* (Hh) pathway is a major regulator of many fundamental processes in vertebrate embryonic development including stem cell maintenance, cell differentiation, tissue polarity and cell proliferation[125]. Constitutive activation of Hh pathway is observed in a wide variety of human cancers including basal cell carcinomas, medulloblastoma and even brain, gastrointestinal, lung, breast and prostate cancers [125]. It is also known that Hh signaling pathway plays a key role during hepatocarcinogenesis[95]. In mammals, the Hh signaling pathways is mainly composed of Hedgehog ligands, the transmembrane protein receptors *Ptch* and *Smo*, the nuclear transcription factors *Gli* and downstream genes[95]. When the Hh signaling pathway is activated, Hh ligands bind Ptch receptor blocking its inhibitory effect on Smo. Smo can thus enters into the cytoplasm to activate the transcriptor factor family Gli, thus inducing the expression of specific genes involved in the regulation of cell growth, proliferation and differentiation[95]. In HCC, Hh signaling pathway is usually abnormally activated; in contrast, in normal liver tissue its signaling is not initiated[126]. Several studies suggest there is a dysfunction of Hh signaling in HCC due to high expression of Hh ligands, in particular *Sonic Hedgehog* ligands, Ptch, Smo and Gli1, all of which regulate c-myc gene expression[127]. Moreover, Kim et al. suggests that in liver cancer tissue, the inhibition of Gli2 gene can reduce the expression of c-myc and increase the expression of p27, thus inhibiting tumor cell growth and proliferation[128].

TGF-β signaling pathway

TGF-β is a secreted protein that mediates growth and proliferation in epithelial cells and in other cell types through several regulatory pathways. Unlike its tumor suppressor function in normal tissue, TGF-β activation promotes tumor growth in cancer tissue [129]. Some changes mediated by TGF-β signaling, including loss of cell polarity, acquisition of motile properties and mesenchymal phenotype during epithelial-mesenchymal transition (EMT), are considered crucial intrinsic modifications of tumor cells [130]. These changes are also associated with extrinsic factors originating from tumor microenvironment such as angiogenesis, inflammation and fibroblast activation. In addition to tumor tissue modifications, alterations in TGF-β signaling pathway can also contribute to tumor growth[129].

The TGF-β signaling occurs through a canonical pathway and a non-canonical pathway. The TGF-β canonical pathway is activated when one of the ligands, TGF-β1, TGF-β2 or TGF-β3, binds TGF-β receptor 2. This complex heterodimerizes with the TGF-β receptor 1 and the kinase domains of both receptors are trans-phosphorylated. This phosphorylation event leads to the recruitment and phosphorylation of SMAD2 and SMAD3 proteins. Their phosphorylation activates a SMAD signaling cascade, resulting in their complexation with SMAD4 and translocation into the nucleus. In the nucleus, SMAD2/3/4 complex causes the transcriptional activation of a wide range of tumor-promoting factors [131]. The less-known TGF-β non-canonical activation pathway is associated with the phosphorylation of several intracellular proteins, including jun N-terminal kinase, p38 MAPK, ERK, or MAP3K[129] (Fig. 1.5).

In a contest of tumor microenvironment, TGF-β orchestrates the homeostasis of the environmental components and tumor cells by balancing the activity of inflammatory cells with tumor cell growth and progression[129]. In a chronically inflamed liver, reversible and irreversible remodeling is often observed, including fibrosis and early cirrhosis [132]. This remodeling is characterized by extracellular matrix (ECM) proteins accumulation, which leads to TGF-β signaling activation. If not stopped, this process can induce cirrhosis and eventually liver failure. Fibrosis due to ECM proteins accumulation is still a reversible step and it can be particularly important for therapeutic approaches aimed at blocking liver diseases progression[129].

A gene expression study performed by Coulouarn et al. both in mouse model and in human tissue, demonstrated that two different TGF-β signaling responses exist, one called *early* TGF-β signaling response and the other termed *late* TGF-β signaling response [133]. The

first signaling response is associated with longer survival than the second one. This is probably possible because the *early* TGFβ signaling reflects the physiologic inflammatory response whereas the *late* TGF-β signaling pattern is associated with a long-term TGFβ activation[129].

The extrinsic effect of TGF-β signaling is the result of tumor cells embedded in ECM-enriched environment[129]. In this condition, TGF-β and other associated factors, including CTGF, are secreted and can thus activate cancer-associated fibroblasts[134]. TGF-β signaling has been also associated with T regulatory cells, by activation of chemokines or by immune presentation of AFP[135]. More recently, TGF-β signaling has also been related to tumor-initiating cells. In fact, stimulation of liver progenitor cells with TGF- β induces their transformation into tumor-initiating cells as shown by TGF- β–induced changes in CD90 and CD133 expression[136]. The intrinsic effects of TGF- β signaling are mostly observed in highly invasive tumors. TGF-β signaling is associated with loss of cell polarity, acquisition of cellular motility, and increased tumor invasion [137]. A very important change in tumor cells is related to E-cadherin expression, a well-known marker of epithelial-mesenchymal transition: in fact in the presence of TGFβ, E-cadherin is shed from tumor cells, making them more invasive[129]. In association with other components of tissue microenvironment such as Ln-5 and CD44, TGF-β promotes the transcription factor *Snail*, another component involved in the epithelial-mesenchymal transition that is often associated with poor prognosis[138]. All these evidences suggest a role of TGF-β signaling in EMT and in making tumors more invasive.

AMPK signaling pathway

AMPK is a highly conserved serine-threonine kinase that plays a key role in linking metabolism and cancer development. Under stressful conditions, such as low glucose level, hypoxia, ischemia or heat shock, AMPK is activated through the increased activity of *AMP/ATP*[101]. Once activated, AMPK suppresses cell proliferation and death, through the inhibition of protein synthesis, in tumor and non-tumor cells. Downstream of AMPK, *TSC1* and *TSC2* proteins are activated, promoting apoptosis.

Clear evidences suggest that AMPK levels are de-regulated in several cancers including HCC. In a recent study, Zheng et al. showed that AMPK was down-regulated in a majority of HCC patients, which presented a worse prognosis [139]. Another study published by Lee et al. demonstrated that AMPK represents a tumor suppressor gene in HCC and its inactivation can lead to hepatocarcinogenesis by destabilizing TP53[140]. Both these studies

underline the key role of AMPK in both HCC onset and progression. Furthermore, it has been demonstrated that activation of *AMPK/TSC1/TSC2* inhibits the onset of various tumors including HCC[139].

c-MET signaling pathway

The *c-Met* proto-oncogene encodes a HGF tyrosine kinase receptor. The binding of HGF to c-MET receptor leads to homo-dimerization, subsequent auto-phosphorylation of downstream residues and downstream activation of MAPK and PI3K pathways[101]. These events promote tumor cell growth, survival, migration, invasion and metastasis[141]. In literature, c-MET is found to be frequently de-regulated in many types of cancer. Moreover, it can have a pivotal role in HCC because its activation can lead to a more aggressive form of HCC with poor outcome[142] (Fig. 1.5).

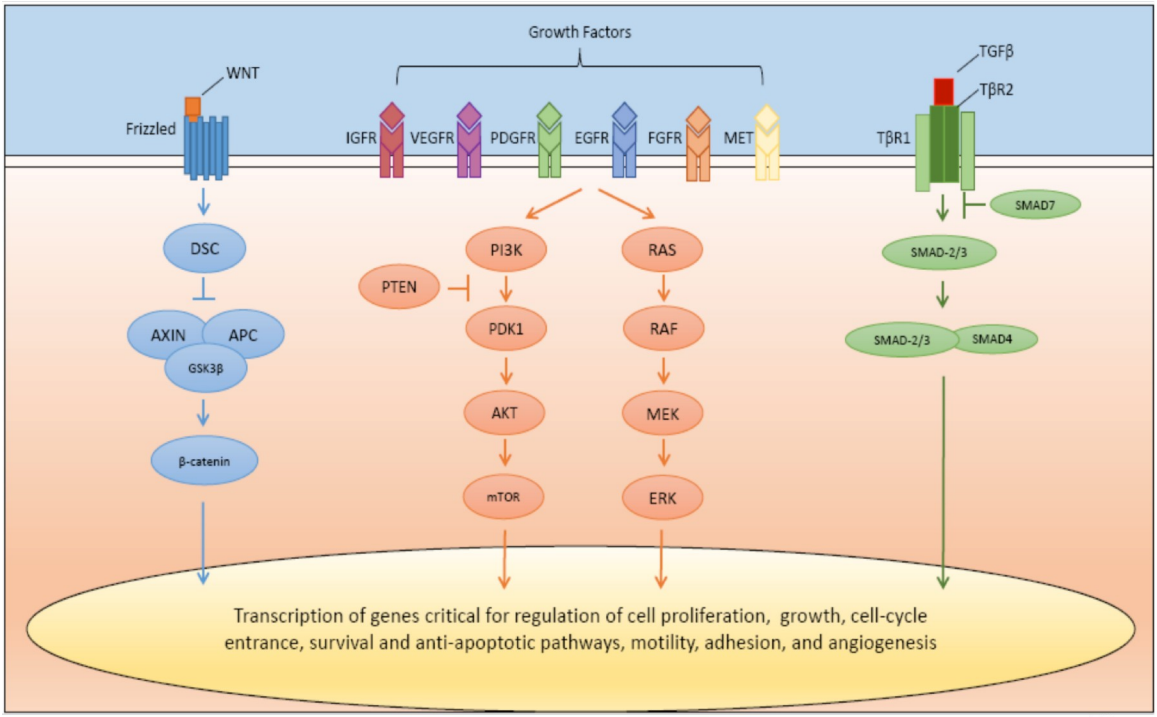

Fig. 1.5 – Schematic representation of the main signal transduction pathways involved in HCC onset[143].

1.3.3.5 Epigenetic alterations in HCC

Genetic alterations are irreversible changes that affect particular DNA sequences. Conversely, epigenetic regulations do not change the sequence of the genome but influence chromatin structure and genes transcription[77]. Epigenetic alterations affect gene products both at transcriptional level and at post-transcriptional level, and add great diversity to the gene regulator network. DNA methylation, histone modification and recently also long non-coding

RNA are the major forms of epigenetic regulations. Changes of the cellular machineries governing those processes are frequently observed in HCC. Epigenetic alterations usually induce activation of oncogenes or inactivation of tumor suppressor genes and recent evidences suggest that epigenetic changes play an important role both in initiation and in development of HCC.

DNA methylation

In non-tumor cells, DNA methylation and de-methylation is a crucial mechanism in regulating gene expression and chromatin structure. The enzyme DNMT catalyzes the addition of methyl groups to cytosine located next to guanine, in the CpG di-nucleotide [144]. CpG di-nucleotides are frequently enriched in particular genomic regions know as *CpG island*, which are located especially in genes promoter. In tumor cells promoter methylation pattern is often changed and promoters' aberrant methylation is a crucial mechanism to inactivate tumor suppressor genes. The hypermethylated CpG islands at the promoter region will prevent the binding of RNA polymerase and transcriptional factors, inhibiting the transcription of target genes[77]. In contrast to hypermethylation, promoter hypomethylation can induce reactivation of transposable elements and insertion to a new location leading to genetic translocations, insertions, exon deletions and chromosomal loss[77].

In HCC, hypermethylation of CpG islands is frequently observed at the promoter region of important tumor suppressor genes. For example, *SOC-1*, which regulates the JAK/STAT signaling pathway, is suppressed in more than 60% of HCC patients due to promoter hypermethylation[7]. The tumor suppressor genes APC and E-cadherin are also hypermethylated in 53% and 49% of HCC patients respectively[8]. Methylation profiling of multi-step HCC tumors suggested that the number of genes methylated gradually increase with the progression of cancer stage. In fact, the observation of tumor suppressor genes hypermethylation in both para-tumor liver tissues and cirrhotic tissues indicates that aberrant promoter methylation occurs in the early stage of hepatocarcinogenesis and increases during cancer progression [145]. Moreover, genome-wide DNA methylation analysis reveals that HCC epigenetic silencing of multiple tumor suppressors can lead to the activation of several oncogenic signaling pathways including Ras, JAK/STAT, and Wnt/β-catenin [146].

In literature, different hypotheses have been proposed trying to explain the aberrant DNA methylation in cancer. One possible mechanism is the aberrant expression of DNMT1, which is usually atypically expressed in cancer. Once overexpressed, DNMT1 can commit methylation errors during DNA replication [147] (Fig. 1.6). The expression of DNMT1, which is

the major enzyme responsible to the maintenance of genomic methylation pattern, is significantly increased in HCC patients [77]. In addition to DNMT1, other DNMT family members, including DNMT3A and DNMT3B, can directly add methyl groups to un-methylated DNA. DNMT3A and DNMT3B are reported to be associated with hyper-methylation of several important tumor suppressor genes, including CDKN2A, CDKN2B, CDH1, and Rb1[148]. DNMT3A and DNMT3B are both significantly overexpressed in HCC compared to non-tumor liver tissues[149] (Fig. 1.6).

Histone acetylation and chromatin remodeling

Chromatin is the fundamental structure of the genome and it is extremely important to gene transcription. In active transcription sites, the chromatin is loosened so that transcriptional factors can enter and bind DNA for transcription initiation. This open chromatin structure is named *euchromatin* [77]. Conversely, some parts of chromatin structure are heavily condensed and the transcriptions of genes located into those regions are inhibited. The condensed chromatin structure is termed *heterochromatin*. Thus, chromatin structure is critically important in regulating gene expression in a temporal and spatial dependent manner[150].

Histone modifications, such as methylation or acetylation, play a pivotal role in chromatin structure regulation. There are two histone modification markers, which can be found in an active transcriptional site. *Trimethylation of H3 lysine 4*, H3K4Me3, is often observed at the promoter region of actively transcribed genes. *Trimethylation of H3 lysine 36*, H3K36Me3, is also closely associated with active transcription. Conversely, *trimethylation of H3 lysine 27*, H3K27Me3, and *trimethylation of H3 lysine 9*, H3K9Me3, are associated with repressed transcription[151] (Fig. 1.6). Histone modifications are catalyzed by several enzymes, which include HMT, HAT, and HDAC. Aberrant expression of those histone modifiers, which further drives epigenetic alterations, is frequently observed in cancer cells. In HCC, overexpression of EZH2, which is the histone methyltransferase for H3K27Me3, has been associated to malignant transformation and poor prognosis of HCC patients[152] (Fig. 1.6). PCAF, which is a well-known HAT, is expressed at low level in HCC, and it can inhibit HCC tumorigenesis both *in vitro* and *in vivo*[153] (Fig. 1.6). Several studies suggest that HDAC specifically induce apoptosis in hepatoma cells but not in primary hepatocytes[154]. These results greatly supported the potential application of HDAC inhibitors in clinical HCC treatment.

In addition to histone modifiers, the ATP-dependent chromatin-remodeling complex is also closely involved in tumorigenesis. This complex uses ATP to mobilize nucleosomes along DNA. The ATP-dependent chromatin remodeling complex family could be further divided into four subfamilies including: the *SWI/SNF* family, the *ISWI* family, the *NuRD/CHD* family, and the *INO80* family [150]. Whole-genome sequencing has identified recurrent somatic mutations in genes involved in the chromatin remodeling complex, including *ARID1A*, *ARID2*, and *BRG1* [155]. The ATPase and putative DNA helicase *RUVBL2* was found to be overexpressed in HCC and they probably contribute to cell malignant transformation[156]. The loss of copy number or the down-regulation of *BRG1* and *BRM* were also frequently observed in HCC patients[157]. In addition, CHD1L has been proven to have diverse oncogenic roles in hepatocarcinogenesis[158].

Long non-coding RNAs

Many non-protein coding transcripts exist in the genome and, recently, emerging evidences suggest that this *long non-coding RNAs* might play important roles in regulating gene expression at post-transcriptional level. Long non-coding RNAs, lncRNAs, can regulate gene transcription either through directly binding to the RNA polymerase II, or changing the activity of the transcriptional co-regulators[77,159]. In addition to transcriptional regulation, lncRNAs can also modulate the post-transcriptional mRNA processing, including mRNA splicing and translation. Furthermore, literature reports that lncRNAs can also be involved in regulating histone methylation and chromatin remodeling [77,160]. Aberrant lncRNAs expression has been observed in several tumors such as HCC, suggesting a critical role of these molecules during tumorigenesis (Fig. 1.6). For example, high expression of lncRNA-HEIH is significantly associated with HCC recurrence and poor prognosis. *In vitro* and *in vivo* functional studies suggested that the overexpression of lncRNA-HEIH can promote HCC tumorigenesis, probably through EZH2[77,161]. In addition, overexpression of lncRNAs *HOTAIR* and *MALAT-1* can help predict tumor recurrence and prognosis of HCC patients[77,162]. All these evidences indicate that lncRNAs might be crucial in HCC initiation and progression.

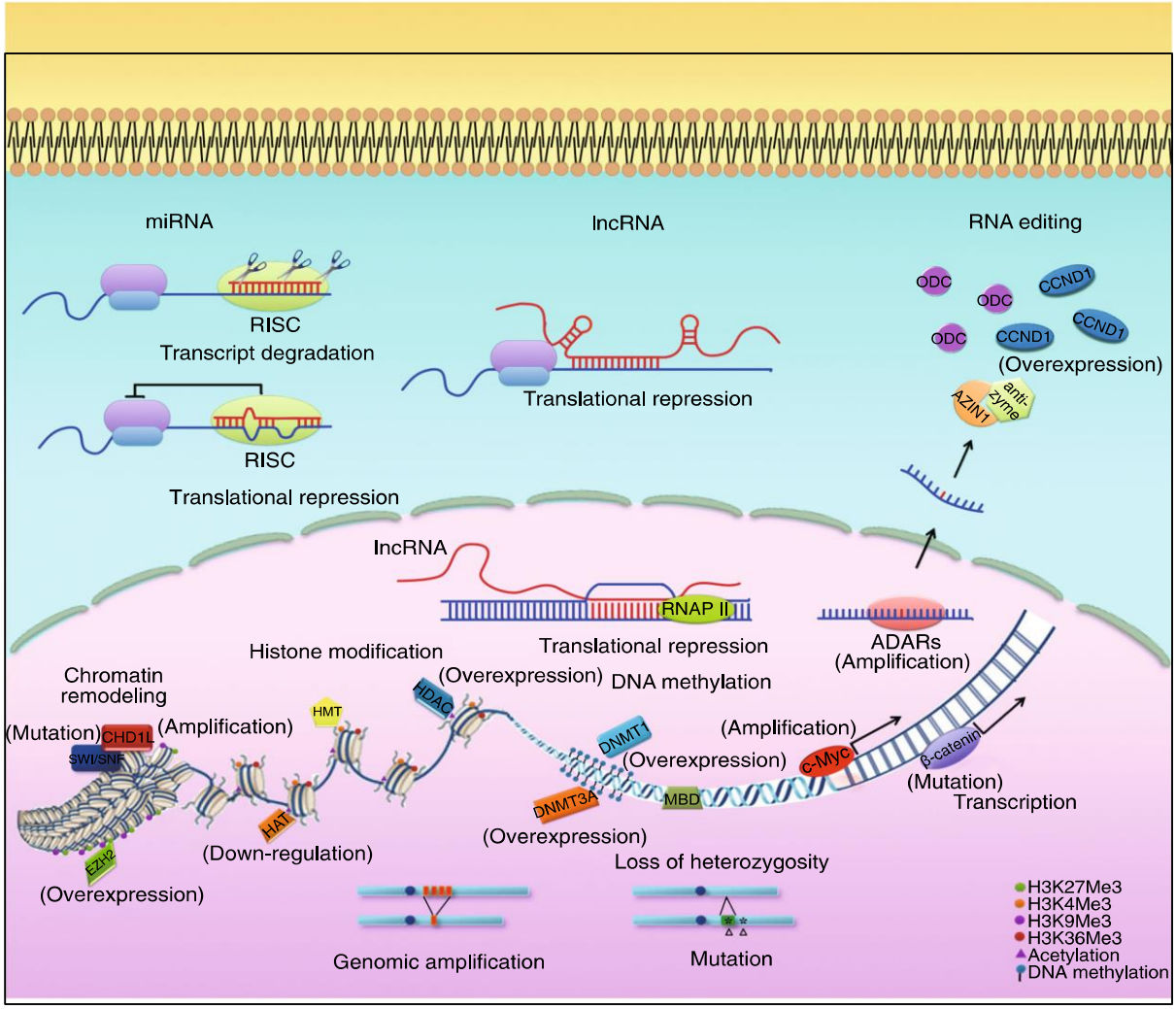

1.3.4 HCC treatment: past, present and future

1.3.4.1 Staging of HCC and current treatment

HCC treatment decisions are complex and strictly depend upon tumor staging. In patients with unresectable disease and tumor staging that falls within criteria, liver transplantation can be curative in a great majority of patients. Unfortunately, most patients will not be candidate for either surgery or transplant[4].

Recently, different HCC staging systems have been proposed but *Barcelona Clinic Liver Cancer* (BCLC) staging system has proved to be the most widely accepted model. In fact, it integrates both tumor characteristics and general health status with hepatic function to provide a clinical algorithm to help guide treatment decision-making according to disease stages[163]. According to BCLC staging system, patients with HCC are divided in five different stages (Fig. 1.7):

- **BCLC 0:** this stage represents the very early HCC stage and refers to patients with a

single tumor ≤ 2cm or *in situ*. Hepatic resection (HR) or liver transplantation (LT) are usually recommended for the treatment of patients with BCLC 0/A stage [164] (Fig. 1.7). However, various risks including insufficient liver function, major blood loss, further injury to the normal parenchyma, and a shortage of liver donors can prevent some patients from undergoing HR or LT [165]. In patients belonging to stage 0 who are not suitable for HR or LT, radiofrequency ablation (RFA) is recognized to be the therapeutic choice. Recently, RFA is shown to be as effective as HR in small HCCs in terms of survival. This evidence suggests that RFA may be the first therapeutic choice for patients with single HCC, which is 2 cm or smaller, even when they can be surgically resected[166].

- **BCLC A:** this stage represents the early HCC stage and includes patients with a single HCC or up to three nodules < 3 cm. Currently, if patients have well-preserved liver function without major vascular or lymphatic invasion, HR is consider to be the standard therapeutic approach for early HCCs [167]. Unfortunately, many patients don't satisfy these criteria because HCC usually occurs in a cirrhotic liver. These patients are usually treated using percutaneous ethanol injection (PEI) or RFA. In fact, RFA has been found to be equally safe and effective as a first-line treatment for a single HCC up to 5 cm in diameter [168]. Because of BCLC staging system categorizes solitary HCC as an early stage of disease irrespective of tumor size, large single HCCs > 5cm without vascular invasion also belong to BCLC A stage[163]. The expected 5-years survival should range between 50% and 75%[169].
- **BCLC B:** this stage represents the intermediate stage and includes patients with asymptomatic, large or multifocal HCCs without evidence of vascular invasion or extrahepatic metastasis. The trans-arterial chemoembolization (TACE) is the recommended therapeutic approach for this stadium of patients[170]. Three-years survival may exceed 50%[169].
- **BCLC C:** this stage represents the advanced HCC stage, to which belong patients who have symptoms and/or vascular invasion or extrahepatic spread. For the treatment of advanced HCC patients, there is not effective systemic chemotherapy. In this context, *Sorafenib*, an oral multi-kinase inhibitor with anti-proliferative and anti-angiogenetic effects, is currently considered as the standard of care for BCLC stage C HCCs[163]. Their survival is less than 10% at 3 years[169].
- **BCLC D:** to this stage belong patients at a terminal stage of disease with very impaired physical status or excessive tumor burden with severe liver damage. These

patients receive symptomatic treatment to avoid suffering. Their survival at 1 years is less than 10%[169].

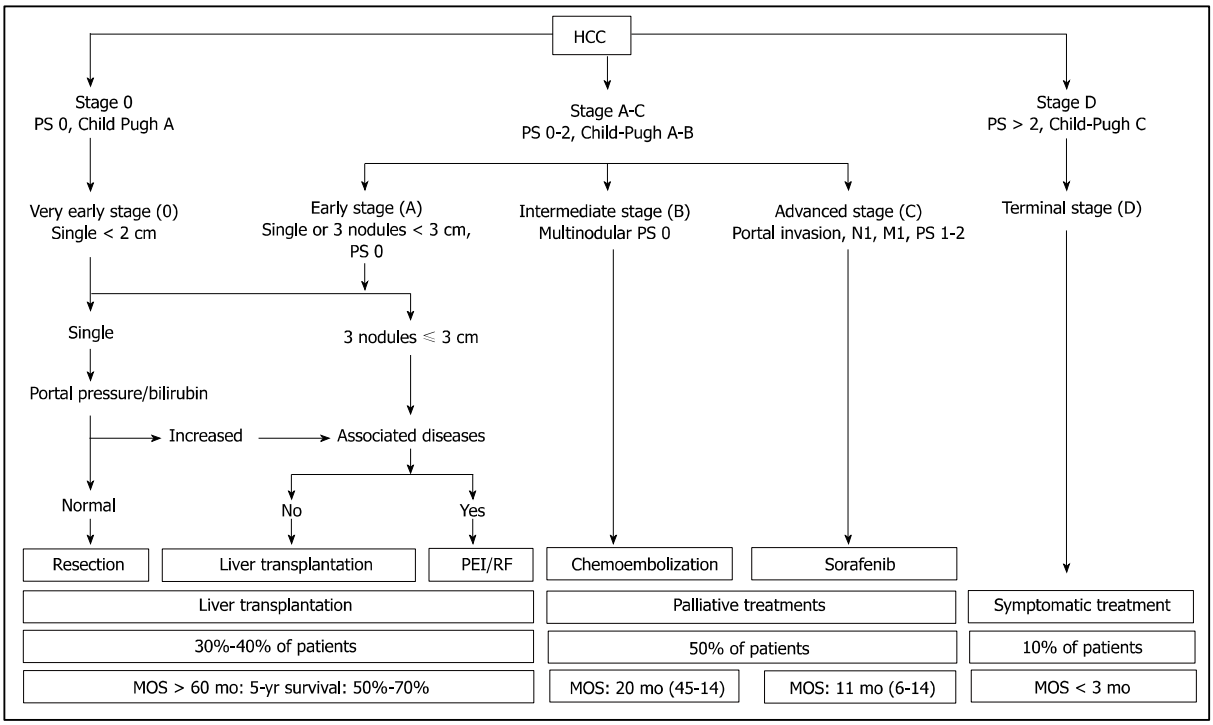

Fig 1.7 - Barcelona Clinic Liver Cancer (BCLC) staging system and treatment strategy[163].

Curative therapy, including surgical approaches such as HR and LT, locoregional therapies, as PEI and FRA, have been proven to have better survival benefits in the very early and early stages of disease[5]. Instead, TACE and redioembolization are primary therapeutic approaches for these patients with preserved liver functions. Unfortunately, if the HCC progresses to an advanced stage, only systemic treatments are indicated even if the prognosis and outcome are very inauspicious for patients[5].

HCC is highly refractory to conventional cytotoxic chemotherapy. Besides chemoresistence, the major side effects of systemic chemotherapy are the poor tolerability by patients with severe hepatic dysfunctions. Chemotherapy was usually offered to patients with advanc00ed HCC. Doxorubicin alone has been used as well as in combination with other chemotherapy agents with no clear evidence of overall survival benefits[171]. Cisplatin, interferon, doxorubicin and fluorouracil regiment was studied in a phase III trial versus single-agent doxorubicin without significant differences in terms of overall survival[171]. A study that enrolled 147 previously untreated HCC patients demonstrated that patients with severe cirrhosis, a tumor mass occupying more than 50% of the entire liver and tumor thrombus in the main portal trunk may not be responsive to chemotherapy [172]. Most of

published studies suggest that the effective response rates of patients to systemic chemotherapy are no more than 25% and there was no evidence that it may improve the overall survival rate in patients with any subset of HCC[5,173]. However, chemotherapy may still considered for patients whose tumors progress while on *Sorafenib* treatment[5].

In the last years, scientists have tried to develop molecular agents able to specifically inhibit proteins involved in the different pathways associated with hepato-carcinogenesis. One of these molecular agents, named *Sorafenib*, is currently the only FDA-approved systemic treatment for HCC[4]. *Sorafenib* is an oral multi-kinase inhibitor with anti-angiogenetic and anti-proliferative actions. It is used for the treatment of asymptomatic HCC patients with well-preserved liver functions who can't receive curative treatment, such as HR or LT, and patients with advanced HCC [4]. Its efficacy and safety in HCC patients were demonstrated by S.H.A.R.P. trial, which enrolled west patients and ORIENTAL trail, which enrolled in Asian-Pacific region patients. In the S.H.A.R.P. phase-III trial, 602 patients, enrolled from different countries, with advanced HCC were randomly assigned to the *Sorafenib* or placebo group. Improvement of median overall survival (10.7 mo Vs 7.0 mo, HR = 0.69, $P < 0.001$) and increased time to progression (5.5 mo Vs 2.8 mo, HR = 0.58, 95% CI: 0.45-0.74, $P < 0.001$) were seen in the *Sorafenib* group. Overall toxicity didn't differ between the treatment and placebo arm (52% Vs 54%)[174]. In 2009 in another phase III trial named ORIENTAL, 226 patients with advanced HCC were randomly divided in two groups: one received *Sorafenib* 400mg twice daily and the other placebo. The group of patients, who took *Sofafenib*, had better median overall survival (6.5 mo Vs 4.2) and time to progression (2.8 mo Vs 1.4 mo) compared to the control group. Only small side effects, including hand-foot syndrome (11%), diarrhea (6%) and fatigue (3%) were found in patients treated with Sorafenib [175]. Thus, FDA approved *Sorafenib* in 2007 in United States and it became the standard care for systemic treatment in advanced HCC patients[5].

Sorafenib has also been studied in combination with other systemic chemotherapeutic agents, such as Doxorubicin. In a phase II trial, patients with advanced HCC were randomly assigned to receive Doxorubicin in combination with *Sorafenib* or Doxorubicin alone. The combined therapy *Sorafenib-Doxorubicin* improved median time to progression (6.4 mo Vs 2.8; $P = 0.02$), median overall survival (13.7 mo Vs 6.5 mo; $P = 0.006$) and progression-free survival (6.0 mo Vs 2.7 mo; $P = 0.006$) compared to Doxorubicin alone[176].

An important aspect that attracts the attention of the scientific community is the drug-resistance to *Sorafenib*, which still remains unclear. The main resistance mechanism could be associated with the genetic heterogeneity; moreover, acquired resistance is possibly related to

the activation of compensatory pathways, including PI3K/AKT and JAK/STAT signaling pathways[6]. The mechanisms associated with the development of *Sorafenib* resistance in HCC patients are really complicated and need further investigation.

1.3.4.2 Molecular targeted therapy based on HCC genetic alterations

It is known that several pathways are implicated in hepatocarcinogenesis, and agents that target these pathways are continuously developed. Effective drugs can be synthesized and used to target a specific HCC subgroup. A molecule that belongs to the oral multi-kinase inhibitors family is *Sunitinib*. It targets several kinase receptors, including VEGF-1/2 and PDGFR-a/b, involved in liver cancer cells proliferation and angiogenesis[4]. It has already demonstrated its preliminary anti-tumour activity and an acceptable safety profile in different phase II trials for advanced HCC patients even if *Sunitinib* seems to induce significant side effects[4]. In a study published in 2011, Huynh et al. wanted to compare the effectiveness of *Sunitinib* relatively to *Sorafenib* using both orthotopic and ectopic xenograft models of HCC. They observed reduced tumour growth, angiogenesis and cell proliferation in both HCC models for the two drugs [177]. However, the antitumor effectiveness of *Sorafenib* was greater than *Sunitinib*. These observations need now to be verified in humans. *Sunitinib* affects large solid intrahepatic tumours but it seems to be unable to oppose to local growth of small tumours and to development of distant micrometastases[178].

Linifanib is a multi-targeted tyrosine kinase inhibitor that targets multiple members of the VEGFR and PDGFR families [179]. It has been demonstrated that in a xenograft model of HCC, *Linifanib* significantly reduces tumour burden. A phase III trial compared the effects of *Linifanib* and *Sorafenib* in patients with advanced HCC. These patients were randomized to *Linifanib* group or *Sorafenib* group and stratified by region (non-Asia/Japan/rest of Asia), ECOG performance status (0/1), vascular invasion or extra-hepatic spread (yes/no), and HBV infection (yes/no). Hazard ratio (HR) for overall survival was 1.046 (95% CI: 0.896, 1.221) and median overall survival (95% CI) was 9.1 months (8.1, 10.2) on *Linifanib* and 9.8 months (8.3, 11.0) on *Sorafenib*. For all pre-specified subgroup analyses, HRs for overall survival ranged from 0.793 to 1.119, and the 95% CI contained 1.0. HR for time to progression was 0.759 (95% CI: 0.643, 0.895; P=0.001) favouring *Linifanib*. Median time to progression (95% CI) was 5.4 months (4.2, 5.6) on *Linifanib* and 4.0 months (2.8, 4.2) on *Sorafenib*. The overall response rate (ORR) was 13.0% on *Linifanib* and 6.9% on *Sorafenib*. In conclusion, overall survival resulted similar in advanced HCC patients treated with *Linifanib* compared to those treated with *Sorafenib*. *Linifanib* had grater time to progression and overall response rate

respect to *Sorafenib* while safety resulted favoured *Sorafenib*[180].

Tivantinib is a new oral selective MET inhibitor. MET is a tyrosine kinase receptor involved in tumor development and metastatic progression. When HGF binds MET receptor, RAS-MAPK and PI3K-AKT signaling pathways are activated [181]. *Tivantinib* acts by blocking growth and inducing apoptosis in human tumor cells that express MET receptors; its antitumor activity was demonstrated in a panel of HCC cell lines and also in murine xenograft models[182]. *Tivantinib* may provide an option for second-line treatment in patients affected by advanced HCC with well-compensated cirrhosis, especially in case of tumors expressing high level of MET. MET overexpression is associated with poor prognosis in HCC patients. *Tivantinib* demonstrated a manageable safety profile and preliminary antitumor activity in patients with advanced HCC[4]. Further studies of *Tivantinib* in a biomarker-selected patient population are warranted and the enrollment for this phase III clinical trial is started[142].

Bevacizumab is a recombinant, humanized monoclonal antibody that targets VEGF and it is one of the main drugs for the treatment of colorectal cancer[183]. In addition to inhibiting tumor growth, growth factor release, and metastasis, *Bevacizumab* can enhance chemotherapeutic agent delivery by normalizing tumor vessels.

Brivanib, a selective inhibitor of FGF and VEGF signaling, has recently been shown to act as a first-line treatment for patients with advanced HCC[184]. In a phase II open-label study published in 2012, *Brivanib* was considered as a second-line therapy in patients with advanced HCC who had not been successfully treated with prior anti-angiogenic molecules[185]. It has been demonstrated that *Brivanib* has a manageable safety profile and it is one of the first agents that shows promising antitumor activity in advanced HCC patients previously treated with *Sorafenib*. Nevertheless, recent data shows that patients treated with *Brivanib* don't reach the primary endpoint of overall survival both in first- and second-line therapy [185]. In 2013 in a multicenter, double blind, randomized, placebo-controlled trial, Llovet and colleagues evaluated *Brivanib* in patients with advanced HCC, who were intolerant to *Sorafenib* or for which *Sorafenib* failed [186]. 395 patients with advanced HCC were randomly assigned (2:1) to receive *Brivanib* 800 mg orally once per day plus best supportive care (BSC) or placebo plus BSC. The authors shown that the median overall survival was 9.4 months for *Brivanib* and 8.2 months for placebo (HR = 0.89; 95.8% CI, 0.69 to 1.15; P=0.3307) whereas the median time to progression was 4.2 months for *Brivanib* and 2.7 months for placebo [186]. Study discontinuation associated with treatment-related adverse events (AEs) occurred in 61 patients (23%) treated with *Brivanib* and in 9 patients who received placebo (7%). The most frequent treatment-related grade 3 to 4 AEs for *Brivanib* included hypertension (17%), fatigue

(13%), hyponatremia (11%), and decreased appetite (10%). In conclusion, in patients with HCC who had been treated with *Sorafenib*, *Brivanib* didn't significantly improve OS. The observed benefit in time to progression warrants further investigation [186]. Currently, two large phase III studies of *Brivanib* in HCC are underway, the BRISK-FL study in first-line therapy and the BRISK-PS study in patients whose disease progressed on or which were intolerant to *Sorafenib*[4].

In addition to these drugs, *Cabozantinib* acts as a dual c-Met/VEGFR2 inhibitor, targeting the tyrosine kinase activity of RET, MET, VEGFR-1, VEGFR-2, VEGFR-3, KIT, TRKB, FLT-3, AXL, and TIE-2. A study proposed in 2012 demonstrated evidence of antitumor activity in a randomized discontinuation phase II trial. Interestingly, the clinical benefits were observed regardless of whether patients had received prior *Sorafenib* treatment[187]. *Cabozantinib* is currently undergoing additional evaluation in HCC to better valuate its efficacy and safety profile in several ongoing clinical trials. Phase III studies should evaluate the effectiveness and tolerability of *Cabozantinib* versus placebo and the overall survival in patients with advanced HCC who have already been treated[4].

Everolimus acts as an inhibitor of mTOR. In a phase III study, *Everolimus* was given to patients with advanced HCC, which progressed during or after *Sorafenib* treatment[188]. Patients aged ≥ 18 years and staged BCLC B or C with preserved liver function whose disease progressed during or after *Sorafenib* treatment or who were *Sorafenib* intolerant, were randomized (2:1) to *Everolimus* 7.5 mg once per day or placebo. 546 patients were enrolled from 18 different countries. 362 patients were treated with *Everolimus* whereas 184 patients took placebo. Randomized patients were stratified by region (Asia versus rest of world) and macro-vascular invasion (yes versus no). The drug was given continuously until disease progression or intolerable toxicity. Median overall survival was 7.56 mo in patients treated with *Everolimus* and 7.33 mo in patients treated with placebo (HR 1.05; 95% CI 0.86–1.27; P = 0.675); the median time to progression was 2.96 mo and 2.60 mo, respectively (HR 0.93; 95% CI 0.75–1.15). The most common side effects in patients treated with *Everolimus* (Vs placebo) were anemia (7.8% v 3.3%), asthenia (7.8% v 5.5%), decreased appetite (6.1% v 0.5%), and hepatitis B viral load increase or reappearance (6.1% v 4.4%). Unfortunately, *Everolimus* didn't improve overall survival in patients with advanced HCC whose disease progressed on or after *Sorafenib* or which were *Sorafenib* intolerant[188].

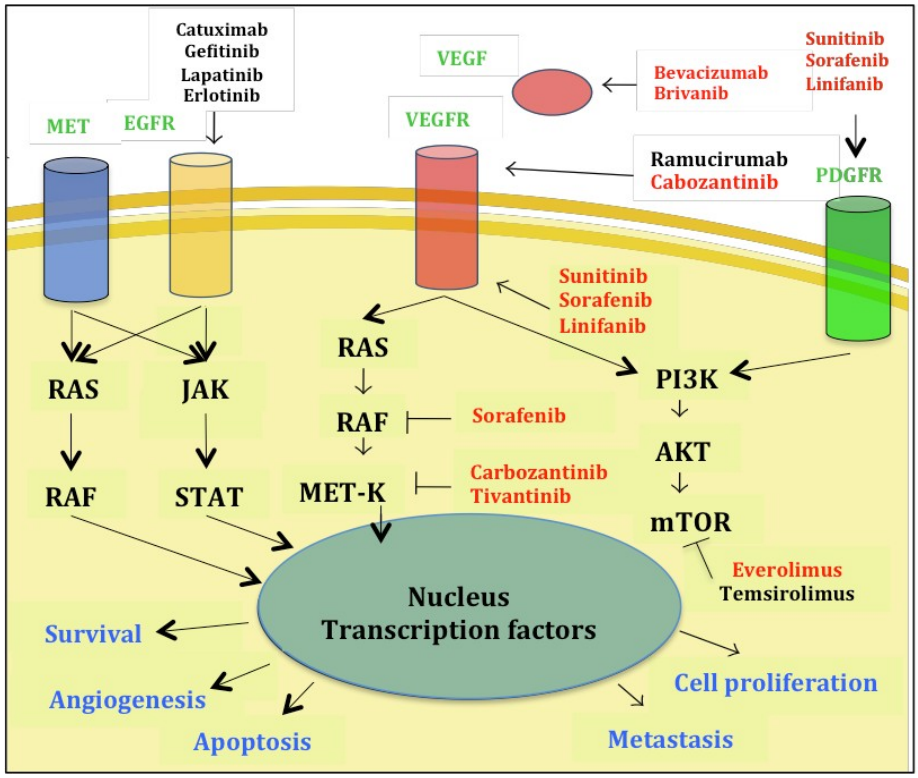

Fig. 1.8 - Molecular action sites of active biochemical agents in HCC treatment.

1.3.4.3 Novel therapeutic approaches: treatment with de-methylating agents

Studies published in the last few years have shown that epigenetic alterations play a pivotal role in cell cancer genome and consequently in tumor biology. In addition, the potential reversibility of epigenetic modifications has led to the development of new therapeutic strategies known as *pharmaco-epigenomics*[189-191]. Therefore, in the last years, several agents have been identified as capable of reversing aberrant epigenetic changes in tumor cells and thus restoring the canonical epigenetic phenotype [192]. In the context of pharmaco-epigenomic approaches, the development of compounds able to inhibit epigenetic processes, including DNA methylation and histone de-acetylation, was associated with the reversal of the epigenetically induced silencing of tumor suppressor genes thus resulting in their concomitant reactivation[193,194].

Drugs that inhibit DNA methylation were discovered in the 1960s and tested in clinical trials in the 1970s[195]. This DNA hypomethylating property is limited to cytosine analogs with 5' modifications of the rings [9]. Among de-methylating agents, the most studied are *5-azacytidine* (Vidaza; 5-aza-CR) and *5-aza-2'-deoxycytidine* (Decitabine; 5-aza-CdR), both of which have shown to de-methylate and restore the function of tumor suppressor

genes[189,196] (Fig. 1.9). Both drugs have been approved by the US FDA for the treatment of myelodysplastic syndrome as well as acute and chronic myeloid leukemia[9].

5-azacytidine and *5-aza-2'-deoxycytidine* are incorporated into DNA where they bind irreversibly DNMTs targeting these enzymes to degradation[197]. In the absence of DNTMs, DNA synthesis results in hypomethylation in the daughter cells and eventually to reactivation of silenced gene expression. Several other 5-modified nucleoside analogs have been described (Fig. 1.9) either in preclinical studies or in early stage clinical trials[198].

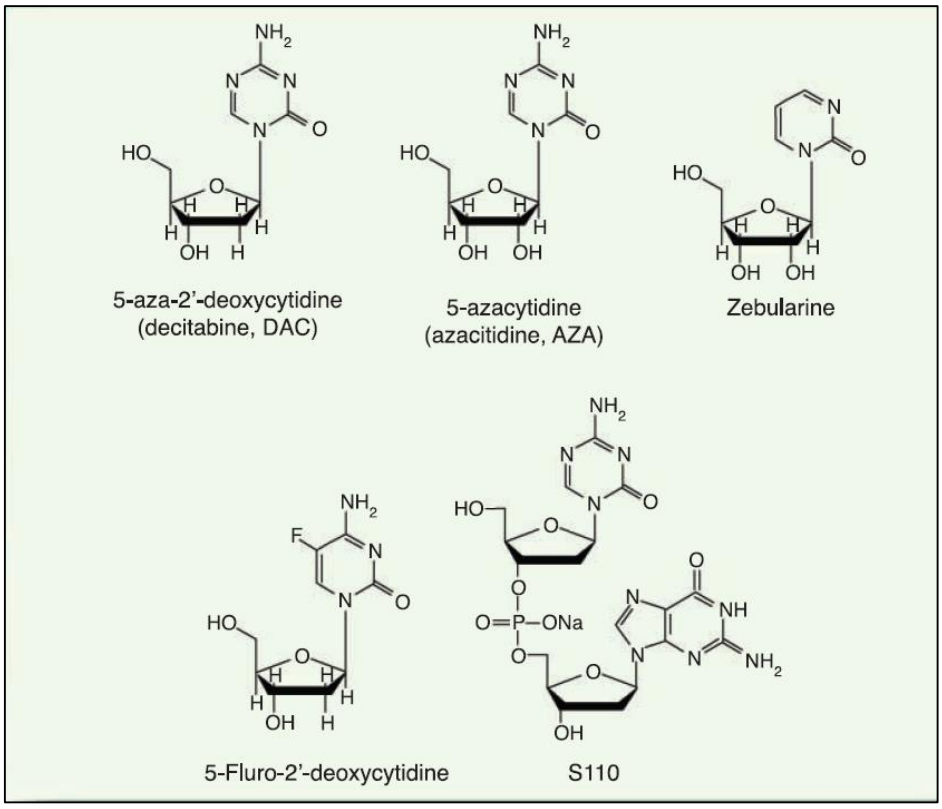

Fig 1.9 – Chemical structure of nucleoside inhibitors of DNA methylation. 5-aza-CR and 5-aza-CdR are the only FDA approved for the treatment of myelodysplastic syndrome[9].

5-azacytidine and *5-aza-2'-deoxycytidine* are efficiently incorporated into cells by specialized transporters, following which their metabolism change. They are phosphorylated by different enzymes to 5-aza-CTP, which is incorporated into RNA molecules and to 5-aza-dCTP, which is incorporated into DNA. A fraction of 5-aza-CDP is also converted to 5-aza-dCDP. Once incorporated into DNA, 5-aza-dCTP forms irreversible covalent bonds with DNMTs, resulting in inhibition of DNA synthesis due to formation of bulky DNA-protein complexes. At high doses, this results in cytotoxic cell death whereas at lower doses, the

complexes are excised and degraded by the proteasome. DNA is repaired, and DNA synthesis restarts in the absence of DNMTs, resulting in hypomethylation of newly synthesized DNA [9] (Fig. 1.10).

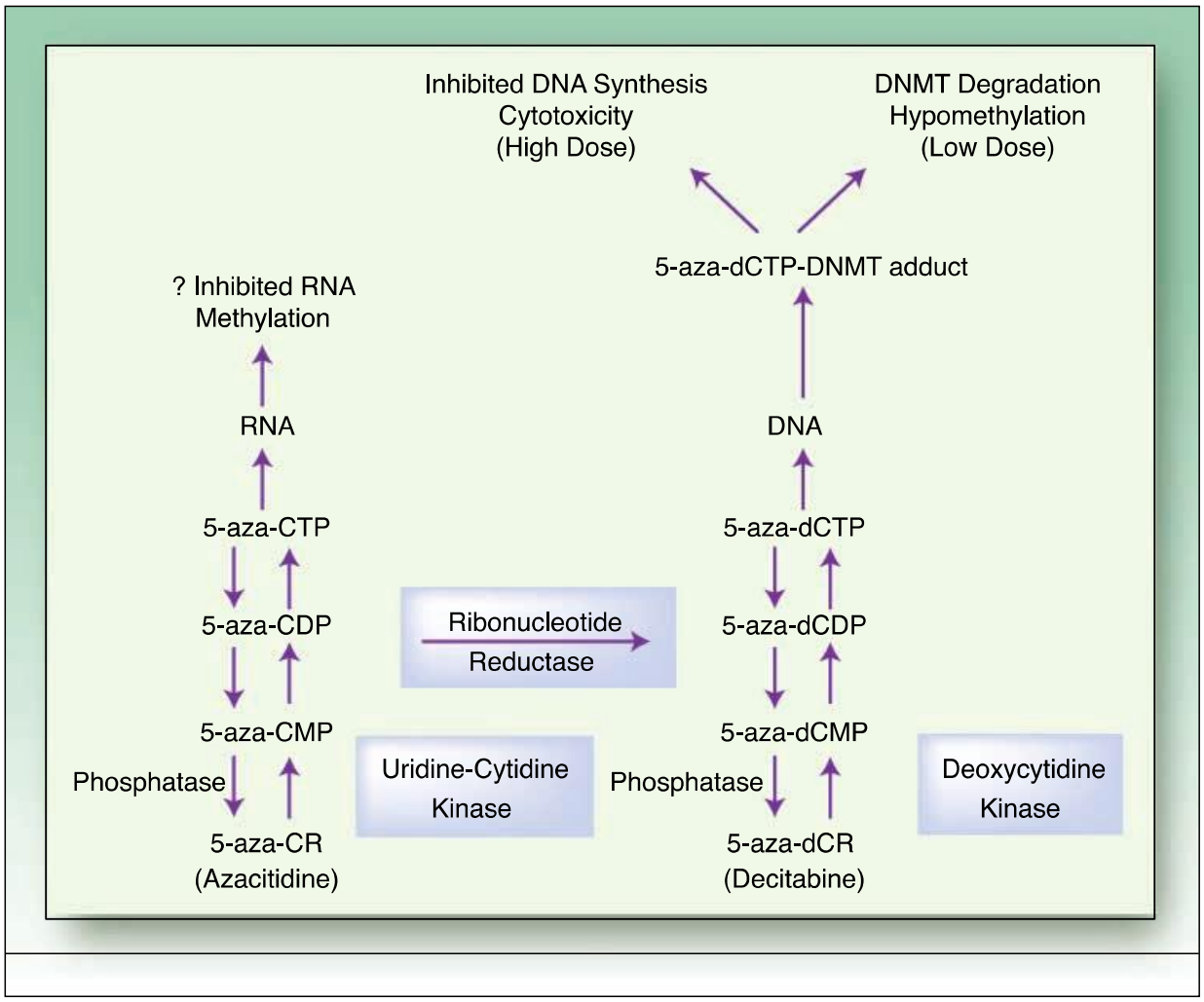

It is important to underline that while inhibiting DNA methylation is a molecularly defined targeted therapy approach, the downstream effects on neoplastic behavior are quite nonspecific[9] (Fig. 1.11). The irreversible covalent bonds of DNMTs with DNA create bulky complexes that can inhibit DNA synthesis and eventually result in cell death by cytotoxicity[199]. In fact, *in vitro* experiments showed that optimal low doses induce hypomethylation, promoting reactivation of genes involved in multiple pathways [190] . Among these, senescence (via P16 activation), apoptosis (via activation of pro-apoptotic genes), stem cell renewal (by abrogating self-renewal signals), invasion (by upregulating inhibitors of motility) and angiogenesis (through angiogenesis inhibitors such as THBS1)[9].

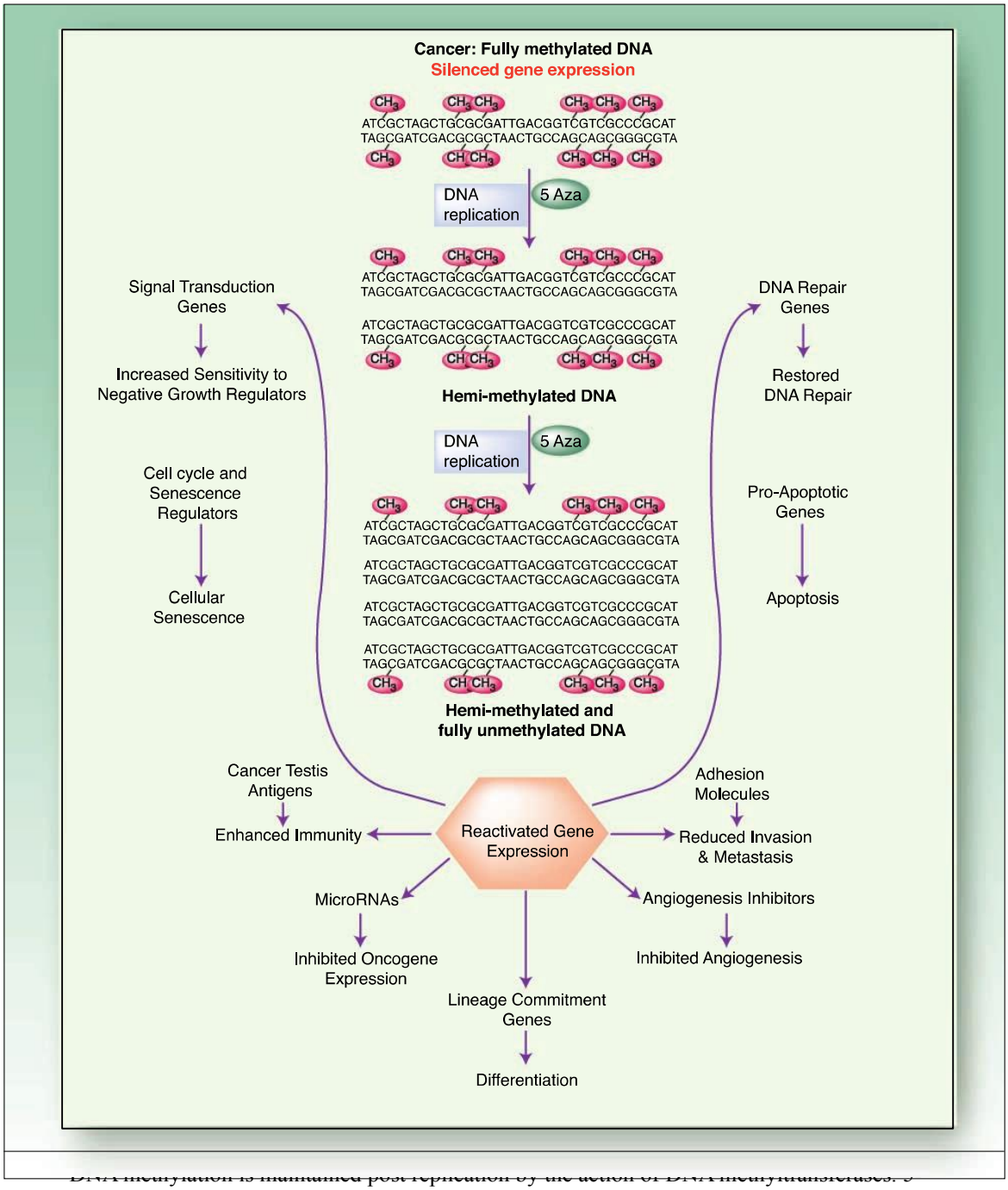

DNA methylation is maintained post-replication by the action of DNA methyltransferases. 5-aza-CR and 5-aza-CdR lead to degradation of the main DNA methyltransferases, and continued replication results in passive demethylation that results in reactivated gene expression, which has effects on multiple different pathways, each of which could contribute to a clinical response[9].

Given the promiscuity of hypermethylation in cancer, it is fair to mention the possibility that hypomethylation can activate those rare oncogenes known to be silenced in cancer (e.g., COX2, EGFR, etc.) [9]. Moreover, there could be the possibility of inducing hypo-methylation in normal cells, adjacent to cancer cells, by inhibiting DNMTs, resulting in the concomitant re-activation of otherwise silenced oncogenes and further in carcinogenesis [200,201]. However, such de-methylating drugs have been shown to act predominantly in rapidly

dividing cancer cells, without any significant effect on normal non-dividing cells[190,192].

1.3.4.4 The use of de-methylating drugs in HCC

Studies published several years ago supported that *5-azacytidine* and *5-aza-2'-deoxycytidine* were not particularly efficient for the treatment of solid tumors [189,202]. A recent study, published in 2011, has indicated that *5-azacytidine* (Vidaza) was actually able to inducing apoptosis in various HCC cell lines by epigenetically reversing the malignant phenotype and also by sensitizing hepatoma cells to TRAIL-induced apoptotic death [203]. Moreover, a Decitabine-modified compound called *2'- deoxy-N4[2-(4-nitrophenyl)ethoxycarbonyl]-5-azacytidine* has shown promising results in inhibiting HCC formation when compared to Decitabine. [204] Specifically, this Decitabine-modified compound is able to reduce global methylation levels in human hepatoma cell lines (HepG2 and Hep3B) and to activate critical tumor suppressor genes. Many studies have also demonstrated *5-azacytidine* and *5-aza-2'-deoxycytidine* roles in unmasking aberrantly methylated tumor suppressor genes which are being silenced in HCC [205,206]. Interestingly, the treatment of various human cell lines with *Zebularine*, another cytosine analogs, resulted in the re-activation of several tumor suppressor genes, including RASSF1A, MST1, p38JNK, caspase-3, SOCS1-3 and SHP1, thus promoting apoptotic cell death and cell growth inhibition[207]. Moreover, it has been also demonstrated that *Zebularine* decreases DNMT1, DNMT3a and DNMT3b levels in the hepatoma cell line HepG2. Through this property, this drug can adjust the expression of several proteins, including p21, Rb PKR, Bcl-2, and MAPK pathway, performing its anti-proliferative and anti-apoptotic effects[208]. In another study published by Andersen and colleagues in 2010, the authors identified a Zebularine-based signature useful in classifying liver cancer cells based on their different drug-response profile whereas drug-sensitive cells exhibited elevated rates of apoptosis, characterized by the upregulation of oncogenic proteins such as E2F1, TNF and MYC. Additionally, Zebularine-based therapy given to xenograft animal models of HCC also showed potent anti-tumor activity[189,209]. In conclusion, Zebularine responsive genes and associated de-methylation signatures were identified as predictors of clinical outcome in HCC patients undergoing epigenetic therapy[189].

A non-nucleoside analog with de-methylating property called *SGI-1027* has been used in some human cancer cell lines to try to reactivate tumor suppressor genes like p16, MLH1 and TIMP3 in RKO human colon carcinoma cell line and to inhibit DNMT1 in Hep3B human hepatoma cell line[210]. Finally, another de-methylating compound with local anesthetic property called *Procaine* was shown to have anti-tumor activity in various HCC cell lines,

including HLE, HuH7 and HuH6, as well as in rodent xenograft model of HCC. Particularly, when *Procaine* was administered in combination with *Trichostatin A*, a histone de-acetylase inhibitor, cell viability decreased in a dose- and time-dependent manner while having no effect on primary hepatocytes. Moreover, *Procaine* inhibited the S/G2/M transition in HLE cell line and restored the expression of several genes such as 16INK4A, HAI-2/PB and 14-3-3δ. The authors observed the same evidences in rodent xenografts of HLE cells, after treatment with high doses of *Procaine*, indicating that this compound could be used in the treatment of HCC[211].

1.4 MicroRNA

MicroRNAs or miRNA are small non-coding RNA molecules containing about 22 nucleotides. MiRNA are found in plants, animals, and some viruses and are involved in RNA silencing and post-transcriptional regulation of gene expression[212].

Encoded by eukaryotic nuclear DNA in plants and animals, miRNAs function via base-pairing with complementary sequences within mRNA molecules resulting in mRNA silencing by one or more of the following processes[213]: cleavage of the mRNA strand into two shorter RNA sequences, destabilization of the mRNA target through shortening of its poly(A) tail, and less efficient translation of mRNA into proteins by ribosomes[214]. MiRNAs derive from regions of RNA transcripts that fold back on themselves to form short hairpins, [215]. The human genome may encode over 1000 miRNAs[216], which are abundant in many mammalian cell types[217] and appear to target about 60% of the genes of humans and other mammals. MiRNAs are well conserved both in plants and in animals. A given miRNA may have hundreds of different mRNA targets, and a given RNA target might be regulated by multiple miRNAs[218].

The first miRNA was discovered in the early 1990s [219]. Nevertheless, microRNA were not recognized as a distinct class of biological regulators until the early 2000s. Since then, miRNA research has revealed different sets of miRNAs expressed in different cell types and tissues[217] with multiple roles in plant and animal development and in many other biological processes including proliferation, differentiation and cells death[220,221]. Aberrant miRNA expression has been implicated in a lot of cellular processes and diseases and miRNA-based therapies are currently under development.

1.4.1 MicroRNA biogenesis

The biogenesis of miRNAs requires a multistep process that begins in the nucleus where RNA polymerase II or III, after binding to the promoter, transcribes a long primary transcript called *pri-miRNA* (Fig. 1.12). This *pri-miRNA* is approximately 1-4 kb long and has a poly(A) tail and a 5'-cap [222]. After that, the microprocessor complex consisting of *Drosha*, an RNase III endonuclease, *DGCR8* and other associated proteins processes the pri-miRNA into approximately 70-nucleotide hairpin-like miRNA precursor called *pre-miRNA*[223]. The *pre-miRNA* is then transported from nucleus to cytoplasm thought *Exportin 5*, which specifically recognizes and binds pre-miRNA. In the cytoplasm, the pre-miRNA is then cleaved by an RNase III endonuclease called *Dicer* into a 20-24 base long dsRNA, which contains both the mature miRNA strand and its complementary strand. This duplex is then separated by helicases, generating a mature ssRNA which is incorporated into the RISC complex to be driven to the target mRNA[224]. Due to the complementarity with its target sequence, the interaction between microRNA and mRNAs typically induces either translation repression, when the complementarity microRNA-mRNA is imperfect, or mRNA degradation, when the mature microRNA binds its target RNA with a perfect complementarity[222]. MicroRNAs regulate mRNA by interacting with their 5'-end and 3'-UTR, although it has recently suggested that microRNA target sites may be located in the 5'-UTR or even at simultaneous 5'- and 3'-UTR interaction sites[225].

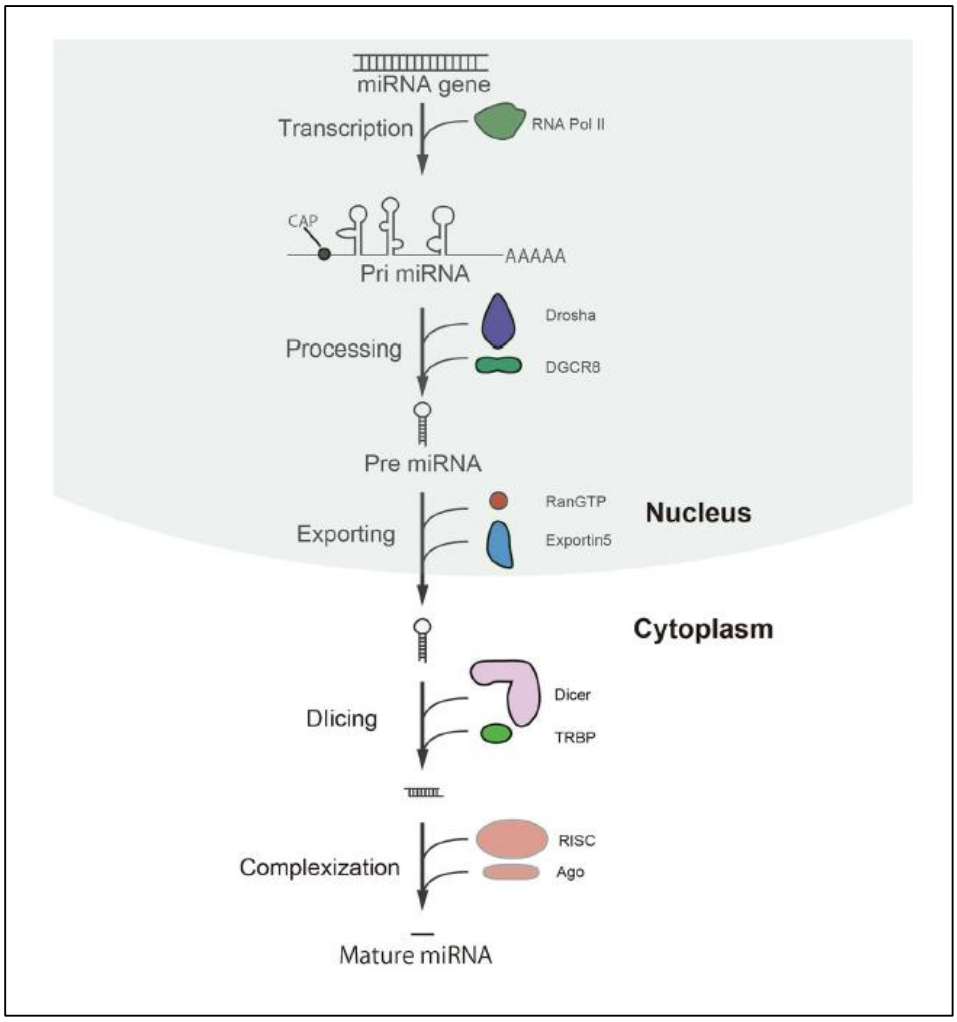

Fig 1.12 – Schematic illustration of miRNA biogenesis[222].

1.4.2 MicroRNA and cancer

Although microRNA are able to negatively regulate the expression of target mRNAs, their expression is also regulated by different mechanisms including translational regulation, methylation and histone de-acetylation, DNA copy alteration and gene mutations affecting proteins involving in processing and maturation [10]. Moreover, literature has been reported that more than 50% of microRNA genes are usually located in the fragile sites of chromosomes or in genomic regions, which often undergo deletions, amplifications and mutations [226]. It is well known that the aberrant expression of many microRNAs is closely related both to the etiology and to clinical outcome of several human cancers, including HCC [10]. MicroRNAs involved in carcinogenesis can be divided into two groups. The first is the so-called *oncomirs* group, in which microRNA act like oncogenes and are able to promote tumor development through the negative regulation of tumor suppressor genes. The second group represents the *anti-oncomirs*, which are tumor suppressor microRNA and are able to inhibit tumor growth by

targeting oncogenes[226]. For this reason, oncomirs are usually upregulated in tumor cells whereas anti-oncomirs are usually downregulated. Currently, in HCC it has been identified a pool of de-regulated microRNA, which are involved in HCC development and progression[10,102].

1.4.2.1 Up-regulated microRNA in HCC

MicroRNA 21 is the most commonly up-regulated miRNA in several human cancers including HCC[227]. This microRNA is one of the most studied microRNAs in HCC because it promotes cell proliferation and migration [10]. *In vitro* studies have shown that microRNA 21 levels are increased in HCC tissues and cell lines, leading to inhibition of some tumor suppressor genes, including pTEN[228], RHOB[229] and PDCD4[230]. Meng et al. demonstrated that the overexpression of microRNA 21 could contribute to HCC growth by modulating its downstream mediators and MMP2 and MMP9 expression, promoting cell proliferation, migration and invasion[228]. Moreover, Bao et al. demonstrated that microRNA 21-mediated suppression of both hSulf-1 and pTEN activated AKT/ERK pathways and EMT in HCC cells, enhanced cell proliferation and migration and promoted tumor growth in HCC xenograft mice models[231]. It is also known that microRNA 21 directly targets MAP2K3, a putative tumor suppressor gene, and inhibits its expression, at both transcriptional and post-transcriptional levels, mainly during HCC carcinogenesis[232]. Tomimaru et al. demonstrated also that microRNA 21 could be involved in the modulation of IFN- α/5-FU response, favoring clinical response and survival[233]. Furthermore, recent studies suggest that microRNA 21 overexpression can be effectively predictive of a worse prognosis in patients with various cancers[234] and it may play a key role in the regulation of anticancer drug sensitivity and resistance[235]. Serum levels of microRNA 21 have also been found to progressively increase from chronic hepatitis to cirrhosis and HCC[10] (Fig. 1.13).

Another important up-regulated microRNA in HCC is *microRNA 221*, which is implicated in hepatocarcinogenesis through different mechanisms. MicroRNA 221 can reduce the expression levels of the anti-proliferative genes CDKN1B/p27 and CDKN1C/p57 leading to an increased tumor cell proliferation[236]. In a study published in 2009, Gramantieri et al. demonstrated also that the over-expression of micron 221 leaded to a down-regulation of *Bmf*, a known inducer of Caspase-3, thus reducing the process of apoptosis in tumor cells [237]. The authors concluded that this microRNA inversely correlates with patient prognosis and reduces the time of recurrences. It is also known that miR-221 targets both DDIT4, a modulator of mTOR, and p27, a cell cycle inhibitor which is associated to tumor stage and metastasis

formation[238]. Another way by which miR-221 overexpression can promote hepatocarcinogenesis is through the stimulation of angiogenetic factors, including CXCL16[239]. Moreover other mechanistic analysis demonstrated that both PTEN and TIMP3 were targeted by miR-221 and these events confer metastatic properties to HCC cells[240]. There are evidences that miR-221 overexpression accelerates the growth of tumorigenic murine hepatic progenitor cells in murine HC, reducing their mean time to death[241]. The silencing of miR-221 using *lentivirus* technique can significantly reduce the growth of the hepatoma xenografts in nude mice[242] (Fig. 1.13).

A recent study published in 2013 demonstrated that also *miR-9* has a key role in the HCC metastatic process[243]. The authors demonstrated that miR-9 was overexpressed in many cell line including Hep12 and once transfected in cells with low metastatic potential, such as HepG2 and SMMC7721, they acquired high invasive properties [243]. A putative target of this microRNA is the mRNA of KLF17 gene, which negatively regulates both the EMT and metastasis formation[10]. It has been demonstrated that the expression levels of KLF17 decrease when miR-9 is overexpressed. Moreover, miR-9 can promote tumor aggressiveness and cell migration inhibiting the production of E-cadherin [244]. The up-regulation of miR-9 in HCC cancer tissue is significantly correlated with aggressive clinic-pathological features and higher tumor staging and risk[245] (Fig. 1.13).

Another microRNA involved in the processes of invasiveness and migration is *miR-224*. During hepatocarcinogenesis, it inhibits apoptosis by blocking API-5[246]. It can also stimulate some targets including PAK4 and MMP9, which increase migration and tumor progression in HepG2 cells [247]. MiRNA-224 can also promote cell proliferation by targeting SMAD4 and this is associated with lower patient survival[248]. A recent study published in 2015 reported that HCC patients with high microRNA 224 serum level showed shorter survival than those with low microRNA 224 serum level. Moreover, serum microRNA 224 concentration reflects tumor stage and liver damage and the coexistence of high microRNA 224 level and pAKT overexpression may represent a potential indicator for poor prognosis in HCC patients[249] (Fig. 1.13).

1.4.2.2 Down-regulated micro RNA in HCC

microRNA 122 is the most abundant miRNA in the liver [250] and it is probably the most important microRNA involved in the process of hepatocarcinogenesis. It is involved in migration, cell invasion and tumor growth through different biomolecular mechanisms[10]. MicroRNA 122 expression can be regulated by liver-enriched transcriptional factors,

including HNF-1α, HNF-3β, HNF-4α, HNF-6 and C/EBP-α[251]. The suppression of microRNA 122 is due to an epigenetic modulation of its expression and its deregulation seems to be involved in many liver diseases [252]. MicroRNA 122-deficent mice develop steatohepatitis and fibrosis [253] and microRNA 122 can also directly interact with HCV genome. The interaction between HCV RNA and microRNA 122, resulting in a heterotrimeric stable structure, enhances HCV translation and protects HCV RNA from degradation[254]. microRNA 122 can also down-regulate HBV replication by targeting sequences located at the coding region of the mRNA for viral polymerase and the 3'-UTR region of the mRNA for core protein of HBV genome via base-paring interactions [255]. Several comparative studies have demonstrated that microRNA 122 is down regulated in HCC tissue compared with adjacent normal tissue and this lower expression in HCC tissue is associated with metastasis and poor prognosis[251]. One of the most important mechanisms by which microRNA 122 acts is the modulation of cancer cell proliferation through cyclin G1 expression. In 2009, Fornari et al. showed that the down-regulation of microRNA 122 up-regulates the level of cyclin G1, promoting cell growth, and down-regulates p53 expression[256]. A recent study published in 2014 showed that HNF-4 α/microRNA 122 controls the hepatocyte epithelial phenotype through modulating RhoA/Rock pathway, suggesting that the loss of microRNA 122 in HCC promotes cancer invasion and metastasis with EMT[257]. Moreover, low levels of microRNA 122 promote overexpression of disintegrin and metalloproteinase as ADAM17[258] and ADAM10[259] that increase migration. A study published by Bai et al. in 2009 demonstrated that cell growth and survival of HCC cells expressing microRNA 122 were significantly reduced upon treatment with *Sorafenib*, a multi-kinase inhibitor, which is actually approved for the treatment of HCC patients[259]. Koberle et al. reported that circulating microRNA 122 levels are positively correlated with liver transaminases and negatively with the Model for End-Stage Liver Disease scores, suggesting that serum microRNA 122 may be a novel biomarker for liver injury[260] (Fig. 1.13).

MicroRNA 34a can inhibit tumor proliferation by different mechanisms. For example, it can decrease the expression of HGFR, reducing phosphorylation of ERK1 and ERK2, which inhibit cell proliferation[261]. miR-34a can also reduce the expression of MACF1 and TPM4, inhibiting the G1 phase of cell cycle thus blocking Lamin A/C, a microtubule actin cross-linking factor, α-tubulin chain 1B and Glial fibrillary acidic protein [10]. MicroRNA 34a seems also able to reduce the expression levels of both CDK6 and CyclinD1, two important cell cycle regulators [262], and Bcl-2, a regulator of apoptosis [263]. In 2012 Yang et al. explained how HBV chronic infection increases TGF-β levels, which reduces microRNA 34a

expression. This stimulates the expression of CCL22, which is a chemokine able to stimulate T regulatory cells and enhance the immune escape. Consequently, the colonization and dissemination of HCC cells are also supported[135]. It is also known that serum levels of microRNA 34a are more elevated in patients with chronic hepatitis C infections than in controls and this is related to the degree of fibrosis [264]. Recently, Xu et al. has published that miR-34a promotes cellular senescence through the negative modulation of telomere pathway in HCC. In fact, this microRNA targets c-Myc and FoxM1, two proteins involved in the activation of hTERT transcription[265] (Fig. 1.13).

Another microRNA significantly down regulated in HCC is *microRNA 101*, which is a antionco-microRNA displaying suppressive effects on cell proliferation, migration and invasion[222]. This microRNA inhibits cell proliferation through the inhibition of three proteins EZH2, c-myc and MCL-1 involved in the apoptotic process [10]. It has been demonstrated that the restoration of microRNA 101 expression inhibits invasion and migration of cultured HCC cells, suggesting that microRNA 101 may play an important role in HCC progression[222]. MicroRNA 101 could exert its pro-apoptotic functions by targeting Bcl-2 and Mcl-1, two anti-apoptotic proteins. MicroRNA 101 significantly repressed Mcl-1 translation and reduced the endogenous protein levels of Mcl-1, whereas the inhibition of microRNA 101 up-regulated Mcl-1 expression and inhibited cell apoptosis [266]. Recently, it was reported that the overexpression of microRNA 101 by lentivirus-mediated systemic delivery, strongly inhibits HCC *in vivo* by repressing many molecular targets, including COX2 and ROCK2, and blocking angiogenesis and EMT of HCC cells[267]. Moreover, the down regulation of microRNA 101 in HCC tissues correlates with tumor aggressiveness and poor prognosis. The expression of serum microRNA 101 in patients with HBV-related HCC was significantly increased compared to healthy controls. This increase was associated with the presence of hepatitis B surface antigens, HBV DNA levels and tumor size[10,268] (Fig. 1.13).

MicroRNA 195 appears to be reduced both at tissue and serum level [10]. In HCC, the reduced levels of this microRNA lead to the loss of suppression of Cyclin D1, CDK6 and E2F3 resulting in pRB phosphorylation. These events include an increase in E2F levels with a higher number of cells in G1/S phase of cell cycle [10,269]. A recent study suggests that serum levels of this miRNA could be useful for differential diagnosis between hepatitis and HCC (Fig. 1.13).

Another important miRNA family frequently down regulated in HCC is *microRNA 200 family*, which consists of two coding clusters microRNA 200b/a/429 and microRNA 200c/141. This miRNA family is an important regulator of EMT and has been implicated in

human carcinogenesis. The zinc finger transcription factors ZEB1 and ZEB2 control the expression of the primary microRNA 200 for both coding cluster[270]. Conversely, ZEB1/2 regulates EMT *via* microRNA 200 family members, where microRNA 200 family members suppress ZEB1/2 production by binding to its 3'-UTR [222]. The ZEB1/2-microRNA 200 feedback loop regulates an EMT signaling axis that may be crucial to tumor progression [271]. MicroRNA 200 family seems to be important for cells migration. A recent study published in 2013 demonstrated that microRNA 200c and microRNA 200b are involved in cell migration through the regulation of E-cadherin and its target ZEB1/2 expression [272]. Moreover, studying the microRNA expression profiles, Dhayat et al. demonstrated that microRNA 200a and microRNA 200b are able to distinguish between cirrhotic and HCC tissue and they can be used as early markers for cirrhosis-associated HCC [273]. Although all members of microRNA 200 family can inhibit ZEB1/2 expression in HCC cell lines, microRNA 200a/141 and microRNA 200b/200c/429 subfamilies participate differently in cancer progression because they down regulate different targets. Wong et al., showed that the microRNA 200b/200c/429 subfamily, but not the microRNA 200a/141 subfamily, inhibited HCC migration modulating the Rho/ROCK-mediated cell cytoskeletal reorganization[274]. In 2014, Lin et al. confirmed that in HepG2 cell line microRNA 141 directly regulates the expression of HNF-3β, which is critical for hepatocyte differentiation and controlling liver-specific gene expression in HCC. The down regulation of HNF-3β by microRNA 141 inhibits cell proliferation and invasion and promotes apoptosis of HepG2 cells[275] (Fig. 1.13).

The *let-7* miRNA family, which consists of 13 members, plays pivotal role in tumorigenesis by acting as a tumor suppressor microRNA. Recently, several studies have demonstrated the role of let-7 in HCC development and progression. Using microarray analysis, Shimizu et al. have found that microRNA let-7c and let-7g promote apoptosis by targeting Bcl-XL, an anti-apoptotic member of the Bcl-2 family, in HCC. This indicates that the restoration of let-7 expression may be a useful therapeutic option for HCC when let-7 expression is absent[276] (Fig. 1.13).

MicroRNA 139-5p is another important downregulated microRNA in HCC. It has been demonstrated that its expression level inversely correlates with HCC metastatic capacity and directly correlates with prognosis[277]. MicroRNA 139-5p negatively regulates ROCK2 protein, a downstream effector of Rho that plays an important role in the tumorigenesis and progression of HCC[278]. ROCK2 increases MMP2 levels, which directly correlated with HCC tumour size, metastasis formation and tumour staging [278,279]. MicroRNA 139-5p is also associated with intestinal inflammation and colorectal cancer development. It has been

demonstrated that miR-139-5p knockout (KO) mice are highly susceptible to colitis and colon cancer, accompanied by elevated proliferation and decreased apoptosis, as well as increased production of inflammatory cytokines, chemokines, and tumorigenic factors. Furthermore, enhanced colon inflammation and colorectal tumor development in miR-139-5p KO mice are due to the regulatory effects of miR-139-5p on its target genes Rap1b and NF-κB, thus affecting the activity of MAPK, NF-κB, and STAT3 signaling pathways[280]. MicroRNA 139-5p was significantly down-regulated also in primary tumor tissues of non-small cell lung cancer (NSCLC) and very low levels were found in NSCLC cell lines. Probably, it promoted apoptosis by acting on Caspase 3 and inhibited cell migration by acting on MMP9 and MMP7. Further, oncogene c-Met was revealed to be a putative target of microRNA 139-5p, which was inversely correlated with microRNA 139-5p expression in NSCLC[281] (Fig. 1.13).

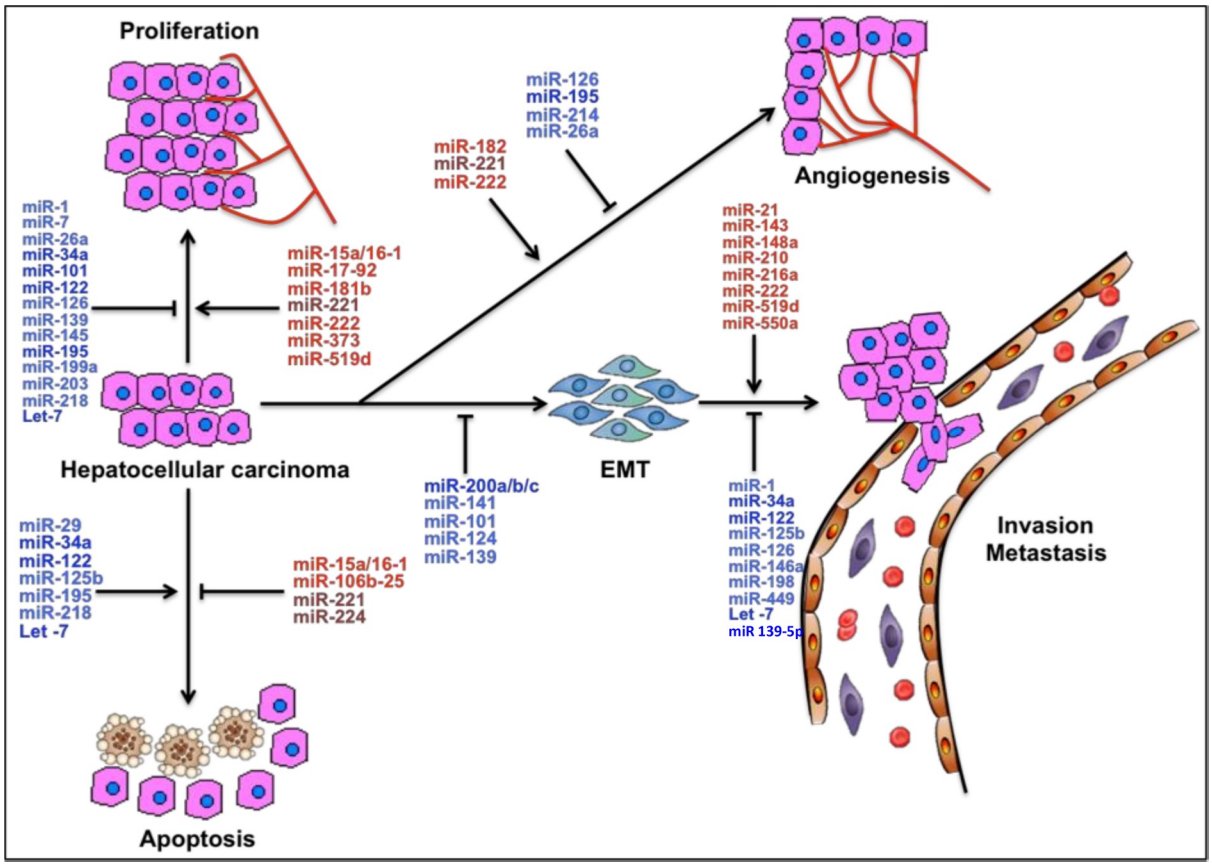

Fig 1.13 – Deregulated microRNA involved in HCC development. In red are indicated the up-regulated microRNA whereas in blue the downregulated microRNAs. EMT = Endothelial-Mesenchymal Transition [222].

2. Aims of the study

Given the modest efficacy of the available therapeutic options for HCC, we tested the effectiveness of 5-azacytidine as a potential novel drug. The effects of 5-azacytidine were evaluated at the phenotypic and molecular level both in cultured HCC cell lines and in a murine subcutaneous xenograft model of HCC. In particular, we analysed the phenotypic effects on cell vitality, proliferation/death, cytoskeleton organization, cell proliferation and migration. At the molecular level we mainly concentrated on the effects 5-azacytidine exerts on miR139-5p/ROCK2/MMP2, a pathway strictly correlated with HCC.

3. Materials and Methods

3.1 Cell cultures

The cell lines using as *in vitro* HCC model are JHH6 and HUH7. These cell lines reflect different phenotypes because HuH7 and JHH6 are assigned to high and medium hepatic differentiation grade respectively on the base of their capacity to synthesize albumin, a well-known marker of hepatic differentiation [282]. HuH7 and JHH6 cell lines derives from a differentiated and undifferentiated hepatoma respectively [283]. Despite the almost undetectable albumin production, JHH6 are able to synthesize ferritin, thus showing a residual hepatic phenotype[284]. As controls, we used both a human hepatocyte cell line called *IHH* and also human hepatocyte-like cells obtained differentiating human embryonic stem cells (hESCs). IHH are hepatocytes immortalized by stabile transfection with a recombinant plasmid containing the early region of SV40 virus. IHH cells retain several differentiated features of normal hepatocyte. Indeed, they display albumin secretion at a level comparable to cultured primary human hepatocytes (30μg/ml per day), besides producing triglyceride (TG)-rich lipoproteins, apolipoprotein B (0.6μg/ml per day), and apolipoprotein A-I (1 μg/ml per day)[285]. Furthermore, IHH cells are polarized forming bile canaliculi-like vacuoles where accumulate exogenous organic anions[285].

JHH6 cell line was cultured in William's Medium (Sigma-Aldrich), whereas HuH7 cell line was grown in DMEM High Glucose Medium (Euroclone). IHH cell line was cultured in Ham's Nutrient Mixture-F12 (Euroclone). All media were supplemented with 10% heat inactivated Fetal Bovin Serum (FBS) (Euroclone, Gibco), 100U/ml penicillin, 100 μg/ml streptomycin and 20mM L-glutamine (Euroclone). In Ham's Nutrient Mixture-F12 medium was also added 1μM Dexamethasone (Sigma-Aldrich) and 10^{6}μM of recombinant human insulin (Humulin). All the cell lines were grown at 37°C in a humidified atmosphere at 5% CO_2. Hepatocyte-like cells were differentiated and grown as reported in the protocol developed by Prof. Elvassore's group[286].

3.2 MicroRNA transfection

In order to evaluate the biological effects of specific microRNAs, we performed transfection assay using *miRNA mimic* or *miRNA inhibitor* molecules. MiRNA mimics are chemically synthetized ds-RNA which mimic naturally occurring miRNAs after transfection into the cell (Fig. 3.1). Only the guide strand is loaded into RNA induced silencing complex

(RISC) with no resulting microRNA activity from the complementary passenger strand. MiRNA inhibitors are single-stranded, modified RNAs which, after transfection, specifically hybridize to mature miRNA, inhibiting its function (Fig 3.1). As control, we used a miRNA Scramble, which is a random sequence miRNA mimics molecule that has been extensively tested in human cell lines and tissues and validated to not produce identifiable effects on known miRNA function.

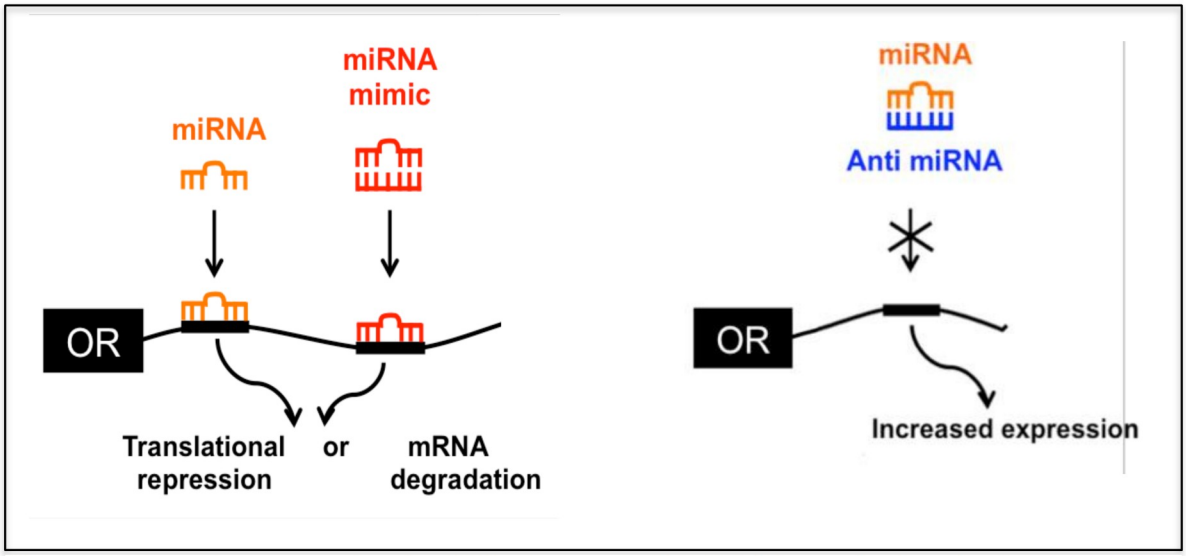

Fig. 3.1 – Schematic representation of *miRNA mimics* and *miRNA inhibitor* mechanism of action.

From a procedural point of view, HCC cell lines were seeded in complete medium at a density of $4.06*10^3$ cells/cm^2 in 6-well plate and allowed to attach overnight. MicroRNA transfections were usually performed the day after seeding and cells were analyzed at 48 hours after transfection as shown in Fig. 3.2.

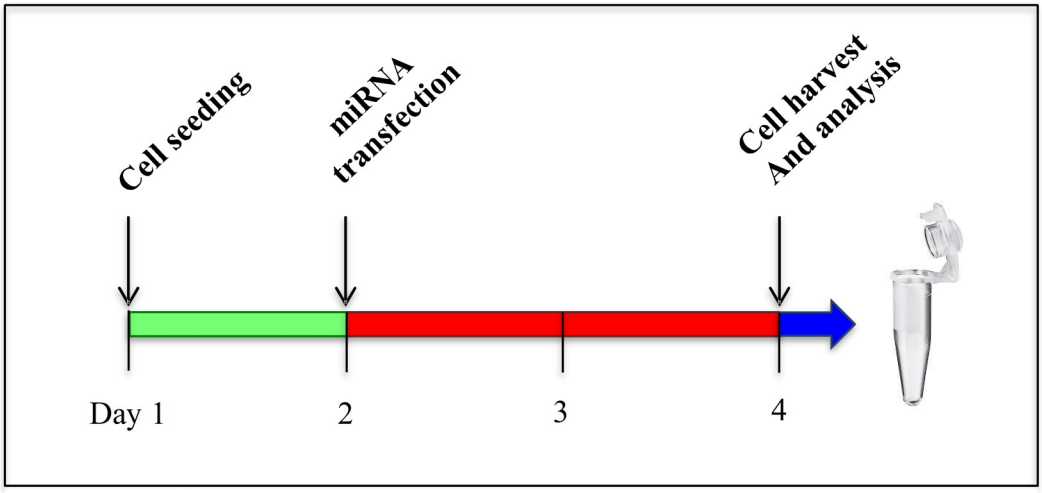

Fig. 3.2 – MiRNA transfection scheme.

1.18µg of liposome (Lipofectamine 2000-1mg/ml, Invitrogen) were mixed in 125 µl of *Optimem medium* (Invitrogen) for 15 minutes at RT. Lipofectamine is a cationic liposome formulation, which complexes with negatively charged nucleic acid molecules to allow them to overcome the electrostatic repulsion of cell membrane [287]. Simultaneously, 1.18 µg of miRNA mimics/miRNA inhibitors/miRNA scramble (Exiquon) were added in 125 µl of *Optimem medium* for 15 minutes and subsequently mixed with the liposome solution prepared as above. 20 minutes are enough to allow miRNA:liposome complexes formation. After that, the mixture was added to 550 µl of *Optimem medium* to reach a final concentration of 100nM and administrated to cells seeded in 6-well plates. After three hours of incubation, the supernatant was replaced by 3ml of specific complete medium (Fig. 3.3)

Regarding MTT assay, 0.078 µg of liposome (Lipofectamin2000-1mg/ml, Invitrogen) were mixed in 50 µl of *Optimem medium* (Invitrogen) for 15 minutes at RT. Simultaneously, 0.078µg of miRNA mimics/miRNA inhibitors/miRNA scramble were added in 50 µl of *Optimem medium* for 15 minutes and subsequently mixed with the liposome solution prepared as above. 20 minutes are enough to allow miRNA:liposome complexes formation. After that, the mixture was added to 100 µl of *Optimem medium* to reach a final concentration of 100nM and administrated to cells seeded in 96-well plate at final density of 3.45*10 ^{3} cell/cm^{2}. After three hours of incubation, the supernatant was replaced by 200 µl of specific complete medium (Fig. 3.3)

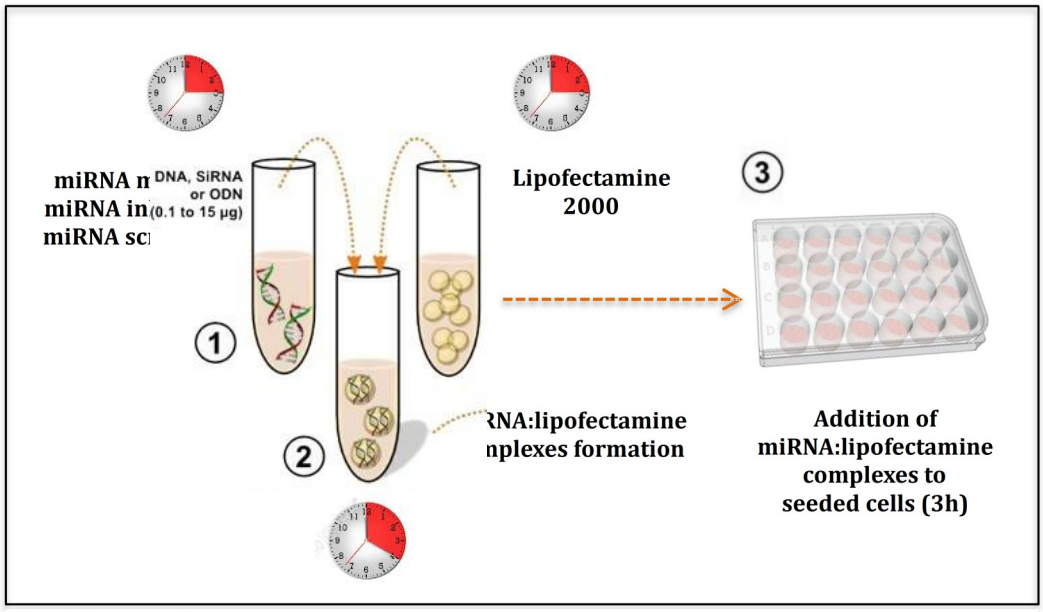

Fig. 3.3 – Transfection protocol.

3.3 Cell counting and vitality assay

To evaluate the morphology, viability and number of cells that have to be sown, it is necessary to perform a thorough examination by light microscope. One of the earliest and most common methods for measuring cell viability is the *Tripan Blu exclusion assay. Tripan Blu* is a 960Da molecule that is cell membrane impermeable and therefore it only enters cells with compromised membranes. Upon its entry into the cell, *Tripan Blu* binds to intracellular proteins thereby giving the cells a blue color. This simple test is used for a direct identification and enumeration of live, unstained, and dead, blue, cells in a given population.
A cell aliquot is usually diluted in an equal volume of 0.04% solution of *Tripan Blu* in 1X Phosphate-Buffer Salin (PBS). After that, it is possible to perform cell counting loading 15 µl of cell re-suspension diluted 1:1 with Tripan Blu 0,04% in 1X PBS in *Thoma's counting chamber* (Exacta-Optech) and watching under microscope (Nikon Eclipse TS100).

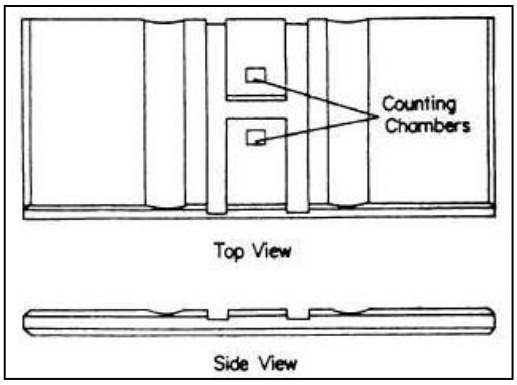

3.4 – Thoma's Counting chamber

After several independent cell counts, it is possible to determinate the number of cells in 1 milliliter of medium through the following formula:

$$Xn = (n_m * 2 * 10^4)$$

where *Xn* represents the cell number in 1ml of medium, n_m is the average number of cells obtained in the different independent counts, 2 is the dilution's factor of *Tripan Blu* and 10^4 represents the conversion's factor of *Thoma's counting chamber*.

3.4 Pharmacological treatment with 5-Azacytidine

5-azacytidine (4-amin-1-β-D-ribofuranosyl-1,3,5-trizan-2(1*H*)-one, trade name *Vidaza*, is a water-soluble cytosine analog with a molecular weight of 244,205g/mol. The pharmaceutical company *Celgene* provides us with the drug powder. We've prepared a stock solution of $41*10^3$µM, diluting 10mg of powder in 1ml of sterile water.

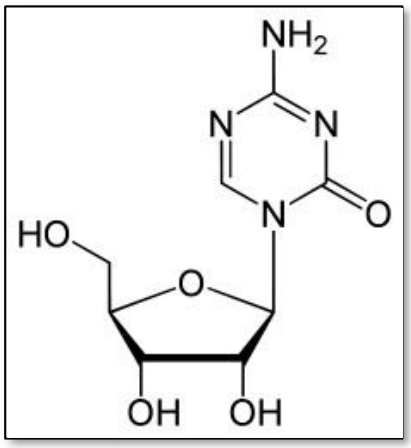

3.5 – Chemical structure of 5-azacytidine ($C_8H_{12}N_4O_5$)

24h before the treatment with 5-azacytidine, the cell lines IHH, JHH6 and HuH7 are usually seeded at specific density, which depends on the type of test performed. The day after the seeding, the cells received the drug for three consecutive days every 24h. This protocol was adopted to mimic the repeated administration cycles used in hematological patients for 5-azacytidine. At the end of the multiple treatments, cells were collected and properly analyzed (Fig 3.6). Cells belonging to JHH6 and IHH cell lines as well as hepatocyte-like cells were treated with 0.8μM and 6μM of 5-azacytidine for three consecutive days every 24h. The highest dose was already found in literature for *in vitro* studies, applied to other kind of tumours [288,289] whereas the lowest dose was chosen to try to mimic drug average plasma concentration found in patients affected by myelodysplastic syndrome[290]. HuH7 cells were also treated with the higher dose 30μM because they are more resistant to 5-azacytidine treatments than the other cell lines.

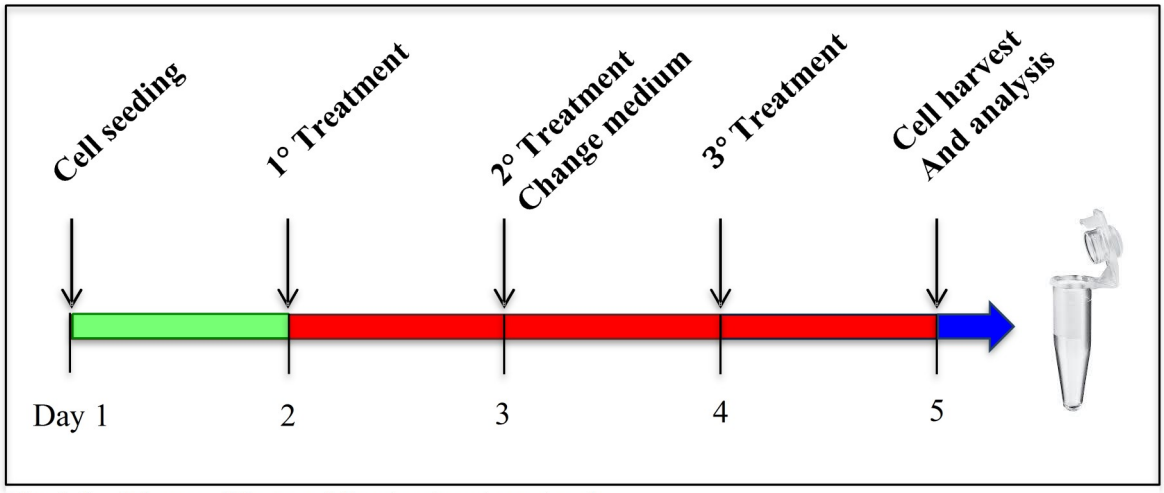

Fig. 3.6 – Scheme of 5-azacytidine treatments protocol.

3.5 MTT assay

MTT assay is a colorimetric test for assessing cell metabolic activity. Under defined conditions, *NAD(P)H-dependent oxidoreductase enzymes* reflect the number of viable cells present in a cell culture. These enzymes are able to reducing the tetrazolium dye *MTT 3-(4,5-dimethylthiazol-2-yl)-2,5-diphenyltetrazolium bromide* (MTT, 4mg/ml in 1X PBS, Sigma-Aldrich) to its insoluble *formazan*, which has a purple colour (Fig. 3.7).

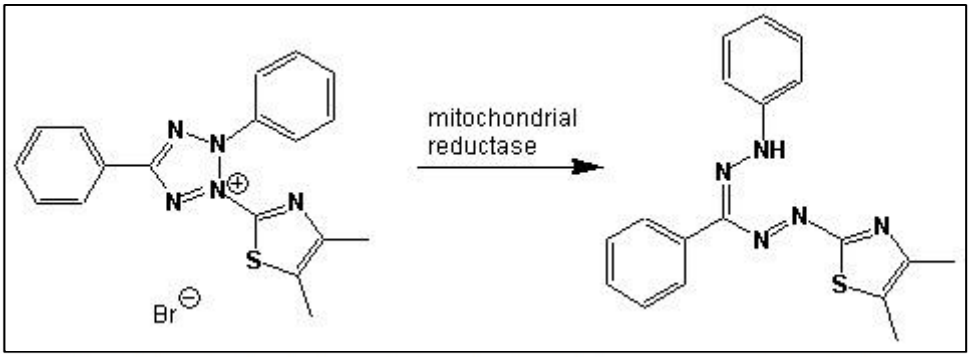

Fig. 3.7 – MTT reduction in live cells by mitochondrial reductase results in the formation of insoluble formazan, characterized by high absorptivity at 570nm.

Regarding 5-azacytidine treatment, JHH6, IHH and HuH7 cells were seeded at $8.6*10^3$ cells/cm^2 in 96-well plates. Hepatocyte-like cells were seeding at $34.4*10^3$ cells/cm^2 because of their low proliferative rate. Regarding miRNA mimics transfection, JHH6 and HuH7 cells were seeded at $3.45*10^3$ cells/cm^2 in 96-well plate. In all cases, MTT is given to cells at the final concentration of 0.5mg/ml. After 4 hours of incubation at 37°C, cell medium is removed and the salt crystals formed inside the cells are solubilized with dimethyl sulfoxide (DMSO). Absorbance is then read at 570nm using a spectrophotometer (Spectra Max Plus 384, Molecular Devices). Cell growth percentage (% G.) is calculated using the following formula:

$$\%\ G. = \left(\frac{OD\ treated\ cells}{OD\ untreated\ cells}\right) * 100$$

From this datum is then easy to obtain the growth inhibition percentage (% G. I.):

$$\%\ G.I. = 100 - \left[\left(\frac{OD\ treated\ cells}{OD\ untreated\ cells}\right) * 100\right] = 100 - \%\ G.$$

3.6 Protein extraction

To obtain protein extracts to be analyzed by Western Blotting analysis, $8.34*10^3$ cells/cm^2 were seeded in 6-well plates. Only for HuH7 cell line, the cell density used was $4.17*10^3$/ cm^2. At the end of 5-azacytidine treatments, cells were collected by centrifugation at 1000 rpm for 5 minutes and rinsed with PBS 1X (NaCl 137 mM, KCl 2.7 mM, Na_2HPO_4 8.1 mM, KH_2PO_4 1.47 mM, pH 7.4). After that, cells were lysed with an *Extraction buffer* consisting of *Tris HCl pH 6.8* (45mM) (Sigma-Aldrich), *N-Lauroylsarcosine* (0.2%) (Fluka). 0.2mM of *Phenylmethanesulfonyl fluoride* (PMSF) (Sigma-Aldrich), 1mM of 1,4-Dithiothreitol (DTT) (Sigma-Aldrich) and proteases inhibitors (2 g/ml of *Aprotinin* and

Pepstatin; Sigma-Aldrich) and phosphatases inhibitors (0.1 mM of *Sodium Orthovanadate* and *Sodium Fluoride*: Sigma-Aldrich). Because of the instability of PMSF in aqueous solution, this component was added to the buffer shortly before use. Twenty μl of *Extraction Buffer*/10^5 cells were added and incubation performed at RT for 5 minutes. Protein extracts were quantified by Bicinchoninic (BCA) protein assay and then stored at -80°C.

3.7 Protein extracts quantification by BCA protein assay

The protein content was determined by the *Bicinchoninic* (BCA) protein assay, which primarily relies on two reactions. First, the peptide bonds in protein reduce Cu^{2+} ions from the copper(II) sulphate to Cu^{+} (a temperature dependent reaction). The amount of Cu^{2+} reduced is proportional to the amount of protein present in the solution. Next, two molecules of bicinchoninic acid chelate with each Cu^{+} ion forming a purple-coloured water-soluble complex that strongly absorbs light at a wavelength of 562 nm (Fig. 3.8). The bicinchoninic acid Cu^{+} complex is influenced in protein samples by the presence of some aminoacids, including cysteine/cystine, tyrosine, and tryptophan. At higher temperatures (37 to 60 °C), peptide bonds assist in the formation of the reaction product. Incubating the BCA assay at higher temperatures is recommended as a way to increase assay sensitivity while minimizing the variances caused by unequal amino acid composition[291].

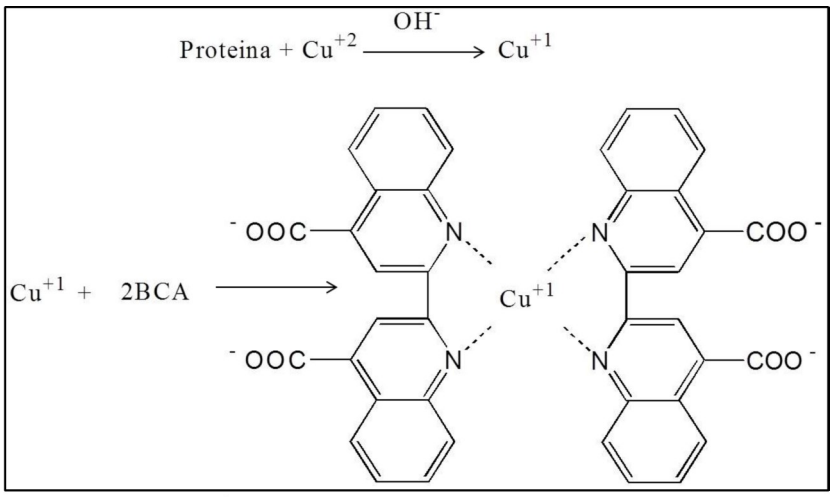

Fig. 3.8 –BCA reaction

BCA protein assay was performed in 96 well flat-bottomed microplate in duplicate. Standards solutions of *Bovine Serum Albumin* (BSA; 2μg/ml; Thermo-Scientific) were prepared to obtain a calibration curve in order to determinate protein extract concentration. 2μl of each standards or protein samples were mixed with freshly prepared working solution

(mixture of BCA and $CuSO_4$ at a ration 50:1) into a 96 well flat-bottomed microplate in duplicate and incubated at 37°C for 30 minutes. Then the samples' absorbance was measured at 570nm using a spectrophotometer (Spectra Max Plus 384, Molecular Devices). The concentration of each protein sample was determined from a plot of concentration against the absorbance obtained for the calibration curve.

3.8 SDS-Page electrophoresis and Western Blot

SDS-PAGE is a technique widely used in molecular biology to separate proteins according to their electrophoretic mobility, a specific property associated with length, conformation and molecular charge. In SDS-PAGE, the chemical denaturant *Sodium Dodecyl Sulphate* (SDS) is added to remove proteins structure and turn the molecules into an unstructured linear chain whose mobility depends only on their length and mass-to-charge ratio. After electrophoretic separation, specific proteins can be identifying by Western Blot analysis in which proteins are transferred to a membrane producing a band for each protein. The membrane is then incubated with labels antibodies specific to the protein of interest[292].

After addition of *Loading Buffer Leammli 6X* (5% of β*mercaptoethanol,* 1.65% of *Sodium Dodecyl Sulphate* (SDS), 10% of glycerol, 0.55M TrisHCl and Bromophenol Blue) and denaturation at 95°C for 5 minutes, 40 μg of protein extract were loaded on 12% or 10% SDS-PAGE (29:1, acrylamide:bis-acrylamide) gel according to Laemmli's procedure [293]. For electrophoretic running, we used a specific *Running Buffer* (0.125M Tris-HCl pH 8.3, 0.96M of glycine and 0.5% of SDS) and an electric field of about 14V/cm. After that, proteins were transferred, using a transblot semi-dry apparatus system (Bio-Rad), onto a 0.22μm nitrocellulose membrane (Schleicher & Schuell), previously hydrated in *Transfer Buffer* (60mM Tris-HCl, 40mM glycine containing 0.05% SDS and 10% methanol) with filter paper. After *sandwich* assembly, proteins transfer was performed using an electric field of 1mA/cm for about 1 hour. Membranes were then stained by *Ponceau S.* (Sigma-Aldrich) to evaluate the efficiency of the transfer and then blocked with appropriate percentage of non-fat dried milk. Afterwards, membranes were incubated with the specific primary antibody and finally with the correspondent HRP-conjugated secondary antibody. The IgG and hybridization conditions used are reported in Table 3.1. Membranes were washed twice by PBS containing 0.05% Tween 20 or 0.05% NP40 and then developed by chemiluminescence's detection kit (*SuperSignal West Pico Chemiluminescent Substrate*; Thermo Scientific-Pierce). Band

intensities were quantified by densitometry (Model GS-700 Imaging Densitometer), Biorad and molecular Analyst software, Biorad). GAPDH was used as internal loading control.

Primary Antibody	Dilution	Non-fat Milk	Incubation Time	Secondary Antibody (1:2000)	Incubation time
PARP (BD Biosciences)	1:1000	5% + 0.05% Tween	O/N at 4°C	Anti-Mouse HRP (Santa Cruz)	1h, RT
BAX (BD Biosciences)	1:250	3% + 0.05% Tween	O/N at 4°C	Anti-Mouse HRP (Santa Cruz)	1h, RT
ROCK 2 (Abcam)	1:1000	5% + 0.05% Tween	O/N at 4°C	Anti-Rabbit HRP (Santa Cruz)	1h, RT
MMP2 (Santa Cruz)	1:1000	5% + 0.05% NP40	O/N at 4°C	Anti-Rabbit HRP (Santa Cruz)	1h, RT
GAPDH (Santa Cruz)	1:1000	5% + 0.05% Tween	O/N at 4°C	Anti-Rabbit HRP (Santa Cruz)	1h, RT

Table 3.1: IgG and hybridization conditions

3.9 Zymography assay

Zymography is generally known as an electrophoretic technique, based on SDS-PAGE, which contains a substrate copolymerized within the polyacrylamide gel matrix, for the detection of enzymatic activity. We used zymography to evaluate the enzymatic activity of *Matrix Metalloprotease 2* (MMP-2), a protein belonging to gelatinase family. MMP-2, as well as MMP-9, regulate cell matrix composition and are known for their ability to cleave one or several extra-cellular matrix constituents [294]. MMP-2 is able to hydrolyzed gelatin, which is embedded into the resolving gel during preparation of acrylamide gel (2.8mg/ml). Samples loaded on SDS-PAGE are concentrated supernatants of treated or untreated cells, grown without serum within 48 hours of their harvesting. In fact serum contains large amount of both MMP-2 and MMP-9 and for this reason human serum has been used as positive control. Samples are normally prepared by the standard SDS-PAGE treatment buffer, under non-reducing condition, i.e. absence of heating and reducing agents, such as 2-mercaptoetanol and dithiothreitol (DTT). Following electrophoresis, the SDS is removed from the zymogram by washing with an appropriated *Wash Buffer* (50mM Tris Hcl, pH 7.5, 5mM $CaCl_2$, 1µM ZnCl, 0.02% NaN_3 and 2.5% Triton X-100) followed by incubation in an appropriate *Digestion Buffer* (50mM Tris Hcl, pH 7.5, 5mM $CaCl_2$, 1µM ZnCl, 0.02% NaN_3) O/N at 37°C. The zymogram is subsequently stained with *Coomassie Brilliant Blue*, and areas of digestion appear as clear bands against a darkly stained background where the substrate has been degraded by the enzyme (Fig. 3.9).

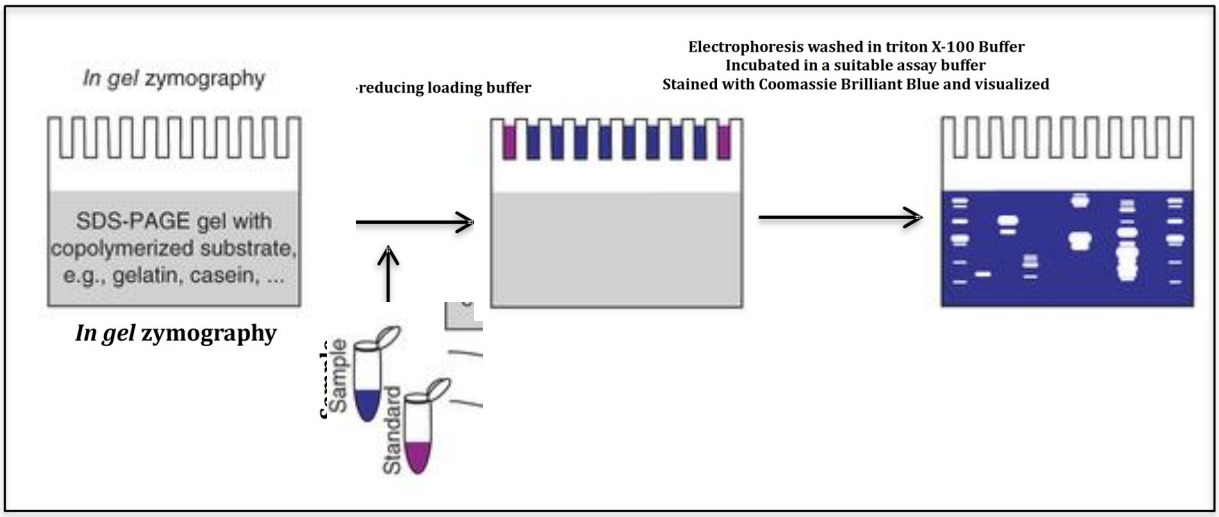

Fig. 3.9 – Schematic representation of Zymography procedure [11]

3.10 Cell cycle analysis

The distribution of cell cycle phases can be analyzed by measuring the thymidine analog *Bromodeoxyuridine* (BrdU; BD-Pharmigen™) incorporation into newly synthetized cellular DNA and *Propidium Iodide* (PI; BD-Pahrmigen™) staining. BrdU is incorporated into newly synthetized DNA in cells entering and progressing through the S phase of the cell cycle. The incorporated BrdU is then stained with specific fluorescently labeled (FITC) anti-BrdU antibody, and the levels of cell-associated BrdU measured by flow cytometer. A dye that binds to total DNA, such as PI, is used in conjugation with immunofluorescent BrdU staining. The anti-BrdU antibody fluorescence intensity is proportional to the amount of newly synthetized DNA whereas PI fluorescence intensity is directly proportional to the total amount of cellular DNA (2n/4n). Values are expressed using a logarithmic scale for FITC and a liner scale for PI. The cell cycle phase distribution is represented in four dials (Fig. 3.6): cells in Q_1 dial represent proliferating cells (DNA content: 2n+X), cells in Q_2 and Q_4 dials are in G2/M phase (DNA content 4n) whereas cells in Q_3 dial are in G_1/G_0 phase and stained only by PI (DNA content: 2n) (Fig. 3.10).

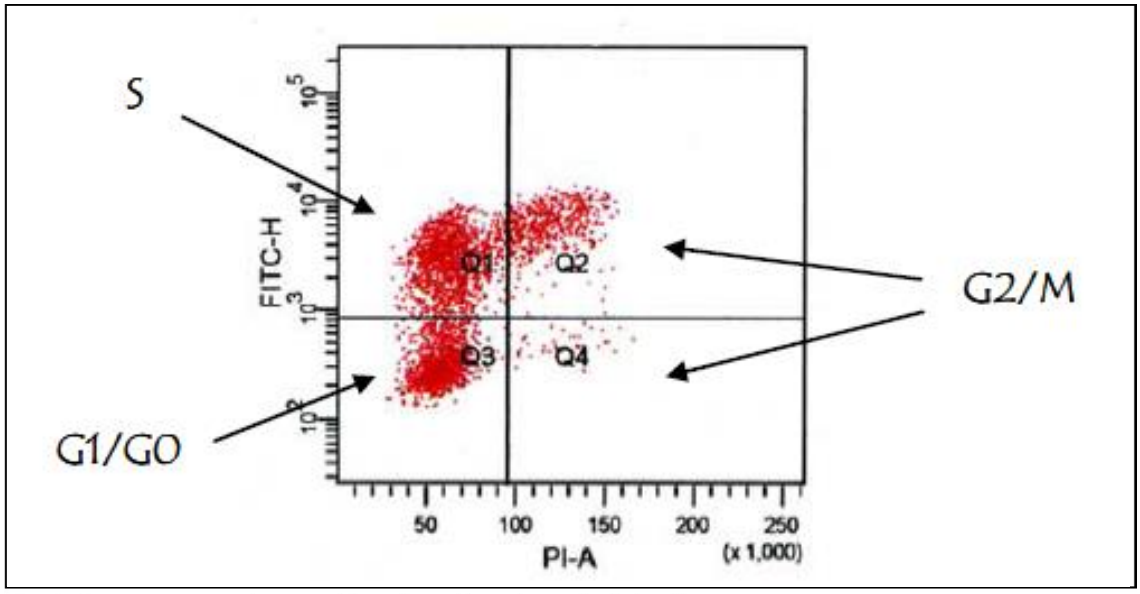

Fig. 3.10 – Representative Dot blot of a cell-cycle analysis by flow cytometer

For cell-cycle analysis, JHH6 and IHH cells were seeded at the density of $8.3*10^3$ cells/cm^2 in 6-well plate whereas HuH7 cells are seeded at $4.1*10^3$ cells/cm^2 in 6-well plate. All cell lines were treated with 5-azacytidine as previously reported (Paragraph 3.2). Twelve hours before harvesting, cells were pulsed with BrdU at a final concentration of 10 μM. Next day, cells were trypsinized and re-suspended in ice cold 70% EtOH at least O/N. These fixed sample could be stored in EtOH at 4°C up to few weeks. Afterwards, a washing step with 1X PBS containing 0.5% BSA was performed and then the cells were incubated with *Acid Solution* (1M HCl in 1X PBS/1% BSA and ddH_2O) to permeabilize their cellular membrane. JHH6 and IHH cells were incubated for 1 hour at RT with the *Acid Solution* whereas HuH7 cells only for 40 minutes. After a further washing step, cells were re-suspended in a *Basic Solution* (0.1M Sodium Borate, pH 8.5) for 2 minutes to bring pH to neutral values. After another washing step, each sample was incubated with *fluorescent-isothiocyanate (FITC)-conjugated mouse monoclonal antibody* (BD PharMigen™) *anti-BrdU* or with *FITC-conjugated mouse IgG_1 Isotype Control*, as background control, for 1 hour at RT in dark. Another washing step preceded incubation with *PI* (4 μl/sample; BD PharMigen™) and *Ribonuclease A* (100 μg/ml; Sigma-Aldrich) for 1 hour. After a final washing step, cells were re-suspended in 500 μl of PBS1X/0.5% BSA and analyzed by the flow-cytometer FACScanto Becton Dickinson using the *DIVA* software.

3.11 Apoptosis Assay – Annexin V Assay

Apoptosis is a physiological genetically programmed process that is characterized by specific morphologic features, including loss of plasma membrane asymmetry and attachment, plasma membrane blebbing, condensation of cytoplasm and nucleus and inter-nucleosomal cleavage of DNA. Loss of plasma membrane is one of the earliest features of apoptosis.

In our samples, apoptosis was evaluated by *Annexin V* assay (Bender-Med, Burlingame, CA) and Propidium Iodide (PI) staining (BD PharMigen ^{TM}). In apoptotic cells, the membrane phospholipid phosphatidylserine (PS) is translocated from the inner to the outer leafter of the plasma membrane. Annexin V is a 35kDa Ca $^{2+}$-dependent phospholipid-binding protein with high affinity to PS and binds PS exposed to apoptotic cell surface. PS translocation precedes the loss of membrane integrity, which characterized the later stage of cells death resulting from either apoptosis or necrosis. As Annexin V is conjugated to a fluorochrome (FITC) it is possible to identify Annexin V positive cells by flow-cytometric analysis. Therefore, Annexin V staining is usually associated with the use of a vital dye, such as Propidium Iodide (PI) to distinguish early apoptosis from late apoptosis. In fact, viable cells with intact membrane exclude PI whereas membranes of damaged cells are permeable to PI. Cells that are considered viable are both Annexin V and PI negative, while cells in early apoptosis are Annexin V positive but PI negative, and cells in late apoptosis or already dead are both Annexin V and PI positive (Fig. 3.11).

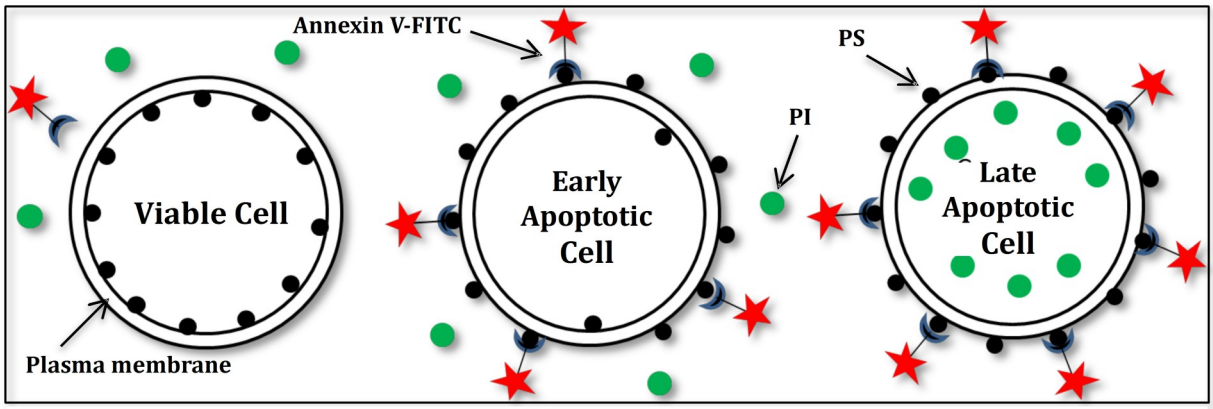

Fig. 3.11 – Diagram showing healthy and apoptotic cells with markers for detection of apoptosis.

After 5-azacytidine treatments, cells were collected and counted. About 2*10 cells were then re-suspended in *Binding Buffer* (10mM Hepes/NaOH, pH 7.4, 140mM NaCl and 2.5mM $CaCl_2$) and incubated with Annexin V-FITC Ig for 15 minutes. Afterwards, cells were sedimented, re-suspended in *Binding Buffer* and incubated with *Propidium Iodide* (PI) for 20

minutes at RT. After a final washing step, cells were re-suspended in 500 µl of PBS 1X/0.5% BSA and analyzed by flow-citometry (FACScanto Becton Dickinson).

3.12 Cytotoxicity assay

Cellular cytotoxicity was evaluated by *Lactate dehydrogenase* (LDH) assay (Bio Vision Product, Mountain View CA). LDH activity is determined by a coupled enzymatic reaction: LDH oxidizes lactate to pyruvate which then reacts with tetrazolium salt to formazan. The formazan dye is water-soluble and can be detected by spectrophotometer at 500nm.

Cells were seeded as in *MTT assay* protocol and, at the end of the appropriate treatment, 100 µl of cellular supernatant were transferred to corresponding wells in an optical clear 96-well plate. 100 µl of *Reaction Solution*, containing Catalyst Solution and Dye Solution at a ratio 1:45, were then added to each well and incubated for 30 minutes at RT protecting plate from light. Absorbance of samples was measured at 500nm using a spectrophotometer (Spectra Max Plus 384, Molecular Devices). As positive control, triton X-100 (1% final concentration) treated cells were considered whereas free medium was used as negative control. The percentage of cytotoxicity was determined according to the formula:

$$Cytotoxicity\ (\%) = \left(\frac{Test\ sample - (-CTR)}{(+CTR) - (-CTR)}\right) * 100$$

Where CTR – is negative control and CTR + is positive control.

3.13 Scratch Assay

The *in vitro* scratch assay is an easy, low-cost and well-developed method to measure cell migration[295]. This test allows to evaluate the capability of the cells to fill in a gap generated with a tip on a cell monolayer.

***Scratch after pharmacological treatment with 5-azacytidine*:**

JHH6 cells were seeded in 3.5cm∅ dishes at the density of $10.4*10^3$ cells/cm^2 in William's complete medium. Conversely, HuH7 cells were seeded at the density of $20.8*10^3$ cells/ cm^2 in DMEM complete medium. 24 hours after seeding, cells were treated with 5-azacytidine for three consecutive days, every 24 hours. At the last drug treatment, scratch was performed on cell monolayer and cells were then grown in medium supplemented only with

1% FBS to reduce proliferation stimuli. Images were acquired at microscope (Leica DM IRB) both after scratching and at 24 or 48 hours (3.12; Protocol A).

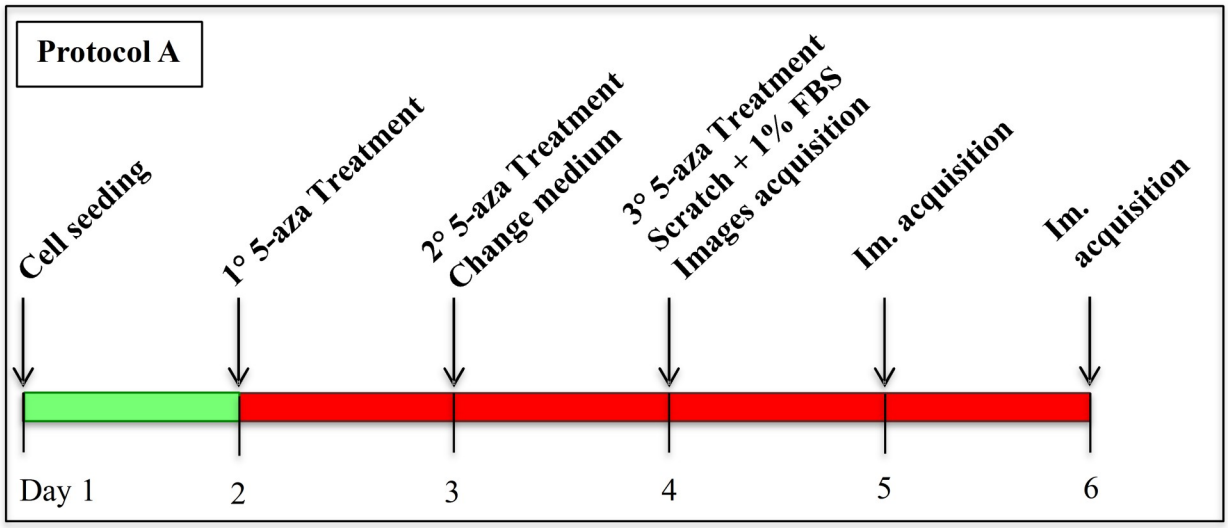

Fig. 3.12 – Scratch assay protocols after 5-azacytidine treatments.

***Scratch after miRNA mimics transfection*:**

HCC cells were seeded in 3.5cm∅ dishes at the density of 6.25*10̊ cells/cm^2 in complete medium. 24 hours after seeding, miRNA mimics transfection was performed as previously reported. Next day, scratch was realized on cell monolayer and cells were then grown in medium with 1% FBS in order to significantly reduce cell proliferation. Images were acquired at microscope (Leica DM IRB) both after scratching and at 24 hours (3.13; Protocol B).

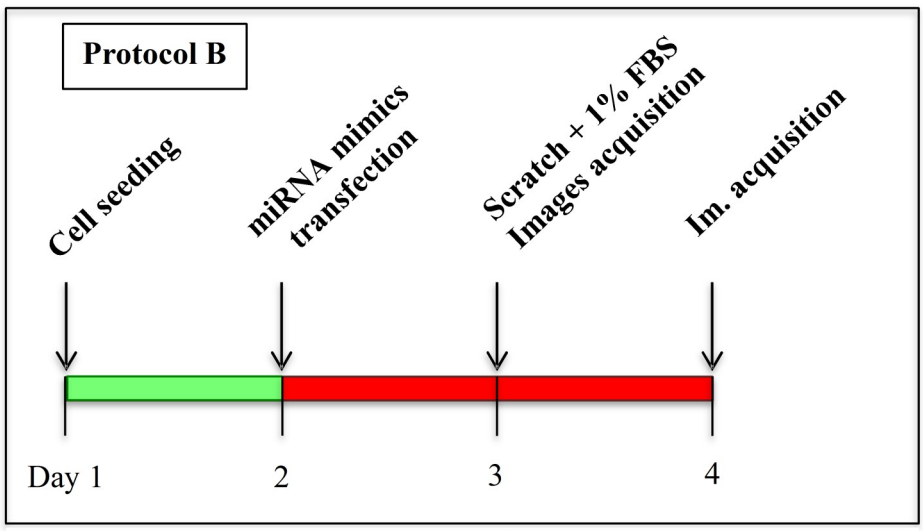

Fig. 3.13 – Scratch assay protocols after miRNA mimics transfection

***Scratch after MMP2 Inhibitor treatment*:**

JHH6 cells were seeded in 3.5cm∅ dishes at the density of $10.4*10^3$ cells/cm^2 in William's complete medium. Conversely, HuH7 cells were seeded at the density of $20.8*10^3$ cells/ cm^2 in DMEM complete medium. At 48h after seeding, cells were treated with 0.1 μM of MMP2 inhibitor (SB-3CT; Selleckchem) for two days consecutively. At the last drug treatment, scratch was performed on cell monolayer and cells were then grown in medium supplemented only with 1% FBS to reduce proliferation stimuli. Images were acquired at microscope (Leica DM IRB) both after scratching and at 24 or 48 hours (3.14; Protocol C).

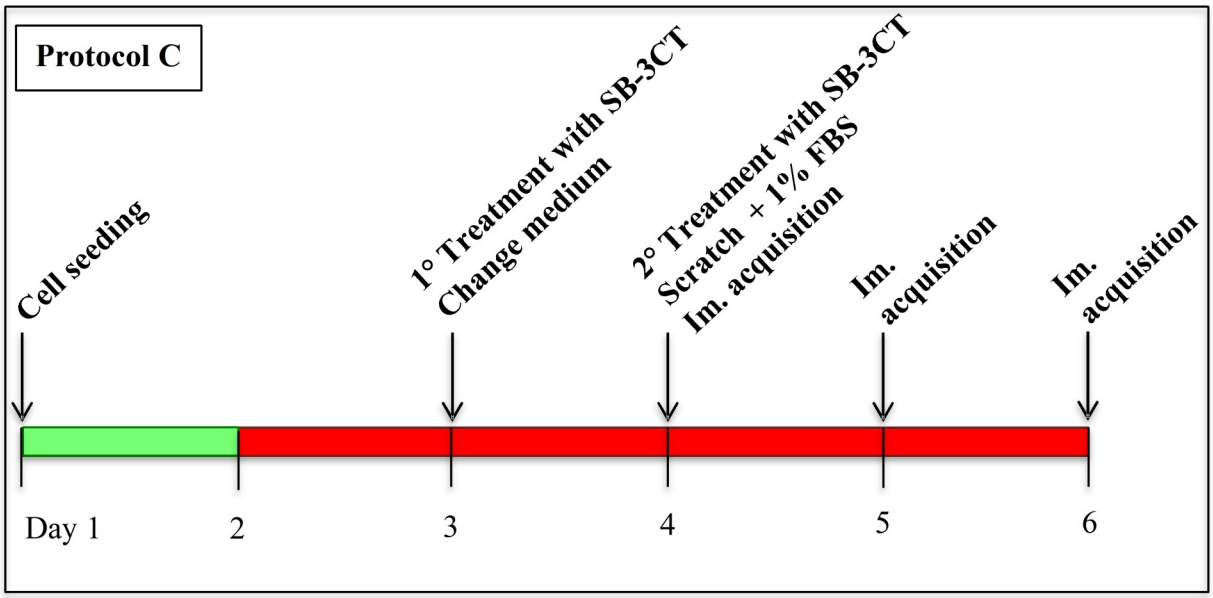

Fig. 3.14 – Scratch assay protocols after MMP2 inhibitor (SB-3CT) treatments.

Scratch after Bortezomib treatment:

JHH6 cells were seeded in 3.5cm∅ dishes at the density of $10.4*10^3$ cells/cm^2 in William's complete medium. Conversely, HuH7 cells were seeded at the density of $20.8*10^3$ cells/ cm^2 in DMEM complete medium. 24 hours after seeding, cells were treated with 10nM or 15nM of Bortezomib () and 48h after drug treatment, scratch was performed on cell monolayer. Cells were then grown in medium supplemented with 1% FBS and images were acquired at microscope (Leica DM IRB) both after scratching and at 24 or 48 hours (3.15; Protocol D).

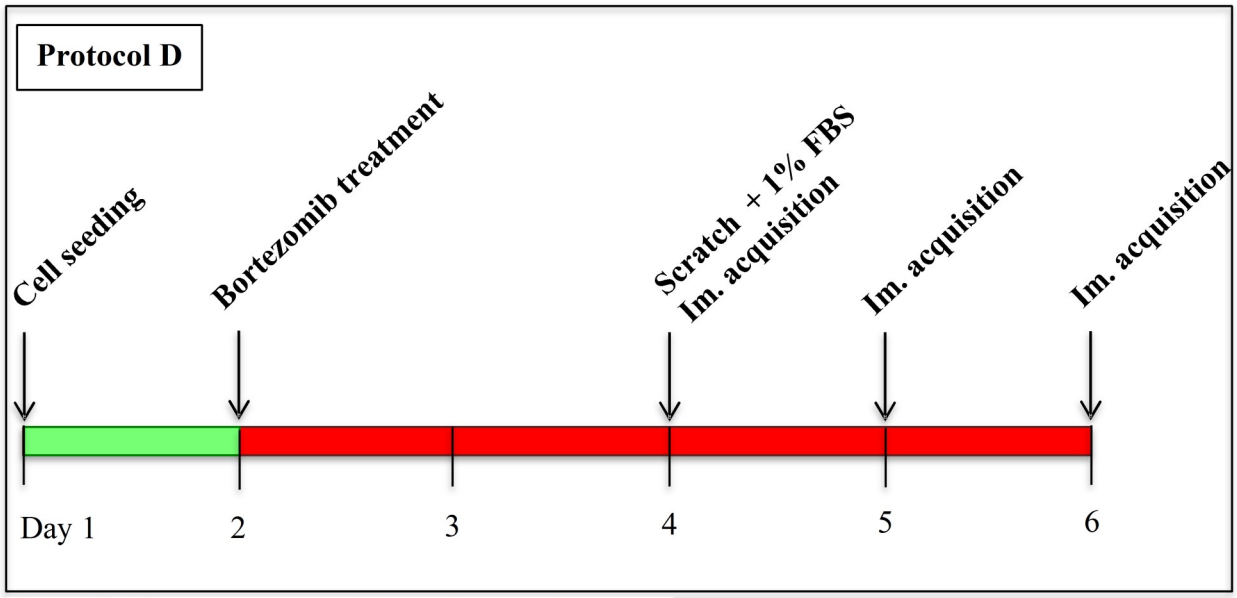

Fig. 3.15 – Scratch assay protocols after *Bortezomib* treatment

Scratch after 5-azacytidine and Bortezomib combined treatment:

JHH6 cells were seeded in 3.5cm∅ dishes at the density of $10.4*10^3$ cells/cm^2 in William's complete medium. Conversely, HuH7 cells were seeded at the density of $20.8*10^3$ cells/ cm^2 in DMEM complete medium. 24 hours after seeding, cells were treated with 10nM or 15nM of *Bortezomib* and 0.8µM or 6µM of 5-Azacytidine. 48h after drugs treatments, scratch was performed on cell monolayer. Cells were then grown in medium supplemented with 1% FBS and images were acquired at microscope (Leica DM IRB) both after scratching and at 24 or 48 hours (3.16; Protocol E).

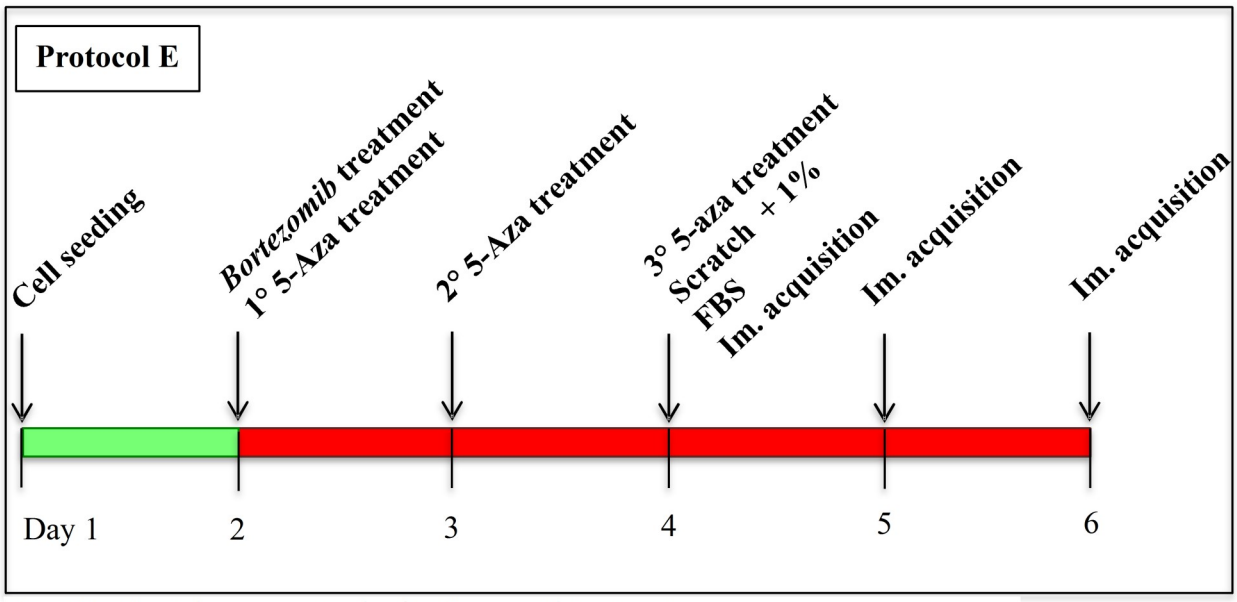

Fig. 3.16 – Scratch assay protocols after *Bortezomib* treatment.

Scratch after ROCK2 Inhibitor treatment:

JHH6 cells were seeded in 3.5cm∅ dishes at the density of $10.4*10^3$ cells/cm^2 in William's complete medium. Conversely, HuH7 cells were seeded at the density of $20.8*10^3$ cells/ cm^2 in DMEM complete medium. At 24h after seeding, scratch was performed on cells monolayer, which was also treated with 50 µM *ROCK2 inhibitor* (Y-27632; Selleckchem) for 4 hours. After that, medium containing inhibitor was replaced with fresh medium supplemented with 1% FBS. Images were acquired at microscope (Leica DM IRB) both after scratching and at 24 or 48 hours (3.17; Protocol F).

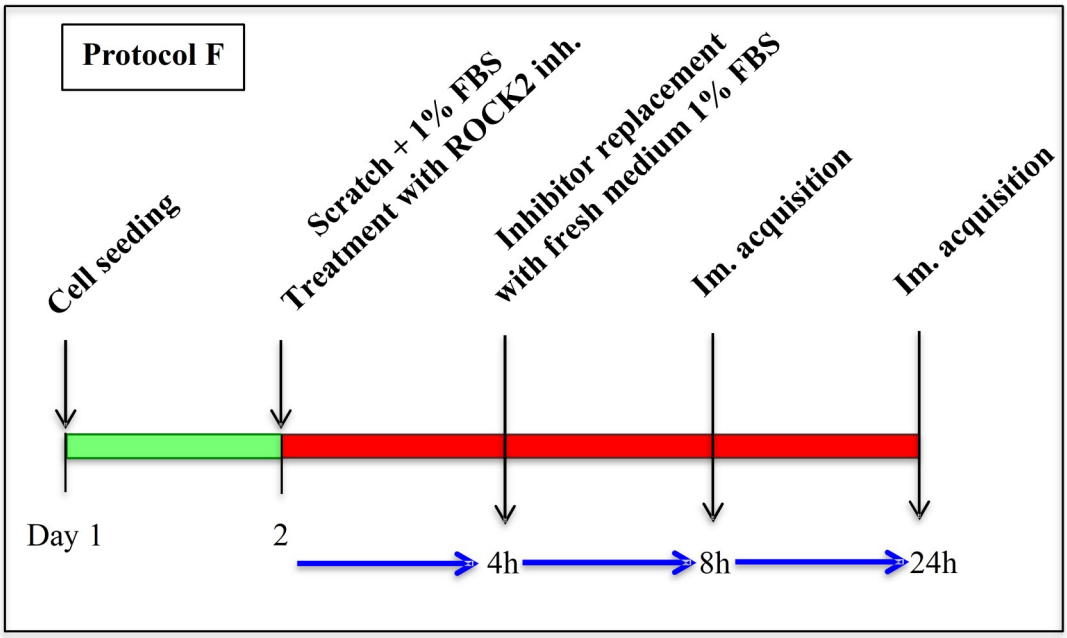

Fig. 3.17 – Scratch assay protocols after ROCK2 inhibitor treatment.

3.14 Fluorescence-Assisted Transmigration Invasion and Motility Assay – F.A.T.I.M.A Assay

The *Fatima assay* allows to evaluate *haptotaxis*, which represents cellular ability to migrate through a gradient of extra cellular matrix proteins[296]. The test involves the use of culture plate inserts (BD-falcon HTS Fluoroblok ^{TM}) containing a *polyethylene terephthalate* (PET) porous membrane to be transversed by the migrating cells labelled with *Dij* (Molecular Probes), a vital fluorescent lipophilic cationic indocarbocyanine dye. Inserts' membranes are coated with *Collagen IV* (Sigma-Aldrich; diluted at 40µg/ml with *Bicarbonate Buffer*, pH 9.6) O/N at 4°C. After that, coated membranes are saturated with specific cell medium

supplemented with 1% BSA. Cells are then harvested and labeled with *Dij*. After saturation, $2*10^4$ cells were re-suspended in 150 µl of specific medium with 0.1% BSA and putted on the top of the insert. 800 µl of specific medium supplemented with 10% FBS and 0.1% BSA were instead putted in the bottom of insert. Cells migration was evaluated hourly through spectrophotometric readings (Infinite f200, TECAN; excitementλ = 535nm; emissionλ = 595nm). Cells migration percentage (*M%*) was obtained using the following formula:

$$M\,\% = \frac{(Bottom\ ti - Bottom\ t0)}{Top\ ti + (Bottom\ ti - Bottom\ t0)}$$

Where *Bottom ti* is the fluorescence value measured on the bottom of transwell at time *i*, *Bottom t0* is the fluorescence value measured on the bottom of transwell at the beginning time, *Top ti* is the fluorescence value measured on the top of transwell at time *i* and $(Bottom\ ti - Bottom\ t0)$ is a correction factor, which considers the eventual cellular aggregate formation on the top of insert that could interfere with cellular migration speed.

3.15 Total RNA extraction

Total RNA was purified from treated and untreated cells by using the *RNeasy Mini Kit* (Qiagen). Briefly, pelleted cells were lysed using *RLT Lysis Buffer* integrated with β *mercaptoethanol*, which breaks protein disulphide bridges. This buffer contains also *guanidinium thyocyanate,* which inactivates *RNase* enzymes preventing RNA degradation. After that, ethanol at 70% was added to precipitate RNA and to promote the interaction between RNA and the silica membrane of columns. The mix was then loaded into the spin columns and centrifuged for 25 second at 13.000 rpm. After that, *Buffer W1* was added to the columns to remove proteins. Afterwards, columns were washed twice using *Buffer RPE* and finally RNA was eluted in 40 µl of *RNase Free Water* centrifuging for 60 seconds at 11.000 rpm. Quantification of total RNA was performed by spectrophotometric determination (NanoDrop ND-100; CelBio).

3.16 MicroRNA extraction with mirVana ™ miRNA Isolation Kit

The mirVana™ miRNA Isolation Kit uses a rapid procedure to isolate small RNAs from tissue and cells using an efficient glass fiber filter (GFF)-based method. The method isolates total RNA ranging in size from kilobases down to 10-mers. Briefly, pelleted cells were lysed adding a specific *Lysis Buffer*, which stabilizes nucleic acids and inactives RNase enzymes. After that, *Homogenete Additive Solution* was added to the samples, which were

then placed in ice for 10 minutes. *Phenol/Clorophorm Solution* was then added to the samples to remove cellular components and to obtain purified RNA. After centrifugation, the aqueous phases were taken and mixed with *Absolute Ethanol* to precipitate RNA. Samples were then loaded into spin columns to immobilize RNA on their specific silica membranes. RNA was washed twice with *Wash Solution 1 and 2* and then eluted in 40 µl of *RNase Free Water* heated at 95°C. Quantification of RNAs was performed by spectrophotometric determination (NanoDrop ND-100; CelBio).

3.17 Quantitative Real-Time PCR

Reverse transcription reactions were performed using 1 µg of each RNA sample. The master mix for reverse transcription was prepared by adding the reagents in the order and in the proportions as reported below:

Components (Applied Biosystems)	**Final concentration**
25mM $MgCl_2$ Solution	5mM
10X PCR Buffer II	1X
dGTP	1mM
dATP	1mM
dCTP	1mM
dTTP	1mM
RNase Inhibitor	1U/µl
MuLV Reverse Transcriptase	2.5U/µl
Random Hexamers	2.5µM

Table 3.2 – Reverse Transcription Master Mix

Using *Random Hexamers* as reverse transcriptase primers, allows samples to incubate at RT for 10 minutes: RT incubation allows for extension of the hexameric primers by reverse transcriptase. The extended primers will then remain annealed to the RNA template upon rising the reaction temperature of 42°C.

Real-Time polymerase chain reaction was performed using the SYBRGreen Master Mix (Applied Biosystems) on a 7900/HT Sequence Detection System (Applied Biosystems). Primers sequences (MWG Eurofins) and their specific T_m are listed in Table 3.3. Amplifications, performed in triplicate, were conducted in a final volume of 35µl of

SYBRGreen Master Mix Buffer, containing 200nM of each primers and 1µl of specific cDNA. 28s rRNA and all the other target genes were submitted to 40 cycles of amplification, precede by 10 minutes of pre-denaturation at 95°C, denaturation at 95°C for 15 seconds, annealing at proper temperature for 60 seconds and extension at 72°C for 30 seconds. A final extension at 72°C for 10 minutes and a dissociation stage (95°C/60°C/95°C 15 seconds each) was finally added. Relative amounts of target mRNAs were normalized by 28s rRNA content according to Pfaffl's method[297].

Gene	Primer pair	Tm	Length (bp)	Amplification Region
E2F1 **NM_005225**	Fw 5'-CCA GGA AAA GGT GTG AAA TC-3' Rv 5'-AAG CGC TTG GTG GTC AGA TT-3'	62°C	74	466-539
E2F2 **NM_004091**	Fw 5'-CAA GTT GTG CGA TGC CTG C-3' Rv 5'-TCC CAA TCC CCT CCA GAT C-3'	65°C	70	644-713
E2F3 **NM_001949**	Fw 5'-AAG TGC CTG ACT CAA TAG AGA GCC-3' Rv 5'-AGT CTC TTC TGG ACA TAA GTA AAC CTC A-3'	62°C	86	1307-1392
E2F7 **NM_203394.2**	Fw 5'-AGG GAT GGA GGT AAA TTG TTT AAC ACT-3' Rv 5'-TTT CCC CAT CTT CAA CTG CAA-3'	65°C	85	233-318
MMP2 **NM_00130251.1**	Fw 5'-CCA TGA TGG AGA GGC AGA CA-3' Rv 5'-TCC GTC CTT ACC GTC AAA GG-3'	60°C	81	391-472
AFT3 **NM_001040619**	Fw 5'-GAG GAT TTT GCT AAC CTG ACG C-3' Rv 5'-CTA CCT CGG CTT TTG TGA TGG-3'	60°C	150	401-551
ATF4 **NM_001675**	Fw 5'-TCT CCA GCG ACA AGG CTA A-3' Rv 5'-CCAA TCT GTC CCG GAG AAG G-3'	60°C	105	1033-1138
DDIT3 **NM-004083.5**	Fw 5'-AAA TCA GAG CTG GAA CCT GAG GA-3' Rv 5'-CCA TCT CTG CAG TTG GAT CAG TC -3'	60°C	91	73-184
ALBUMIN **NM_000477.5**	Fw 5'-CCT GTT GCC AAA GCT CGA TG-3' Rv 5'-GAA ATC TCT GGC TCA GGC GA -3'	60°C	139	676-815
28S **M11167**	Fw 5'-TGG GAA TGC AGC CCA AAG-3' Rw 5'-CCT TAC GGT ACT TGT TGA CTA TGC-3'	60°C	84	282-365

Table 3.3 –Primers and annealing temperatures.

3.18 MicroRNA quantitative Real-Time PCR

MicroRNA reverse transcription reactions were performed using *miRCURY LNÅ™ Universal RT microRNA PCR kit* (Exiqon). This kit units two important features: first, it provides template for all microRNA Real-Time PCR assays. This allows to reduce technical variation and consumption of reagents. Second, both PCR amplification primers (forward and reverse) are microRNA specific and optimized with LNA™ (*Locked Nucleid Acid*) increasing sensitivity and accuracy of microRNA quantification.

From an experimental point of view, a *poly-A* tail is added to the mature microRNA template (Fig. 3.13, step 1A). cDNA is then synthesized using a poly-T primer with a 3' degenerate anchor and a 5' universal tag (step 1B). To obtain newly cDNA, 20ng of each RNA sample were added to *Reaction Buffer 5X*, which contains both poly-A tail and poly-T primer, *RNase Free Water* and *Enzyme Mix*, which contains the *poly-A-polymerase* and the *reverse transcriptase*. Then samples were incubated at 42°C for 1 hours and finally at 95°C for 5 minutes. The cDNA template is then amplified using microRNA-specific and LNA™-enhanced forward and reverse primers (Fig. 3.18, step 2A). Each sample was diluted 80 times with *RNase Free Water* and then mixed with *SYBRGreen Master Mix* and *miRNA Primer Mix*, containing both forward and reverse primers (Fig. 3.18, step 2B). 5s rRNA and all the other target microRNAs were submitted to 40 cycles of amplification, precede by 10 minutes of pre-denaturation at 95°C, denaturation at 95°C for 15 seconds and annealing at 60°C for 60 seconds, followed by a finally dissociation stage (95°C/60°C/95°C 15 seconds each). Relative amounts of target microRNAs were normalized by 5s rRNA content.

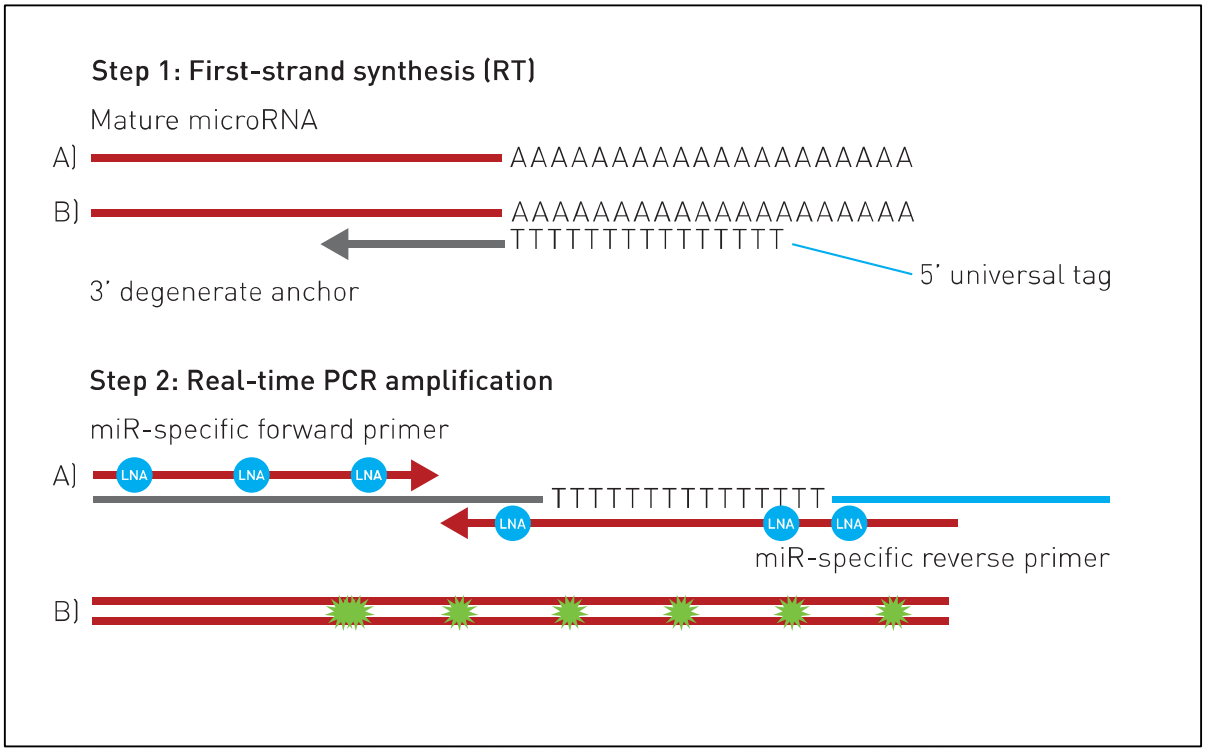

Fig. 3.18 – Schematic outline of the *miRCURY LNA TM Universal RT microRNA PCR System*.

3.19 Immunofluorescence assay

HCC cells were seeded on slides placed in each well of 6-weel plates, as previously described. After the specific treatment, cells were fixed in 4% *paraformaldehyde* for 20 minutes at RT. Afterwards cells were washed twice with 1X PBS and incubated with 0.1M *glycine* in order to mask the aldehyde bonds discovered by fixation treatment, reducing the background staining. After two washes in 1X PBS, cells were incubated with 0.1 % Triton X-100 for 5 minutes at RT to permeabilize cell membranes allowing antibodies entry. Cells were then saturated in 1% BSA/1X PBS and incubated with the specific primary antibody (anti β-tubulin III antibody diluted 1:60, rabbit, Sigma-Aldrich) 1 hour at RT in a humid chamber. After two quick washes, cells were incubated with the secondary antibody (Alexa Fluor 488 diluted 1:400, anti-rabbit, Invitrogen) conjugated with *fitc* for 45 minutes at RT in a humid chamber in dark. Finally, cells were incubated with *Dapi* (1:2500 in 1X PBS; n-9564; Sigma-Aldrich) for 5 minutes at RT e then mounted using *Moviol Mounted solution* (Mowiol® 4-88, Fluka). Images were acquired with Leica DM-2000 microscope.

3.20 *In vivo* experiments

In order to confirm the effectiveness of 5-azacytine treatments in more complex system, *in vivo* experiment were performed in collaboration with Dott.ssa Urska Kamensek

and Dott.ssa Maja Cemazar from the Oncology Institute of Ljubljana. A subcutaneous *Xenograft* model of HCC in SCID (*Severe Combined Immuno Deficiency*) mice was used[298].

Cell lines and experimental animals:

HuH7 cell line was used in the experiments. For the induction of the tumors, HuH7 cells were propagated in Dulbecco's modified Eagle's medium with 10%-heat inactivated fetal bovine serum, 2mM glutamine, 100 U penicillin/0.1 mg/ml streptomycin (Gibco, Live technologies) in a humidified incubator at 37°C with 5% CO_2. 8 week-old female SCID mice (Charles Rivers) were used. For induction of subcutaneous tumours, a suspension of 10^7 cells in 0.1 ml of *NaCl* was injected into the right flank of mice. When tumours reached 30-40 mm^3, animals were randomly divided into experimental groups and subjected to a specific experimental protocol. When mass tumour reached 250 mm^3 mice were sacrificed.

5-azacytidine treatments:

A stock solution of 5-azacytidine (5-aza) was diluted in endotoxin free water to the working of concentration of 0.01µg/µl and frozen down in working aliquots that were thawed each day of the experiment. Mice were treated by intra-tumour injections of 50µL (0,5µg of 5-aza) of the solution to the $40mm^3$ of tumour volume on three consecutive days. Regarding the control group, mice were treated with the same volumes of endotoxin free water without 5-aza. In the long-term evaluation group the treatments were repeated 6 days after the first round of treatments.

Therapeutic effectiveness:

Half of the mice (12) were used for the short-term evaluation. In this group mice were sacrificed two days after the first round of 5-azacytidine treatments and tumours were excised. Half of the tumour was snap frozen in liquid N_2 for the RNA and proteins analysis and the other half was fixated in formalin for the histological analysis. RNA was purified from 20mg of tumour mass using *miRCURY LNA™ Universal RT microRNA PCR kit* (Exiqon), after manual homogenization, and analysed as previously described (Paragraph 3.17). Proteins were extracted from 20-30mg of tumour mass using *RIPA Buffer* consisting of 20mM *Tris Base* pH 7.5, 2.5mM *EDTA*, 1% *Triton*, 10% *Glycerol*, 1% *Deoxycholic acid*, 0.1% *SDS*, 50mM *NaF* and 10mM *Sodyum Pyrophosphate tetrabasic*. After the integration of proteases and phosphatase inhibitors, *RIPA Buffer* was added to the piece of tumour, which was

manually homogenized. Afterwards, proteins extract was incubated on ice for 20 minutes and then centrifuged at 13.000 rpm for 20 minutes at 4°C. Proteins quantification was performed by *BCA assay*, as previously reported.

The other half of the mice (12) was used for the long-term evaluation. The therapeutic effect of the 5-azacytidine treatments was determined using the tumour growth delay assay. Tumours were measured in three perpendicular directions (a, b, c) every 2–3 days using a digital caliper. Tumour volume was calculated by the formula: $V = a \times b \times c \times \pi/6$. Tumour growth was followed until tumours reached an average volume of 250 mm^3, and then the animals were sacrificed and tumours excised for the RNA and histological analysis. The tumour growth curves were plotted for each individual mouse and for the group average. Additionally, for the long-term evaluation group Kaplan Meier survival graph was plotted, where the tumour volume of 250 mm^3 was counted as an event.

3.21 Statistical analysis

If not otherwise indicated, data are expressed as the mean ± SEM, and statistical significance (*P value*) was calculated using *Instat 2.0* and *Graphpad 6.1* softwares. P values $\leq$ 0.05 were considered to be statistically significant.

4. Results

The cell lines employed in this work as *in vitro* HCC model are JHH6 and HuH7. These cell lines have different phenotypes being HuH7 and JHH6 characterized by medium and low hepatic differentiation grade, respectively, on the base of their capacity to synthesize albumin, a well-known marker of hepatic differentiation[282]. As controls, we used an immortalized human hepatocyte cell line (*IHH)* and human hepatocyte-like cells obtained differentiating human embryonic stem cells (hESCs) [286]. IHH cells retain several features of normal hepatocyte such as the ability to produce physiological levels of albumin, triglyceride (TG)-rich lipoproteins and apolipoproteins[285]. Hepatocyte-like cells are positive for several differentiation hepatic markers including albumin and cytochrome P450-3A, show albumin secretion, glycogen storage and indocyanine green incorporation[286]. Furthermore, they proliferate less than IHH cells, as shown by cell counting and antigen ki67 immuno-staining, indicating a higher differentiation grade compared to IHH [286].

In the result reported below a multiple administration protocol of 5-azacytidine was used (see protocol of Figure 3.6) to mimic, at least in part, the multiple administration protocols followed in the clinic for the treatment of hematological disorders [299]. The range of drug concentration employed (0.8μM-30μM) was chosen to include the average blood concentration reachable in humans[290] and the typical concentration used for *in vitro* testing[288,289]. In particular, JHH6 resulted to be more sensible to the drug and thus the 0.8μM-6μM range was used; for HuH7, which resulted to be more resistant, the 0.8μM-30μM range was used. For IHH and human hepatocyte-like cells the upper drug concentration was kept at 6μM. In fact, the effects observed at this drug concentration were comparable to those observed at highest concentration of 30 μM.

The analysis of the effects of 5-azacytidine started with the characterization of the phenotypic effects followed by the study of the molecule mechanism of action of the drug.

4.1 Phenotypic effects of 5-azacytidine *in vitro*

4.1.1 Cell morphology and cell counting

We first evaluated the effect of 5-azacytidine treatments on tumor and non-tumor cells morphology. Treated tumor cells (JHH6 and HuH7) appeared to be larger than untreated cells and with widespread cytoplasmic granulation (Fig. 4.1 e Fig. 4.2, black arrows). Furthermore, treated cells were more multi-nucleated compared to untreated cells (Fig. 4.1 e Fig. 4.2, black

arrows) and plasma membranes were often indented. These morphological features increased in a dose-dependent manner.

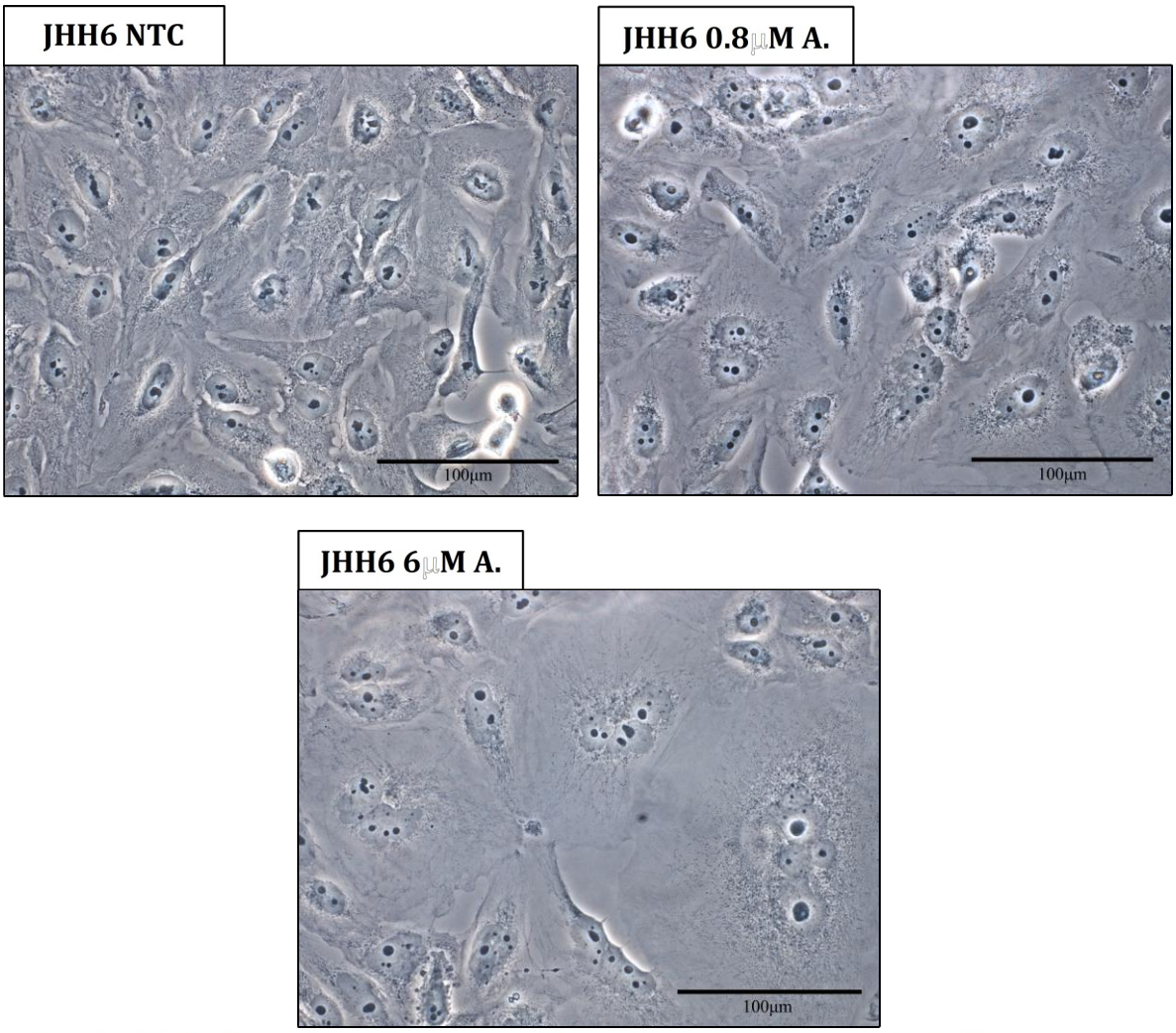

Fig. 4.1 – JHH6 cells morphology after 5-azacytidine treatments. Images are acquired with phase-contrast microscope (Leica DM 2000). Magnification 40X, (bar = 100µm).

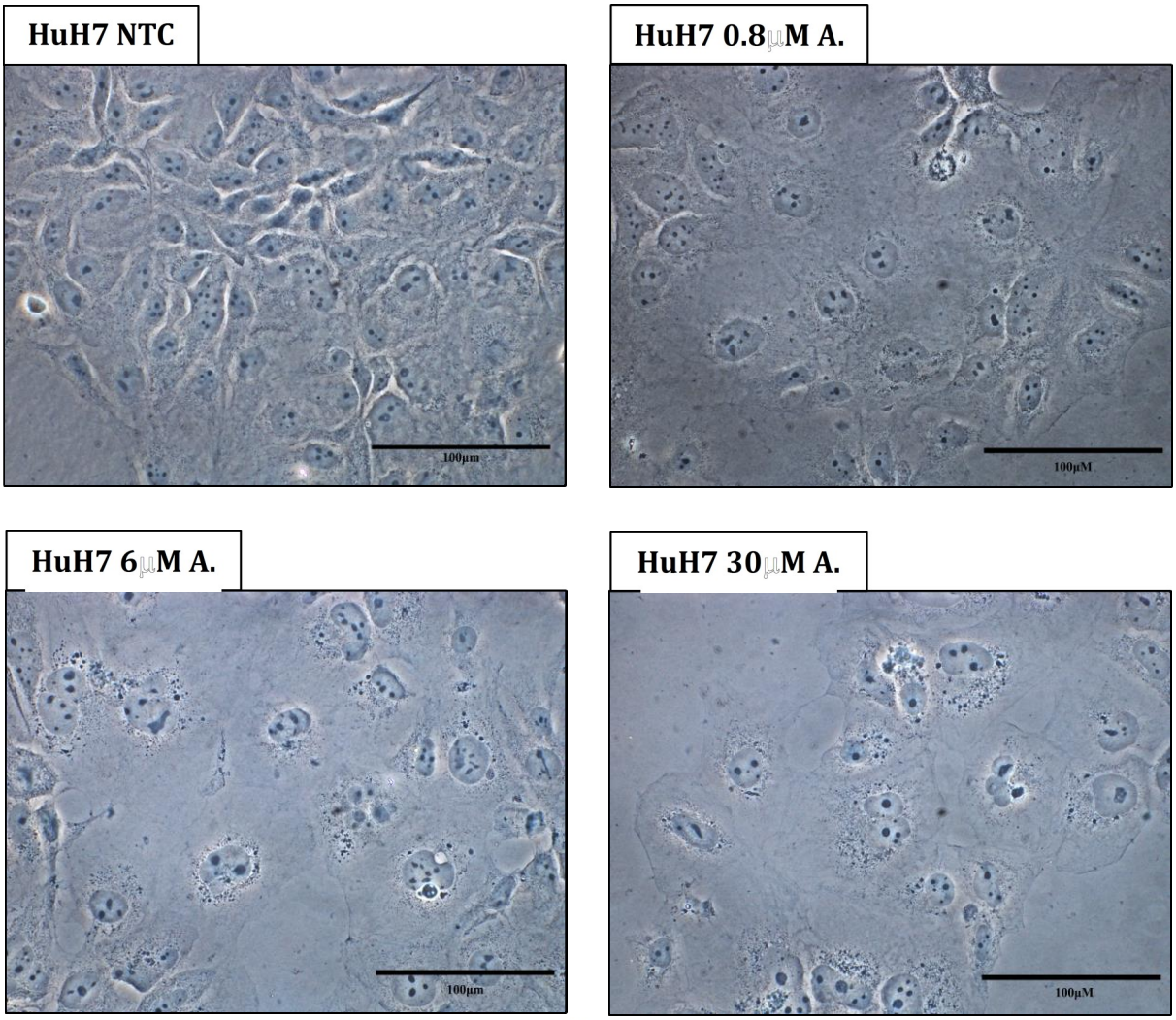

Fig. 4.2 – HuH7 cells morphology after 5-azacytidine treatments. Images are acquired with phase-contrast microscope (Leica DM 2000). Magnification 40X, (bar = 100µm).

In contrast to JHH6 and HuH7, the non-tumor cells IHH didn't show strong signs of stress. In fact, their polygonal-like shape, typical of healthy hepatocytes, was maintained and no evident cytoplasmic granulation was observed. Nuclei appeared somewhat less regular only in cells treated with the highest dose of 5-azacytidine (Fig 4.3, black arrows).

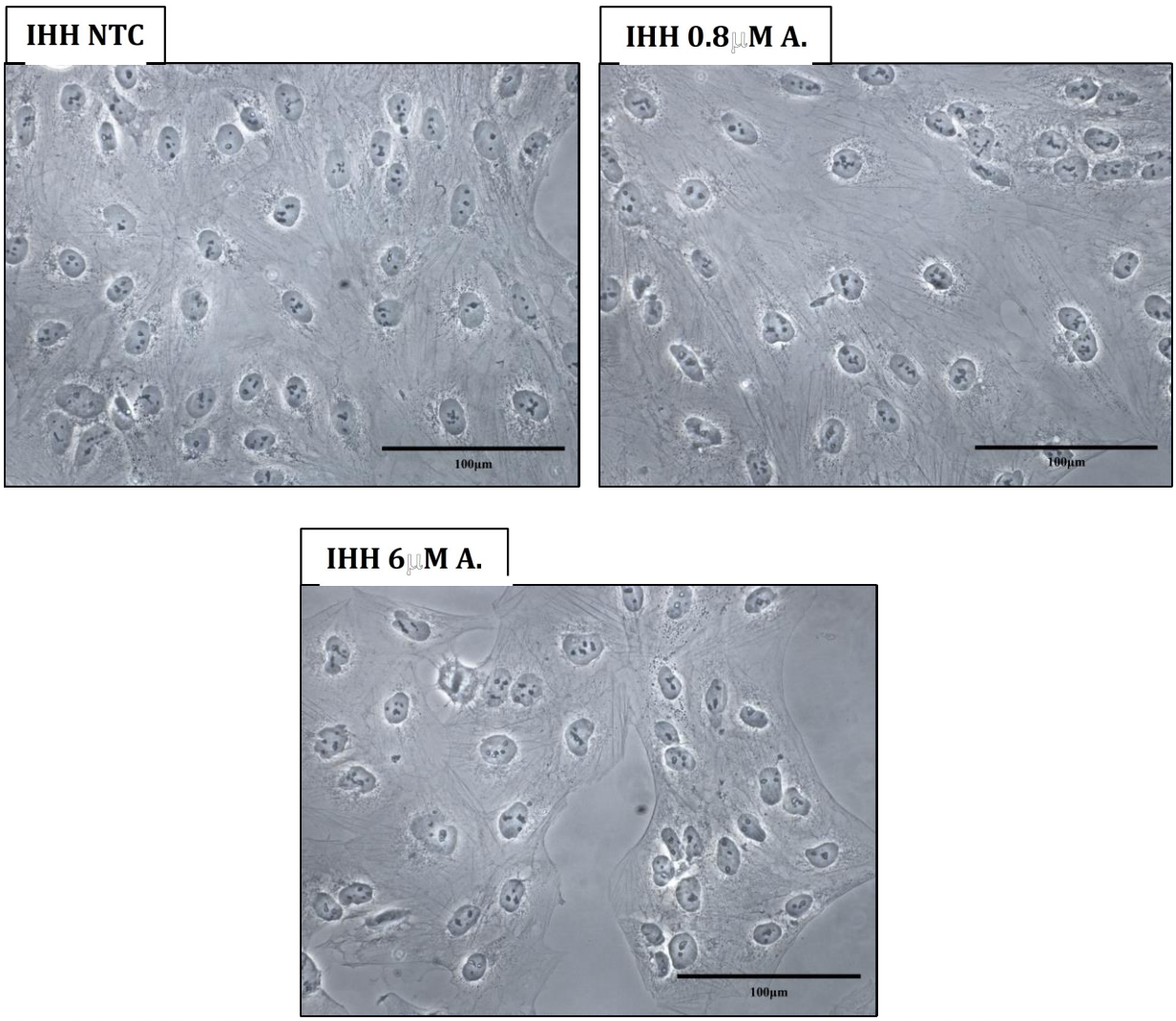

Fig. 4.3 – IHH cells morphology after 5-azacytidine treatments. Images are acquired with phase-contrast microscope (Leica DM 2000). Magnification 40X, (bar = 100µm).

Hepatocyte-like cells (obtained using a specific differentiation protocol developed by Prof. Elvassore's group, University of Padova [286]), the second non-tumor cell type considered, were not significantly affected by 5-azacytidine treatments. They maintained their typical polygonal shape without granules formation into the cytoplasm. Moreover, both plasma membranes and nuclei were smooth and regular (Fig.4.4).

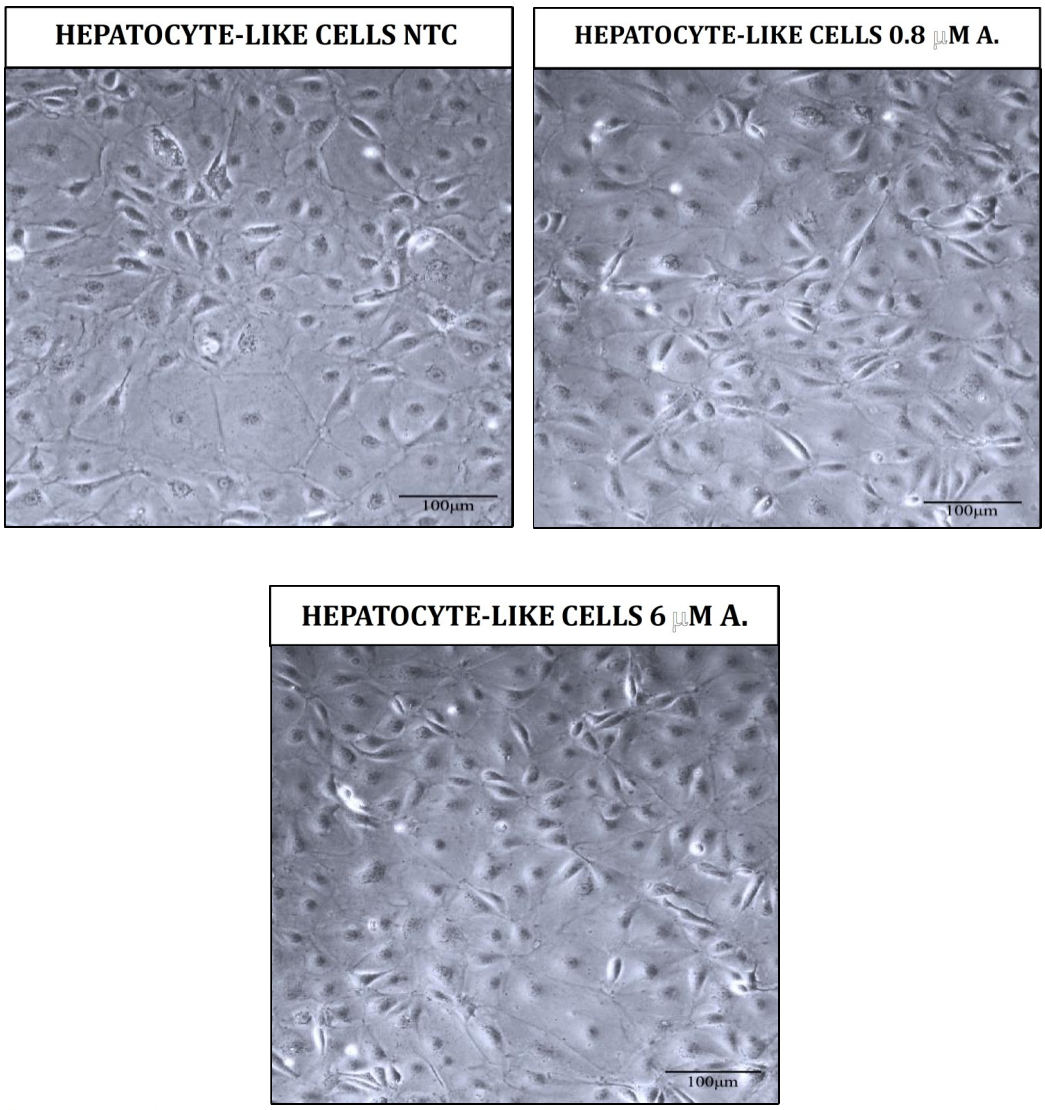

Fig. 4.4 – Hepatocyte-like cells morphology after 5-azacytidine administrations. Images are acquired with phase-contrast microscope (Leica DM 2000). Magnification 20X, (bar = 100µm).

Regarding cell counting, we noticed a reduction in the amount of JHH6 cells number of about 40% and 60% after the treatments with 0.8µM and 6µM of 5-azacytidine respectively (Fig. 4.5). In HuH7 cell line, cell number decreased of about 34% after the treatment with the lowest dose 0.8 µM. Instead, after the administrations of 6 µM and 30 µM of drug, the percentage of cells, respect to untreated cells, further decreased of about 50% and 75% respectively (Fig. 4.5). IHH cells were significantly affected only by treatments with the highest dose of drug. In fact, as shown in Fig. 4.5, IHH cell number was reduced of about 50% after the administrations of the 6µM dose. On the contrary, the number of hepatocyte-like cells was not decreased after the treatments with 0.8 µM and 6 µM doses of 5-azacytidine, indicating a higher resistance of these cells to the drug.

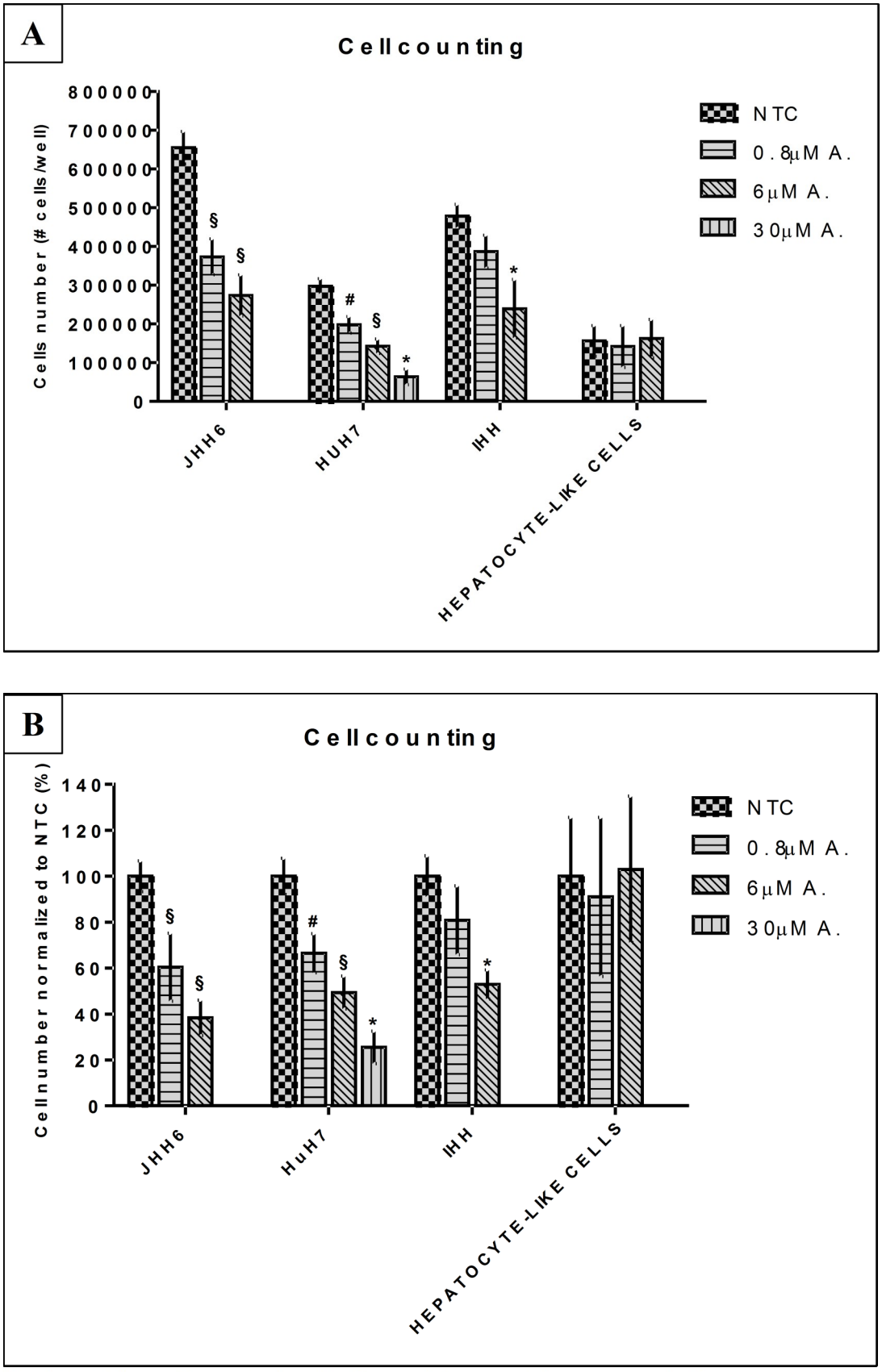

Fig. 4.5 – Cell counting evaluation after 5-azacytidine repeated treatments. (A) Data are expressed as cell number/well whereas in (B) data are expressed as a percentage and normalized to NTC. P#<0.05, P§< 0.005 and P*<0.0001 respect to NTC (Non Treated Cells). Data are expressed as mean ± SEM; n = 10.

4.1.2 Cell viability

We also studied the effect of 5-azacytidine treatments on cells viability. Performing MTT assay, which allows assessing cells metabolic activity and indirectly cell proliferation, we observed an increased sensibility of JHH6 compared to HuH7 (Fig. 4.6), in agreement with the cell counting data. Indeed, the highest dose of 30 μM inhibited the proliferation of HuH7 cells as much as the dose of 6μM in JHH6 cells (Fig. 4.6).

IHH cells were also affected by 5-azacytidine treatments even if their sensitivity was reduced compared to that of JHH6 cells and similar to that of HuH7 cells. IHH are immortalized hepatocytes and still own a high proliferative rate. Being that 5-azacytidine is incorporated into newly synthetized DNA, cells with higher proliferative ability incorporate more drug than the less proliferating ones. This can explain the effect of 5-azacytidine, which, however, is more contained than in the HCC tumor cells. As expected, due to the lower proliferation rate[286], hepatocyte-like cells did not have major detrimental effect on cell viability (Fig. 4.6). Compared to IHH, hepatocyte-like cells better resemble the features of mature hepatocytes, which, under physiological conditions, have a low rate of proliferation and start to grow mostly in response to liver injuries.

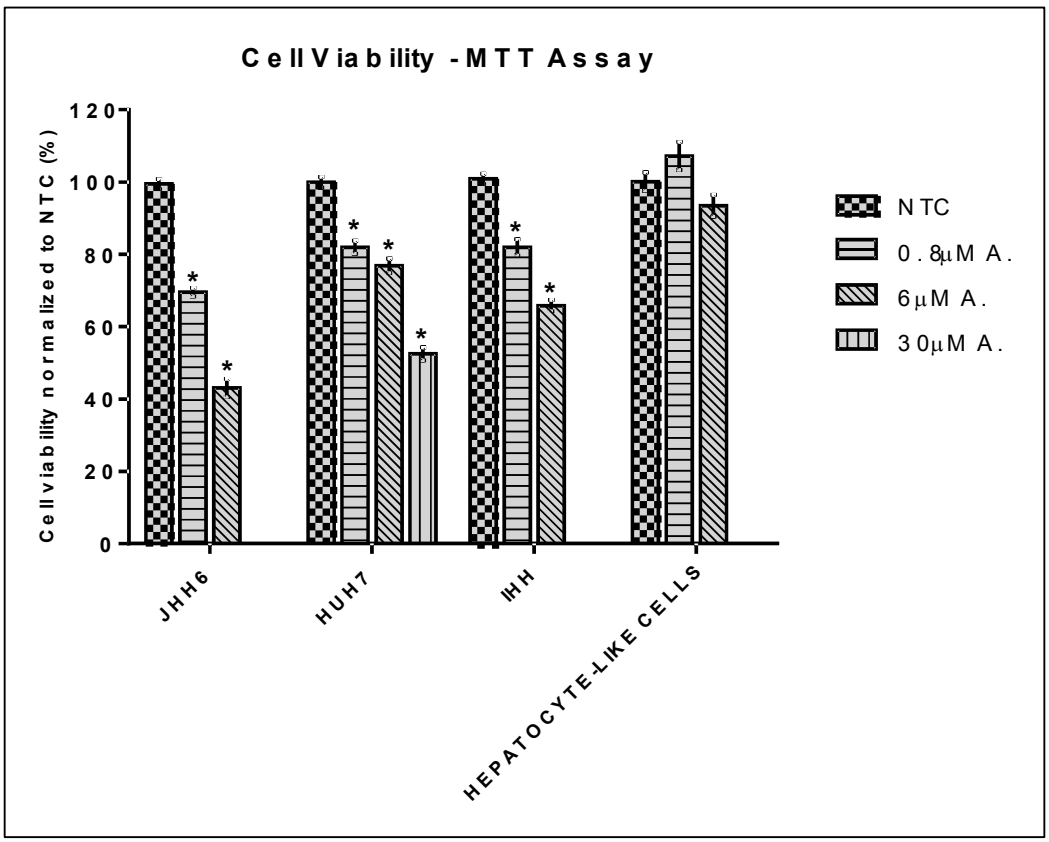

Fig. 4.6 – Cell viability evaluation after 5-azacytidine repeated treatments. P*< 0.0001 respect to NTC (Non Treated Cells). Data are expressed as mean ± SEM; n = 16.

4.1.3 Cell cycle phase distribution

Cell cycle progression was evaluated by flow cytometry after Bromodeoxyuridine (BrdU) pulse and DNA staining by Propidium Iodide (PI). This technique allows to identify the newly synthesized DNA which incorporated BrdU, and the total DNA content by the staining with PI, thus permitting to distinguish cells in the different phases of cell cycle[300].

In JHH6, treatments with 0.8μM and 6μM of 5-azacytidine caused a reduction of about 40% and 50% of S phase cells, respectively, compared to untreated cells, as reported in a representative experiment in Fig 4.7 and summarized in Fig. 4.8. We also noticed an increase in G1/G0 cells (36% after 0.8μM and 47% after 6μM treatments, respectively) compared to untreated cells. Moreover, an increase of about 34% (0.8μM treatments) and 46% (6μM treatments) of phase G2/M cells respect to untreated cells was observed.

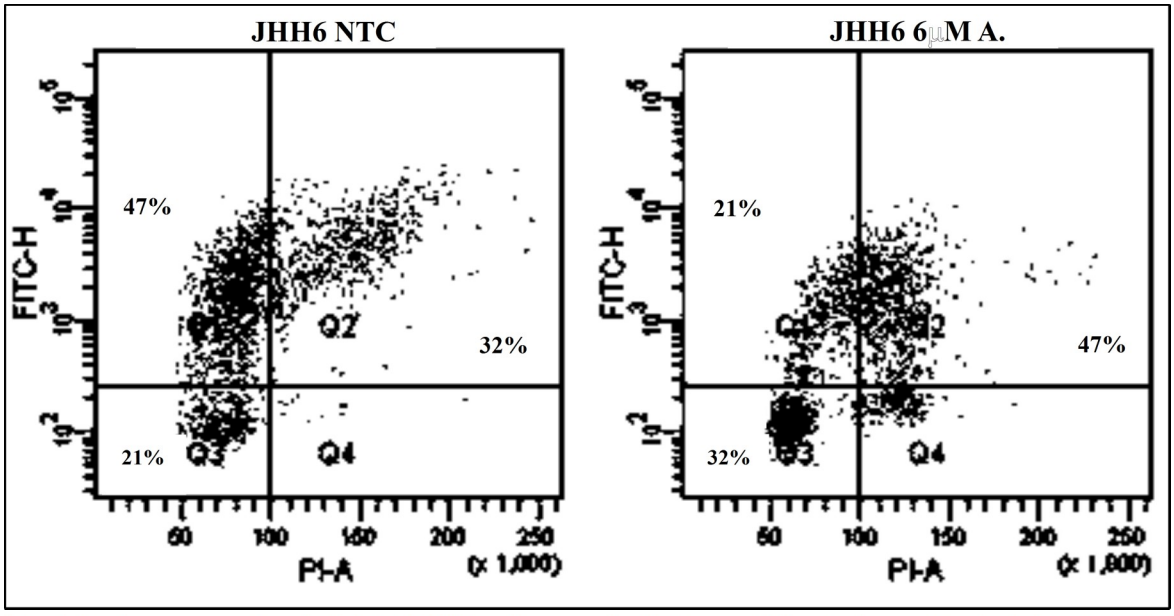

Fig. 4.7 – A representative dot blot of JHH6 cells treated with 5-azacytidine is shown. On the left untreated cells whereas on the right cells treated with the dose 6 μM. Q1: S-phase cells; Q2/Q4: G2/M phase cells; Q3: G1/G0 phase cells. PI-A: Propidium Iodide staining; FITC-H: FITC labeled Ig anti BrdU.

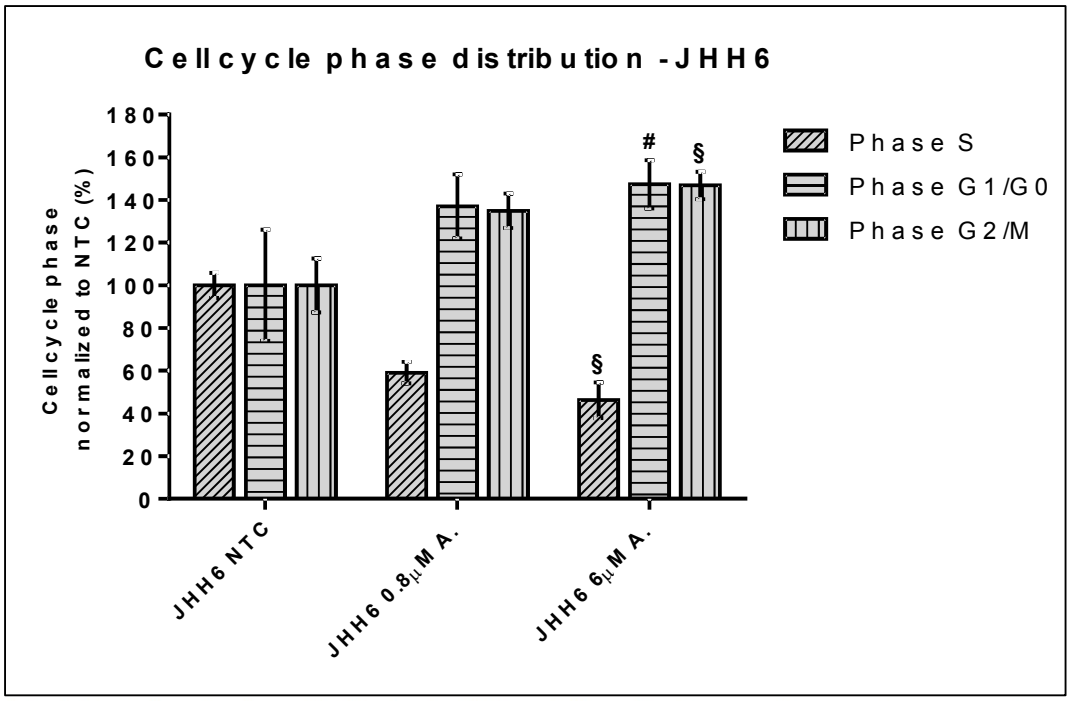

Fig. 4.8 – Cell cycle phase distribution in JHH6 cell line after 5-azacytidine repeated treatments. P#<0.05 and P§<0.005 respect to NTC (Non Treated Cells). Data, normalized to NTC, are expressed as mean ± SEM; n=6 for JHH6 NT and JHH6 6μM A.; n=2 for JHH6 0.8μM A.

HuH7 cells also responded in a dose-dependent fashion to 5-azacytidine. As shown in Fig. 4.9 and summarized in Fig. 4.10, the amount of S phase cells progressively decreased and the percentage of G1/G0-G2/M phase cells progressively increased.

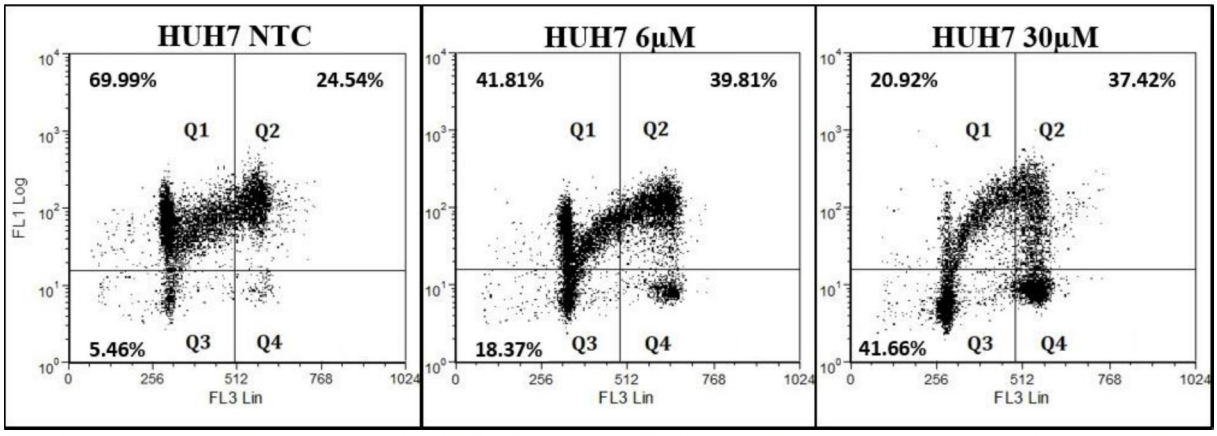

Fig. 4.9 – A representative dot blot of HuH7 cells treated with 5-azacytidine is shown. One the left untreated cells whereas in the middle and on the right cells treated with the doses 6μM and 30μM respectively. Q1:S phase cells; Q2/Q4:G2/M phase cells; Q3:G1/G0 phase cells. FL3 Lin: Propidium Iodide staining; FL1 Log: FITC labeled Ig anti BrdU.

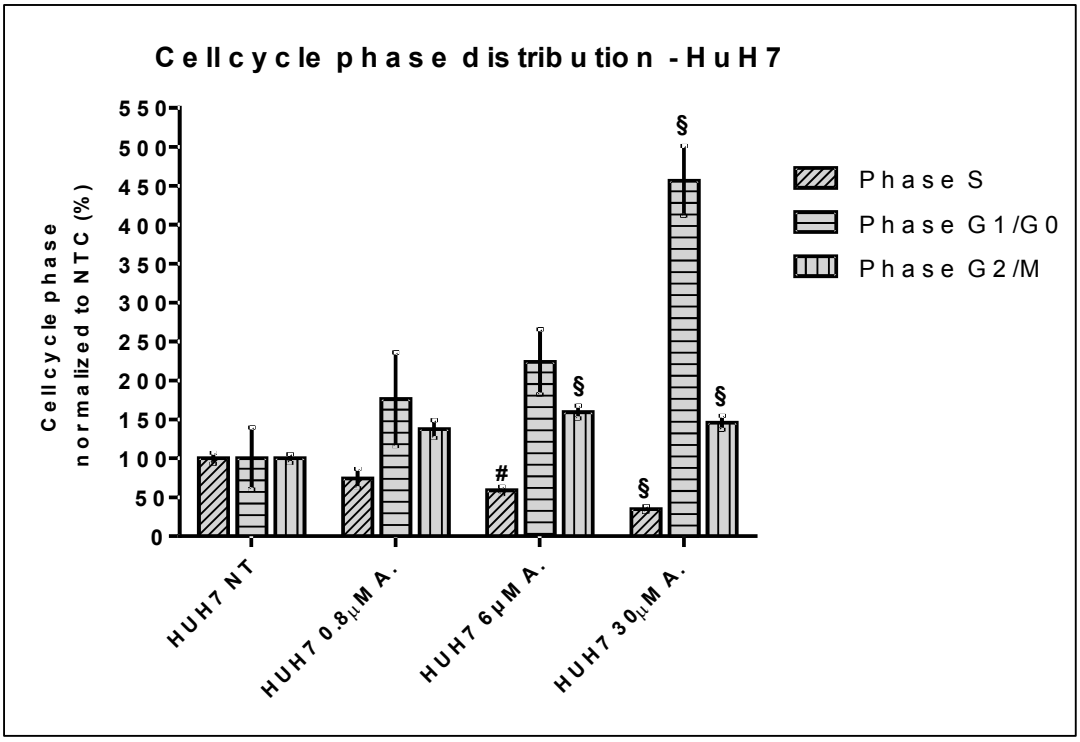

Fig. 4.10 – Cell cycle phase distribution in HuH7 cell line after 5-azacytidine repeated treatments. P#< 0.05, P§<0.005 respect to NTC (Non Treated Cells). Data are expressed as mean ± SEM; n=3 for HuH7 NT, HuH7 6μM A. and HuH7 30μM A.; n=2 for HuH7 0.8μM A.

Regarding cell phases distribution in IHH cell line, we observed differences only with the 6μM dose (Fig. 4.11 and in Fig. 4.12) where we observed a significant decrease of about 55% in S phase cell and a strong increase of cells in G2/M phase. Due to the extremely low proliferation rate of hepatocyte-like cells a cell cycle analysis was not possible.

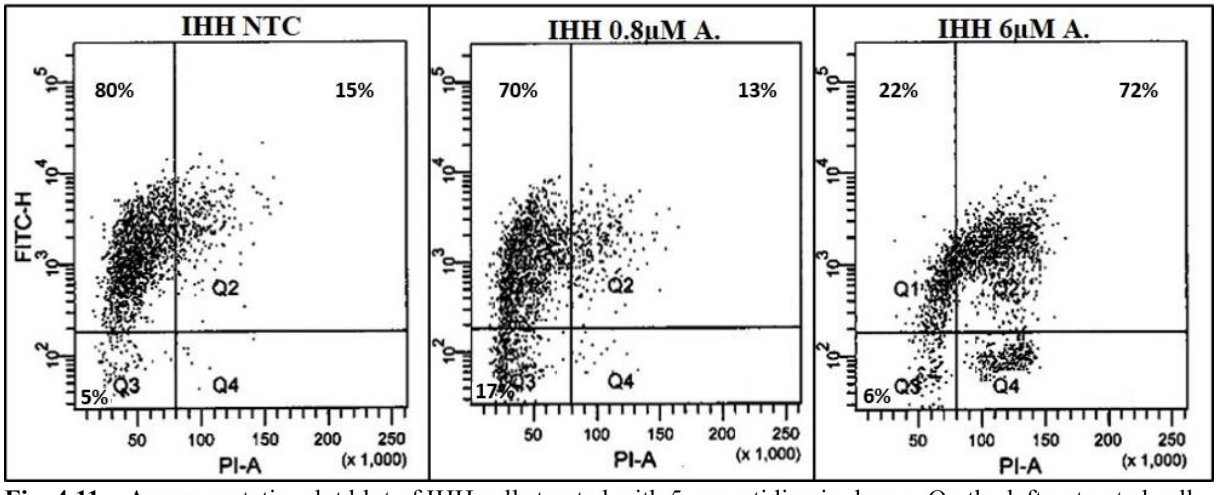

Fig. 4.11 – A representative dot blot of IHH cells treated with 5-azacytidine is shown. On the left untreated cells whereas in the middle and on the right cells treated with the doses 0.8 μM and 6 μM respectively. Q1:S phase cells; Q2/Q4:G2/M phase cells; Q3:G1/G0 phase cells. FL3 Lin: Propidium Iodide staining; FL1 Log: FITC labeled Ig anti BrdU.

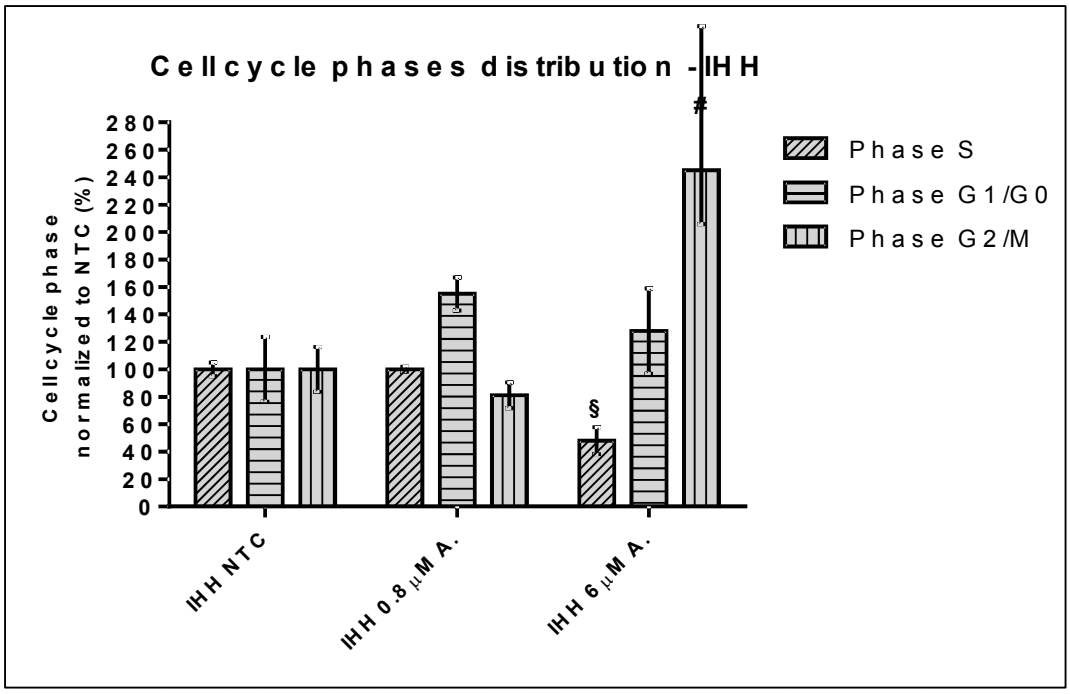

Fig. 4.12 – Cell cycle phases distribution in IHH cell line after 5-azacytidine repeated treatments. P#<0.05 and P§<0.005 respect to NTC (Non Treated Cells). Data are expressed as mean ± SEM. n=5 for IHH NTC and IHH 6µM A.; n=2 for IHH 0.8µM A.

4.1.4 Cell death

To check whether the 5-azacitydine could induce apoptosis in HCC cell lines and in IHH control cells, we performed western blotting analysis to evaluate the protein levels of some key apoptotic markers, including *PARP* and the pro-apoptotic protein *Bax*. Due to the fact that hepatocyte-like cell are produced in microplate [286], only a small amount of cell was available and thus they were not considered for further testing despite being the ideal control system.

PARP is a nuclear enzyme that catalyses the transfer of ADP-ribose polymers onto itself and other nuclear proteins in response to DNA strand breaks. During late apoptosis, PARP-1 is cleaved by Caspases 3 and 7 in two fragments of 89kDa and 24kDa respectively[301]. The cleavage inactivates PARP, preventing its binding to DNA[301]. We observed that both HCC cell lines showed no cleaved PARP bands thus indicating a negligible apoptosis following 5-azacytidine treatments (Fig. 4.13). A similar observation was done for IHH (Fig 4.14).

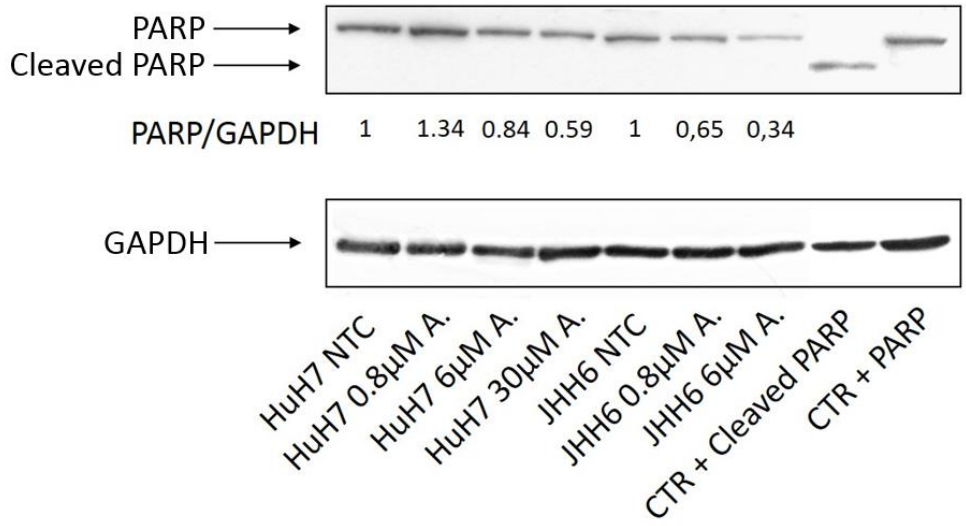

Fig. 4.13 – A representative immunoblotting for the detection of full cleaved and cleaved PARP isoforms in both HCC cell lines is shown. CTR + cleaved PARP is represented by Jurkat cells treated with 1μM of *Staurosporine*, a protein kinase inhibitor widely use to induce cell apoptosis, whereas CTR + PARP is represented by untreated Jurkat cells. The ratio between PARP and GAPDH is normalized to NTC (Non Treated Cells) of each cell line.

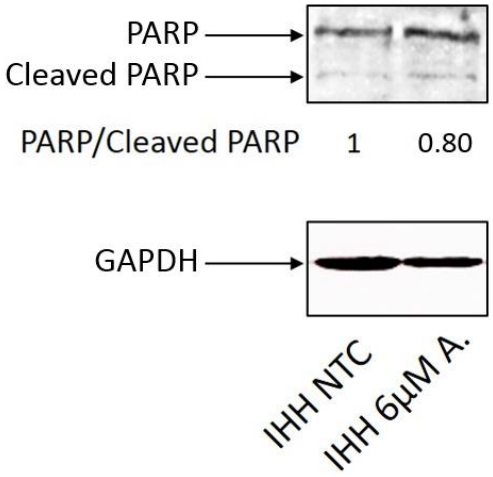

Fig. 4.14 – A representative immunoblotting for the detection of full length and cleaved PARP isoforms in IHH cell lines is shown. The ratio between full length PARP and cleaved PARP is normalized to NTC (Non Treated cells).

The lack of significant apoptosis was also confirmed by evaluating the expression levels of Bax protein, which is a pro-apoptotic member of Bcl-2 protein family and it has been shown to be involved in p53-mediated apoptosis [302]. As shown in Fig 4.15 and 4.16, the levels of Bax protein did not change significantly after 5-azacytidine treatments.

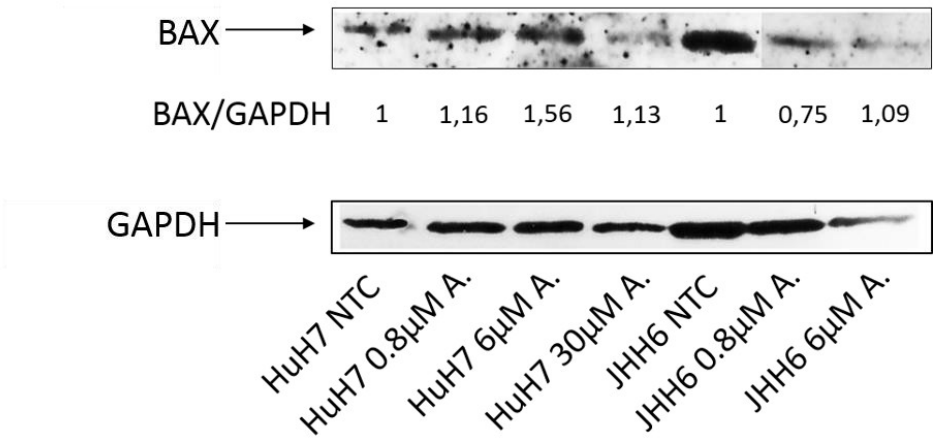

Fig. 4.15 – A representative immunoblotting for the detection of BAX in JHH6 and HuH7 cell lines is shown. The ratio between BAX and GAPDH is normalized to NTC (Non Treated Cells) of each cell line.

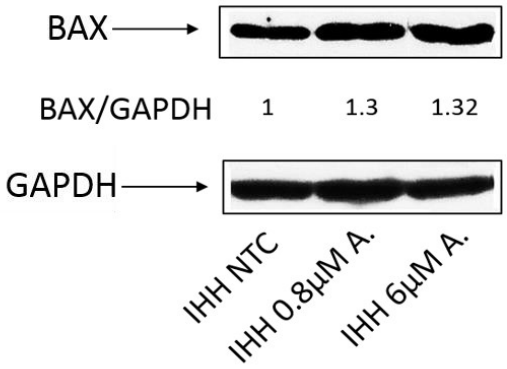

Fig. 4.16 – A representative immunoblotting for the detection of BAX in IHH cell lines is shown. The ratio between BAX and GAPDH is normalized to NTC (Non Treated Cells).

In agreement with the above observations, *Annexin V* test, which allows detecting the presence of phosphatidylserine on cell membranes of apoptotic cells, didn't show any significant percentage of apoptotic cells (Fig. 4.17).

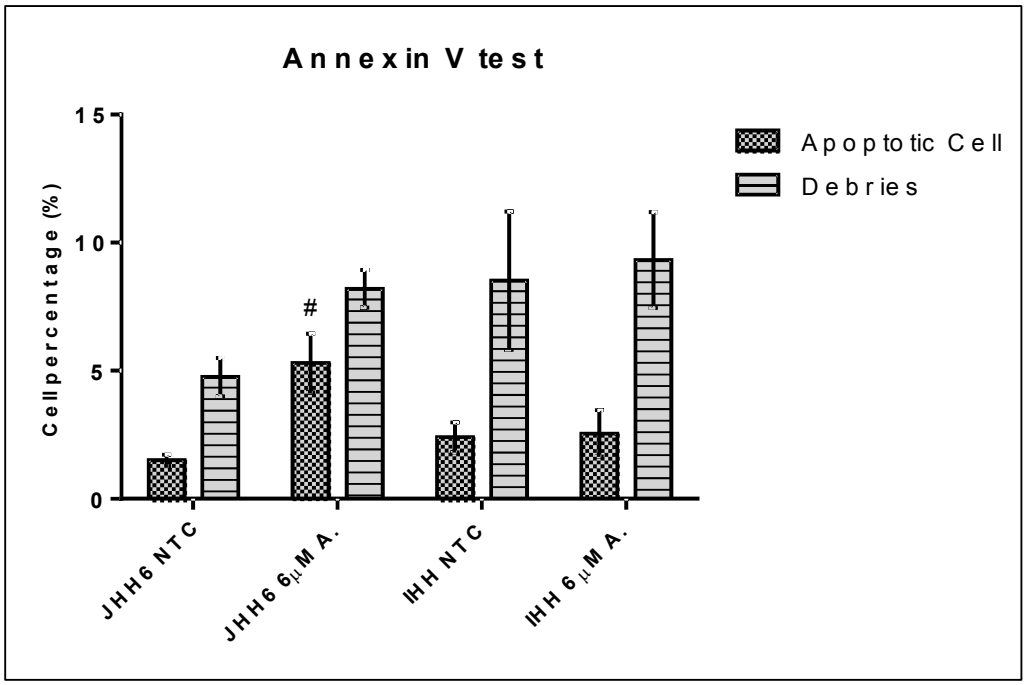

Fig. 4.17 – Apoptotic cell evaluation after 5-azacytidine repeated administrations. JHH6 and IHH cells are subjected to *Annexin V* test and analyzed by flow cytometry. P# < 0.05 respect to NTC (Non Treated Cells). n=4.

4.1.5 Necrosis

To fully characterizing the 5-zacytidine effects on the phenotype of the considered cell lines, we performed the *LDH assay* to evaluate the necrotic effect. This colorimetric assay allows to quantitatively measuring the enzymatic activity of *Lactate Dehydrogenase* (LDH), released into the medium by damaged cells, and thus considered a biomarker for cellular necrosis. As positive control, cells were treated with 10% Triton X-100, a non-ionic surfactant used to induce the complete cell lysis.

As shown in Fig. 4.18, no significant release of LDH was observed after 5-azacytidine administrations, both in tumor and control cell lines.

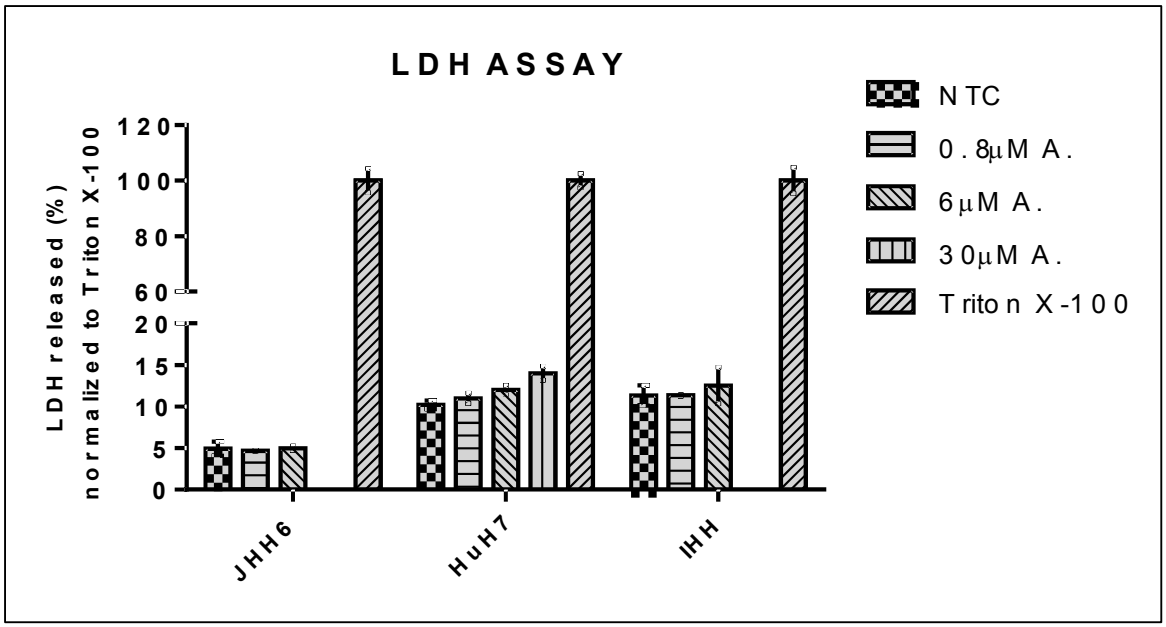

Fig. 4.18 – Measure of LDH released after 5-azacytidine administrations in JHH6, HuH7 and IHH cells. Data, normalized to Triton X-100, are expressed as mean ± SEM, n=12.

4.1.6 Cell migration

The effects of 5-azacytidine on tumor cells migratory ability were evaluated in the first instance by performing *Scratch assay*. This test allows evaluating the ability of the cells to fill in a gap generated with a tip on a cell monolayer. Scratch was performed the same day (day 3) of the last repeated treatment (see materials and methods, scheme 3.6) and healing was measured within 24 or 48 hours, depending on tumor cell line. Cells were maintained in complete medium with low FBS concentration (1%) in order to reduce as much as possible proliferation, a fact that can interfere with the evaluation of migration.

As shown in Fig. 4.19 and in Fig. 4.20, JHH6 migration was inhibited by about 40% and 75% after 0.8μM and 6μM administrations, respectively.

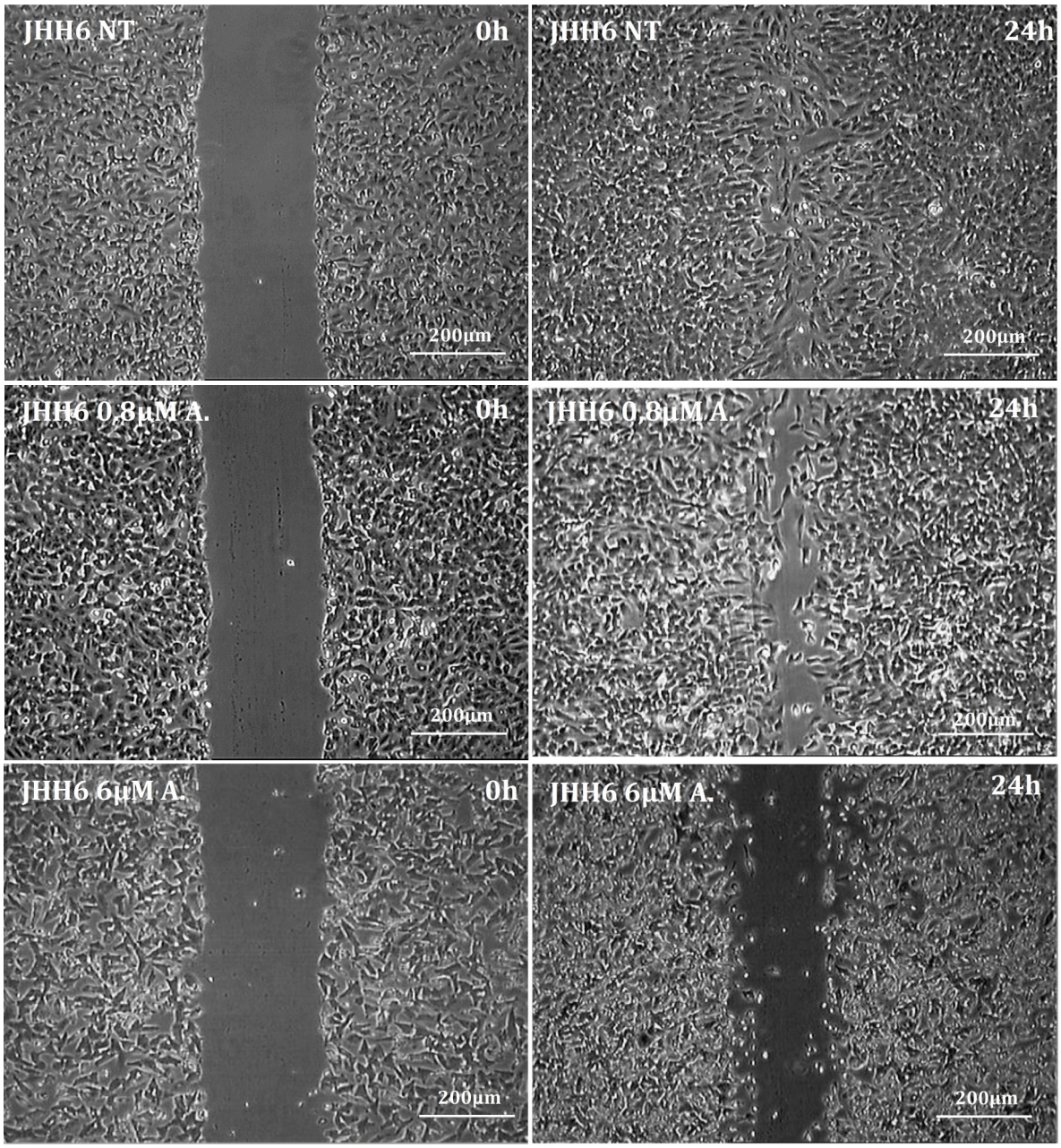

Fig. 4.19 – Representative images of *scratch assay* in JHH6 cells. Scratch is performed at the same day of last drug treatment and its healing is evaluated within 24 hours. Images are acquired with Leica DM IRB microscope. Magnification 5X (bar = 200µm).

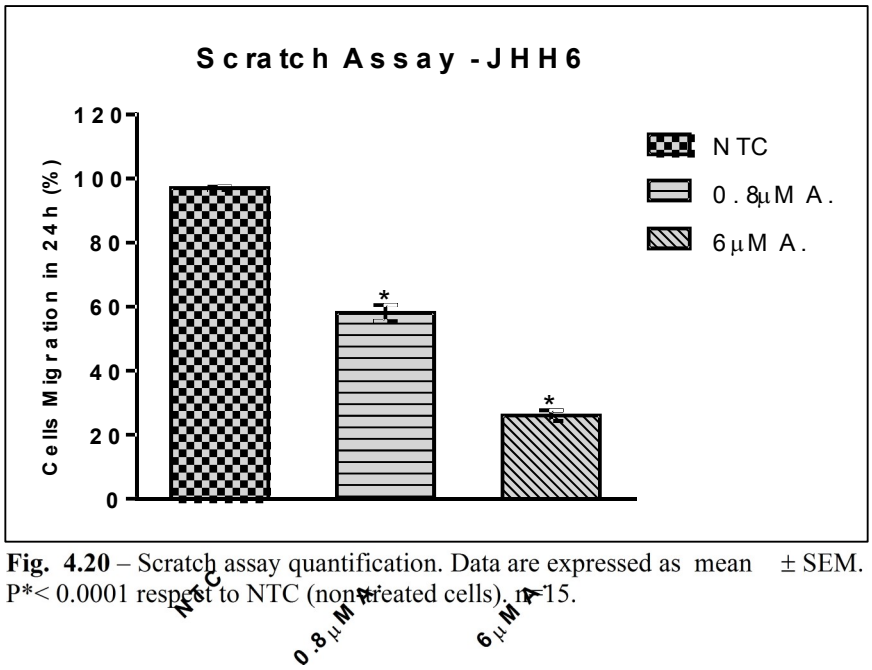

Fig. 4.20 – Scratch assay quantification. Data are expressed as mean ± SEM. P*< 0.0001 respect to NTC (non-treated cells). n=15.

To further characterize the anti-migratory effects of 5-azacytidine, we studied, in collaboration with Prof. Caserta and Prof Guido's group of Federico II's University, Naples, this phenomenon by time-lapse microscopy. In these set of experiments, in addition of being maintained in 1% FBS, cells were also treated by *Mitomycin C*, a compound able to block cell duplication[303]. Our data indicate that 5-azacytidine can significantly reduce the speed of migration (Fig. 4.21). Notably, *Mitomycin C*/5-azacytidine treated cells displayed a reduction in migration speed comparable to that of 5-azacytidine alone. This suggests that the reduction in cell migration due to 5-azacytidine, is not substantially influenced by cell proliferation.

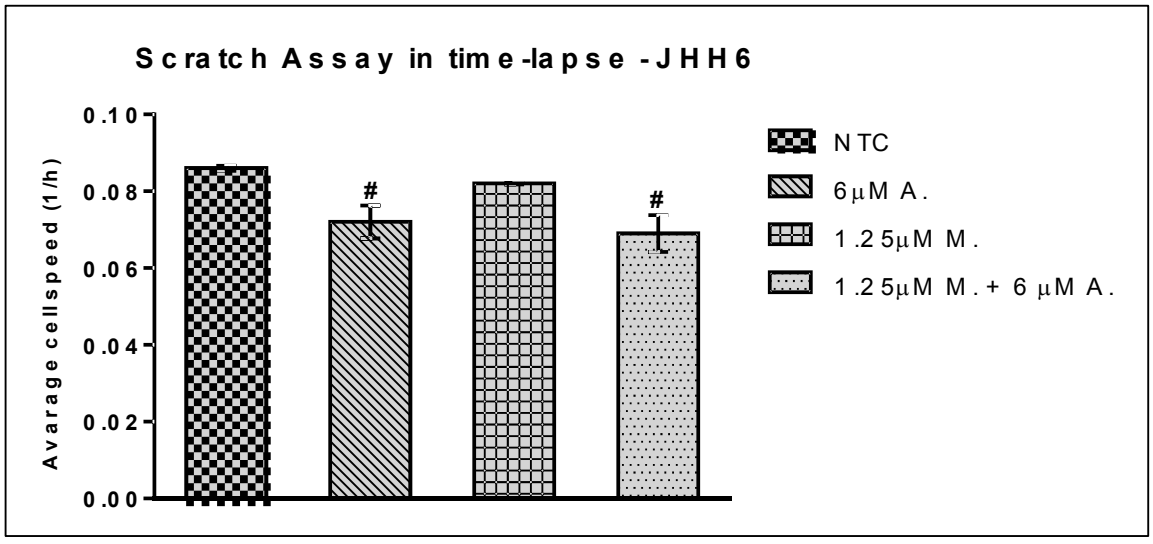

Fig. 4.21 – Quantification of scratch assay in time-lapse. Differences in terms of cell speed reduction are not observed between JHH6 treated with 5-azacytidine/Mitomycin C and cells treated with 5-azacytidine alone compared to each control. Data are expressed as mean ± standard deviation, n=3.

Also in the case of HuH7 cell line, we observed a dose-dependent decrease in cell migration (Fig 4.22 and Fig. 4.23). In particular, 0.8μM, 6μM and 30μM of 5-azacytidine reduced cell migration by about 30%, 40% and 70%, respectively.

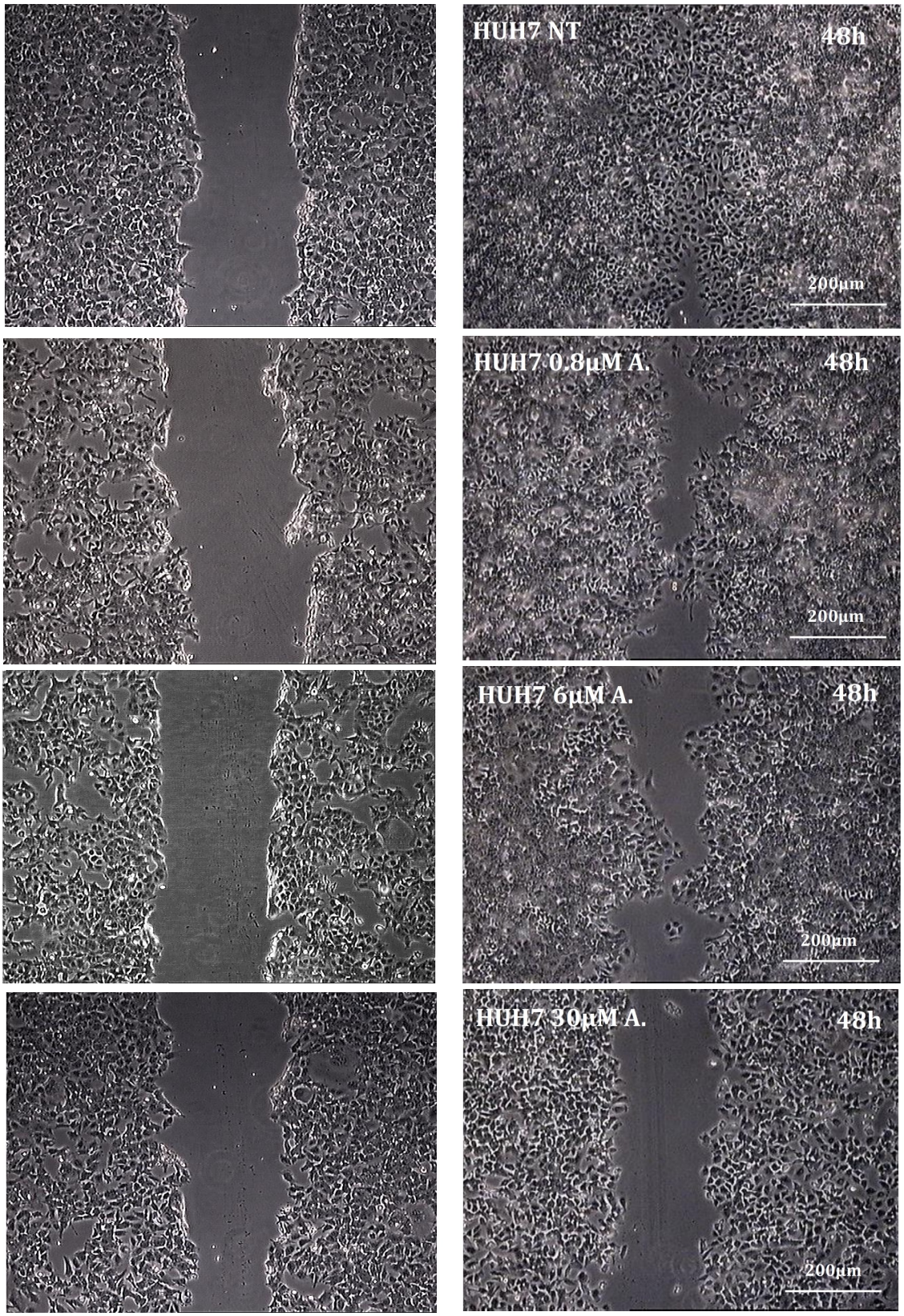

Fig. 4.22 – Representative images of *scratch assay* in HuH7 cells. Scratch is performed at the same day of last drug treatment and its healing is evaluated within 48 hours. Images are acquired with Leica DM IRB microscope. Magnification 5X (bar = 200μm).

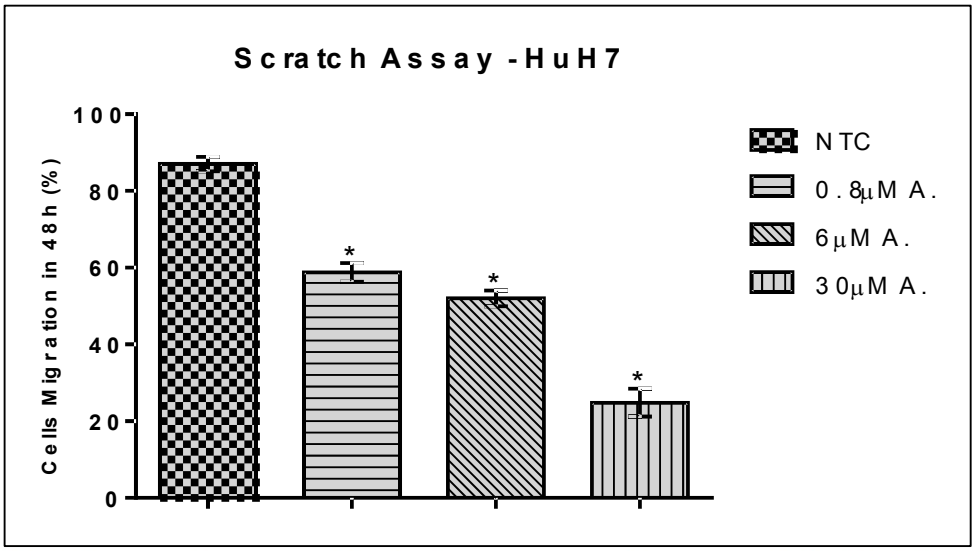

Fig. 4.23 – Scratch assay quantification. Data are expressed as mean ± SEM. P*< 0.0001 respect to NTC (Non Treated cells). n=15.

The migration test above reported were performed using cells cultured on plastic surface. To better mimicking the physiological situation where cells are in contact with the extracellular matrix, we used the FATIMA assay. This test allows to evaluate the ability of cells, stimulated by a serum gradient, to migrate through a membrane coated by extra-cellular matrix proteins[296]. The test involves the use of culture plate inserts containing a *polyethylene terephthalate* (PET) porous membrane. The cells, labelled by the vital fluorescent lipophilic cationic molecule *Dij*, go through the porous membrane and their amount can be then counted. Membranes of inserts are coated with Collagen IV, a key component of extra-cellular matrix; cell migration is evaluated hourly through spectrophotometric readings.

In JHH6 cells, we observed a dose-dependent decrease in cellular migratory ability, which reached 30% and 50% in cells treated with 0.8μM and 6μM of 5-azacytidine respectively after 7 hours (Fig. 4.24).

In HuH7 cells, we also observed a powerful decrease in cell migration. As shown in Fig 4.25, the doses 6μM and 30μM of drug reduced of about 50% the cell migratory capability compared to non-treated cells. Comparable results were obtained using collagen type I (data not shown). This indicates that the anti-migratory effect of 5-azacytidine is maintained also in the presence of different components of the extracellular matrix, thus giving a general value to our observations.

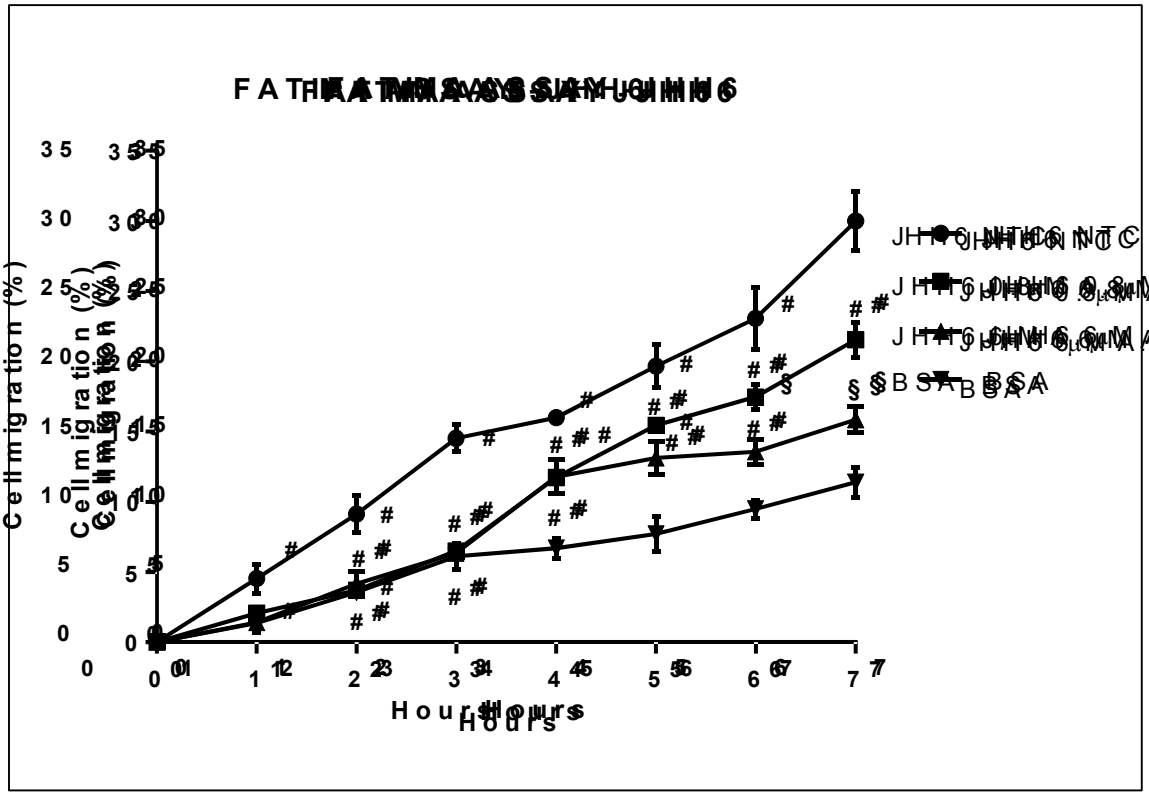

Fig. 4.24 – Evaluation of cell migration percentage in JHH6 cell line by FATIMA assay. Stimulated by a serum gradient, JHH6 cells migrate through collagen IV coated membranes of specific culture plate inserts. Cell migration is evaluated hourly through spectrophotometric readings. Data are expressed as mean ± SEM. P#< 0.05 and P§<0.005 respect to NTC (Non Treated Cells). n=4.

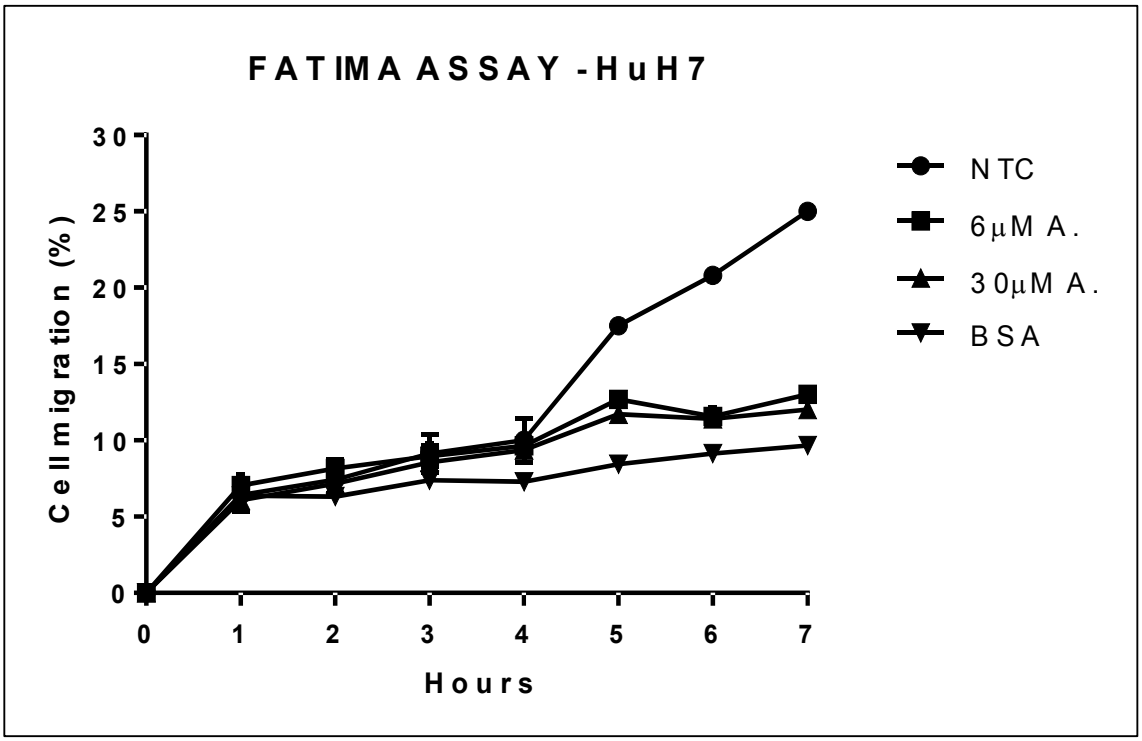

Fig. 4.25 – Evaluation of cell migration percentage in HuH7 cell line by FATIMA assay. Stimulated by a serum gradient, HuH7 cells migrate through collagen IV coated membranes of specific culture plate inserts. Cell migration is evaluated hourly through spectrophotometric readings. Data are expressed as mean ± SEM. n=2.

Moreover, we studied the alterations of the adhesion ability of tumor cells to the growth surface, which resulted to be reduced by 5-azacytidine treatments in a dose-dependent way (data not shown).

4.1.7 Cytoskeletal structure

As above reported, 5-azacytidine affects cellular proliferation and migration, two biological phenomenon strictly correlated with the remodelling of the cytoskeleton structure. To explore the 5-azacytidine effects on the structure of cytoskeleton, we performed cell immunostaining assay in treated and non-treated cells. In particular, we focussed on the detection of β-tubulin, a protein that polymerizes into microtubules, a major component of the eukaryotic cytoskeleton[304]. Most JHH6 cells treated by 5-azacytidine appeared to increase in size and to be either multinucleated or to show nuclear fragmentation, in contrast to non-treated cells. Furthermore, treated cells showedβ-tubulin accumulation in the peri-nuclear region (Fig. 4.26).

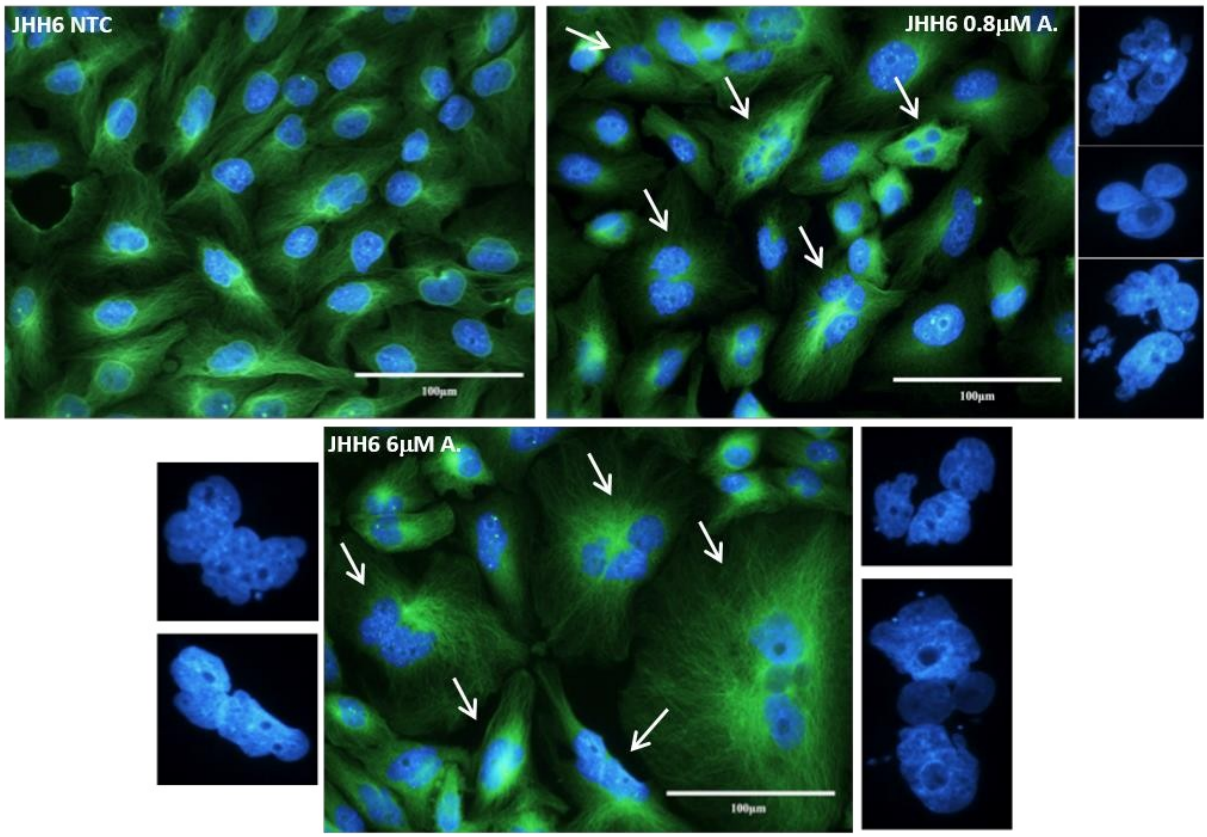

Fig. 4.26 – Immunostaining of β-tubulin in JHH6 cells. Treated cells show multinuclear formations and peri-nuclear tubulin accumulation (white arrows) whereas non-treated cells own regular nuclei and structured organization of β-tubulin. Images are acquired with Leica DM 2000 microscope. Green = β-tubulin, Blue=DAPI. Magnification 40X. (bar=100µm)

These phenotypic features together with the absence of pro-apoptotic markers (see Fig 4.13-Fig. 4.16) and the block of cells in G2/M phase, suggest that 5-azacytidine could induce a specific phenomenon known as *Mitotic Catastrophe* [305]. *Mitotic catastrophe* is characterized by the occurrence of aberrant mitosis, or mis-segregation of the chromosomes, followed by cell division and inhibition of the dynamic reorganization of microtubules. Nuclear envelopes form around individual chromosomes or groups of chromosomes forming large non-viable cells with multiple micronuclei, which are morphologically distinguishable from apoptotic cells[305]. In JHH6 cell line, we analyzed also the expression of a major mitotic catastrophe marker, phospho-Ser10 histone H3 [306]. We noticed that 5-azacytidine-treated cells showed a higher amount of phospho-Ser10 histone H3 compared to un-treated ones. These evidences suggested that 5-azacytidine treatments may induce cell death via mitotic catastrophe.

HuH7 cells showed morphological features similar to those of JHH6. As shown in Fig. 4.27, the drug treatment induced an increased size, multi-nucleation or nuclear fragmentation and β-tubulin accumulation at a peri-nuclear level (white arrows) in a dose-dependent manner.

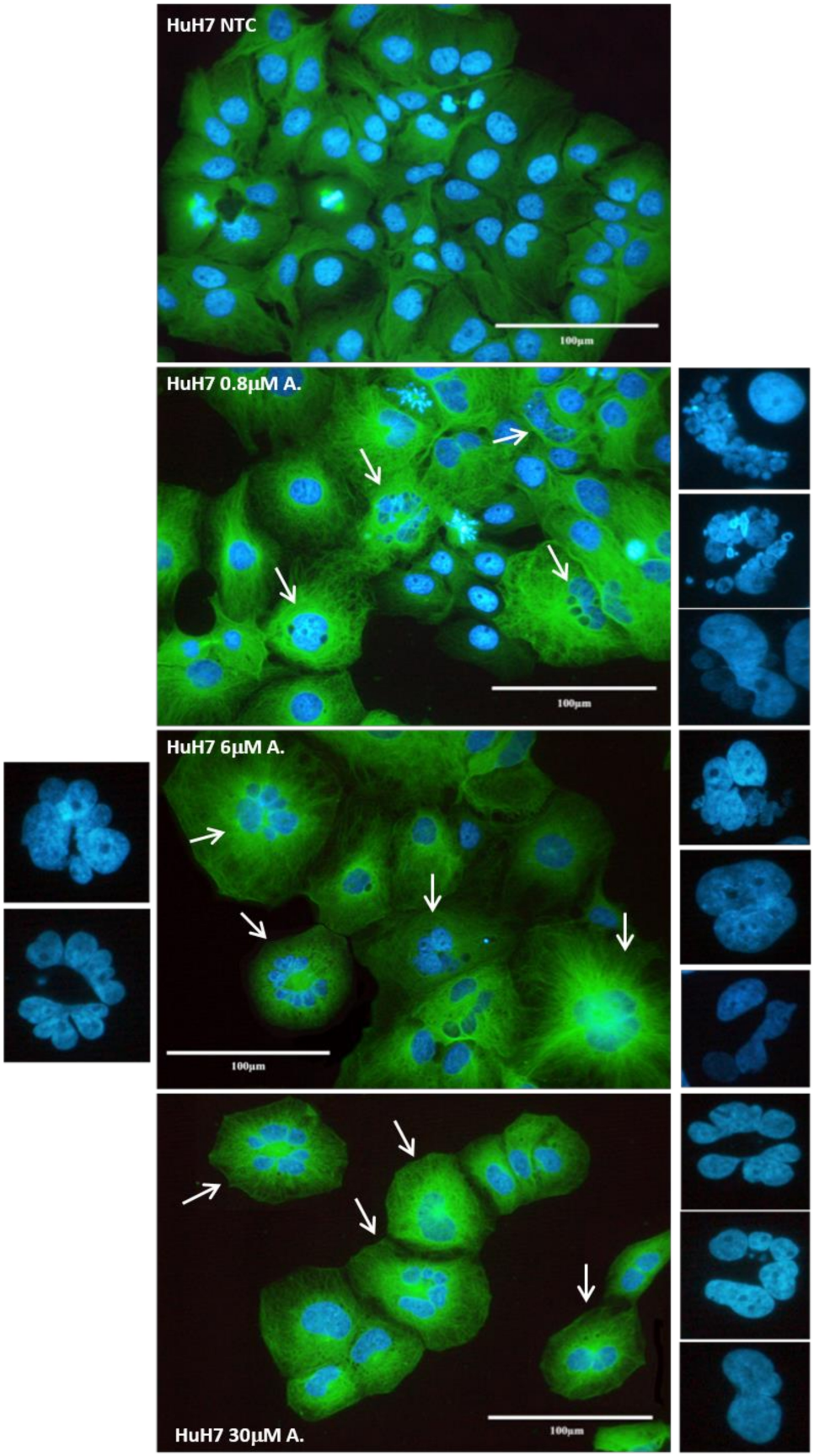

Fig. 4.27 – Immunostaining of β-tubulin in HuH7 cells. Treated cells show multinuclear formations and peri-nuclear tubulin accumulation (white arrows) whereas non-treated cells own regular nuclei and structured organization oβ-tubulin. Images are acquired with Leica DM 2000 microscope. Green=β-tubulin, Blue=DAPI. Magnification 40X. (bar=100µm).

Regarding IHH cells, they didn't seem particularly affected by 5-azacytidine treatments. As shown in Fig. 4.28, they generally kept regular nuclei and a structured distribution of β-tubulin without significant accumulation at a peri-nuclear level. In addition, the cell size was maintained compared to untreated cells. This observation is in line with the reduced sensitivity of this control cell line toward 5-azacytidine effects (see the above results).

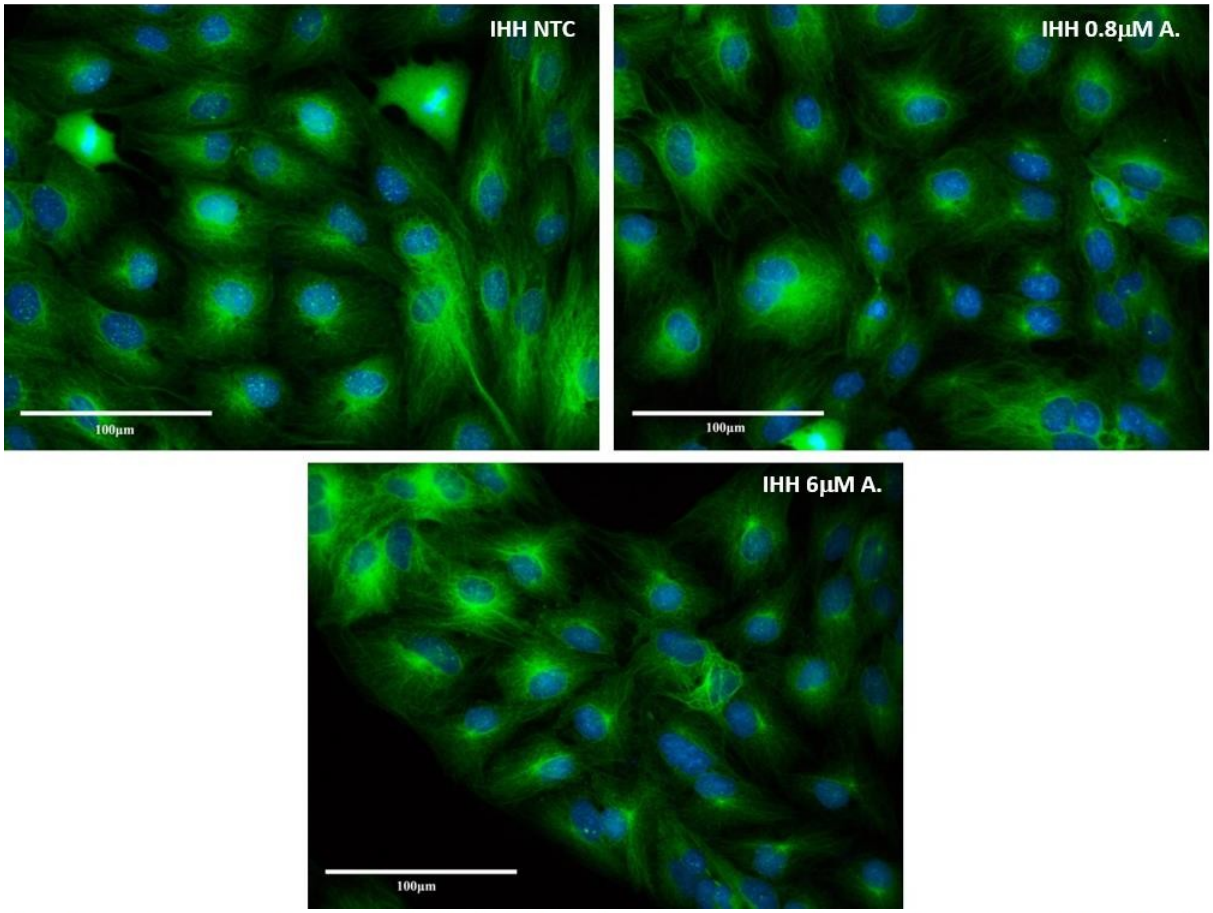

Fig. 4.28 – Immunostaining of β-tubulin in IHH cells. After 5-azacytidine administrations, IHH cells show regular nuclei and structured β-tubulin organization as shown in untreated cells. Images are acquired with Leica DM 2000 microscope. Green = β-tubulin, Blue=DAPI. Magnification 40X (bar=100µm).

4.2 Molecular effects of 5-azacytidine *in vitro*

The important phenotypic effects observed for 5-azacytidine, prompted us to explore the molecular mechanisms responsible for these phenotypes. The investigation is based on our previous analysis conducted at the gene and miRNA expression level. The results about the gene and miRNA expression profile are summarized in the next two paragraphs.

4.2.1 Gene expression profile

The data we obtained by microarray analysis, suggested that in JHH6 cell line 5-azacytidine (6μM) induced the deregulation of about 2200 genes. Many of these were involved in cellular processes such as cell cycle regulation, cell communication and adhesion, cell death and cell proliferation and growth. Thanks to freely available software, it was possible to get specific information about the biological, biochemical and molecular functions of the proteins encoded by the differentially regulated mRNA. The software that we used for the analysis is called *Onto-Express*. This is a novel tool able to automatically translating such lists of differentially regulated genes into functional profiles[307]. *Onto-Express* builds functional profiles for the following categories: biochemical function, biological process, cellular role, cellular component, molecular function and chromosome location. Statistical significance values are calculated for each category[307]. The Onto-Express analysis revealed that about 60% of the deregulated genes (1313) were involved in the most important cellular processes, such as cell cycle regulation, proliferation and cell death. Deregulated genes were also associated with metabolic processes and their regulation. In Fig. 4.29 it is reported a pie chart showing all the molecular processes in which the deregulated genes are involved.

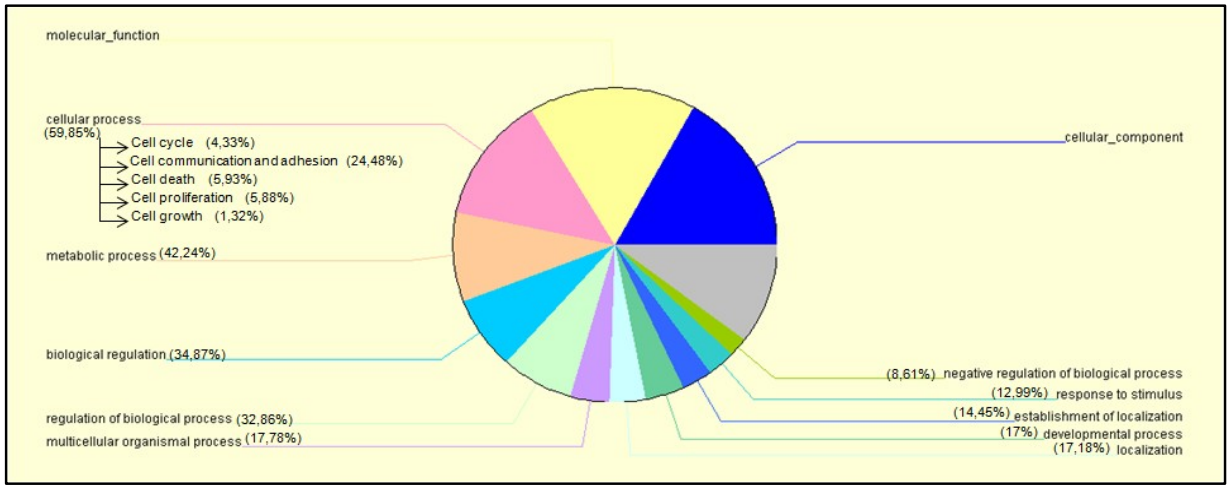

Fig. 4.29 – Pie chart obtained by Onto-express is shown. The chart represents all the different biological and molecular processes in which genes de-regulated by 5-azacytidine repeated treatments are involved.

Another software that we have used to analyse data obtained by microarray analysis, is *Pathway-express*. *Pathway-express* is a tool for the analysis of signalling pathways that allows understanding in which signalling pathways are placed proteins encode by the deregulated genes[308]. The analysis allows to obtain different cartoons specific for each pathway showing the up or down-regulation of proteins based on the up or down-regulation of their mRNAs. Pathways are listed based on their statistical significance expressed by an

Impact Factor value [308]. An output example obtained from *Pathways-expressed* is shown in Fig. 4.30.

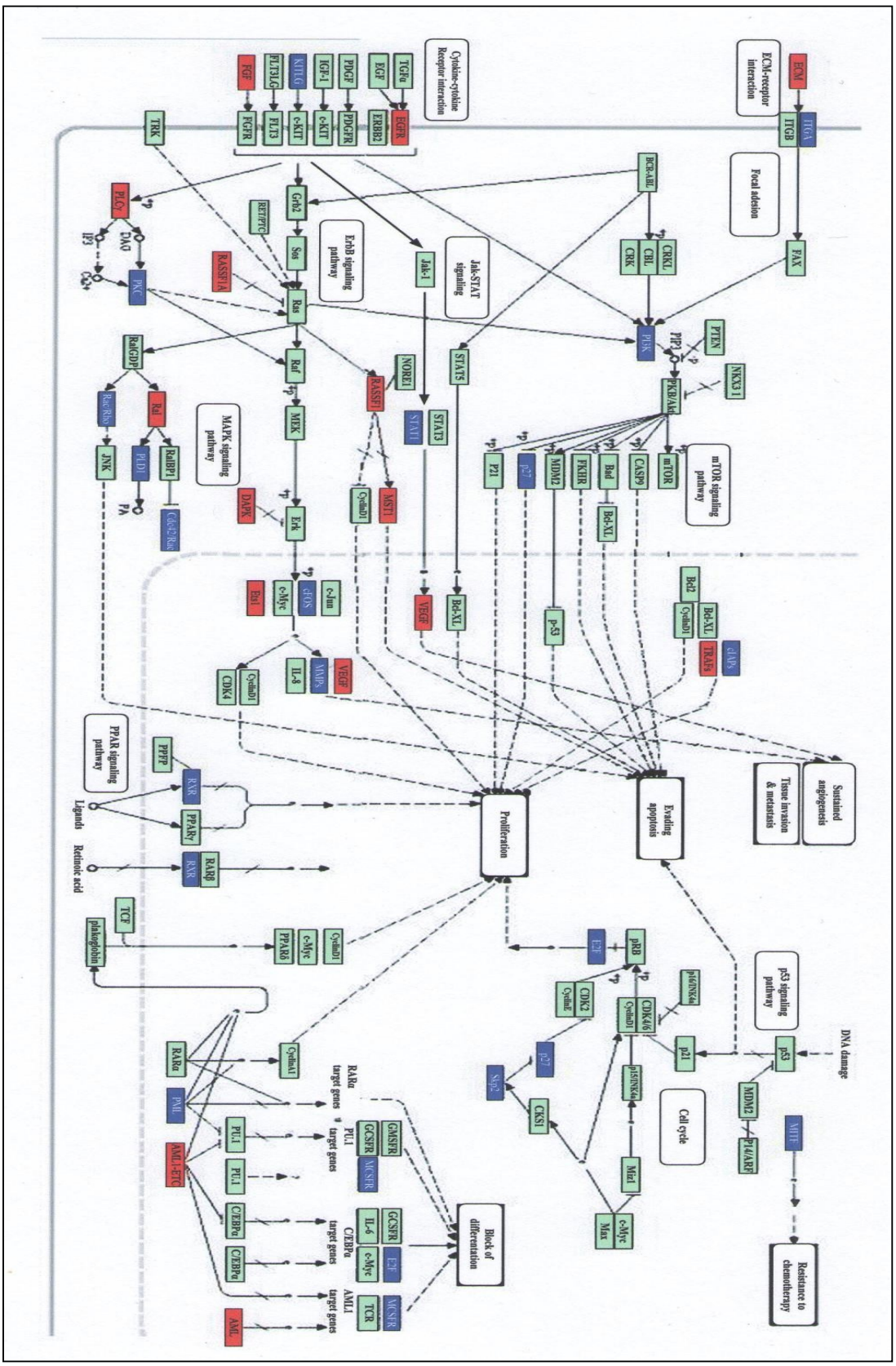

Fig. 4.30 – A summary scheme obtained by Pathway-express showing the main biological pathways in which several deregulated genes are involved. Impact Factor = 60.2; p=0.013

The analysis carried out by *Pathway-Express* shows a significant down-regulation of genes belonging to the E2F transcription factors family. The E2F transcription factors are key regulators of cell cycle progression that can be divided into 4 subgroups based on their main function, i.e. activation or inhibition of cell proliferation. The activating E2Fs, that include E2F1, E2F2 and E2F3 are required for the transactivation of target genes involved in the G1/S transition and, hence, for the correct progression through the cell cycle [309]. E2F1, E2F2 and E2F3 resulted to be down regulated after 5-azacytidine treatments (6μM) in JHH6 (Tab 4.1). E2F7 belongs to E2F7 subgroup and are considered to be transcriptional repressor [309]. Acting with E2F8, E2F7 negatively regulates E2F1 transcription blocking cell proliferation[309]. Notably, in the microarray analysis, E2F7 resulted to be significantly up regulated (Tab 4.1).

Always regarding cell proliferation, an important oncogene that resulted to be down regulated after 5-azacytidine treatments, was PI3K. PI3K pathway is a critical signal transduction system linking oncogenes with multiple receptor classes and with many essential cellular functions[118]. It is perhaps the most commonly activated signalling pathway in human cancer.

Another important proto-oncogene that resulted strongly down regulated by 5-azacytidine was c-FOS, which belongs to Fos transcription factors family. C-FOS encodes a 62kDa protein, which forms heterodimer with c-Jun, resulting in the formation of AP-1 complex[310]. In turn, this complex binds DNA at AP-1 specific sites present on promoter and enhancer regions of target genes thus converting extracellular signals into changes of gene expression[310]. It is known that c-Fos and AP-1 complex plays an important role in many cellular functions and it has been found to be overexpressed in a variety of cancers.

With regard to cell migration, we noticed that 5-azacytidine treatments decreased the mRNA levels of different genes associated with the migration process. For example Fibronectin 1, a glycoprotein of the extracellular matrix, resulted significantly down regulated. Fibronectin 1 is involved in cell adhesion, growth, migration and differentiation. Fibronectin has also been implicated in carcinoma development [311]. For example in lung carcinoma, Fibronectin expression is increased, especially in non-small cell lung carcinoma[311]. The adhesion of lung carcinoma cells to Fibronectin enhances tumorigenicity and confers resistance to apoptosis-inducing chemotherapeutic agents[311].

Genes that encode for several integrin subunits were also down regulated, including β4 subunit, αX subunit and α3 subunit. Both Fibronectin 1 and integrins are key regulators of cell migration process. Integrins activation promotes many signalling pathways causing invasion, migration and proliferation and in fact they result up-regulated in actively migrating cells, as

are tumour cells[312]. In addition to regulate cell migration and adhesion, integrins are also involved in the cytoskeletal re-organization[312].

Two other important genes that were deregulated after 5-azacytidine administrations were MMP2 and TIMP3. MMP2 belongs to *Gelatinases* family and plays a key role in the degradation of type IV collagen and gelatine, the two main component of ECM [313]. Increased expression of MMP2 and MMP9, the second component of Gelatinases family, is reported in many tumours, including ovarian, breast, prostate tumours and melanoma[313]. A significant association has been reported between tumour aggression and increased levels of MMP-2 and MMP-9 in many experimental and clinical studies[314]. Increased MMP-2 and MMP-9 expression has also been documented to correlate with cancer invasion[314]. TIMP-3 is an inhibitor of MMPs and was shown to induce apoptosis and inhibit growth of tumour cells and is, thus, consider to be a tumour suppressor[315]. It has been also frequently observed the promoter methylation of TIMP-3 in adenocarcinomas of the oesophagus and stomach. Notably, the impairment of TIMP-3 expression seems to be of clinical and prognostic relevance in these cancers[315].

Finally, genes ATF3, ATF4 and DDI3 were found to be significantly up regulated after 5-azacytidine treatments. ATF3 and ATF4 are members of ATF/CREB family of transcription factors and play a key role in stress responses [316]. In the last years, many evidences suggested an important role of these proteins also in migration processes. For example, a recent study demonstrated that AFT3 suppressed metastasis of bladder cancer and its decreased expression was also associated with bladder cancer progression and reduced survival of patients[317]. It has been also showed that ATF3 promotes the formation of MDM2/ATF3/MMP2 complex that facilities the degradation of MMP2, which subsequently leads to inhibition of cell invasion, in oesophageal squamous cell carcinoma [318]. DDIT3, also called CHOP, is a bZip transcription factor belonging to C/EBP family. DDIT3 is a key ER stress-response product involved in cell death. A recent study suggested that suppressing ER-MAPKs-CHOP signalling axis by using either inhibitors (4-PBA, SP, SB, or U0126) or knocking-down CHOP expression, did not grossly affect the rate of cell death but showed prominent effects on cell migration in HCC cell lines[319].

Cellular Processes	Gene	Fold change (NTC Vs 6μM A.)
Cell cycle	E2F1	-2.57
	E2F2	-2.36
	E2F7	+3.6
Cell Proliferation	PI3K	-2.57
	C-Fos	-11.96
Cell Migration	Fibronectin 1	-10.2
	B4 integrin subunit	-16.7
	αX integrin subunit	-4.2
	A3 integrin subunit	-2.66
	RAC	-2.16
	MMP2	-7.9
	TIMP3	+2.3
Stress response and cell migration	ATF3	+6.94
	ATF4	+4.38
	DDIT3	+8.31

Table 4.1 – Fold change values of genes, which are differentially expressed after 5-azacytidine treatments (6μM). Genes are divided on the base of the cellular process in which they are usually involved. Genes differentially expressed in treated cells respect to untreated ones are identified using a $p \leq 0.05$.

In this thesis, we confirmed by qRT-PCR the differential regulation of some of the above genes deregulated by 5-azacytidine. As shown in Fig. 4.31, we confirmed the effective down-regulation of E2F1, E2F2 and E2F3 in JHH6 cells and the significant up-regulation of E2F7. With regard to genes involved in cell migration process, qRT-PCR confirmed the dose-dependent up-regulation of ATF3, ATF4 and DDIT3 and the significant down-regulation of MMP2 mRNA levels following 5-azacytidine treatments (Fig. 4.32).

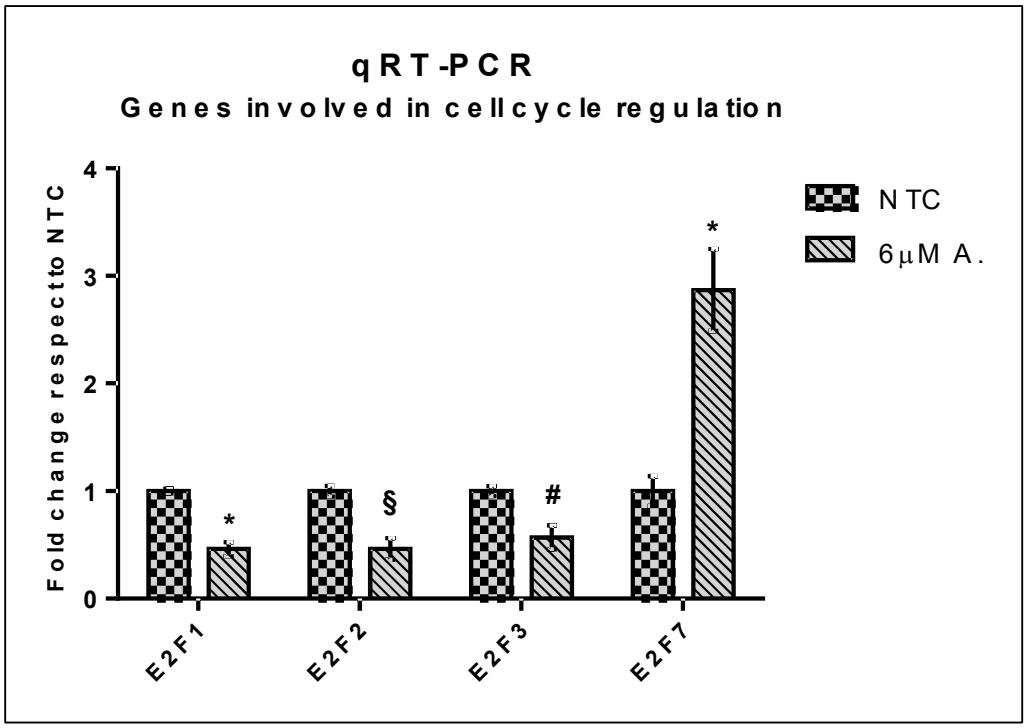

Fig. 4.31 – Analysis of mRNA expression levels of genes involved in cell cycle regulation by qRT-PCR in JHH6 cells. P#<0.05, P§< 0.005 and P*<0.0001 respect to NTC (Non Treated Cells). Data, normalized to NTC, are expressed as mean ± SEM, n=9.

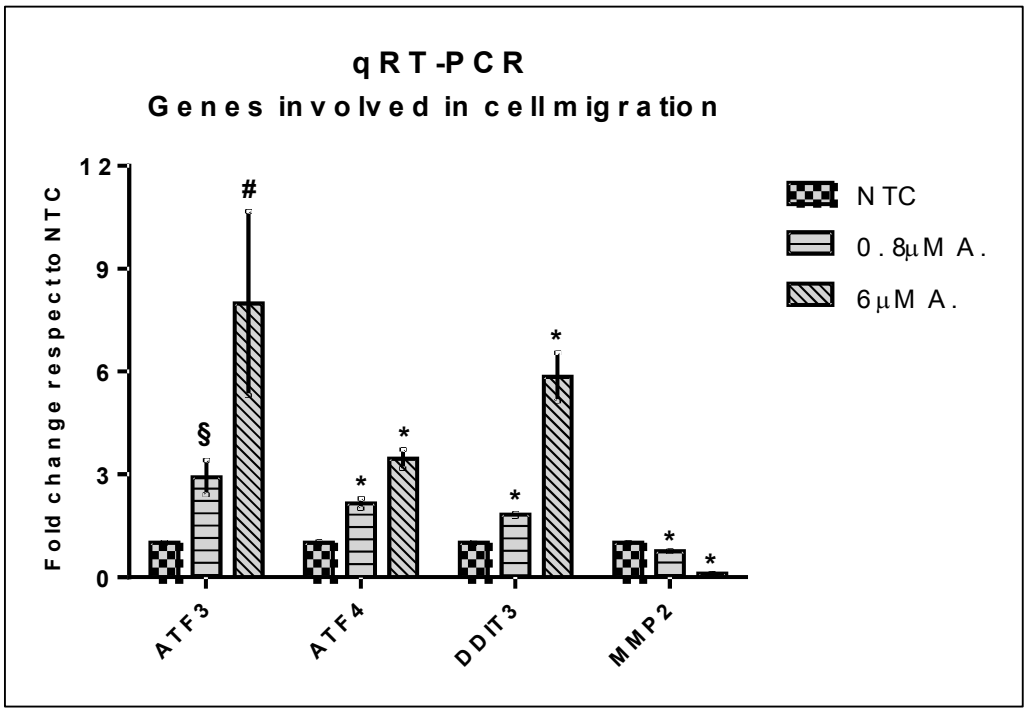

Fig. 4.32 – Analysis of mRNA expression levels of genes involved in cell migration by qRT-PCR in JHH6 cells. P#<0.05, P§< 0.005 and P*<0.0001 respect to NTC (Non Treated Cells). Data, normalized to NTC, are expressed as mean ± SEM, n=9.

With regard to HuH7 cells, we confirmed the decrease of E2F1 (6 μM) and E2F2/E2F3 mRNA levels (0.8 μM and 6 μM) (Fig. 4.33). Moreover, in line with JHH6, also E2F7 was up regulated.

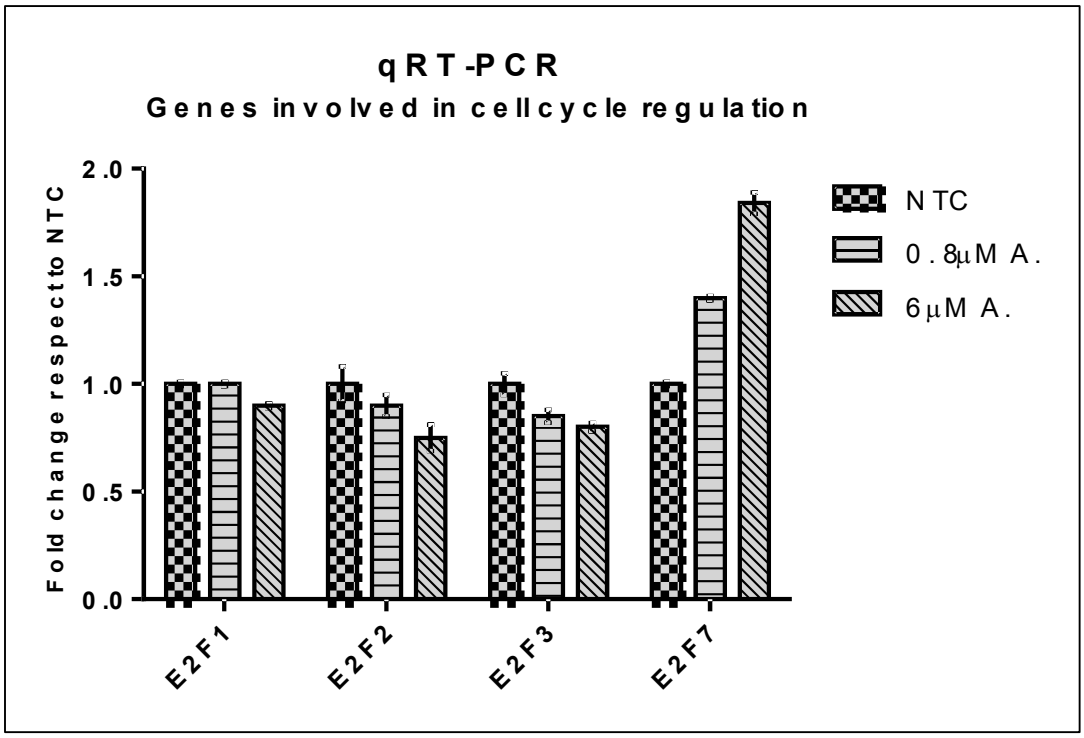

Fig. 4.33 – Analysis of mRNA expression levels of genes involved in cell cycle regulation by qRT-PCR in HuH7 cells. P#<0.05, P§< 0.005 and P*<0.0001 respect to NTC (Non Treated Cells). Data, normalized to NTC, are expressed as mean ± SEM, n=3.

Regarding genes involved in cell migration, we observed a dose-dependent up regulation of the mRNA levels of all analysed genes, as previously observed in JHH6 cell line. (Fig. 4.34)

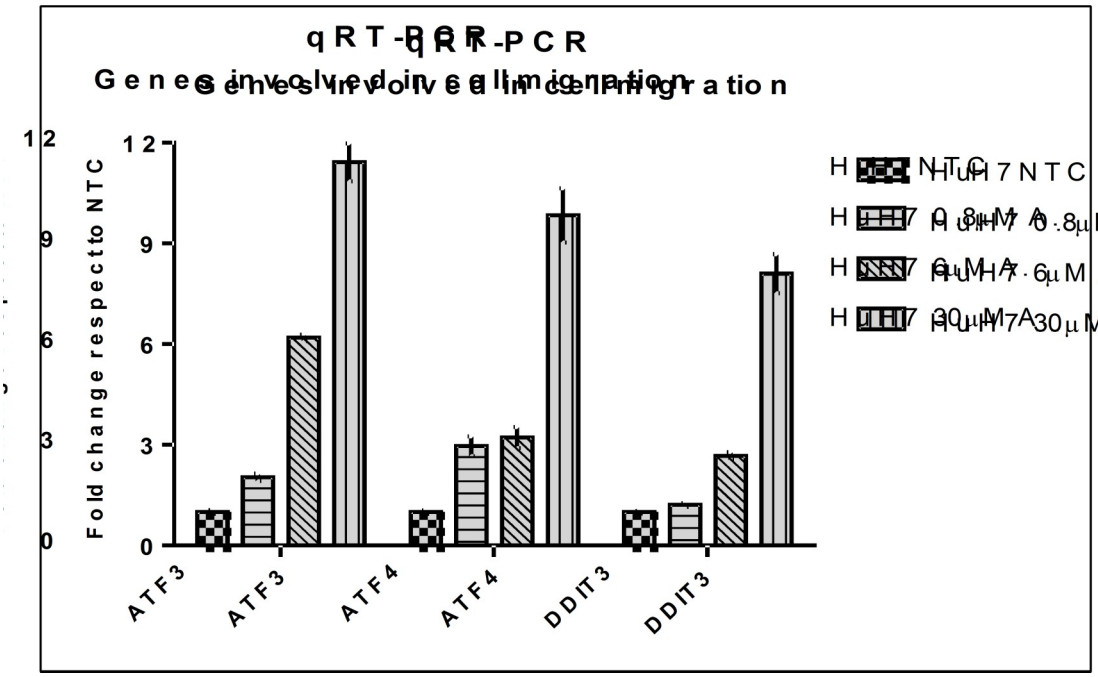

Fig. 4.34 – Analysis of mRNA expression levels of genes involved in cell cycle regulation by qRT-PCR in HuH7 cells. Data, normalized to NTC, are expressed as mean ± SEM, n=3.

4.2.2 MiRNA expression profile

In addition to studying the effects of 5-azacytidine on gene expression, we have previously evaluated the expression profile of microRNAs, being these molecules implicated in many cancers including HCC. Microarray analysis found 14 microRNAs differentially expressed after the treatment with 5-azacytidine (6µM). Of these, four were up regulated and 9 were down regulated (Table 4.2)

microRNA	Fold change (6μM A. Vs NTC)	p-value
miR 1280	2.62	0.03
miR 139-5p	2.5	0.05
miR 1308	2.38	0.032
miR 663	2.28	0.04
miR 193b	0.486	0.046
miR 23b	0.473	0.047
miR 181a	0.428	0.037
miR 210	0.423	0.046
miR 23b*	0.406	0.035
miR 452	0.395	0.046
miR 34a	0.386	0.035
miR 30a*	0.352	0.037
miR 27b	0.304	0.027

Table 4.2 – Fold change values of microRNAs, which are differentially expressed after treatments with 6μM of 5-azacytidine. miRNAs differentially expressed in treated cells respect to untreated ones are identified using a $p \leq 0.05$.

Due to the direct involvement of miR 139-5p in HCC [277], we focussed on this miRNA. Mir 139-5p is located at 11q13.4 and it has anti-oncogenic and anti-metastatic activity in humans[320]. MiR-139-5p has been shown to be down regulated in a variety of cancers, including gastric cancer, breast cancer, non-small cell lung cancer and colorectal carcinoma[281]. Recently, it has been shown that miR 139-5p is often down-regulated in HCC tissue compared to adjacent non-tumour tissue and it seems to be involved in the regulation of EMT and metastasis of HCC cells [321]. There are different proteins shown to be targets of miR-139-5p. For example, miR 139-5p recognizes the 3′ un-translated region of ZEB1 and ZEB2 in HCC. Notably, the targeting of these proteins inhibits metastasis and invasion in HCC cells[321]. Another important target of miR 139-5p is ROCK2, a novel oncogene often associated with aggressive tumour behaviour and in fact its overexpression has been shown in several types of cancer [322]. ROCK2 is frequently overexpressed in human HCC and confers motility and invasive capability to HCC cells both *in vitro* and *in vivo*[277]. In HCC, down-regulation of miR 139-5p was associated with poor patients prognosis and features of metastatic tumours, such as venous invasion, microsatellite formation, absence of tumour

encapsulation, and reduced differentiation[277]. Overexpression of miR 139-5p in HCC cells significantly reduced cell migration and invasion *in vitro* and the incidence and severity of lung metastasis in orthotropic liver tumours in mice[277]. ROCK2 protein expression was associated inversely with miR-139 expression in the HCC cells. Interestingly, only the protein but not the mRNA of ROCK2 was modulated by miR 139-5p, suggesting this regulation is post-transcriptional[277].

We confirmed by qRT-PCR the up-regulation of miR 139-5p in JHH6 extending this observation also to HuH7 cell line. As shown in Fig. 4.35, 5-azacytidine (0.8 μM and 6 μM) significantly up regulated miR 139-5p in JHH6 cells; in HuH7 the up regulation was evident at 30 μM.

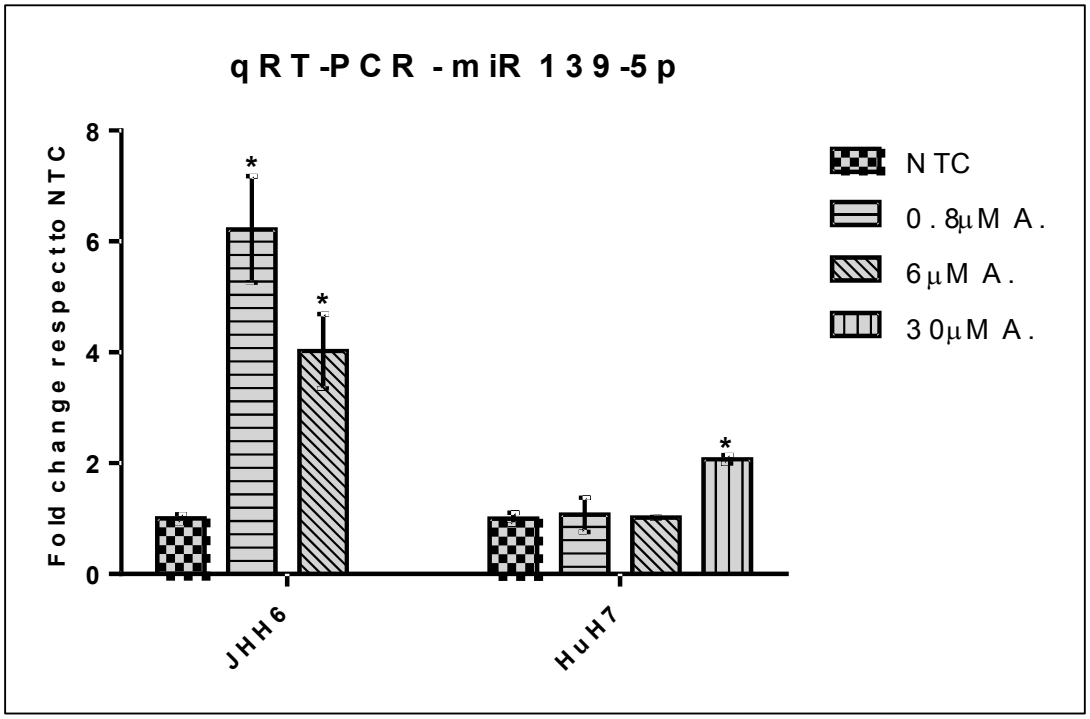

Fig. 4.35 – Analysis of miR 139-5p expression levels by qRT-PCR in JHH6 and HuH7 cells. P*<0.0001 respect to NTC (Non Treated Cells). Data, normalized to NTC, are mean ± SEM, n=9.

4.2.3 5-azacytidine and miRNA 139-5p

To prove that the up regulation of miRNA 139-5p is functionally involved in the phenotypic effects induced by 5-azacytidine, HCC cell were transfected by a *miRNA mimic* corresponding to miRNA 139-5p. MiRNA mimics are chemically synthetized ds-RNA, which mimic naturally occurring miRNAs after transfection into the cell. Only the guide strand is loaded into RNA induced silencing complex (RISC) with no resulting microRNA activity

from the complementary passenger strand. As control, we used a miRNA Scramble sequence. This is a random miRNA sequence, which has been validated not to produce identifiable effects in cells. MiRNA-139-5p mimic was transfected into JHH6 and HuH7 at the concentration of 100nM, being this amount found to be optimal to investigate influences on cell phenotype. Viability (MTT assay) was performed at the optimal time point of 48 hours after transfection. In line with the effect of 5-azacytidine (Fig. 4.36), miR 139-5p mimic significantly decreased cell viability both in JHH6 and in HuH7 cells of about 15% and 20% respectively.

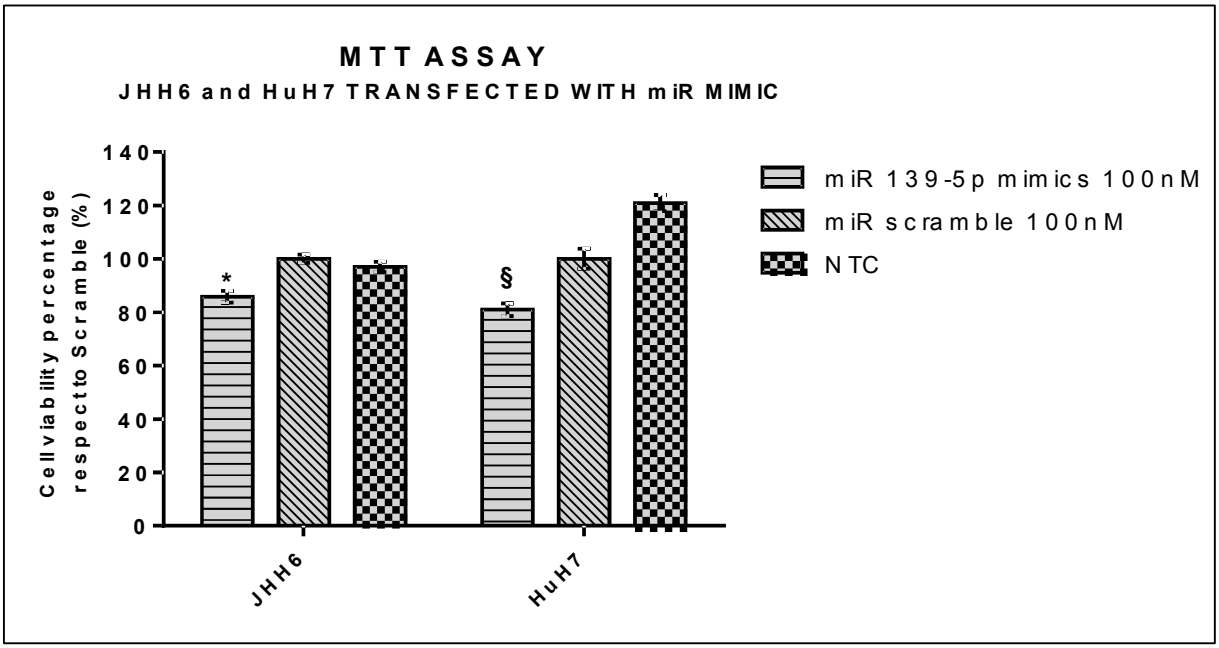

Fig. 4.36 – Evaluation of tumour cell viability after miR-139-5p mimic transfection by MTT assay. P§< 0.005, P*<0.0001 respect to scramble. Data, normalized to scramble, are expressed as mean ± SEM, n=12.

Moreover, miR-139-5p mimic did not elicit any significant necrosis (LDH assay) compared to miRNA scramble (Fig. 4.37), further confirming the observation done for 5-azacytidine.

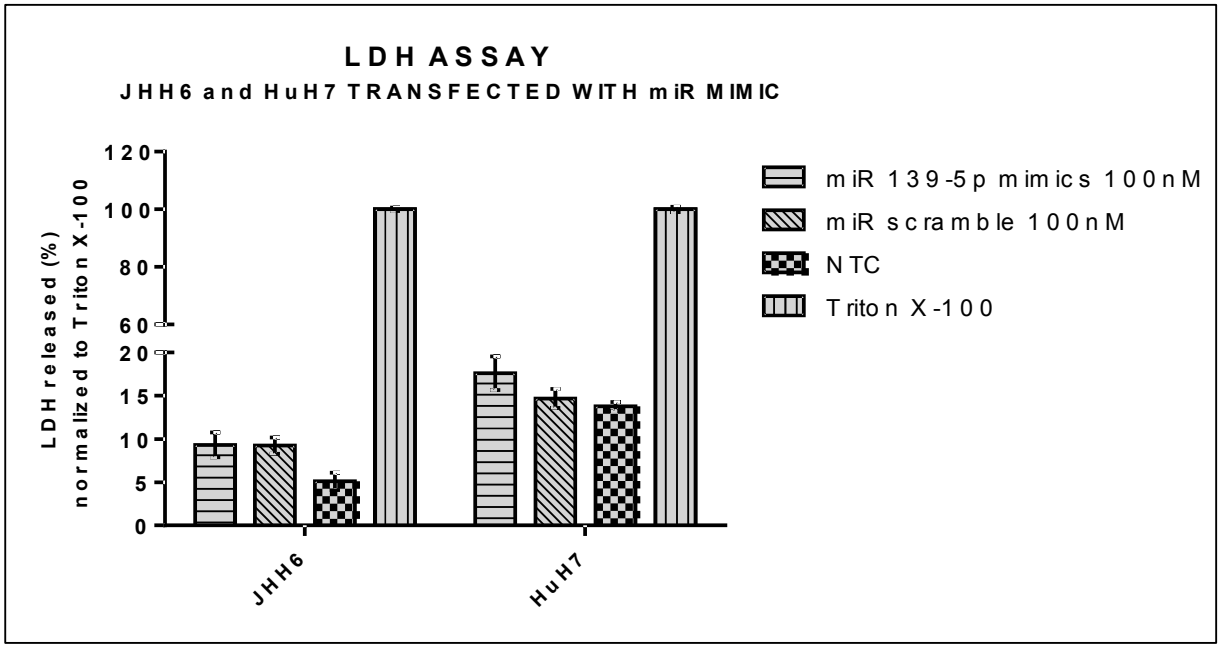

Fig. 4.37 – Measure of LDH released after miR 139-5p mimic transfection in tumour cells. Data, normalized to Triton X-100, are expressed as mean ± SEM, n=6.

The reduction in cell viability was confirmed also at the cell counting level where the percentage of miR 139-5p mimic-treated cells decreased compared to that of scramble-treated cells of about 25% in both JHH6 and HuH7 (Fig. 4.38).

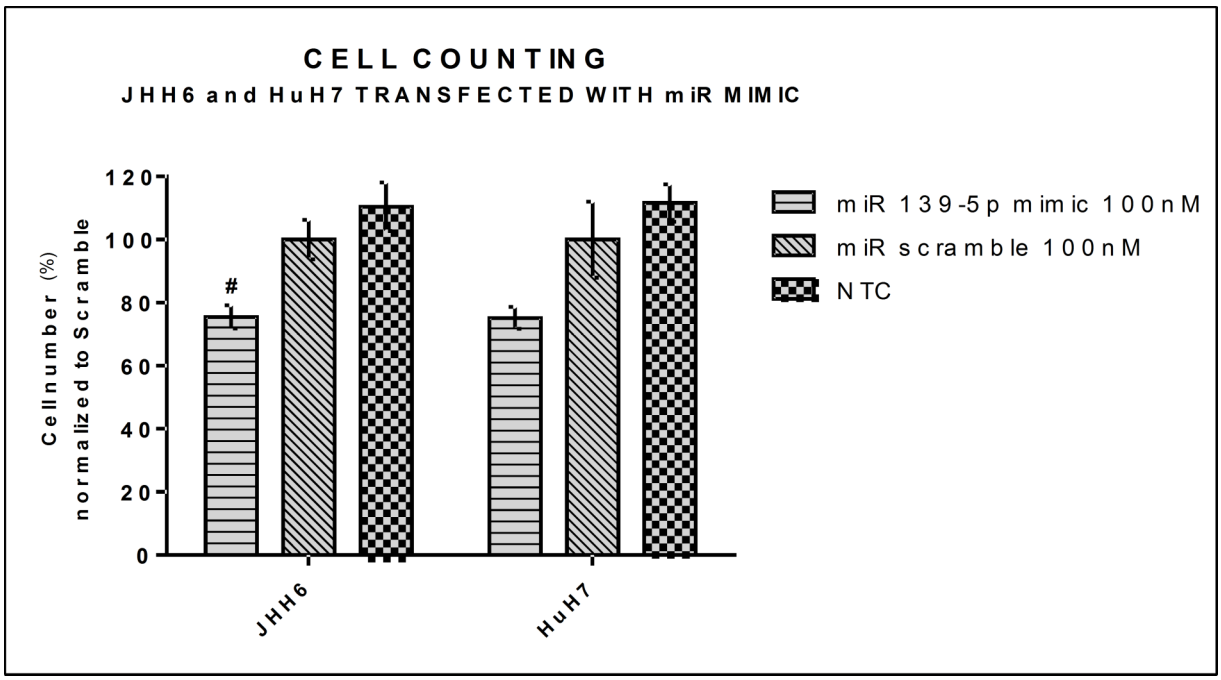

Fig. 4.38 – Evaluation of tumour cell number after 48 hours from miR 139-5p transfection. P#<0.05. Data are expressed as mean ± SEM. The percentage of miR 139-5p mimic-treated cells and NTC cells are normalized to scrambled-treated cells. n=6 in JHH6, n=2 in HuH7.

In line with the effects of 5-azacytidine, in JHH6 (Fig. 4.39), miR 139-5p mimic significantly increased the percentage of G2/M phase cells whereas decreased the percentage of G1/G0 phase cells compared to the miRNA scrambled. Together the above data indicate that miRNA 139-5p can mimic, at least from the qualitative point of view, the effects of 5-azacytidine on cell vitality, necrosis, number and cell cycle phase distribution.

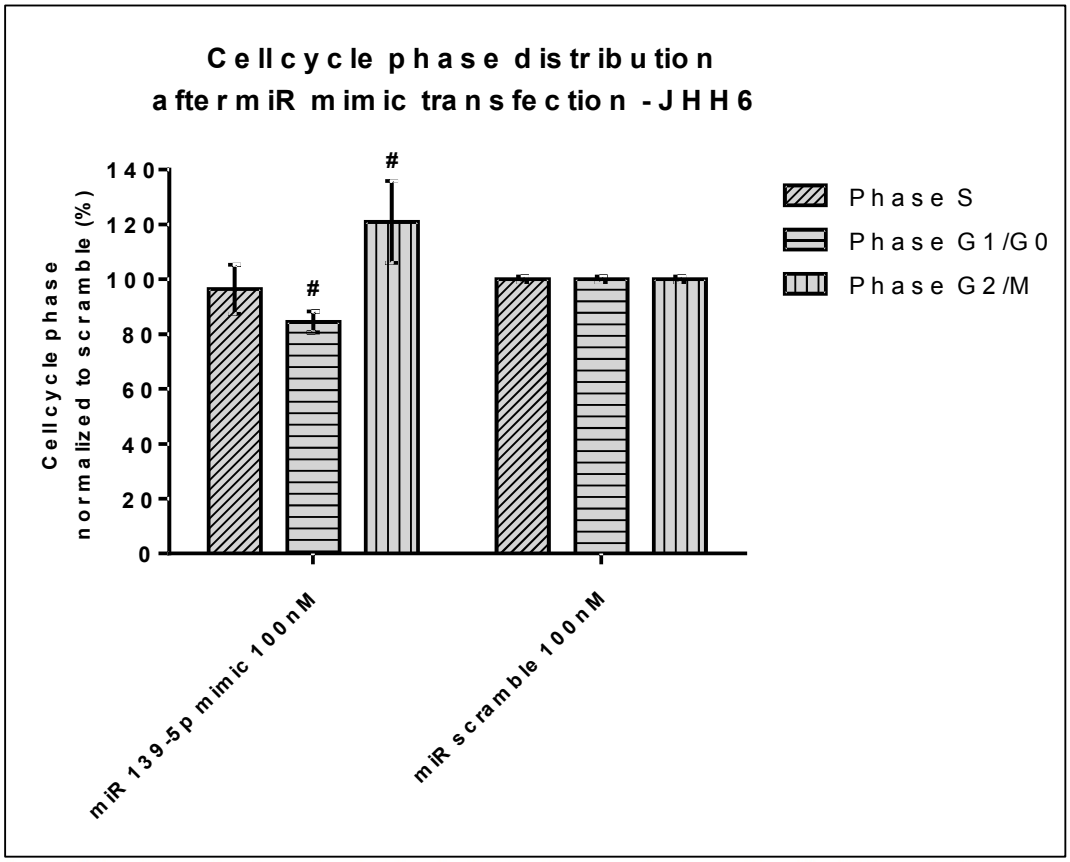

Fig. 4.39 - Cell cycle phase distribution in JHH6 after transfection with miR 139-5p mimic and miR scramble. P# < 0.05 respect to scramble. Data, normalized to scramble, are expressed as mean ± SEM; n=3.

The alteration of cell cytoskeleton induced by 5-azacytidine (Fig 4.26 and Fig 4.27), prompted us to verify whether miR 139-5p mimic could contribute to generate this phenotype. In analogy with 5-azacytidine, cytoskeleton was analysed checking the organization of the cellular β-tubulin. After miR 139-5p mimic transfection, some cells showed the specific features that we had already seen in JHH6 treated with 5-azacytidine. In fact, as shown in Fig. 4.40, miR139-5p mimic-treated cells had more multi-nuclear formation and altered β-tubulin organization compared to scramble-treated cells. These evidences, associated with the G2/M phase block seen in cell cycle analysis, suggested that miR 139-5p could be effectively involved in the strong cytoskeletal alterations induced by 5-azacytidine and also promote mitotic catastrophe.

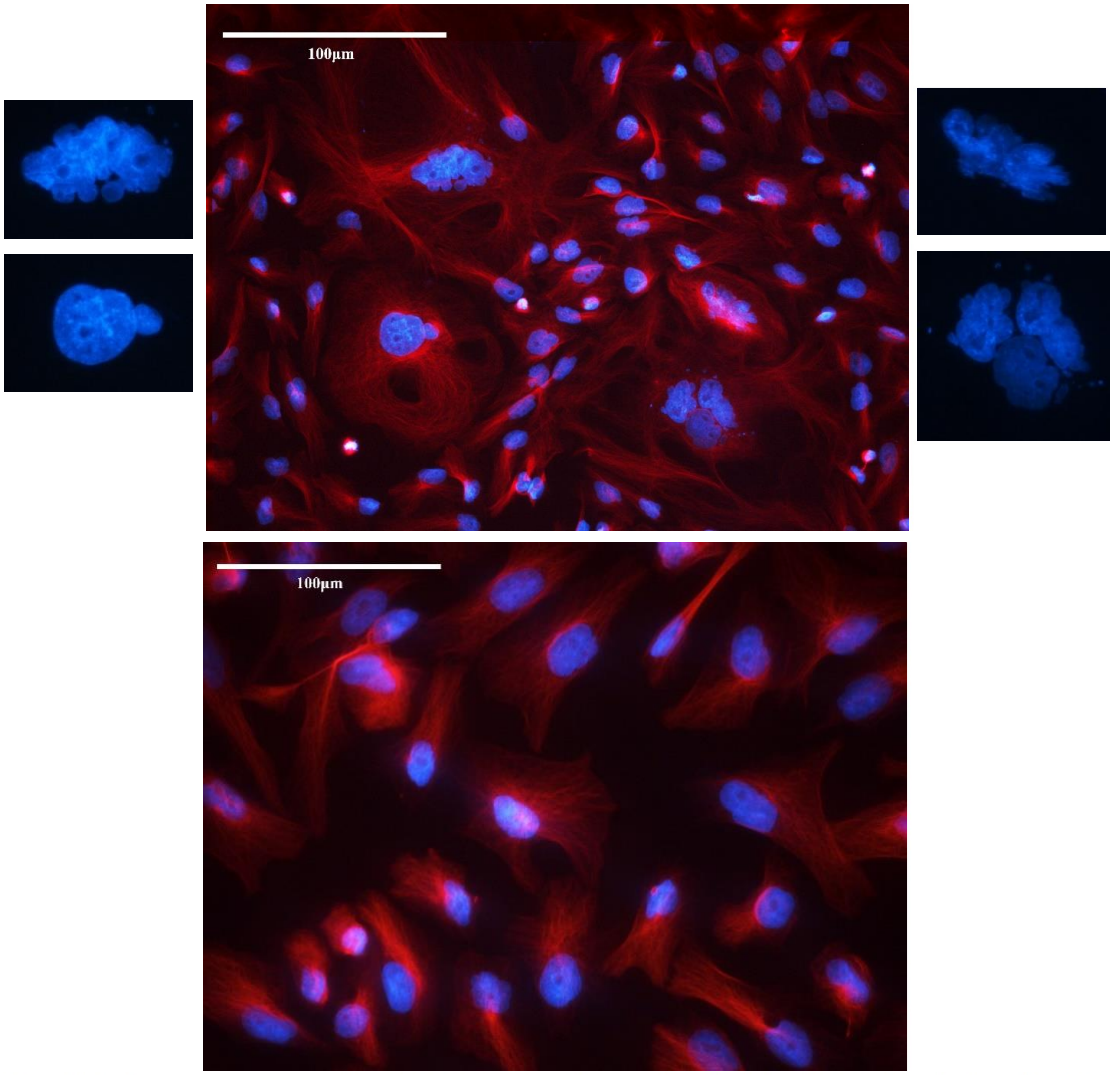

Fig. 4.40 – Immunostaining of β-tubulin in JHH6 cells transfected with miR 139-5p mimic. miR 139-5p mimic-treated cells show multinuclear formations and altered β-tubulin organization (white arrows) whereas scramble-treated cells own regular nuclei and structured organization of β-tubulin. Images are acquired with Leica DM 2000 microscope. Red=β-tubulin, Blue=DAPI. Magnification 40X. (bar=100µm).

4.2.4 5-azacytidine and ROCK2

After proving that miR 139-5p was significantly up-regulated following 5-azacytidine and that its overexpression can mimic the phenotype induced by 5-azacytidine, we evaluated the protein level of ROCK2 [323], one of miR 139-5p demonstrated target. ROCK2, as ROCK1, belongs to the Rho-associated coiled-coil kinase (ROCK) family and is a serine/threonine kinase. ROCK2 is primarily localized to the cytoplasm in association with *Vimentin* and actin stress fibres[324]. The small Rho-GTPase superfamily subclass of Rho proteins, which predominantly includes *RhoA, RhoB* and *RhoC*, are the most studied ROCK regulators. They bind to a specific domain in their active, GTP-charged state, enhancing ROCK catalytic activity fibres[324]. The ROCK proteins phosphorylate an abundant array of downstream targets, which modify filamentous-actin ultra-structural assemblies that are important for the regulation of cell contractility, motility and morphology [324]. Increased ROCK2 expression is correlated with poor prognosis in many human cancers, including HCC, breast cancer and lung cancer[278]. Recently, emerging evidences link the biological functions of ROCK2 to tumour metastasis. For example, the overexpression of ROCK2 in HCC is significantly correlated with the presence of tumour microsatellite formation, and the stable knockdown of ROCK2 markedly reduced HCC migration and invasion *in vivo* and *in vitro*[323].

As shown in a represented immunoblotting in Fig. 4.41 and summarized in Fig. 4.42, we observed a dose-dependent reduction in ROCK2 protein levels in both JHH6 and HuH7 cell lines following 5-azacytidine treatments. JHH6 showed a decrease in ROCK2 protein levels of about 35% and 50% after treatments with 0.8µM and 6µM of 5-azacytidine, respectively. In HuH7 cells, we noticed a reduction of about 40% and 60% of ROCK2 following the administrations of 5-azacytidine at the concentration of 0.8µM and 6µM/30µM, respectively.

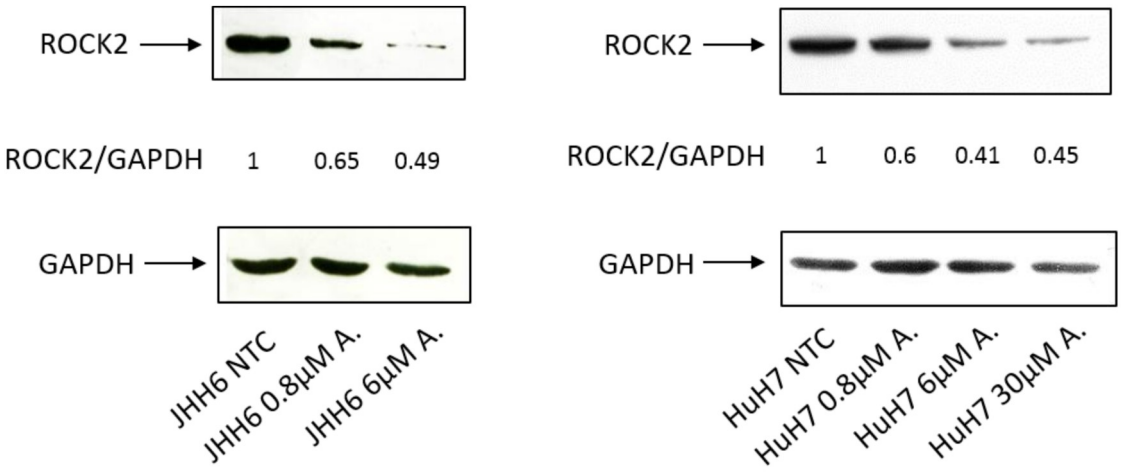

Fig. 4.41 – A representative immunoblotting for the detection of ROCK2 in JHH6 and HuH7 cell lines is shown. The ratio between ROCK2 and GAPDH is normalized to NTC (Non Treated Cells) of each cell line.

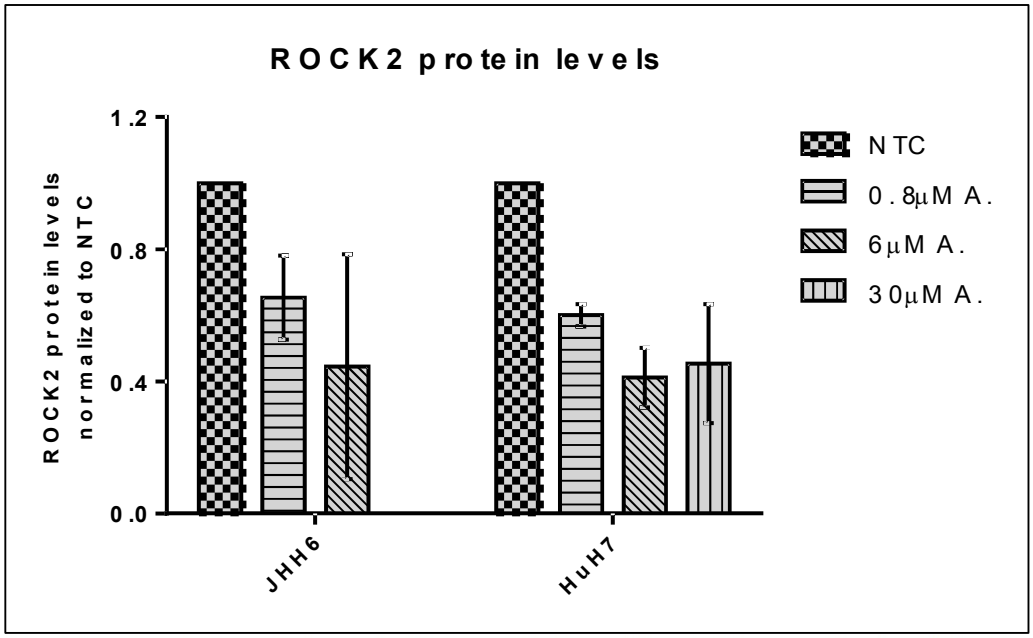

Fig. 4.42 – ROCK2 protein levels in JHH6 and HuH7 cell lines. Data, normalized to NTC (Non Treated Cell), are expressed as mean ± SEM; n=3.

4.2.5 5-azacytidine and MMP2

After proving that ROCK2 protein levels strongly decreased after 5-azacytidine administrations, we checked any possible differences in the protein level of a ROCK2 target, i.e. the metalloproteinase MMP2. MMP2 is a proteolythic enzyme that degrades some components of ECM including collagen type IV favouring cell migration[325]. ROCK2 is an important regulator of MMP2 expression through a mechanism in which ROCK2 stabilizes

MMP2 preventing proteasome degradation[278]. Notably, in HCC, ROCK2 is positively correlated with MMP2[278].

Western blotting analysis showed a dose-dependent reduction of MMP2 protein levels after 5-azacytidine administrations in both JHH6 and HuH7 (Fig. 4.43, Fig. 4.44).

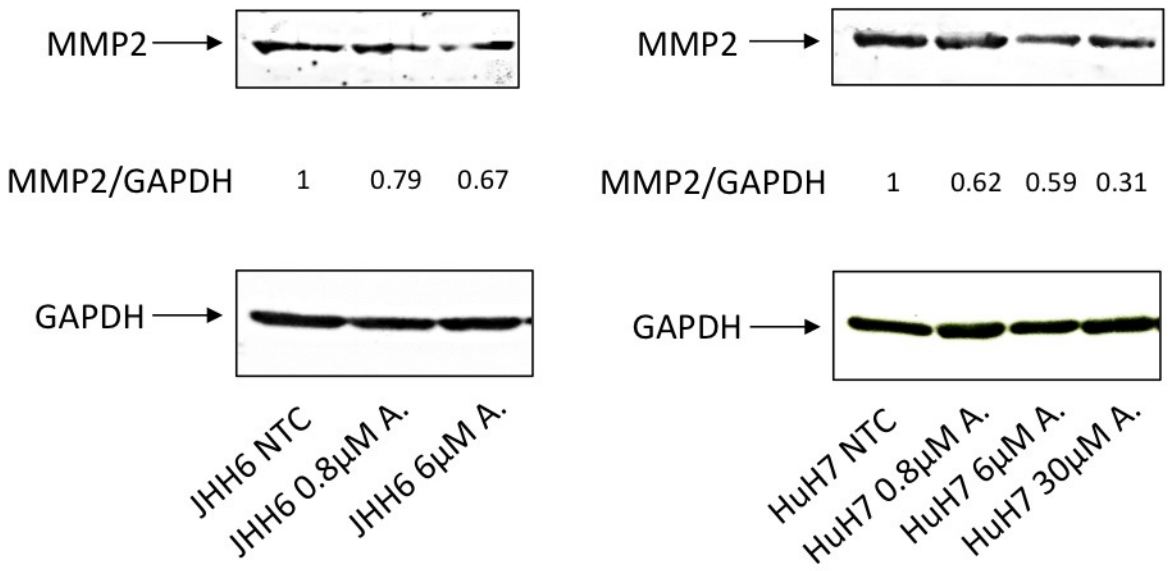

Fig. 4.43 – A representative immunoblotting for the detection of MMP2 in JHH6 and HuH7 cell lines is shown. The ratio between MMP2 and GAPDH is normalized to NTC (Non Treated Cells) of each cell line.

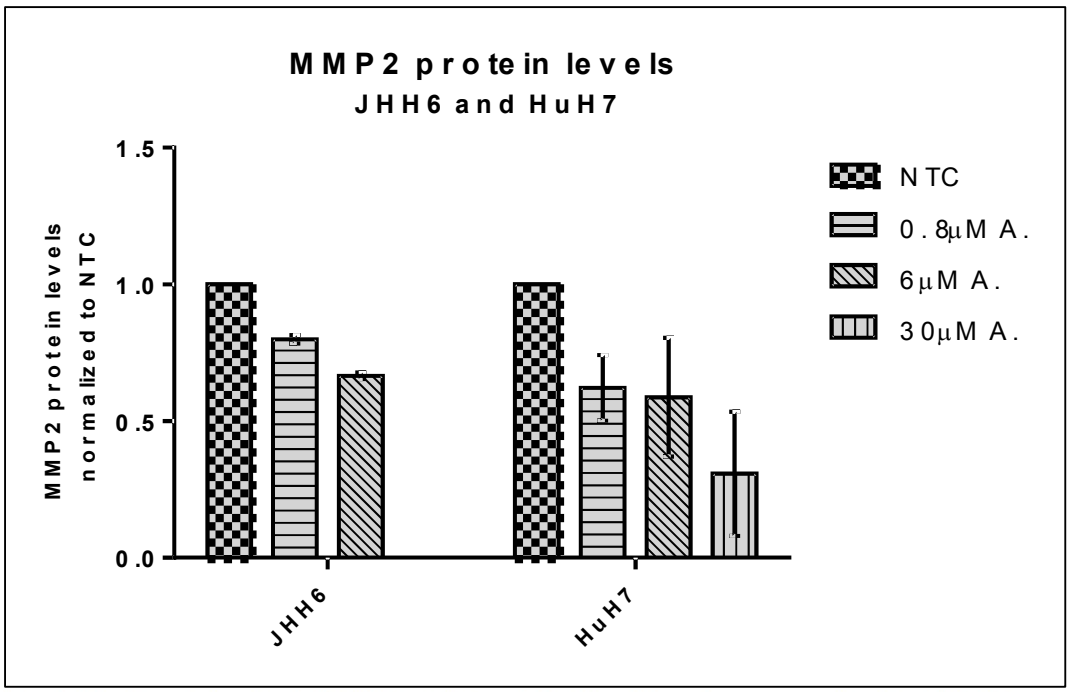

Fig. 4.44 – Protein levels of MMP2 in JHH6 and HuH7 cell line. Data, normalized to NTC (Non Treated Cell), are expressed as mean ± SEM; n=3.

To further proving the involvement of MMP2 in 5-azacytidine effects, we evaluated the enzymatic activity of MMP2 by zymography. This is an electrophoretic technique used to study the enzyme hydrolytic activity evaluating substrate degradation [11]. Gelatin, the substrate of MMP2, is embedded into the resolving gel during the preparation of acrylamide gel. Samples loaded on SDS-PAGE derive from concentrated supernatants of treated/untreated cells, grown without serum within 48 hours of their harvesting. As human serum contains large amount of both MMP-2 and MMP-9, this was used as positive control. Following electrophoresis, the SDS is removed from the zymogram by washing with an appropriated *Wash Buffer* followed by incubation in an appropriate *Digestion Buffer* O/N at 37°C. The zymogram is subsequently stained with *Coomassie Brilliant Blue*, and areas of digestion appear as clear bands against a darkly stained background where the substrate has been degraded by the enzyme. As shown in a representative zymogram (Fig. 4.45) and summarized in Fig. 4.46, in the supernatants of JHH6 treated by 5-azacytidine, the extent of substrate digestion was significantly reduced compared to control. Notably, the effect was dose-dependent. Thus, our data prove that 5-azacytidine reduces MMP2 level together with its activity.

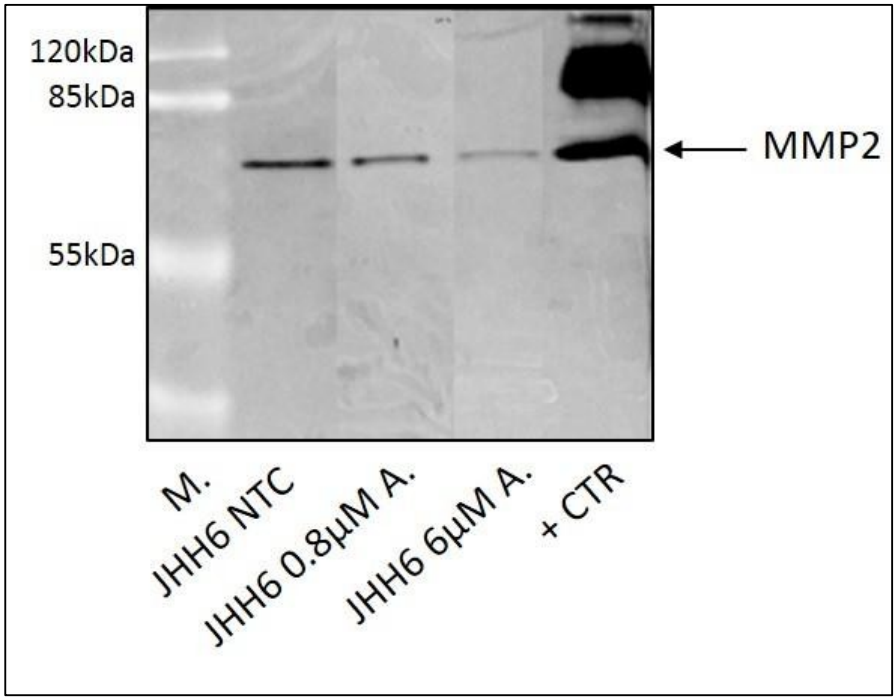

Fig. 4.45 – A representative zymogram obtained from the analysis of JHH6 supernatants is shown. M is marker and + CTR is human serum that contains large amount of MMP-2.

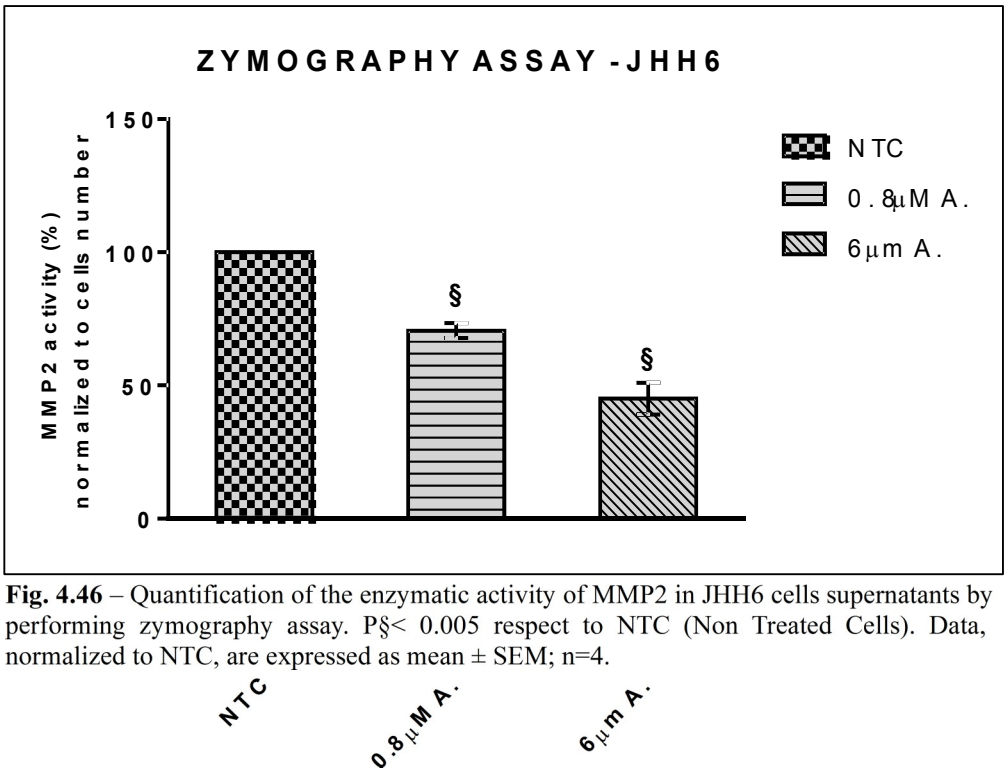

Fig. 4.46 – Quantification of the enzymatic activity of MMP2 in JHH6 cells supernatants by performing zymography assay. P§< 0.005 respect to NTC (Non Treated Cells). Data, normalized to NTC, are expressed as mean ± SEM; n=4.

4.2.6 miR 139-5p, ROCK2 and MMP2 pathway

After demonstrating that 5-azacytidine significantly reduced the protein levels of both ROCK2 and MMP2, we investigated whether these effects could depend on the up regulation of miRNA 139-5p. Following miR 139-5p mimic transfection, ROCK2 protein level strongly decreased in both JHH6 and HuH7 (Fig. 4.47 and Fig. 4.48). Notably, cells transfected with the anti-miR 139-5p tended to show higher level of ROCK2 proteins compared to control cells. This can be due to the inhibitory action of anti-miR 139-5p which binds to miR 139-5p reducing its function in treated cells and, in turn, the effect on ROCK2 protein.

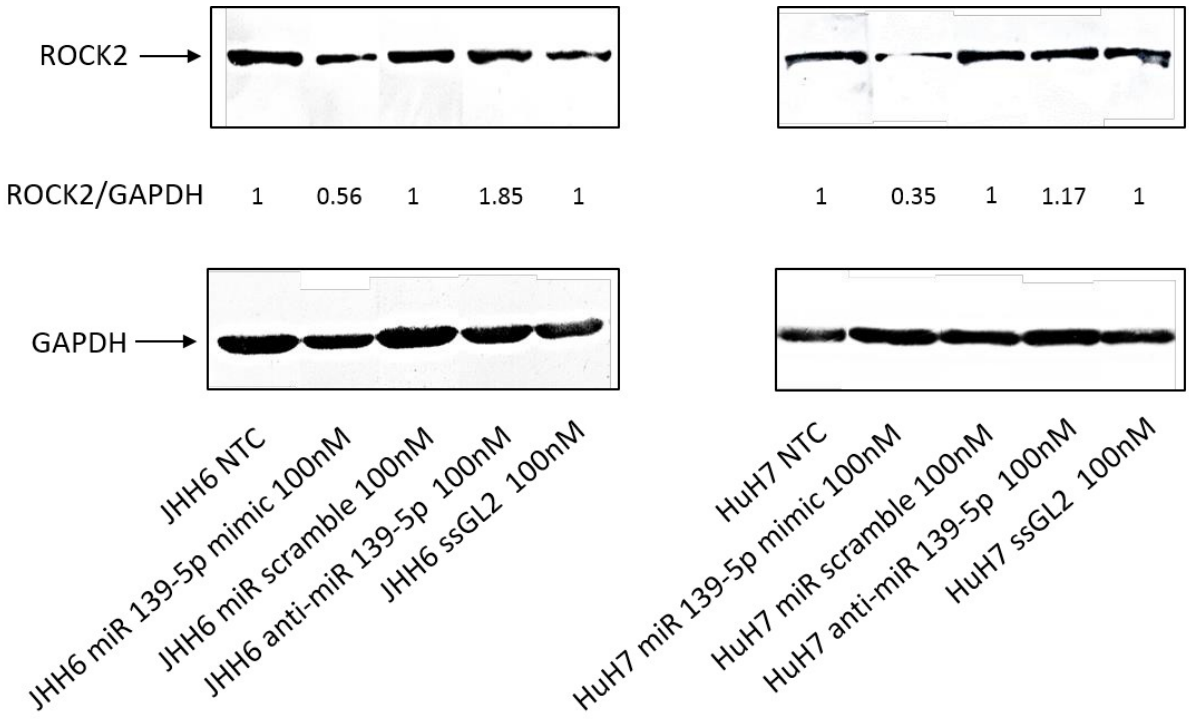

Fig. 4.47 – A representative immunoblotting for the detection of ROCK2 in JHH6 and HuH7 cells transfected with miR 139-5p is shown. The ratio between ROCK2 and GAPDH is normalized to scramble in NTC (Non Treated Cells) and miR 139-5p mimic-treated cells whereas the ratio between ROCK2 and GAPDH is normalized to ssGL2 in anti-miR 139-5p-tretaed cells.

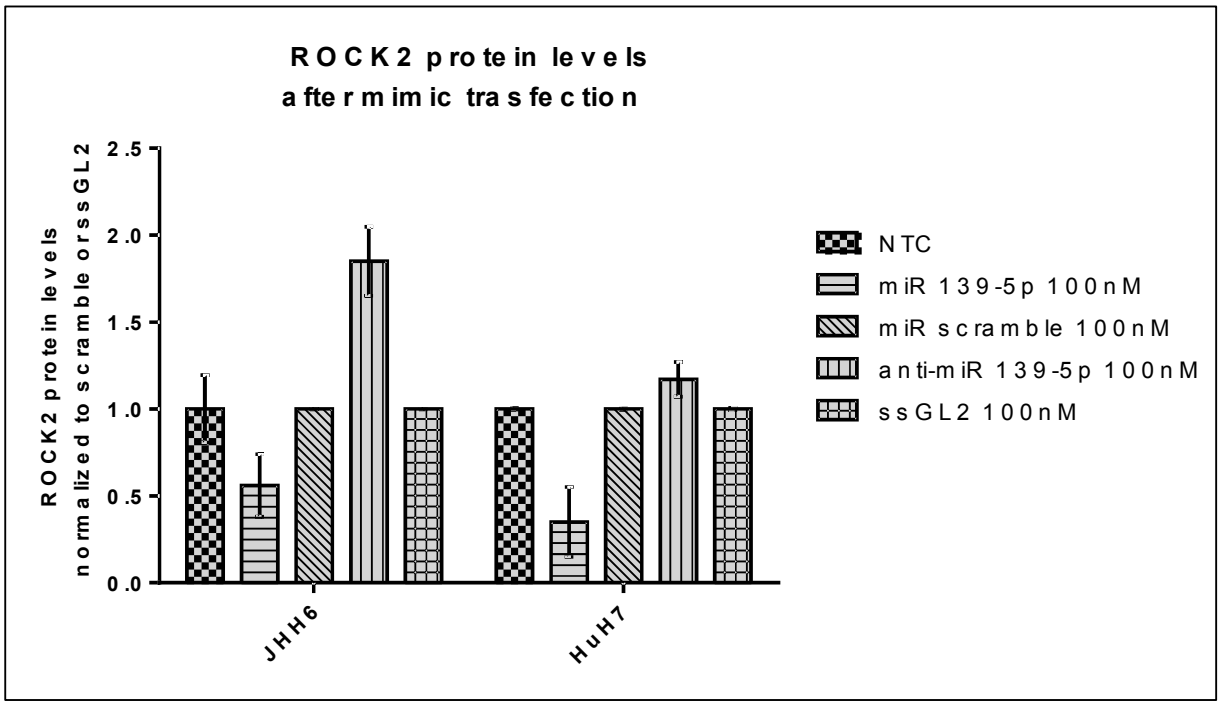

Fig. 4.48 – ROCK2 protein levels in JHH6 and HuH7 cells transfected with miR 139-5p mimic. The amount of ROCK2 protein in miR 139-5p mimic-treated cells and NTC (Non Treated Cells) is normalized to scramble whereas ROCK2 protein levels in anti-139-5p-treated cells are normalized to ssGL2-treated cells. Data are expressed as mean ± SEM; n=2.

Finally, preliminary data suggested that also MMP2 protein levels decreased after miR 139-5p mimic transfection (Fig. 4.49). Together these data confirm in our model the existence of the miR 139-5p, ROCK2 and MMP2 pathway[277], which our findings indicate to be affected by 5-azacytidine.

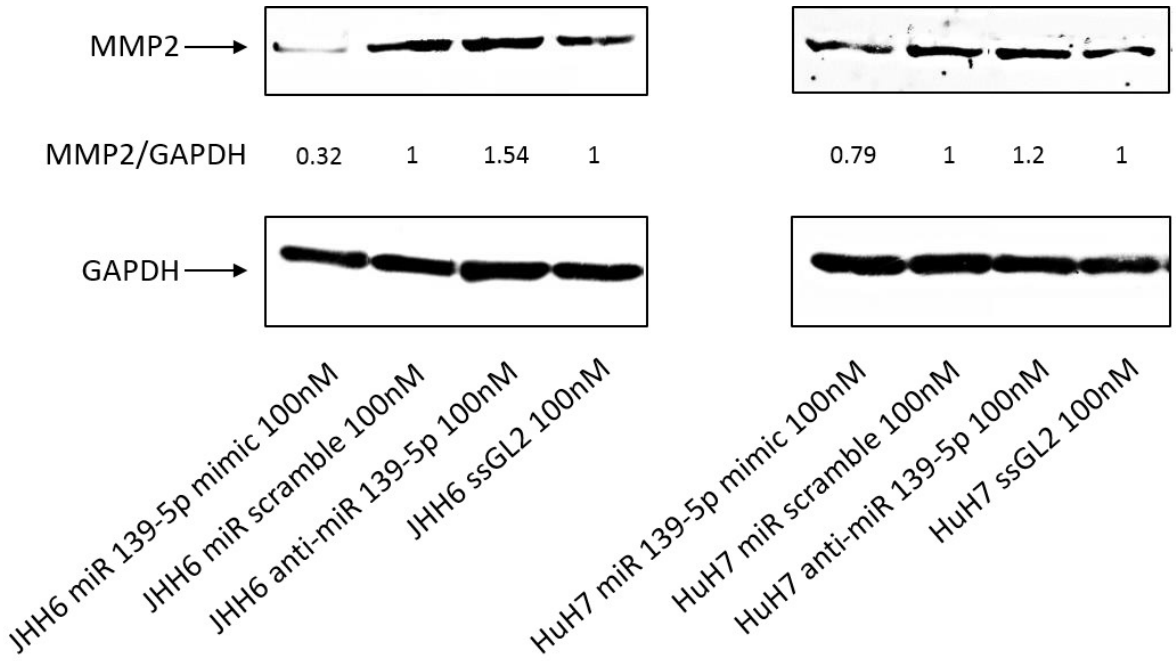

Fig. 4.49 – A representative immunoblotting for the detection of MMP2 in JHH6 and HuH7 cells transfected with miR 139-5p is shown. The ratio between MMP2 and GAPDH is normalized to scramble in miR 139-5p mimic-treated cells whereas the ratio between MMP2 and GAPDH is normalized to ssGL2 in anti-miR 139-5p-tretaed cells.

4.2.7 The effects of miRNA 139-5p transfection on HCC cell migration

After proving that miRNA 139-5p is unregulated by 5-azacytidine, we evaluated the effects of miRNA 139-5p up regulation on tumour cells migration. We performed the scratch assay test on tumour cells after 24 hours from miR 139-5p mimic transfection. The scratch healing was observed within 24 hours. As shown in Fig. 4.50, miR 139-5p mimics-transfected cells migrated about 15% less than scramble-treated cells. These evidences suggested that miR 139-5p expression levels can modulate HCC cell migration.

In HuH7 cells, it was not possible to perform this type of experiment. In fact, HuH7 cells grew in colonies and, reducing the number of cells to transfect, we did not achieve a sufficiently dense area to perform scratch.

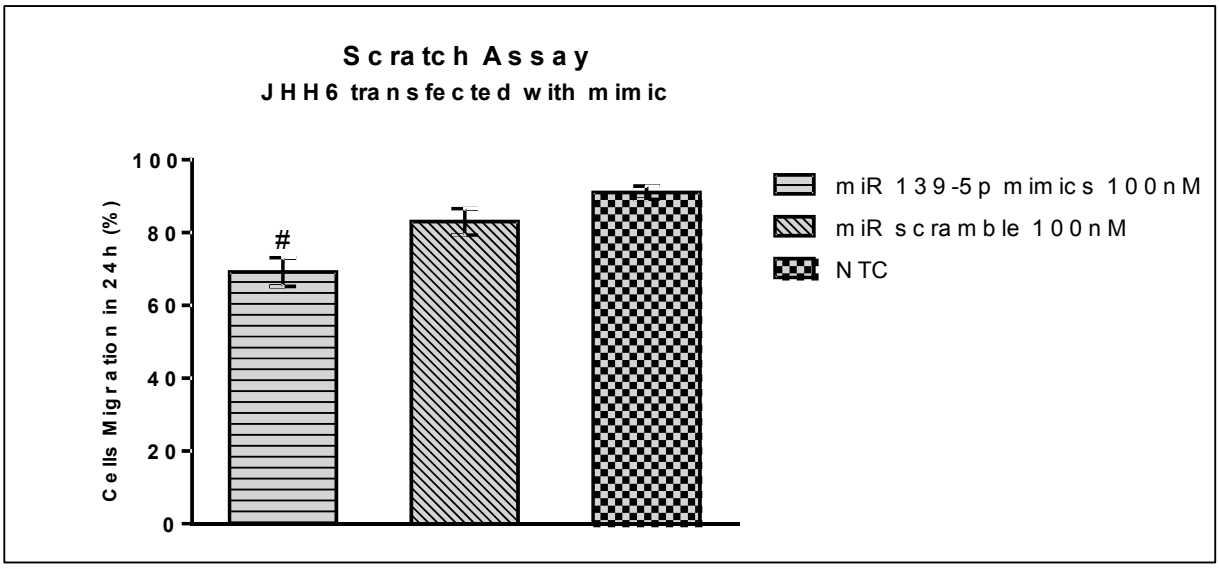

Fig. 4.50 - Scratch assay quantification in JHH6 cells transfected with miR-139-5p mimic. Data are expressed as mean ± SEM. P#< 0.05 respect to scramble. n=12.

4.2.8 ROCK2 and HCC cell migration

After proving that ROCK2 is reduced by 5-azacytidine via the up regulation of miRNA 139-5p, we evaluated the effects of ROCK2 inhibition of tumor cells migration. We performed the scratch test on tumor cell treated by 50μM of a commercial ROCK inhibitor named Y-27632. Y-27632 is a cell-permeable, highly potent and selective inhibitor of ROCK. Y-27632 inhibits ROCK2 by competing with ATP for binding to the catalytic site. After 4 hours of incubation, medium containing ROCK inhibitor was replaced with fresh medium and the scratch healing was observed within 24 hours.

With regard to JHH6 cells, we noticed a decrease in cell migration after 8 hours from scratch. At longer time points (24 hours, Fig. 4.51 and Fig. 4.52) the effect was relieved.

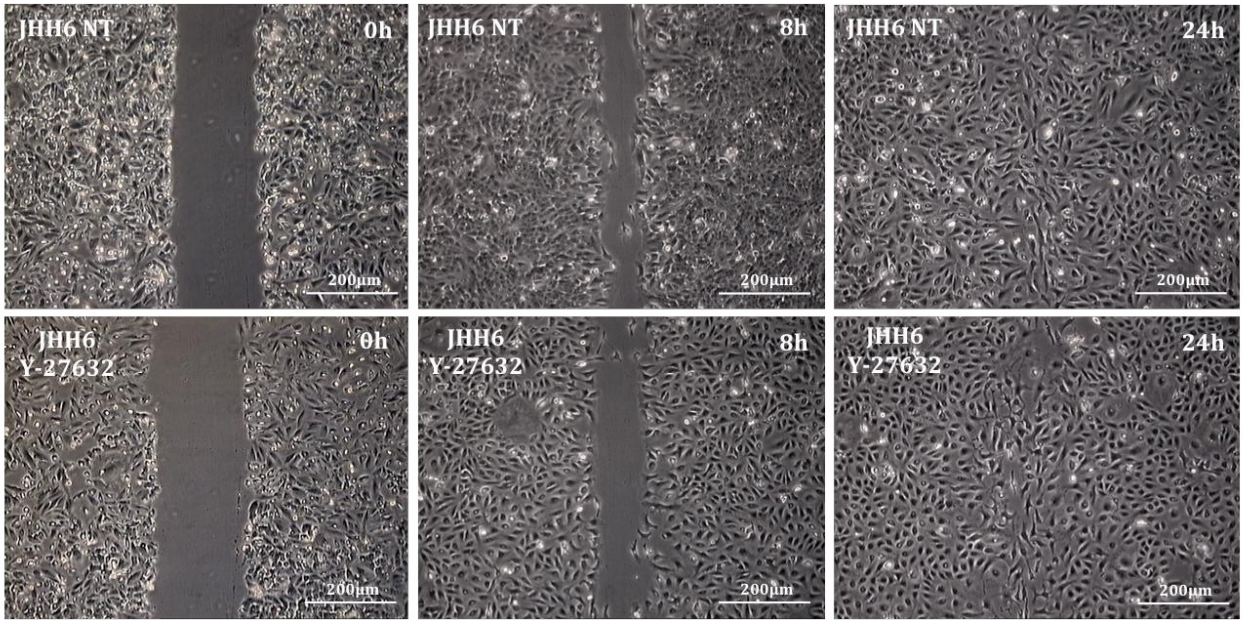

Fig. 4.51 – Representative images of scratch assay in JHH6 cells treated with Rock inhibitor (Y-27632). Images are acquired with Leica DM IRB microscope. Magnification 5X (bar = 200µm).

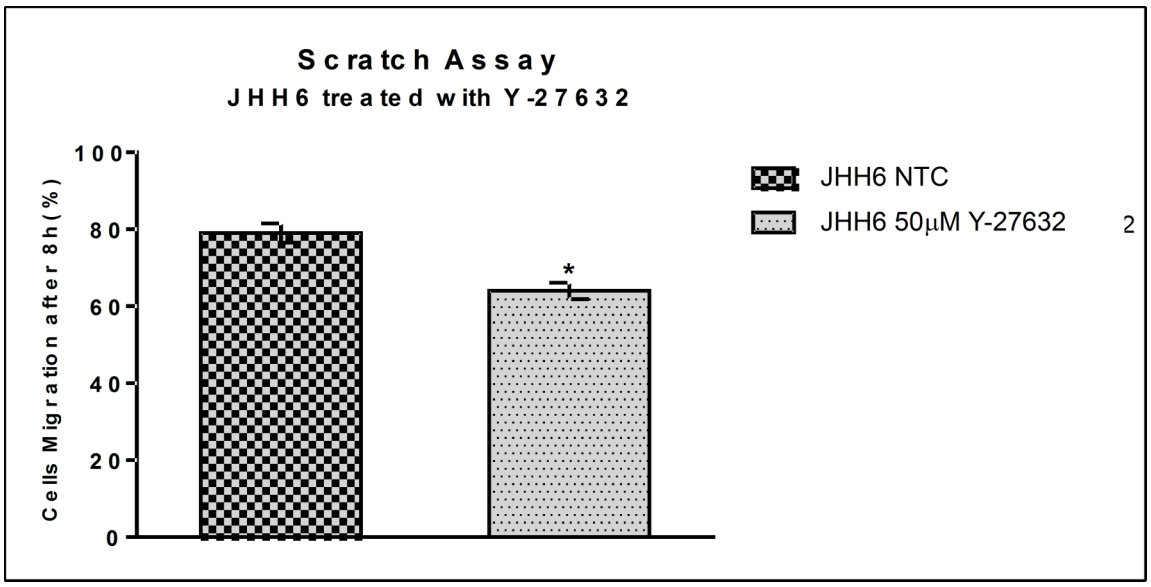

Fig. 4.52 – Scratch assay quantification in JHH6 cells treated with ROCK2 inhibitor. Data are mean ± SEM. P*< 0.0001 respect NTC (Non Treated cells). n=12

HuH7 cells treated with ROCK2 inhibitor showed a reduced migratory ability at 8 hours and 24 hours from scratch. At longer time points (48 hours) (Fig. 4.53 and Fig. 4.54) the effect was relieved.

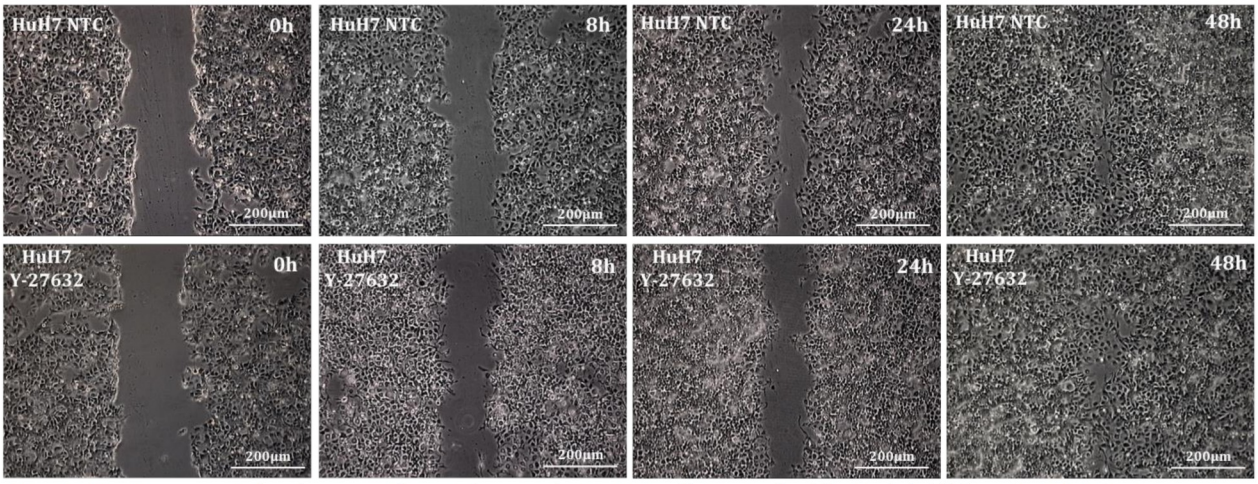

Fig. 4.53 – Representative images of scratch assay in HuH7 cells treated with Rock inhibitor (Y-27632). Images are acquired with Leica DM IRB microscope. Magnification 5X (bar = 200µm).

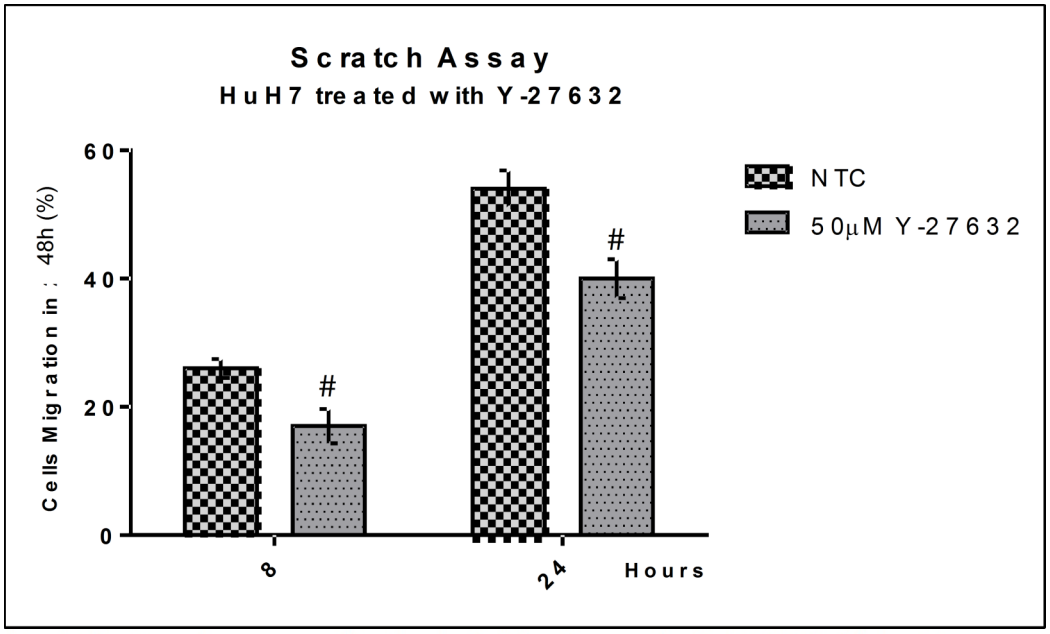

Fig. 4.54 – Scratch assay quantification in HuH7 cells treated with ROCK2 inhibitor. Data are mean ± SEM. P#< 0.05 respect NTC (Non Treated cells). n=10.

Together these observations suggest that ROCK2 is involved in the 5-azacytdine-mediated reduction of cell migration. However, the more contained effect compared to 5-azacytidine may indicate that 5-azacytidine exert this effect also *via* other molecular pathways. This observation supports the idea that ROCK2 is functionally involved in the 5-azacytidine mediated impairment of cell migration in our model.

In line with the effects on cell migration, ROCK2 inhibition clearly subverted the cytoskeleton organization. By evaluating β-tubulin (Fig. 4.55), in JHH6 ROCK2 inhibitor

induced the formation of evident alterations in the cytoskeletal structure, such as a more elongated shape, cytoplasmic extroflexions and a general disorganization of β-tubulin.

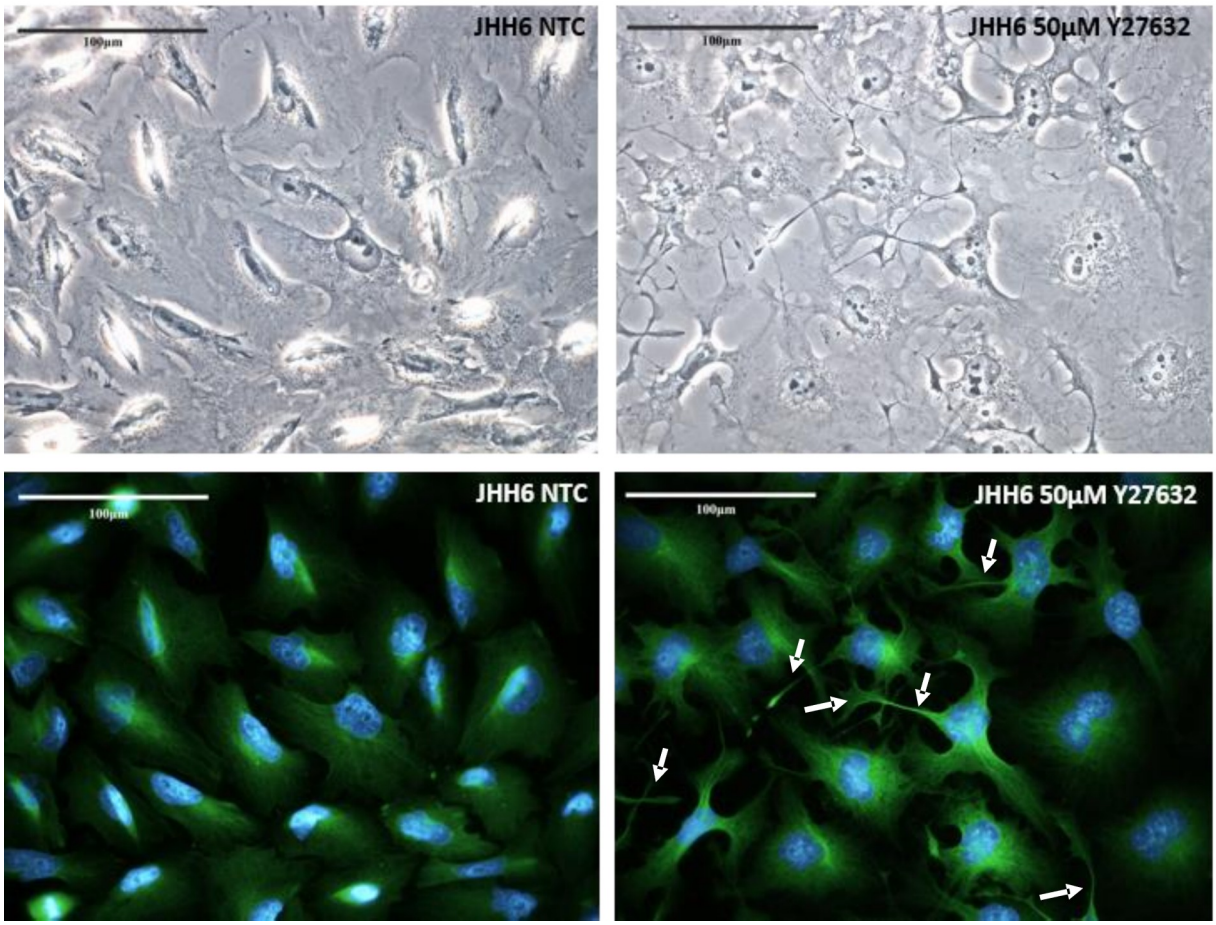

Fig. 4.55 – Immunostaining of β-tubulin in JHH6 cells treated with Y27632. Rock2 inhibitor-treated cells show elongated shape and cytoplasmic extroflexions (white arrows) whereas NTC cells own structured organization of β-tubulin. Images are acquired with Leica DM 2000 microscope. Green=β-tubulin, Blue=DAPI. Magnification 40X. (bar=100µm)

Similar findings were observed in HuH7 (Fig. 4.56).

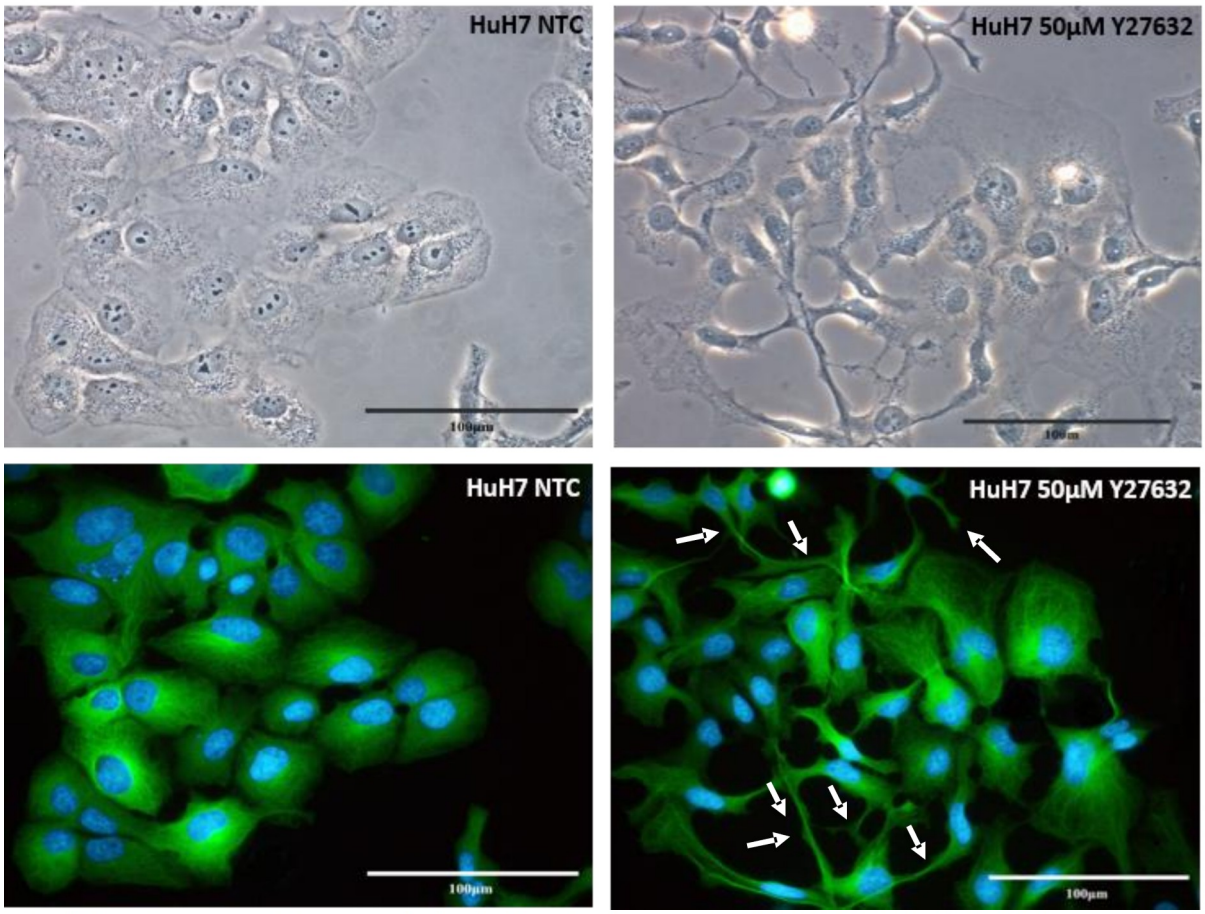

Fig. 4.56 – Immunostaining ofβ-tubulin in HuH7 cells treated with Y27632. Rock2 inhibitor-treated cells show elongated shape and cytoplasmic extroflexions (white arrows) whereas NTC cells own structured organization of β-tubulin. Images are acquired with Leica DM 2000 microscope. Green=β-tubulin, Blue=DAPI. Magnification 40X. (bar=100µm)

The general alteration of the cytoskeleton observed is reminiscent of the disorganization induced by 5-azacytidine. This supports the idea that ROCK2 is involved in the 5-azacytidine-mediated disorganization of the cytoskeleton.

We also evaluated the effect of ROCK2 inhibitor on tumour cell viability by performing MTT assay (data not shown). After 8 and 24 hours from the treatment with the ROCK2 inhibitor, we observed a reduced cell viability of tumour treated-cells compared to un-treated ones. These evidences suggest that ROCK2 might play a key role not only in HCC migration but also in tumour cell viability and proliferation.

4.2.9 MMP2 and HCC cell migration

After proving that MMP2 is strongly down regulated after 5-azacytidine administrations *via* miRNA 139-5p up regulation and the consequent ROCK2 down regulation, we evaluated the functional role of MMP2 in cell migratory ability using a specific

inhibitor of the *Gelatinase* family called SB-3CT. Using the scratch assay, 48h from seeding, tumor cells were treated with 0.1μM of SB-3CT. The next day, the scratch was performed on cell culture monolayer. Cell were maintained in the presence of MMP2 inhibitor and 1% FBS in order to reduce as much as possible proliferative stimuli. As shown in Fig. 4.57 and summarized in Fig. 4.58, JHH6 cells treated with 0.1μM of MMP2 inhibitor, exhibited impaired migration compared to control.

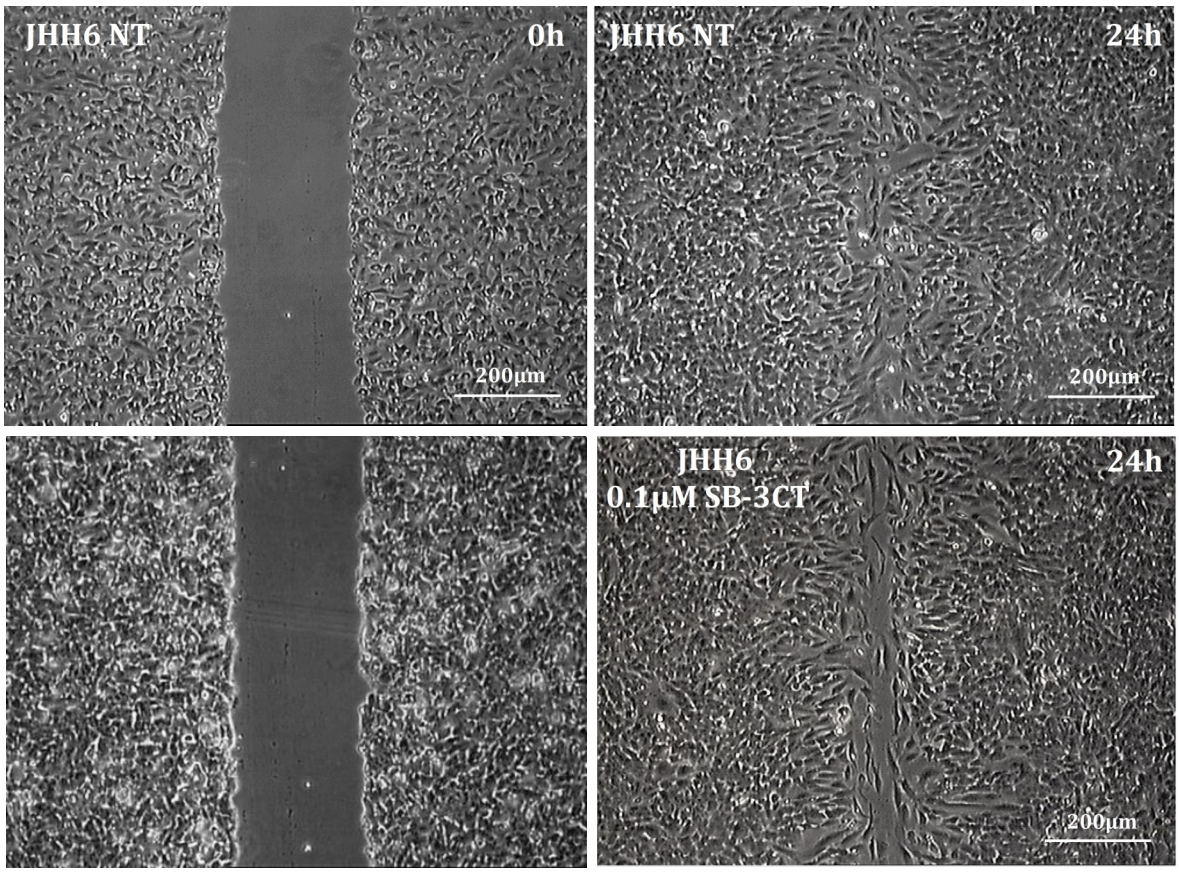

Fig. 4.57 – Representative images of *scratch assay* in JHH6 cells treated with MMP2 inhibitor (SB-3CT). Scratch is performed after two consecutive treatments with MMP2 inhibitor and its healing is evaluated within 24 hours. Images are acquired with Leica DM IRB microscope. Magnification 5X (bar = 200μm).

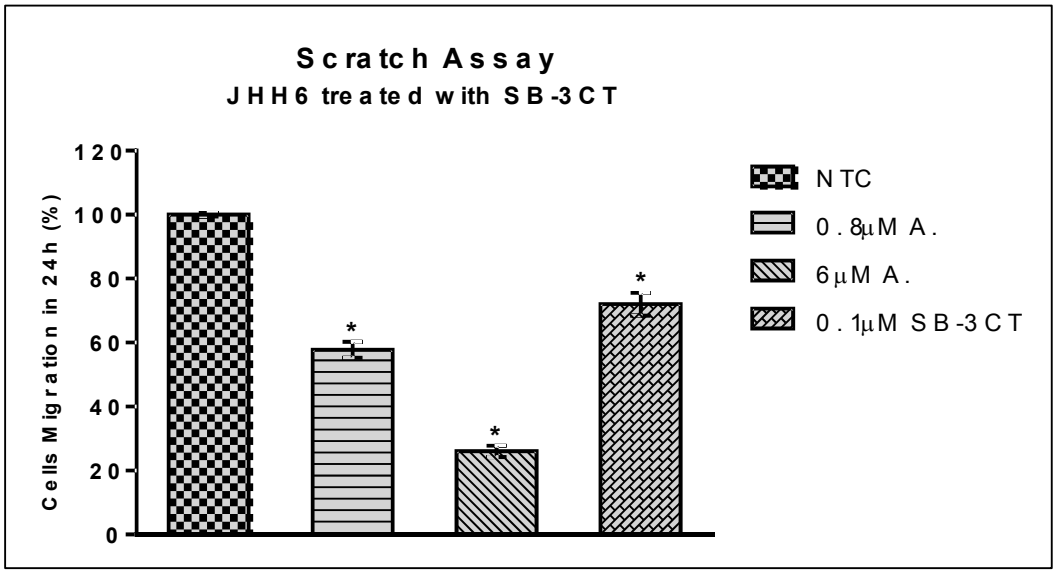

Fig. 4.58 – Scratch assay quantification in JHH6 cells treated with 5-azacytidine or with MMP2 inhibitor. Data are expressed as mean ± SEM. P*< 0.0001 respect to NTC (Non Treated Cells). n=15.

Similar trend was observed for HuH7 (Fig. 4.59 and Fig. 4.60). This observation supports the idea that MMP2 is functionally involved in the 5-azacytidine mediated impairment of cell migration in our model.

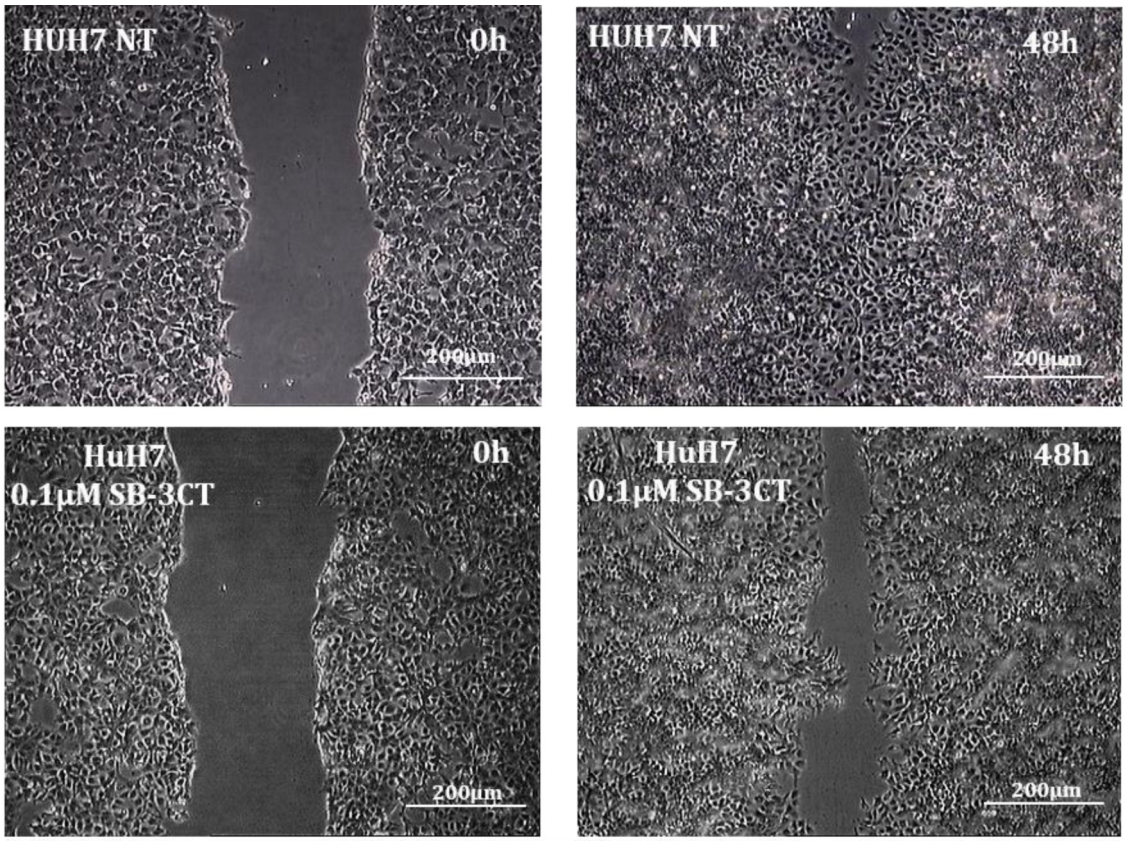

Fig. 4.59 – Representative images of *scratch assay* in HuH7 cells treated with MMP2 inhibitor (SB-3CT). Scratch is performed after two consecutive treatments with MMP2 inhibitor and its healing is evaluated within 48 hours. Images are acquired with Leica DM IRB microscope. Magnification 5X (bar = 200μm).

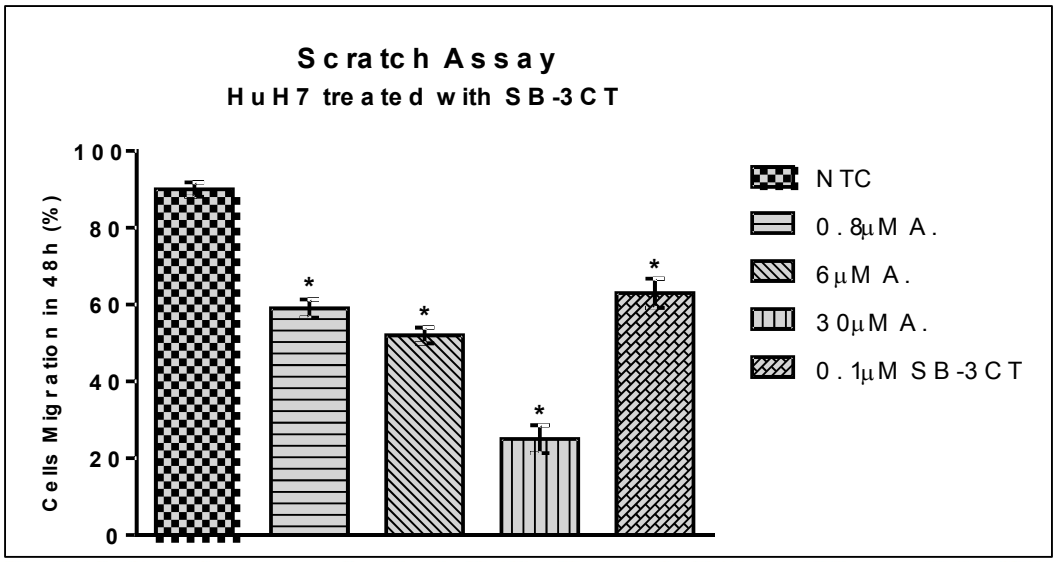

Fig. 4.60 – Scratch assay quantification in HuH7 cells treated with 5-azacytidine or with MMP2 inhibitor. Data are expressed as mean ± SEM. P*< 0.0001 respect to NTC (Non Treated Cells). n=15.

To further proving this concept, we studied the effects on cell migration of the increase of MMP2 levels. It has been proposed that ROCK2 can inhibit the degradation of MMP2 that occurs via proteasome[278]. Based on this, we inhibited proteasome activity and observed the effects on cell migration. Tumor cells were simultaneously treated with 5-azacytidine and with the proteasome inhibitor *Bortezomib*. As shown in Fig. 4.61 and summarized in Fig 4.62, in JHH6 cells treated by both 5-azacytidine and *Bortezomib*, the migratory ability was improved compared to the cell treated by 5-azacytidine alone. Notably, *Bortezomib* alone did no further improve the migratory capacity probably indicating that over a certain level of MMP2 no further increase can occur.

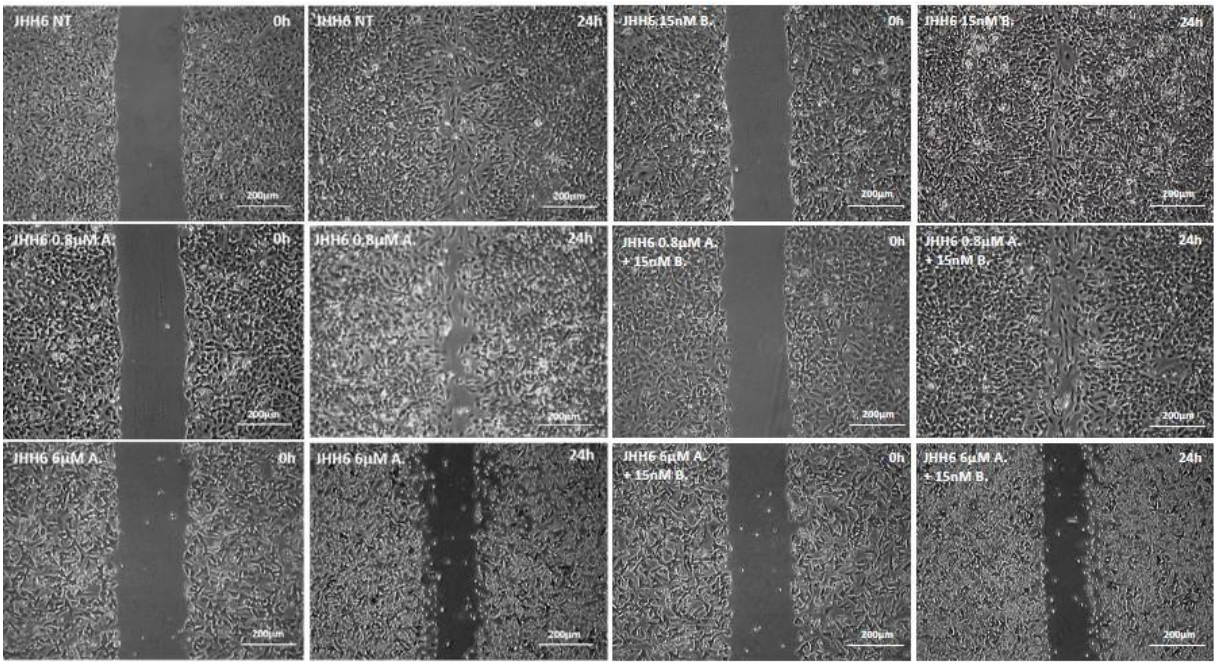

Fig. 4.61 – Representative images of scratch assay in JHH6 cells treated with 5-azacytidine or with combined treatment 5-azacytidine/*Bortezomib*. Images are acquired with Leica DM IRB microscope. Magnification 5X (bar = 200μm).

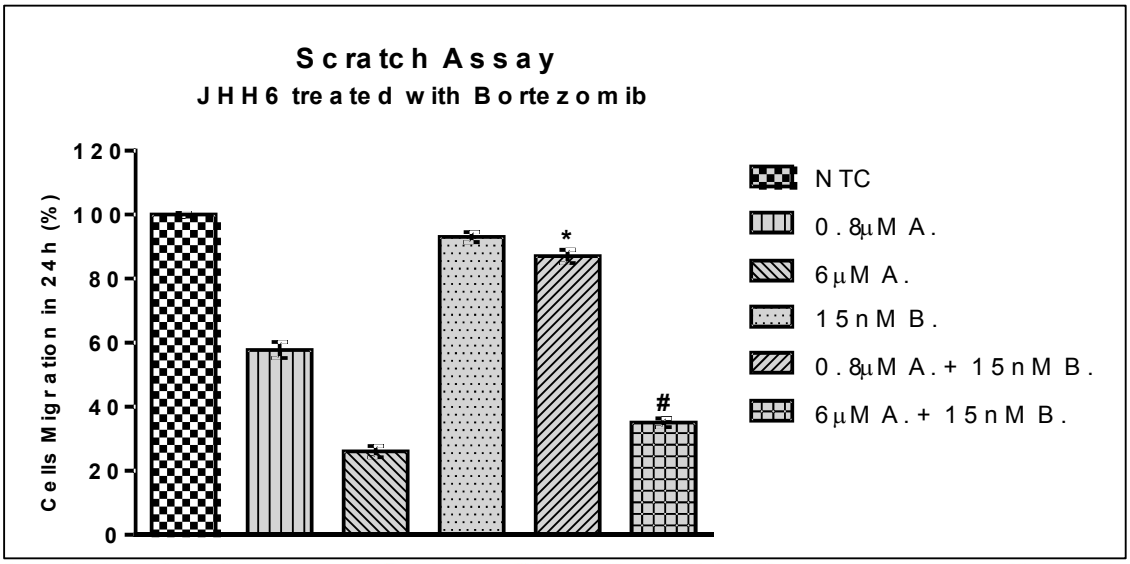

Fig. 4.62 – Scratch assay quantification in JHH6 cells treated with 5-azacytidine or with combined treatment 5-azacytidine/*Bortezomib*. Data are expressed as mean ± SEM. P*< 0.0001 respect to 0.8μM treated cells, P#< 0.05 respect to 6μM treated cells. n=15

Also in HuH7 cells treated simultaneously by 5-azacytidine and *Bortezomib,* cell migratory ability was restored in a dose-dependent manner (Fig. 4.63). In particular, cells treated with the two lower doses of 5-azacytidine and 10nM of *Bortezomib* increased their

migratory ability of about 30% whereas the migration percentage of HuH7 treated with 30µM of 5-azacytidine and 10nM of *Bortezomib* rose of about 50% (Fig. 4.64).

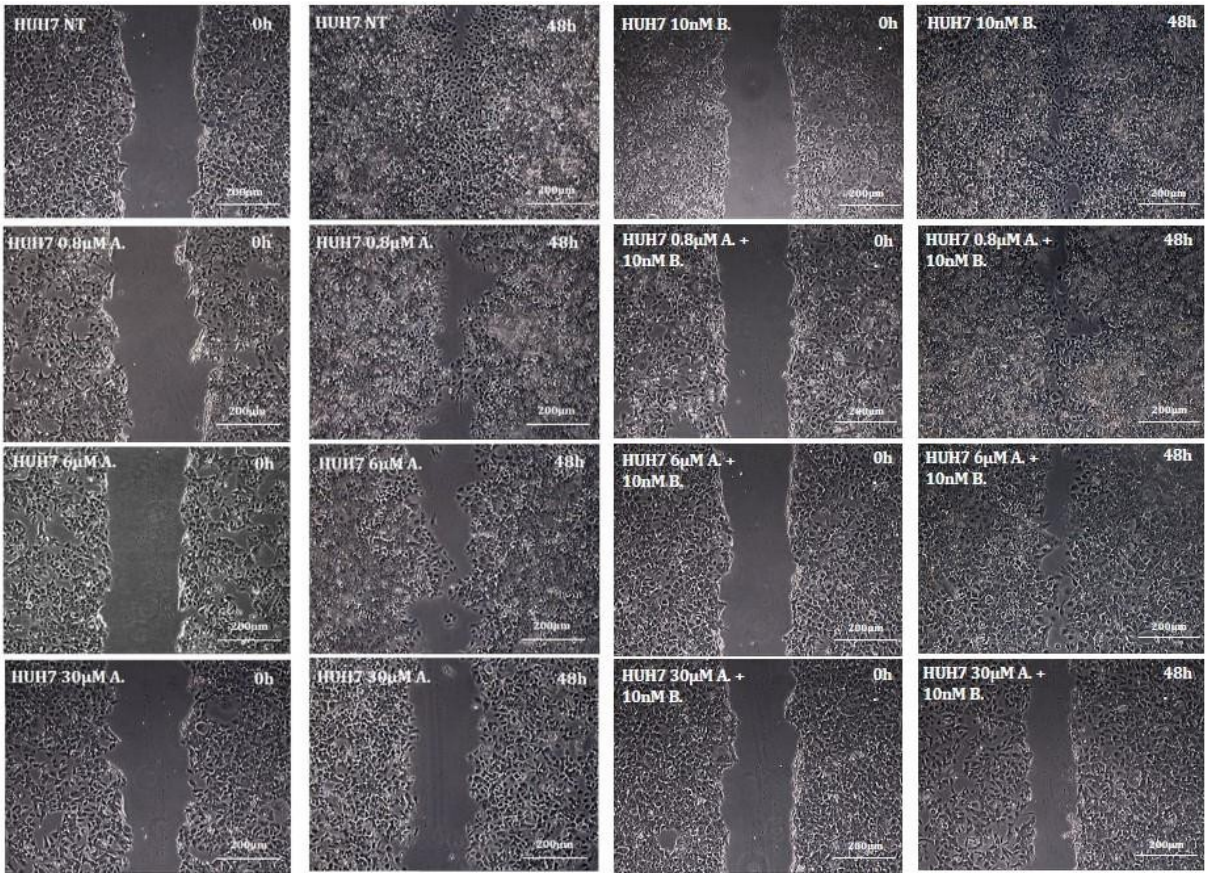

Fig. 4.63 – Representative images of scratch assay in HuH7 cells treated with 5-azacytidine or with combined treatment 5-azacytidine/*Bortezomib*. Images are acquired with Leica DM IRB microscope. Magnification 5X (bar = 200µm).

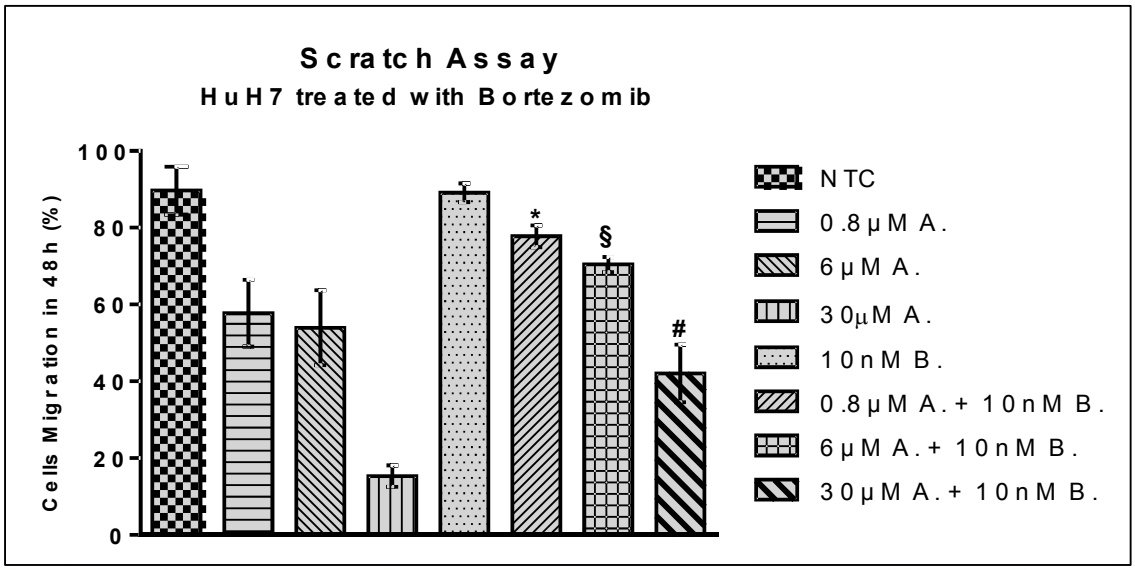

Fig. 4.64 – Scratch assay quantification in HuH7 cells treated with 5-azacytidine or with combined treatment 5-azacytidine/*Bortezomib*. Data are expressed as mean ± SEM. P*< 0.0001 respect to 0.8µM-treated cells, P§<0.005 respect to 6µM-treated cells and P#< 0.05 respect to 30µM -treated cells. n=15

4.3 Effects of 5-azacytidine *in vivo*

In order to confirm the effectiveness of 5-azacytine in a more complex system and to confirm *in vivo* the molecular mechanisms of action observed *in vitro*, a subcutaneous xenograft mouse model of HCC has been considered. These experiments were done in collaboration with Dott.ssa Urska Kamensekand Dott.ssa Maja Cemazar of the Oncology Institute of Ljubljana, Slovenia. A suspension of 10^7 HuH7 cells in 0.1 ml of *NaCl* was injected subcutaneously into the right flank of SCID (*Severe Combined Immuno Deficiency*) mice[298]. As JHH6 cannot graft in the animals, this cell type was not considered for the mice model. When tumours reached 30-40 mm^3, animals were randomly divided into two experimental groups (5-azacytidine group Vs control group). In the 5-azacytidine group, mice were treated by intra-tumour injections of 0.4µg of 5-azacytidine in three consecutive days (Figure 4.65). The 5-azacytidine dosage of 0.4µg was used to resemble the most effective *in vitro* concentration (30µM). Mice belonging to the control group were treated with the same volumes of endotoxin free water without 5-azacytidine. Two different experimental protocols were followed: a short-term and a long-term evaluation protocol. In the first case, mice were sacrificed two days after the first round of 5-azacytidine treatments (Fig. 4.65). In the long-term evaluation protocol mice were sacrificed when mass tumour reached 300 mm^3, which corresponded to either 9 or 16 days after the second round of treatments (Fig. 4.65).

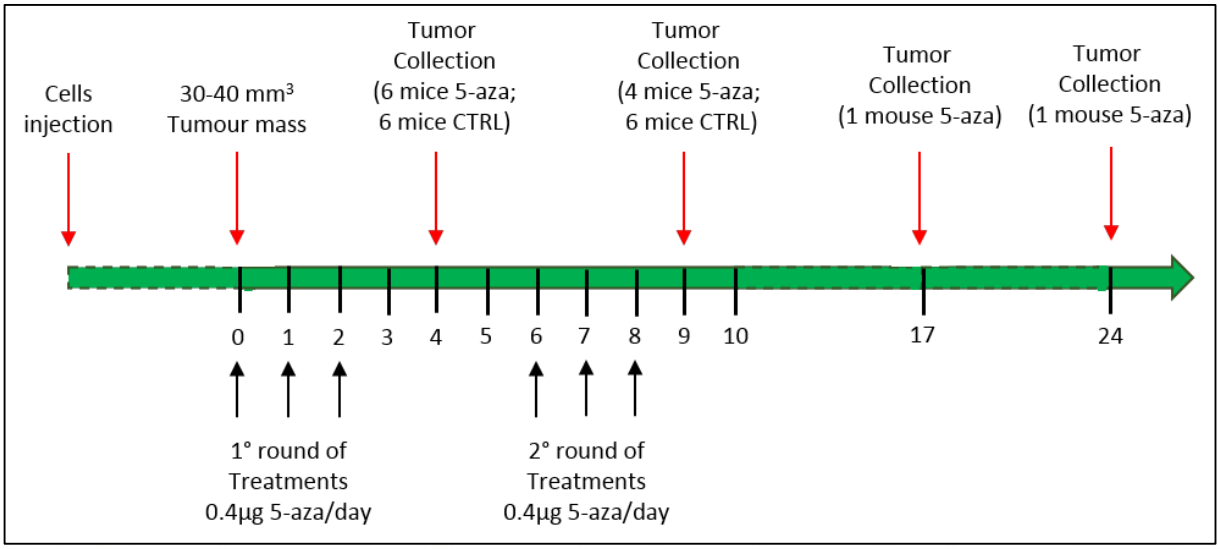

Fig. 4.65 – Schematic representation of the two experimental protocols performed by using murine Xenograft model.

4.3.1 Effects of 5-azacytidine on tumor mass growth and animal survival

As shown in Fig. 4.66, significant differences in term of tumor size were already observed after the first round of drug treatments between treated and untreated mice. These differences were maintained during the second round of 5-azacytidine administrations and until the end of the experiments. However, we observed that after each cycle treatment the tumour starts re-growing, thus in the future we would test the effects of a continuous administration of the drug. Notably, tumor mass reached 300mm ^{3} 10 days after the beginning of the experimental protocol in control mice; in contrast, the growth of the tumor mass in treated mice was remarkably delayed reaching the critical volume 17-24 days after the beginning of the test procedures (Fig. 4.66).

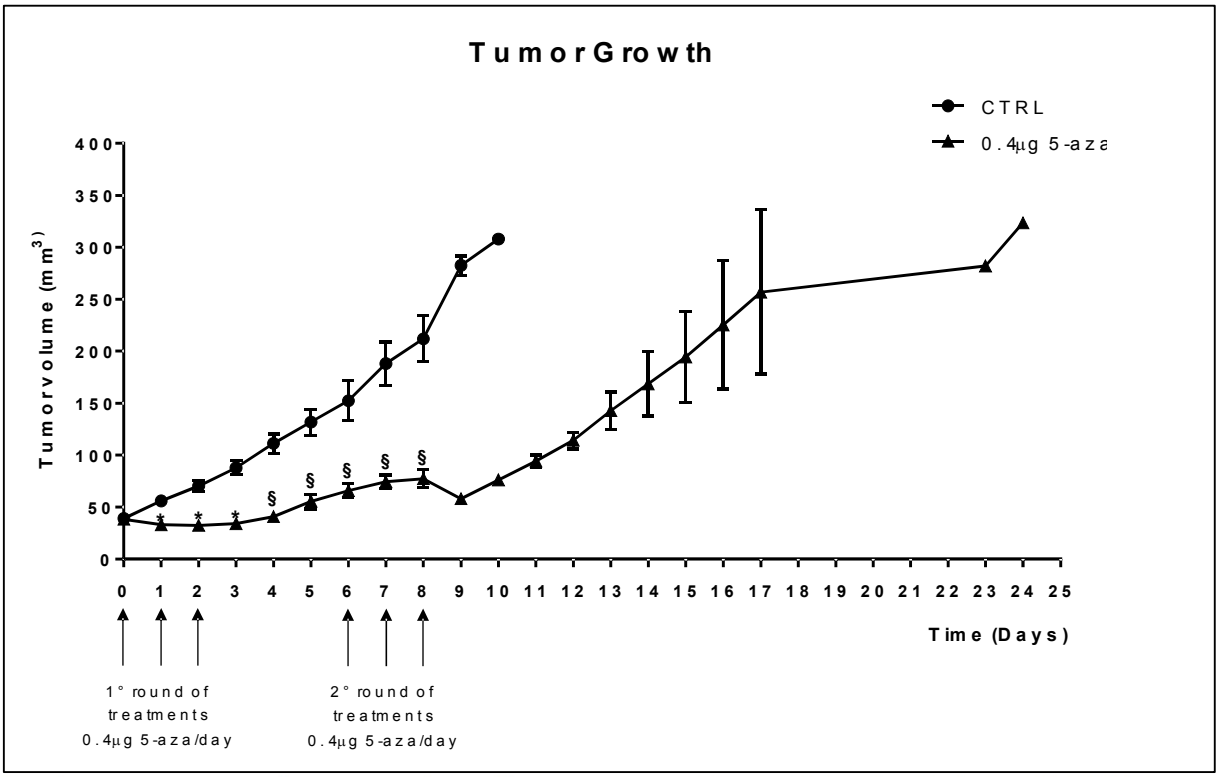

Fig. 4.66 – Comparison of tumor growth trend between 5-azacytidine-treated and control mice. P*<0.0001 and P§<0.005 respect to CTRL (Control mice). Data are expressed as mean ± SEM. The number of animals tested has already been indicated in Fig. 4.65.

Not only 5-azacytidine delayed tumor mass growth, it also improved animal survival as treated mice lived about twice respect to control animals (Fig 4.67).

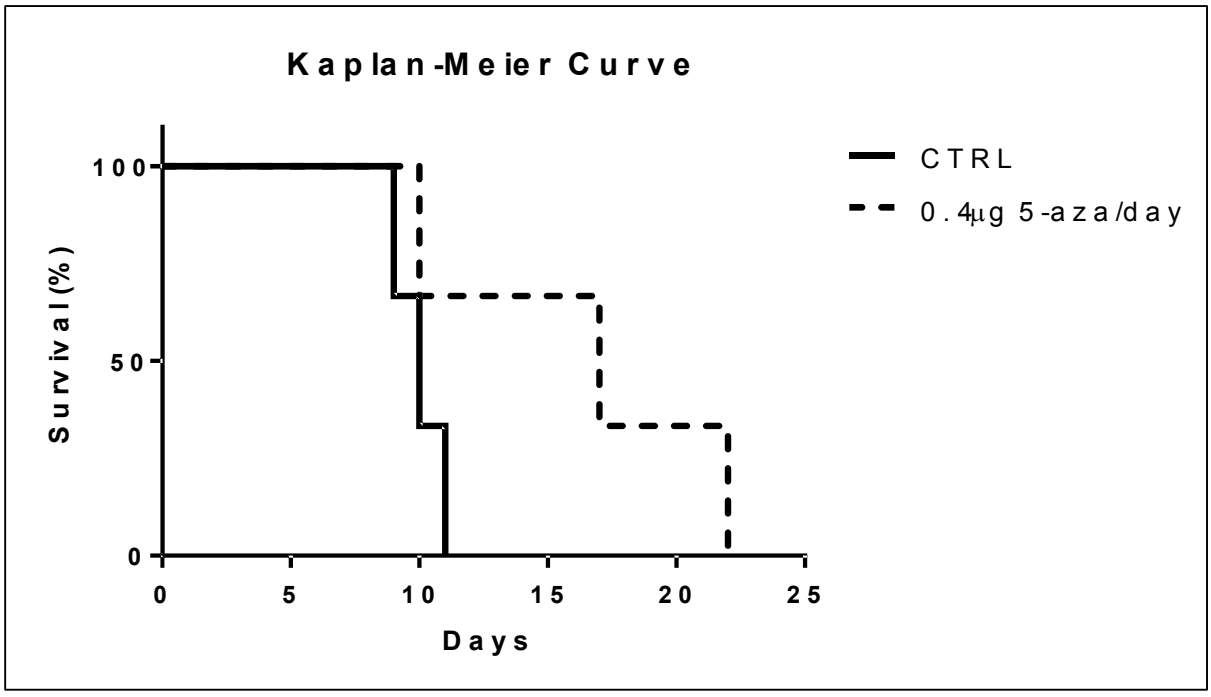

Fig. 4.67 – Kaplan-Meier Curve. Data are expressed as mean ± SEM. Mice treated with 0.4 µg 5-aza/day=3; CTRL (Control) mice =3.

4.3.2 Molecular effects of 5-azacytidine *in vivo*

We then wanted to confirm *in vivo* the molecular pathway affected by 5-azacytidine *in vitro* (miRNA 139-5p, ROCK2, MMP2). Tumor masses from the short-term protocol were collected and the levels of miRNA 139-5p, ROCK2, MMP2 evaluated. As shown in Fig. 4.68, a significant increase in miRNA 139-5p levels was observed in treated vs non-treated animals.

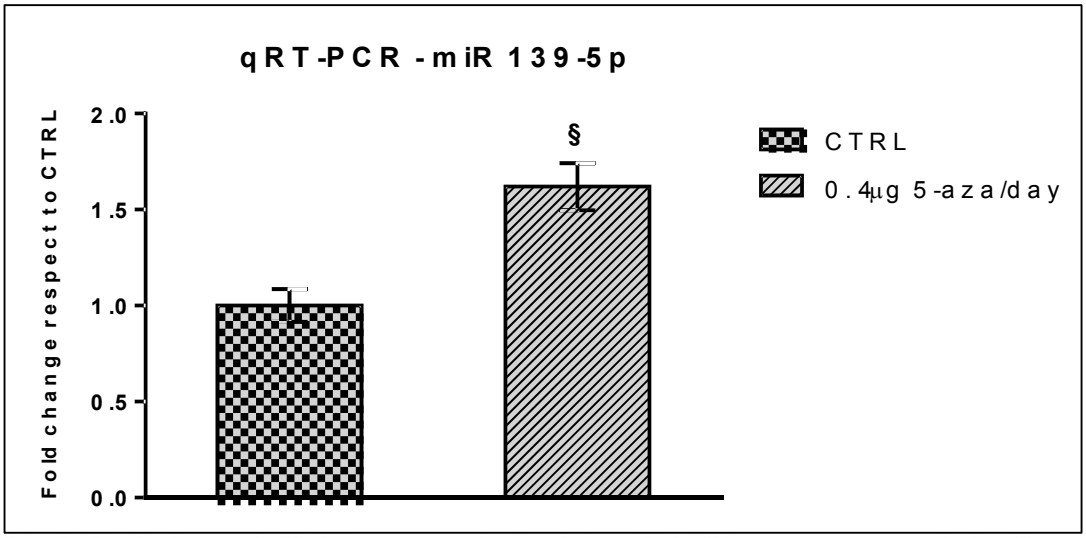

Fig. 4.68 – Analysis of miR 139-5p expression levels by qRT-PCR in tumour masses obtained from 5-azacytidine treated and control mice. P§<0.005 respect to CTRL (Control mice). Data, normalized to CTRL, are mean ± SEM. n=9.

Moreover, as shown in Fig 4.69 and summarized in Fig. 4.70, we observed a strong reduction of ROCK2 protein levels in tumor masses collected from treated mice compared to control animals. Finally, also for MMP2 protein, we noticed a strong decrease in protein levels in 5-azacytidine treated mice compared to control animals. Collectively, the above data confirm *in vivo* the molecular effects of 5-azacytidine observed *in vitro*.

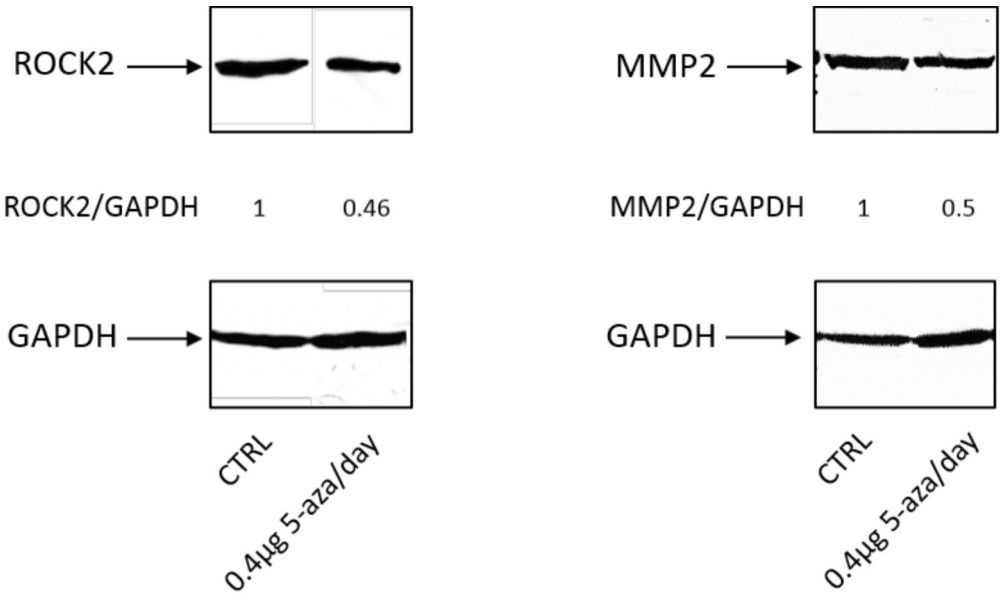

Fig. 4.69 – A representative immunoblotting for the detection of ROCK2 and MMP2 protein levels, in 5-azacytidine treated and control mice, is shown. The ratio ROCK2/GAPDH and MMP2/GAPDH is normalized to CTRL (Control mice).

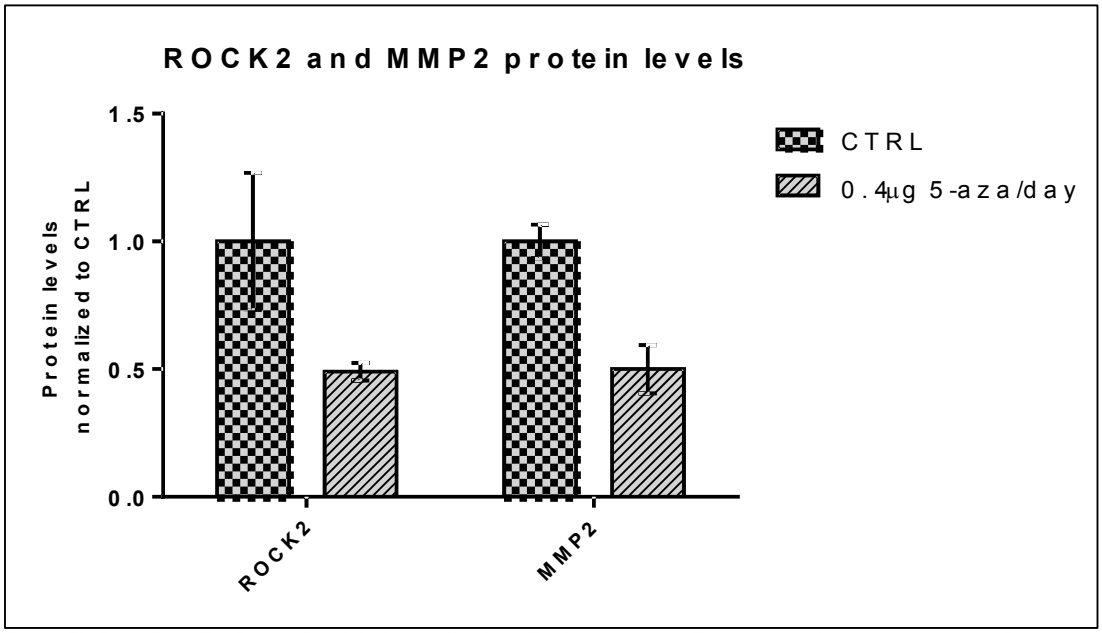

Fig. 4.70 – ROCK2 and MMP2 protein levels in 5-azacytidine treated mice compared to control animals. Data, normalized to CTRL (Control mice), are expressed as mean ± SEM; n=3.

Finally, the histological analysis of tumor tissues collected from treated mice showed the peculiar presence of polygonal shape structures similar to those of the hepatic lobules (Fig. 4.71).

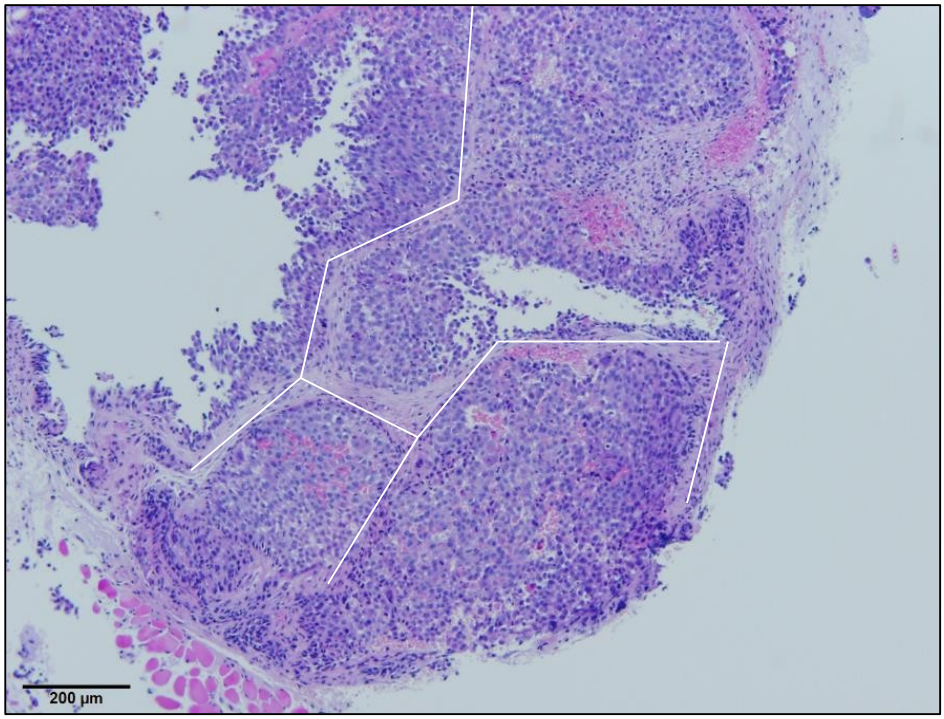

Fig. 4.71 - Haematoxylin eosin staining. The tumour mass was obtained from a 5-azacytidine-treated animal at day 4. Indicated in white is the polygonal shape of the pseudo hepatic lobules. Magnification 5X (bar=200µm).

These evidences, not observed in control mice, suggest that 5-azacytidine treatments may induce a sort of differentiation of cells belonging to treated tumor mass. This hypothesis is supported by the detected overexpression of albumin, a well-known marker of hepatic differentiation[282], in tumor masses collected from 5-azacytidine treated mice compared to control animals (Fig. 4.72). Moreover, the up-regulation of albumin after 5-azacytidine administrations was not observed *in vitro*, suggesting that the de-differentiation process may require a more complex system to occur.

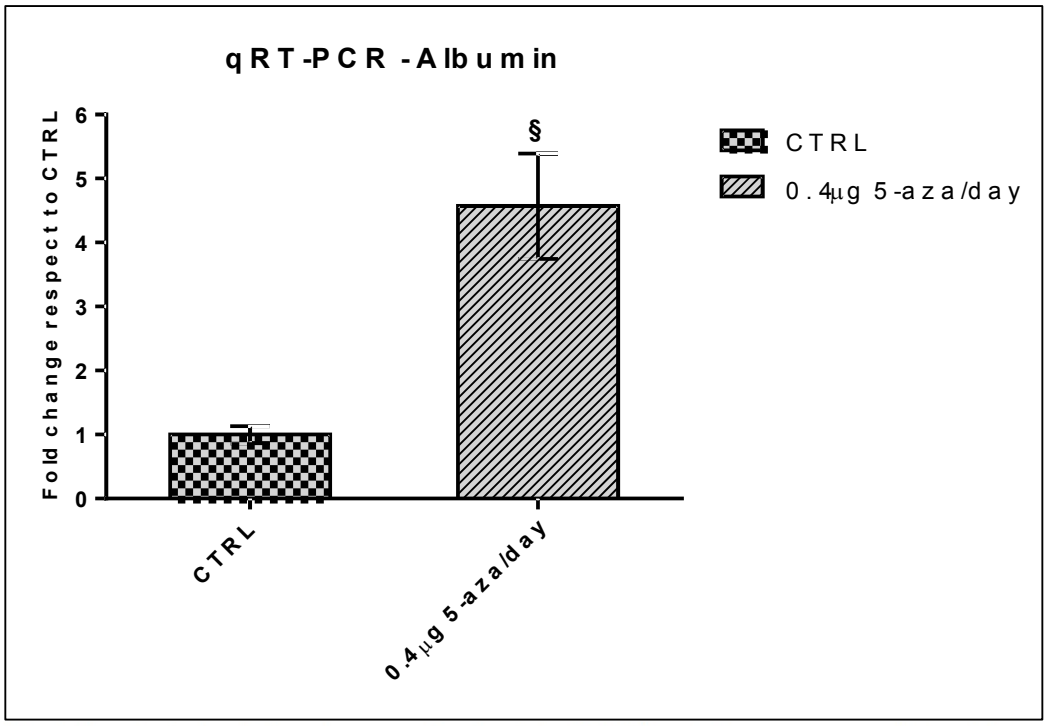

Fig. 4.72 – Analysis of albumin expression levels by RT-PCR in tumour masses obtained from 5-azacytidine treated and control mice. P§<0.005 respect to CTRL (Control mice). Data, normalized to CTRL, are mean ± SEM. n=9.

5. Discussion

5.1 HCC is a widespread cancer with poor prognosis and very limited therapeutic options.

Primary liver cancer (PLC) is the fifth most common cancer in the world and the third leading cause cancer-related deaths worldwide, with approximately 600.000 deaths annually [1]. HCC is the most represented liver primary cancer [2], which accounts for approximately 85% of all PLC[1]. The estimated incidence of new cases of HCC is about 500.000-1.000.000 per year even if an important difference has been noted between countries [2]. In fact, most cases of HCC occur in Asia where several regions have a very high incidence. Although the incidence of HCC in developed countries is relatively low, it is rising annually[18]. For example in the United States there has been an increase of about 80% in the annual incidence of HCC from 1.4/100.000 (cases/inhabitants) per year in the eighties to 2.4/100.000 per year in the nineties[2]. Other developed countries have noted similar increasing trends, for example Italy but also United Kingdom and Canada. This increase is related to migration flow from parts of the world with high prevalence, such as sub-Saharan Africa and Asia, being associated with a parallel increase in hospitalization and mortality for HCC[19].

Only in the very early stages of disease, there are real possibilities to heal from HCC. In fact, in these cases, liver transplantation and surgically resection of tumor can be curative in a great majority of patients. Unfortunately, being HCC often asymptomatic in its early stages, most patients will not be candidate for either surgery or transplant[4]. If the HCC progresses to an advanced stage, only systemic treatments are indicated even if the prognosis and outcome are very inauspicious for patients [5]. Currently the only FDA-approved systemic treatment for HCC[4] is an oral multi-kinase inhibitor called *Sorafenib*. It is used for the treatment of HCC patients with well-preserved liver functions that cannot receive curative treatment and patients with advanced HCC[4]. *Sorafenib*, however, can only induce 3-month improvement in both median survival and time of progression. Moreover, it is not uncommon that patients develop drug-resistance to *Sorafenib* treatment.

The above considerations clearly indicate that novel therapeutic treatments for HCC are urgently required.

5.2 HCC is one of the leading cancers in which aberrant methylation occurs

In contrast to the genetic alterations that cause irreversible changes to particular DNA sequences, epigenetic regulations do not change the sequence of the genome but influence chromatin structure and genes transcription [77]. Epigenetic alterations usually induce activation of oncogenes or inactivation of tumor suppressor genes and recent evidences suggest that epigenetic changes play an important role both in initiation and in development of HCC. In HCC, hyper-methylation of CpG islands is frequently observed at the promoter region of important tumor suppressor genes, including SOC1, APC and E-Cadherin, which are hyper-methylated in most HCC patients[7,8]. Methylation profiling of multi-step HCC tumors suggested that the number of methylated genes gradually increase with the progression of cancer stage. In fact, the observation of tumor suppressor genes hyper-methylation in both para-tumor liver tissues and cirrhotic tissues indicates that aberrant promoter methylation occurs in the early stage of hepatocarcinogenesis and increases during cancer progression [145]. Moreover, genome-wide DNA methylation analysis reveals that HCC epigenetic silencing of multiple tumor suppressors can lead to the activation of several oncogenic signaling pathways including Ras, JAK/STAT, and Wnt/β-catenin [146]. Given the importance of DNA hyper-methylation in hepatocarcinogenesis, the pharmaceutical company producing 5-azacytidine (commercial name *Vidaza*) named Celgene asked us to investigate the effects of 5-azacytidine in HCC. So far 5-azacytidine, a de-methylating agent able to restore the function of tumor suppressor genes, has been approved by the US FDA for the treatment of myelodysplastic syndrome and acute and chronic myeloid leukemia[9].

Based on the above consideration, we started to study on the effects of 5-azacytidine treatments on HCC cell line models and in particular on JHH6 and HuH7 cell lines.

5.3 Phenotypic effects of 5-azacytidine on HCC cell lines

5.3.1 Cell vitality and number

The two HCC cell lines chosen to perform all the experiments discussed in this thesis are the JHH6 and HuH7 cell lines. These cell lines have different phenotypes: HuH7 and JHH6 are assigned to high and medium hepatic differentiation grade respectively on the base of their capacity to synthesize albumin, a well-known marker of hepatic differentiation[282]. HuH7 and JHH6 cell lines derives from a differentiated and undifferentiated hepatoma respectively[283]. For this reason, JHH6 cell line represents a more aggressive HCC model than

HuH7 cells. Thus, the use of HCC cell lines with different differentiation grade allowed us detect phenotypic-dependent effects of 5-azacytidine. In this regard, it clearly results from our data that JHH6 are more sensible than HuH7 (see for example the cell counting and the vitality data, Figure 4.5 and 4.6). A possible interpretation of this observation is that being less differentiated, JHH6 may have a promoter methylation pattern different and more prone to be subverted by 5-azacytidine compared to HuH7. Notably, it is known that DNA methylation status change during HCC progression and it is also related to clinic-pathological and histological features[326]. Thus, it is feasible than in the less differentiated JHH6, the methylation pattern differs from the more differentiated HuH7. The improved sensibility of JHH6 compared to HuH7 may also depend on the presence in JHH6 of a drug extrusion machinery less effective in JHH6 compared to HuH7. Consequently, the drug dose that can reside in the cell is higher in JHH6 compared to HuH7. Regardless of the reasons for the dissimilar sensitivity to 5-azacytidine, our data indicate that the drug is active against HCC cells with different phenotypes. Thus in principle 5-azacytidine has the potential to be active also against HCC with different differentiation grade *in vivo*.

5.3.2 Cell proliferation

Whereas the reduction in cell vitality and number is not significantly dependent on cell necrosis and apoptosis (Figures 4.13, 4.15 and 4.18), our data indicate a strong effect on cell proliferation induced by 5-azacytidine. In particular, we observed a cell cycle block in the G1/S and G2/M (Figures 4.8 and 4.10).

The G1/S block is in line with the down regulation of the S phase promoting genes E2F1-3 (Figure 4.31 and 4.33) and with the upregulation of the S phase inhibitory gene E2F7. The fact that 5-azacytidine reduces the expression of E2F1-3, indicates that its action cannot be direct on these genes. Indeed, the action of 5-azacytidine is to subvert the promoter methylation pattern activating the transcription. Thus, it is possible that the drug reactivates the expression of cellular genes negative regulating E2F1-3 expression. In this regard, it is feasible that 5-azacytidine reactivates the expression of miRNAs affecting the level of E2F1-3. However, our miRNA expression data (Table 4.2) do not show the upregulation of miRNAs known to target E2F1-3. It is thus possible that other miRNAs are upregulated by 5-azacytidine but we could not detect them because of the sensibility of the detection system (miRNoma). In this regard, it is known that the quantitative real time PCR approach is more sensible than miRNoma analysis. An alternative to the upregulation of E2F1-3 targeting miRNA, is that 5-azacytidine promotes the expression of gene affecting E2F1-3 stability. In

contrast to the E2F1-3 expression down regulation, the upregulation of the cell cycle inhibitor E2F7 may directly depend on the demethylation of its promoter by 5-azacytine. Obviously, further investigation about the molecular effects of 5-azacytidine on the expression level of cell cycle promoter/inhibitors belonging to the E2Fs family is necessary (work in progress). Among these, we need to verify the methylation pattern of E2F7 promoter before and after 5-azacytidine treatment.

The G2/M block we observed in HCC cell lines (Figures 4.8 and 4.10) is in line with the observation of the occurrence of bigger cells, compared to controls (Figures 4.1, 4.2, 4.3 and 4.4). These findings indicate that many of the HCC treated cells increase their size in order to duplicate but, being blocked in G2, they cannot progress toward the M phase and thus maintain the bigger size. The impossibility to progress towards the M phase is in line with the subverted organization of the cell cytoskeleton evidenced by β-tubulin staining (Figure 4.26 and 4.27). In particular, compared to non-treated cells, β-tubulin displayed an accumulation in the peri-nuclear region. The above observation together with the absences of pro-apoptotic markers suggest that 5-azacytidine could induce a specific cell death phenomenon known as *Mitotic Catastrophe*[327]. *Mitotic catastrophe* is a recently discovered phenomenon, characterized by the occurrence of aberrant mitosis, or mis-segregation of the chromosomes, followed by cell division and inhibition of the dynamic reorganization of microtubules. Nuclear envelopes form around individual chromosomes or groups of chromosomes forming large non-viable cells with multiple micronuclei, which are morphologically distinguishable from apoptotic cells[327]. Mitotic catastrophe induces mitotic damage and directs the defective cell to one of three possible anti-proliferative fates. Defective mitotic cells can engage the cell death machinery and undergo death in mitosis, when cyclin B levels remain high. Alternatively, defective cells can exit mitosis, known as slippage, and undergo cell death execution during G1 in the subsequent cell cycle. This last fate may contribute to explain the G1 block we observed. Finally, defective cells can exit mitosis and undergo senescence [327]. It is clear that mitotic catastrophe is always accompanied by mitotic arrest; however, the mechanisms that dictate cell fate following mitotic catastrophe remain unclear. It was originally proposed that death signals gradually accumulate during mitotic arrest, and therefore the length of mitotic arrest determines cell fate[327]. Mitotic catastrophe can be induced by different mechanisms including mitotic perturbation and DNA damage. If mitotic perturbation occurs, microtubules do not stick properly to chromosomes at their kinetochore, promoting a network of signals to recruit mitotic checkpoint components to kinetochores. This event allows the formation of an inhibitory complex named *Mitotic checkpoint Complex*,

consisting of Mad2, ubR1 and BuB3 as well as Cdc20, that binds to and potently inhibits APC by sequestering CdC20, thereby preventing mitotic exit [327]. Improper kinetochore-microtubule attachment also causes reduced tension across the spindle apparatus, which inhibits the APC through a mechanism involving Aurora B kinase. Instead, following DNA damage, activated ATR and ATM promote the activation of the *DNA damage checkpoints*, including Chk1 and Chk2, which transduce the DNA damage signal downstream. Genomic stress activates the G1 checkpoint, which prevents S phase entry by inhibition of DNA replication. At this point, Chk2, which is activated by ATM, phosphorylates and suppresses the phosphatase Cdc25-A, thereby preventing activation of cyclin E/cdk2 and thus halting the cell cycle. The S phase checkpoint is activated in response to replication errors and DNA damage that occurs during S phase, whereas the G2 checkpoint deals with cells that have either undergone DNA damage in G2, or they have escaped the G1 and S phase checkpoints. At G2, Chk1, which is activated by ATR, phosphorylates and suppresses Cdc25-A, -B, and -C thereby preventing cyclin B/cdk1 activation and causing G2 arrest[328-330]. G2 arrest is also initiated by MK2 which inactivates Cdc25-B and -C [328]. Thus, the G2 checkpoint is the last opportunity to halt the cycle and repair DNA damage in cells that have escaped the G1 and S phase checkpoints. Abrogated or compromised G2 checkpoint will allow premature mitotic entry of defective cells that fail to undergo proper chromosome segregation thereby leading to mitotic catastrophe. The mitotic catastrophe markers most studied are cyclin B, Aurora B and also the H3 phosphorylation mediated by Aurora A kinase. We started to study the molecular mechanism underlying the 5-azacytidine-mediated mitotic death evaluated the H3 phosphorylation on serine 10 (data not shown) by immunostaining assay. We observed a significantly dose-dependent increase of H3 phosphorylation in treated cells respect to control cells. In the future, we plan to analyse other specific markers to definitively prove the induction of mitotic catastrophe by 5-azacytidine treatment.

In conclusion our data indicate a potent anti-proliferative effects of 5-azacytidine which is exerted via a G1/S and G2/M blocks. Whereas the molecular mechanisms responsible for these effects deserve further investigation, our data clearly point towards the potent effect of 5-azacytidine.

5.3.3 Cell migration

In agreement with the subverted cytoskeleton structure induced by 5-azacytidine, also cell migration was importantly affected. We evaluated cells migratory ability firstly by performing scratch assay, an easy test that allows evaluating the ability of cells to fill in a gap

generated with a tip on a cell monolayer. 5-azacytidine induced a dose-dependent decrease of cell migratory ability in both cell lines (Figures 4.20 and 4.23). Regarding to JHH6 cells, a set of time-lapse microscopy experiments were also performed in collaboration with Prof. Caserta and Prof. Guido's group of Federico II's University, Naples. In this case, in addition of being maintained in 1% FBS, cell were also treated with Mytomycin C, a chemical compound able to block cell duplication. These set of experiments allowed us to understand how the residual cell proliferation influenced migration data. The results obtained clearly indicated that Mytomycin C/5-azacytidine treated cells displayed a reduction in migration speed comparable to that of 5-azacytidine alone. These data suggested that the reduction in cell migration due to 5-azacytidine is not substantially influenced by residual cell proliferation. Considering that scratch assay was performed using cell grown on plastic surface, to better mimicking the physiological condition where cells are in contact with extracellular matrix, we performed the FATIMA assay. This test allows studying the ability of cells, stimulated by a serum gradient, to migrate through a membrane coated with extracellular matrix proteins, such as Collagen IV. We observed that 5-azacytidine administrations inhibited significantly JHH6 and HuH7 cell migratory ability. Notably, higher dose of the drug were necessary for HuH7 further pointing towards the increased resistance of this cell line to 5-azacytidine (compare Figure 4.24 with 4.25). Comparable results were obtained also coating trans-well membranes with Collagen I, another key component of extracellular matrix, indicating that the anti-migratory effect of 5-azacytidine is really coat-independent. Thus, the potent anti-migratory effect observed together with the anti-proliferative activity of 5-azacytidine, makes this compound potentially appropriate for HCC treatment.

5.4 Phenotypic effects of 5-azacytidine on control liver cells

As control cells, we used a human hepatocyte cell line called *IHH* and human hepatocyte-like cells obtained differentiating human embryonic stem cells (hESCs). IHH are hepatocytes immortalized by stabile transfection with a recombinant plasmid containing the early region of SV40 virus. IHH cells retain several differentiated features of normal hepatocyte. Hepatocyte-like cells were instead obtained using a specific differentiation protocol developed by Prof. Elvassore's group[286]. They can be considered phenotypically very close to mature hepatocytes being positive for hepatic markers including albumin and cytochrome P450-3A and shows albumin secretion, glycogen storage and indocyanine green incorporation. IHH and human hepatocyte-like cells were used to mimic the normal

hepatocyte thus allowing to start the exploration about the possible side effects of 5-azacytdine on normal liver cells. The ideal control cell would have been represented by isolated human hepatocyte. However, the difficulties to obtain such cells both in terms of ethic and quantity issues, prompted us to consider more "friendly" cells such as *IHH* and human hepatocyte-like cells. Our data indicate that *IHH* and human hepatocyte-like cells are significantly less sensitive to 5-azacytidine compared to the HCC cell lines. This observation anticipates that *in vivo* the drug may affect predominantly the tumor cells compared to the normal liver cells thus preserving the liver functions. Whereas these data deserve further confirmation *in vivo*, they represents an encouraging observation for the use of 5-azacytidine.

Despite the reduced sensibility shown by IHH cells to 5-azacytidine, the effect on cell viability and counting is not negligible (see Figures 4.5 and 4.6). In contrast, in hepatocyte-like cells, 5-azacytidine effect is far less evident if not absent (Figures 4.5 and 4.6). A possible interpretation of this observation is based on the fact that the extent of 5-azacytidine effect depends on its incorporation into DNA that in turn is a function of the cell replication rate. As IHH are faster proliferating cells compared to hepatocyte-like cells[331], it is reasonable that IHH are more affected than hepatocyte-like cells. Thus, this observation indicates that, whereas 5-azacytidine effects on the non-tumorigenic liver cells is more contained compared to hepatocarcinoma cells, in case of concomitant liver regenerating phenomenon (cirrhosis, surgical intervention etc.) caution should be exercised in the use of 5-azacytidine. Indeed, under this condition, 5-azacytidine may influence the regenerative process impairing liver functions.

In contrast to the HCC cell lines, the control cells IHH and hepatocyte-like cells, did not show important morphological changes in the cell shape (Figures 4.3 and 4.4). In fact, in both cases, cells maintained their polygonal-like shape without cytoplasmic granulation and both nuclei and plasma membranes were smooth. Moreover, in IHH treated cells a structured distribution of β-tubulin without significant accumulation at a peri-nuclear level was observed (Figure 4.28). These observation are in line with the reduced impact of 5-azacytidine on control cell viability and support the milder effect on non-tumorigenic liver cells. In agreement with the morphological, viability and cell counting data, also at the cell cycle level, 5-azacytidine showed a milder impact on the control IHH cells (Figure 4.12). Hepatocyte-like cells were not used for cell cycle analysis due to the small amount available following the differentiation process (obtained by a microfluidic approach) and to the fact that ki67 staining did not show major signs of proliferation[331].

As observed for the HCC cell lines considered, also in IHH the reduction in cell vitality and number is not significantly dependent on cell necrosis and apoptosis (Figures 4.14, 4.16 and 4.18). Due to the fact that hepatocyte-like cells are produced in a very small amount, they were not considered for necrotic and apoptotic testing.

5.5 Molecular effects of 5-azacytidine on HCC cell lines

After observing the important phenotypic aspects induced by 5-azacytidine repeated administrations, we started to explore the molecular mechanisms responsible for these phenotypes. In particular, we performed two type of microarray analysis, one made to evaluate gene expression changes and the other to analyze miRNA deregulation in tumor treated cells.

5.5.1 Gene and miRNA expression profile

The data obtained by microarray analysis gave us many information about both gene expression modification and miRNA deregulation. In fact, we found that in JHH6 cell line 5-azacytidine (6μM) induced the deregulation of about 2200 genes. Many of these were involved in the main cellular processing, such as cell cycle regulation, cell proliferation and growth, cell communication and cell death. Relevant for the present investigation, we observed the down regulation of the expression of E2F1-3 and the upregulation of E2F7, already discussed in 5.3.2. Moreover, also the expression of the oncogenes PI3K and c-FOS was downregulated in treated cells compared to non-treated cells. This further support the potent anti-proliferative effect of 5-azacytidine. The fact that different molecular pathways involved in cell proliferation are affected by 5-azacytidine, indicates a pleiotropic effect of this drug and provides the basis for the potent anti-proliferative effect. Obviously, as also discussed for E2Fs, the role of PI3K and c-FOS down regulation needs further studies to fully understanding their role in the 5-azacytidine mediated effect.

In agreement with the potent anti-migratory effect of 5-azacytidine and in addition to the subverted cytoskeleton structure ofβ-tubulin (Figures 4.26 and 4.27), we observed the down regulation of many different genes involved in the migration and adhesion processes. Among these, many subunits of integrines proteins (β4, αX, α3), Rac and MMP2, showed a significant down-regulation. MMP2 is one of the most important proteins that promote tumor cells migration and invasionand its overexpression is often correlated with poor prognosis and outcome in many type of tumors [313,314]. Moreover, also ATF3 and ATF4 were found to be

upregulated. Notably, their reduced expression was associated with bladder cancer progression and reduced survival of patients [317]. Moreover ATF3 promotes the formation of MDM2/ATF3/MMP2 complex that facilities MMP2 degradation (see also the scheme of Figure 5.1), thus inhibiting cell migration in esophageal squamous cell carcinoma [318]. Taken together, these data demonstrate that, as observed for the anti-proliferative effects, also for the anti-migratory effect, 5-azacytidine affects different pathways thus explaining its potent effect.

In addition to studying the effects of 5-azacytidine on gene expression, we have previously evaluated the expression profile of miRNAs, being these molecules particularly important in the development of many cancers including HCC. Microarray analysis found 14 miRNAs differentially expressed after 5-azacytidine administrations and of these 4 resulted up-regulated whereas 9 were down-regulated. Due to the known involvement of miR 139-5p in HCC development [277], we mainly focused on this miRNA. We confirmed by qRT-PCR the up-regulation of miR 139-5p in both HCC cell lines, finding greater up-regulation in JHH6 cell line. Probably, this can contribute to explain the increased sensitivity of JHH6 cells compared to HuH7 to 5-azacytidine.

5.5.2. Role of miR139-5p ROCK2, MMP2 in 5-azacytidine effects

Starting from our miRNoma data, we focused our attention of the upregulation of miR139 5p by 5-azacytidine since the downregulation of this miRNA in HCC is associated with poor patients prognosis and features of metastatic tumors [277]. Moreover, overexpression of miR 139-5p in HCC cells significantly reduces cell migration and invasion *in vitro* and the incidence and severity of lung metastasis in orthotropic liver tumors in mice[277]. Our data indicate that miR139-5p upregulation is not an epiphenomenon of 5-azacytidine as shown by the functional assays we performed. Indeed, miR139-5p *per se* can: 1) significantly decrease cell viability and number (Figures 4.36 and 4.38), 2) induce a G2/M phase block (Figure 4.39) and 3) influence the cytoskeletal structure of cells and the migratory ability (Figure 4.40 and 4.50). Thus, miR 139-5p overexpression (obtained by transfection of pre-synthetized molecules) can reproduce the effects triggered by 5-azacytidine. Notably, the extent of the effects induced by miR139-5p is reduced compared to that of 5-azacytdine. This however may depend on the fact that, as discussed above, 5-azacytidine exerts its effects affecting multiple pathways. In contrast, it is convincible that miR139-5p has a more restricted field of action.

Given the known effect of miR139-5p on ROCK2[277], we studied the variation of ROCK2 levels following 5-azacytidine or miR139-5p administration. Moreover, as ROCK2 stabilizes MMP2 promoting its pro-migratory activity, also MMP2 was studied. Importantly, the Rho/ROCK2 signaling is frequently altered in human HCC by multiple mechanisms and consequently implicated in HCC metastasis[323]. Moreover, in HCC MMP2 is a master regulator of tumor metastasis. Additionally, it is known that ROCK2 and MMP2 are markedly overexpressed in HCCs compared with the corresponding adjacent tissue[323].

Our data show that both ROCK2 and MMP2 proteins are significantly down-regulated by 5-azacytidine in both HCC cell lines considered (Figures 4.42 and 4.44). Moreover, preliminary data confirm the directly involvement of miR 139-5p in the down-regulation of ROCK2 and MMP2 protein levels in our cellular models (Figures 4.48 and 4.49). Notably, the chemical inhibition of ROCK2 protein significantly affected cell migration (Figures 4.52 and 4.54) and proliferation (data not shown). In addition, MMP2 chemical inhibition (Figures 4.58 and 4.60) resulted in a reduction of HCC cell migration. In contrast, the inhibition of MMP2 degradation obtained *via* proteasome inhibition, partially restored cell migratory ability (Figure 4.62 and 4.64). Taken together, our data support the functional involvement of ROCK2 and MMP2 in 5-azacytidine mediated effects indicating miR139-5p/ROCK2/MMP2 pathway as being responsible to the 5-azacytidine induced effects.

The Rho/ROCK signaling pathway is not only involved in cell migration, it also plays a role in cell proliferation. Indeed, ROCK2 directly activates by phosphorylation many substrates including GFAP and MLC [332], which are involved in the control of different aspects of cell proliferation (see the scheme of Figure 5.1). Based on this, in the next future we plan to study the phosphorylation status of these ROCK2 substrates. This will allow understanding their role in the 5-azacytidine mediated effects for what concerns cell cycle progression. This investigation may result to be important for the mechanistic interpretation of the cytokinesis errors induced by 5-azacytidine we observed (Figures 4.26 and 4.27).

Despite the important role of the miR139-5p /ROCK2 role in the regulation of MMP2 levels, our data suggest that this mechanism may not be the only one responsible for the phenomenon.

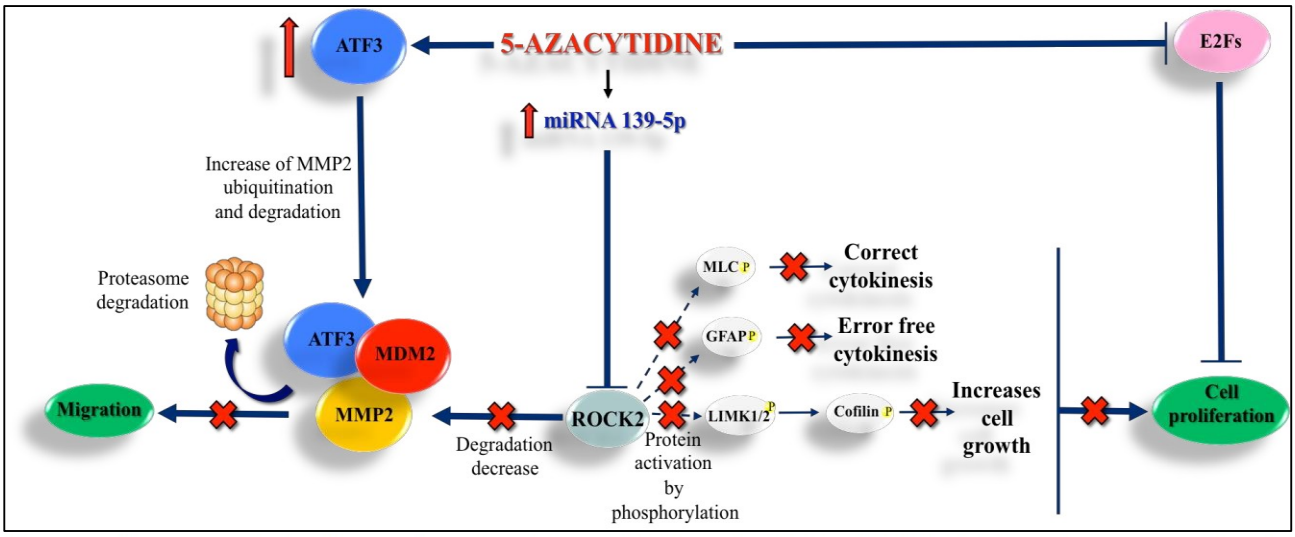

Fig. 5.1 – The proposed signalling pathway involving miR 139-5p, ROCK2 and MMP2 that is partially responsible of the inhibition of both cell migration and proliferation. miR 139-5p/ROCK2/MMP2 pathways is probably directly regulated by 5-azacytidine.

Indeed, our gene expression data (Table 4.1), confirmed by quantitative real time PCR (Figures 4.32 and 4.34), indicate that ATF3 is upregulated. In some type of cancer [318], ATF3 could promote the formation of MDM2/ATF3/MMP2 complex thus enhancing the degradation of MMP2 and thus resulting in the inhibition of cell migration and invasion. In addition, in the last years, many evidences suggested an important role for ATF3 in migration processes. For example, a recent study demonstrated that AFT3 suppressed metastasis of bladder cancer and its decreased expression was also associated with bladder cancer progression and reduced survival of patients [317]. So far, none is known in HCC, but our data suggest that also in this kind of cancer ATF3 may play an important role with regard to migration. Further studies are required to fully elucidating ATF3 role in 5-azacytidine mediated effects.

Finally, in order to be completely sure that 5-azacytidine directly activates miR 139-5p/ROCK2/MMP2 signaling pathway, a methylation analysis of miR139-5p promoter will be soon performed. Furthermore, we will analyze also the methylation status of ATF3 promoter to definitely confirm its activation by 5-azacytidine.

5.6 Effects of 5-azacytidine in a subcutaneous xenograft model of HCC

To confirm the effectiveness of 5-azacytidine also in an *in vivo* system and to confirm the molecular mechanism of action observed *in vitro*, a subcutaneous murine xenograft model

of HCC has been used. These experiments were done in collaboration with Dott.ssa Urska Kamensek and Dott.ssa Maja Cemazar of the oncology Institute of Ljubljana, Slovenia.

Significant differences in term of tumor size were already observed after the first round of 5-azacytidine treatments between treated and untreated mice (Figure 4.66). These relative differences were maintained during the second round of administrations and until the end of the protocol. However, we noticed that after each cycle treatment the tumor growth tended to restart. For this reason, we will test the effects of a continuous administration of drug. Notably, we did not use a special delivery system for 5-azacytdidine (just direct tumor injection), thus it is possible that the effect of the drug could be improved using a controlled delivery system. It is reasonable to suppose that a delivery system able to favor drug permanence in the tumor and to modulate the delivery over time, may result in a more potent effect. It should not be forgotten that, despite being injected intra-tumor, the drug might be removed by the tumor vessel thus reducing significantly the effects. Beside these consideration, a proper delivery system will be necessary to prove the efficacy of 5-azacytidine when injected systemically, i.e. the normal route for future application in humans. Despite the limitation of delivery, not only 5-azacytidine reduced tumor mass growth, it also increased animal survival as treated mice lived about twice respect to control animals (Figure 4.67). This observation is particularly promising for future investigation of 5-azacytidine effects anti HCC. In this regard, to further explore the effectiveness of 5-azacytidine we have in progress experiments in an orthotropic syngeneic rat model of HCC[333].

Besides showing the potential therapeutic value of 5-azacytidine *in vivo*, our data confirmed the alteration of the miR 139-5p/ROCK2/MMP2 pathway by 5-azacytidine. A significant increase in miRNA 139-5p level together with the down regulation of ROCK2 and MMP2 protein levels were observed in tumor masses collected from treated mice compared to control animals (Figures 4.68 and 4.70). These data together with the relevance of the miR 139-5p/ROCK2/MMP2 pathway in HCC patients [277], strongly suggest that 5-azacytidine may be of therapeutic value in humans.

Interestingly, histological analysis suggested a sort of differentiation effect of 5-azacytidine *in vivo*. In fact, we noticed the formation of pseudo hepatic lobules in tumor tissue collected by treated mice and not visible in tissue derived from control animals (Figure 4.71). Moreover, we observed a higher expression of albumin (Figure 4.72), a well-known marker of hepatic differentiation. These data suggest that 5-azacytidine might promote a differentiation process *in vivo,* perhaps enhancing the acquisition of more normal characteristics to cancer cells. Interestingly, *in vitro* we could not see improved albumin expression following 5-

azacytidine treatments (data not shown). This might depend on the fact that the absence of the proper extracellular environment *in vitro* does not allow the differentiation effect promoted by 5-azacytidine.

Finally, the data obtained *in vivo* were obtained using HuH7 and not JHH6 as this last cell line cannot graft in the mouse. To overcome this limitation, we are in the processes to develop a *Zebrafish* model of HCC were JHH6 can be successfully grafted. Preliminary observation (data not shown) indicate that also in this animal model 5-azacytdine is effective in reducing the growth of the tumor mass made by JHH6. When confirmed, this observation would further strength the concept of the therapeutic value of 5-azacytidine in HCC.

6. Conclusion

In this thesis we explored the effectiveness of 5-azacytidine against HCC *in vitro* and *in vivo*. The data obtained indicate the great effectiveness of 5-azacytidine. Moreover, they show that a molecular mechanism by which 5-azacytidine exerts its effect goes through the targeting of miR 139-5p/ROCK2/MMP2 pathway. Our observation together with the relevance of miR 139-5p/ROCK2/MMP2 pathway in HCC patients suggest that 5-azacytidine have the potential to be of great therapeutic value in HCC.

Acknowledgements

I would like to sincerely thank my two supervisors, Prof. Mario Grassi and Prof Gabriele Grassi. In particular Prof. Gabriele Grassi has been my supervisor since the beginning of my studies and he has always suggested and encouraged me during these three hard years.

I thank my colleagues, Dott.ssa Barbara Dapas and Dott.ssa Rossella Farra for having always supported and helped me.

I would like to sincerely thank Prof. Nicola Elvassore and Dott.ssa Cristina Zennaro because they give me the opportunity to learn new amazing techniques. They've always shown to believe in me and in my way of working.

I would like to thank all people in lab, Barbara, Fleur, Anna, Paola for the funny lunch-breaks and, in particular, for the indispensable coffee-breaks. You are nice neighbors.

Very very special thanks to my family, my parents and my sister, who have always been close to me and have always supported my choices. We are a strong family that fight the difficulties together and this thesis are dedicated to us.

Many thanks to all my friends, near and far, new and old. I love you and I'm fine with you.

Last but not least, a special thanks to Andrea, who has always supported me and endured. You daily drive me through joys and difficulties of life and for that and much more I love you!!

…And now...Let's Get The Party Started!!!

References

1 Kumar, M., Zhao, X. & Wang, X. W. Molecular carcinogenesis of hepatocellular carcinoma and intrahepatic cholangiocarcinoma: one step closer to personalized medicine? *Cell & bioscience* **1**, 5, doi:10.1186/2045-3701-1-5 (2011).

2 Gomaa, A. I., Khan, S. A., Toledano, M. B., Waked, I. & Taylor-Robinson, S. D. Hepatocellular carcinoma: epidemiology, risk factors and pathogenesis. *World journal of gastroenterology : WJG* **14**, 4300-4308 (2008).

3 Di Bisceglie, A. M. Hepatitis B and hepatocellular carcinoma. *Hepatology* **49**, S56-60, doi:10.1002/hep.22962 (2009).

4 Bertino, G. *et al.* Hepatocellular carcinoma: novel molecular targets in carcinogenesis for future therapies. *BioMed research international* **2014**, 203693, doi:10.1155/2014/203693 (2014).

5 Chen, K. W. *et al.* Current systemic treatment of hepatocellular carcinoma: A review of the literature. *World journal of hepatology* **7**, 1412-1420, doi:10.4254/wjh.v7.i10.1412 (2015).

6 Zhai, B. & Sun, X. Y. Mechanisms of resistance to sorafenib and the corresponding strategies in hepatocellular carcinoma. *World journal of hepatology* **5**, 345-352, doi:10.4254/wjh.v5.i7.345 (2013).

7 Yoshikawa, H. *et al.* SOCS-1, a negative regulator of the JAK/STAT pathway, is silenced by methylation in human hepatocellular carcinoma and shows growth-suppression activity. *Nature genetics* **28**, 29-35, doi:10.1038/88225 (2001).

8 Yang, B., Guo, M., Herman, J. G. & Clark, D. P. Aberrant promoter methylation profiles of tumor suppressor genes in hepatocellular carcinoma. *The American journal of pathology* **163**, 1101-1107, doi:10.1016/S0002-9440(10)63469-4 (2003).

9 Issa, J. P. & Kantarjian, H. M. Targeting DNA methylation. *Clinical cancer research : an official journal of the American Association for Cancer Research* **15**, 3938-3946, doi:10.1158/1078-0432.CCR-08-2783 (2009).

10 Bronte, F. *et al.* HepatomiRNoma: The proposal of a new network of targets for diagnosis, prognosis and therapy in hepatocellular carcinoma. *Critical reviews in oncology/hematology*, doi:10.1016/j.critrevonc.2015.09.007 (2015).

11 Vandooren, J., Geurts, N., Martens, E., Van den Steen, P. E. & Opdenakker, G. Zymography methods for visualizing hydrolytic enzymes. *Nature methods* **10**, 211-220, doi:10.1038/nmeth.2371 (2013).

12 Martini, F. H. *Anatomia Umana*. 3° edn, (2004).

13 Ramadori, G., Moriconi, F., Malik, I. & Dudas, J. Physiology and pathophysiology of liver inflammation, damage and repair. *Journal of physiology and pharmacology : an official journal of the Polish Physiological Society* **59 Suppl 1**, 107-117 (2008).

14 Geerts, A. History, heterogeneity, developmental biology, and functions of quiescent hepatic stellate cells. *Seminars in liver disease* **21**, 311-335, doi:10.1055/s-2001-17550 (2001).

15 Knittel, T. *et al.* Expression and regulation of cell adhesion molecules by hepatic stellate cells (HSC) of rat liver: involvement of HSC in recruitment of inflammatory cells during hepatic tissue repair. *The American journal of pathology* **154**, 153-167 (1999).

16 Bishayee, A. The role of inflammation and liver cancer. *Advances in experimental medicine and biology* **816**, 401-435, doi:10.1007/978-3-0348-0837-8_16 (2014).

17 El-Serag, H. B. & Rudolph, K. L. Hepatocellular carcinoma: epidemiology and molecular carcinogenesis. *Gastroenterology* **132**, 2557-2576, doi:10.1053/j.gastro.2007.04.061 (2007).

18 Di Bisceglie, A. M. Epidemiology and clinical presentation of hepatocellular carcinoma. *Journal of vascular and interventional radiology : JVIR* **13**, S169-171 (2002).

19 Montalto, G. *et al.* Epidemiology, risk factors, and natural history of hepatocellular carcinoma. *Annals of the New York Academy of Sciences* **963**, 13-20 (2002).

20 Parikh, S. & Hyman, D. Hepatocellular cancer: a guide for the internist. *The American journal of medicine* **120**, 194-202, doi:10.1016/j.amjmed.2006.11.020 (2007).

21 Sharma, D. S., Mhatre, V., Heigrujam, M., Talapatra, K. & Mallik, S. Portal dosimetry for pretreatment verification of IMRT plan: a comparison with 2D ion chamber array. *Journal of applied clinical medical physics / American College of Medical Physics* **11**, 3268 (2010).

22 Bartenschlager, R., Lohmann, V. & Penin, F. The molecular and structural basis of advanced antiviral therapy for hepatitis C virus infection. *Nature reviews. Microbiology* **11**, 482-496, doi:10.1038/nrmicro3046 (2013).

23 Hoshida, Y., Fuchs, B. C., Bardeesy, N., Baumert, T. F. & Chung, R. T. Pathogenesis and prevention of hepatitis C virus-induced hepatocellular carcinoma. *Journal of hepatology* **61**, S79-90, doi:10.1016/j.jhep.2014.07.010 (2014).

24 Suruki, R. Y. *et al.* Host immune status and incidence of hepatocellular carcinoma among subjects infected with hepatitis C virus: a nested case-control study in Japan. *Cancer epidemiology, biomarkers & prevention : a publication of the American Association for Cancer Research, cosponsored by the American Society of Preventive Oncology* **15**, 2521-2525, doi:10.1158/1055-9965.EPI-06-0485 (2006).

25 Michielsen, P. P., Francque, S. M. & van Dongen, J. L. Viral hepatitis and hepatocellular carcinoma. *World journal of surgical oncology* **3**, 27, doi:10.1186/1477-7819-3-27 (2005).

26 Lai, M. M. & Ware, C. F. Hepatitis C virus core protein: possible roles in viral pathogenesis. *Current topics in microbiology and immunology* **242**, 117-134 (2000).

27 Okuda, M. *et al.* Mitochondrial injury, oxidative stress, and antioxidant gene expression are induced by hepatitis C virus core protein. *Gastroenterology* **122**, 366-375 (2002).

28 Kwun, H. J. & Jang, K. L. Dual effects of hepatitis C virus Core protein on the transcription of cyclin-dependent kinase inhibitor p21 gene. *Journal of viral hepatitis* **10**, 249-255 (2003).

29 Reyes, G. R. The nonstructural NS5A protein of hepatitis C virus: an expanding, multifunctional role in enhancing hepatitis C virus pathogenesis. *Journal of biomedical science* **9**, 187-197, doi:59419 (2002).

30 Poordad, F. & Dieterich, D. Treating hepatitis C: current standard of care and emerging direct-acting antiviral agents. *Journal of viral hepatitis* **19**, 449-464, doi:10.1111/j.1365-2893.2012.01617.x (2012).

31 Pockros, P. J. New direct-acting antivirals in the development for hepatitis C virus infection. *Therapeutic advances in gastroenterology* **3**, 191-202, doi:10.1177/1756283X10363055 (2010).

32 Gane, E. J. *et al.* Nucleotide polymerase inhibitor sofosbuvir plus ribavirin for hepatitis C. *The New England journal of medicine* **368**, 34-44, doi:10.1056/NEJMoa1208953 (2013).

33 Au, J. S. & Pockros, P. J. Novel therapeutic approaches for hepatitis C. *Clinical pharmacology and therapeutics* **95**, 78-88, doi:10.1038/clpt.2013.206 (2014).

34 Tellinghuisen, T. L., Foss, K. L. & Treadaway, J. Regulation of hepatitis C virion production via phosphorylation of the NS5A protein. *PLoS pathogens* **4**, e1000032, doi:10.1371/journal.ppat.1000032 (2008).

35 Sulkowski, M. S. *et al.* Daclatasvir plus sofosbuvir for previously treated or untreated chronic HCV infection. *The New England journal of medicine* **370**, 211-221, doi:10.1056/NEJMoa1306218 (2014).

36 Fung, J., Lai, C. L. & Yuen, M. F. Hepatitis B and C virus-related carcinogenesis. *Clinical microbiology and infection : the official publication of the European Society of Clinical Microbiology and Infectious Diseases* **15**, 964-970, doi:10.1111/j.1469-0691.2009.03035.x (2009).

37 Bruix, J. & Llovet, J. M. Hepatitis B virus and hepatocellular carcinoma. *Journal of hepatology* **39 Suppl 1**, S59-63 (2003).

38 Kremsdorf, D., Soussan, P., Paterlini-Brechot, P. & Brechot, C. Hepatitis B virus-related hepatocellular carcinoma: paradigms for viral-related human carcinogenesis. *Oncogene* **25**, 3823-3833, doi:10.1038/sj.onc.1209559 (2006).

39 Bonilla Guerrero, R. & Roberts, L. R. The role of hepatitis B virus integrations in the pathogenesis of human hepatocellular carcinoma. *Journal of hepatology* **42**, 760-777, doi:10.1016/j.jhep.2005.02.005 (2005).

40 Rossner, M. T. Review: hepatitis B virus X-gene product: a promiscuous transcriptional activator. *Journal of medical virology* **36**, 101-117 (1992).

41 Tai, P. C., Suk, F. M., Gerlich, W. H., Neurath, A. R. & Shih, C. Hypermodification and immune escape of an internally deleted middle-envelope (M) protein of frequent and predominant hepatitis B virus variants. *Virology* **292**, 44-58, doi:10.1006/viro.2001.1239 (2002).

42 Ikeda, K. *et al.* A multivariate analysis of risk factors for hepatocellular carcinogenesis: a prospective observation of 795 patients with viral and alcoholic cirrhosis. *Hepatology* **18**, 47-53 (1993).

43 Davila, J. A., Morgan, R. O., Shaib, Y., McGlynn, K. A. & El-Serag, H. B. Diabetes increases the risk of hepatocellular carcinoma in the United States: a population based case control study. *Gut* **54**, 533-539, doi:10.1136/gut.2004.052167 (2005).

44 Montella, M. *et al.* Coffee and tea consumption and risk of hepatocellular carcinoma in Italy. *International journal of cancer. Journal international du cancer* **120**, 1555-1559, doi:10.1002/ijc.22509 (2007).

45 Tanaka, K. *et al.* Inverse association between coffee drinking and the risk of hepatocellular carcinoma: a case-control study in Japan. *Cancer science* **98**, 214-218, doi:10.1111/j.1349-7006.2006.00368.x (2007).

46 Cavin, C., Holzhauser, D., Constable, A., Huggett, A. C. & Schilter, B. The coffee-specific diterpenes cafestol and kahweol protect against aflatoxin B1-induced genotoxicity through a dual mechanism. *Carcinogenesis* **19**, 1369-1375 (1998).

47 Bravi, F. *et al.* Coffee drinking and hepatocellular carcinoma risk: a meta-analysis. *Hepatology* **46**, 430-435, doi:10.1002/hep.21708 (2007).

48 Wolk, A. *et al.* A prospective study of obesity and cancer risk (Sweden). *Cancer causes & control : CCC* **12**, 13-21 (2001).

49 Moller, H., Mellemgaard, A., Lindvig, K. & Olsen, J. H. Obesity and cancer risk: a Danish record-linkage study. *European journal of cancer* **30A**, 344-350 (1994).

50 Hwang, S. J. *et al.* Hepatic steatosis in chronic hepatitis C virus infection: prevalence and clinical correlation. *Journal of gastroenterology and hepatology* **16**, 190-195 (2001).

51 Bugianesi, E. *et al.* Relative contribution of iron burden, HFE mutations, and insulin resistance to fibrosis in nonalcoholic fatty liver. *Hepatology* **39**, 179-187, doi:10.1002/hep.20023 (2004).

52 Garner, R. C., Miller, E. C. & Miller, J. A. Liver microsomal metabolism of aflatoxin B 1 to a reactive derivative toxic to Salmonella typhimurium TA 1530. *Cancer research* **32**, 2058-2066 (1972).

53 Qian, G. S. *et al.* A follow-up study of urinary markers of aflatoxin exposure and liver cancer risk in Shanghai, People's Republic of China. *Cancer epidemiology, biomarkers & prevention : a publication of the American Association for Cancer Research, cosponsored by the American Society of Preventive Oncology* **3**, 3-10 (1994).

54 Ezzat, S. *et al.* Associations of pesticides, HCV, HBV, and hepatocellular carcinoma in Egypt. *International journal of hygiene and environmental health* **208**, 329-339 (2005).

55 Smith, B. W. & Adams, L. A. Non-alcoholic fatty liver disease. *Critical reviews in clinical laboratory sciences* **48**, 97-113, doi:10.3109/10408363.2011.596521 (2011).

56 Oda, K., Uto, H., Mawatari, S. & Ido, A. Clinical features of hepatocellular carcinoma associated with nonalcoholic fatty liver disease: a review of human studies. *Clinical journal of gastroenterology* **8**, 1-9, doi:10.1007/s12328-014-0548-5 (2015).

57 Starley, B. Q., Calcagno, C. J. & Harrison, S. A. Nonalcoholic fatty liver disease and hepatocellular carcinoma: a weighty connection. *Hepatology* **51**, 1820-1832, doi:10.1002/hep.23594 (2010).

58 Bugianesi, E. *et al.* Expanding the natural history of nonalcoholic steatohepatitis: from cryptogenic cirrhosis to hepatocellular carcinoma. *Gastroenterology* **123**, 134-140 (2002).

59 Marrero, J. A. *et al.* NAFLD may be a common underlying liver disease in patients with hepatocellular carcinoma in the United States. *Hepatology* **36**, 1349-1354, doi:10.1053/jhep.2002.36939 (2002).

60 Leggett, B. A., Halliday, J. W., Brown, N. N., Bryant, S. & Powell, L. W. Prevalence of haemochromatosis amongst asymptomatic Australians. *British journal of haematology* **74**, 525-530 (1990).

61 Feder, J. N. *et al.* A novel MHC class I-like gene is mutated in patients with hereditary haemochromatosis. *Nature genetics* **13**, 399-408, doi:10.1038/ng0896-399 (1996).

62 Jouanolle, A. M. *et al.* A candidate gene for hemochromatosis: frequency of the C282Y and H63D mutations. *Human genetics* **100**, 544-547 (1997).

63 Fargion, S. *et al.* Survival and prognostic factors in 212 Italian patients with genetic hemochromatosis. *Hepatology* **15**, 655-659 (1992).

64 Bradbear, R. A. *et al.* Cohort study of internal malignancy in genetic hemochromatosis and other chronic nonalcoholic liver diseases. *Journal of the National Cancer Institute* **75**, 81-84 (1985).

65 Strohmeyer, G., Niederau, C. & Stremmel, W. Survival and causes of death in hemochromatosis. Observations in 163 patients. *Annals of the New York Academy of Sciences* **526**, 245-257 (1988).

66 Hsing, A. W. *et al.* Cancer risk following primary hemochromatosis: a population-based cohort study in Denmark. *International journal of cancer. Journal international du cancer* **60**, 160-162 (1995).

67 Niederau, C. *et al.* Survival and causes of death in cirrhotic and in noncirrhotic patients with primary hemochromatosis. *The New England journal of medicine* **313**, 1256-1262, doi:10.1056/NEJM198511143132004 (1985).

68 Marra, M. *et al.* Molecular targets and oxidative stress biomarkers in hepatocellular carcinoma: an overview. *Journal of translational medicine* **9**, 171, doi:10.1186/1479-5876-9-171 (2011).

69 Hanahan, D. & Weinberg, R. A. The hallmarks of cancer. *Cell* **100**, 57-70 (2000).

70 Teoh, N. C. Proliferative drive and liver carcinogenesis: too much of a good thing? *Journal of gastroenterology and hepatology* **24**, 1817-1825, doi:10.1111/j.1440-1746.2009.06121.x (2009).

71 Farazi, P. A. & DePinho, R. A. Hepatocellular carcinoma pathogenesis: from genes to environment. *Nature reviews. Cancer* **6**, 674-687, doi:10.1038/nrc1934 (2006).

72 Watanabe, S. *et al.* Morphologic studies of the liver cell dysplasia. *Cancer* **51**, 2197-2205 (1983).

73 Le Bail, B., Bernard, P. H., Carles, J., Balabaud, C. & Bioulac-Sage, P. Prevalence of liver cell dysplasia and association with HCC in a series of 100 cirrhotic liver explants. *Journal of hepatology* **27**, 835-842 (1997).

74 Lee, R. G., Tsamandas, A. C. & Demetris, A. J. Large cell change (liver cell dysplasia) and hepatocellular carcinoma in cirrhosis: matched case-control study, pathological analysis, and pathogenetic hypothesis. *Hepatology* **26**, 1415-1422, doi:10.1002/hep.510260607 (1997).

75 Feitelson, M. A. *et al.* Genetic mechanisms of hepatocarcinogenesis. *Oncogene* **21**, 2593-2604, doi:10.1038/sj.onc.1205434 (2002).

76 Boige, V. *et al.* Concerted nonsyntenic allelic losses in hyperploid hepatocellular carcinoma as determined by a high-resolution allelotype. *Cancer research* **57**, 1986-1990 (1997).

77 Liu, M., Jiang, L. & Guan, X. Y. The genetic and epigenetic alterations in human hepatocellular carcinoma: a recent update. *Protein & cell* **5**, 673-691, doi:10.1007/s13238-014-0065-9 (2014).

78 Guan, X. Y. *et al.* Recurrent chromosome alterations in hepatocellular carcinoma detected by comparative genomic hybridization. *Genes, chromosomes & cancer* **29**, 110-116 (2000).

79 Kondo, Y. *et al.* Genetic instability and aberrant DNA methylation in chronic hepatitis and cirrhosis--A comprehensive study of loss of heterozygosity and microsatellite instability at 39 loci and DNA hypermethylation on 8 CpG islands in microdissected specimens from patients with hepatocellular carcinoma. *Hepatology* **32**, 970-979, doi:10.1053/jhep.2000.19797 (2000).

80 Ma, N. F. *et al.* Isolation and characterization of a novel oncogene, amplified in liver cancer 1, within a commonly amplified region at 1q21 in hepatocellular carcinoma. *Hepatology* **47**, 503-510, doi:10.1002/hep.22072 (2008).

81 Chen, L. *et al.* Clinical significance of CHD1L in hepatocellular carcinoma and therapeutic potentials of virus-mediated CHD1L depletion. *Gut* **60**, 534-543, doi:10.1136/gut.2010.224071 (2011).

82 Liu, L. *et al.* Maelstrom promotes hepatocellular carcinoma metastasis by inducing epithelial-mesenchymal transition by way of Akt/GSK-3beta/Snail signaling. *Hepatology* **59**, 531-543, doi:10.1002/hep.26677 (2014).

83 Okamoto, H., Yasui, K., Zhao, C., Arii, S. & Inazawa, J. PTK2 and EIF3S3 genes may be amplification targets at 8q23-q24 and are associated with large hepatocellular carcinomas. *Hepatology* **38**, 1242-1249, doi:10.1053/jhep.2003.50457 (2003).

84 Santoni-Rugiu, E., Jensen, M. R. & Thorgeirsson, S. S. Disruption of the pRb/E2F pathway and inhibition of apoptosis are major oncogenic events in liver constitutively expressing c-myc and transforming growth factor alpha. *Cancer research* **58**, 123-134 (1998).

85 Parada, L. A. *et al.* Frequent rearrangements of chromosomes 1, 7, and 8 in primary liver cancer. *Genes, chromosomes & cancer* **23**, 26-35 (1998).

86 Liu, M. *et al.* Serum and glucocorticoid kinase 3 at 8q13.1 promotes cell proliferation and survival in hepatocellular carcinoma. *Hepatology* **55**, 1754-1765, doi:10.1002/hep.25584 (2012).

87 Iwata, N. *et al.* Frequent hypermethylation of CpG islands and loss of expression of the 14-3-3 sigma gene in human hepatocellular carcinoma. *Oncogene* **19**, 5298-5302, doi:10.1038/sj.onc.1203898 (2000).

88 Yuan, B. Z. *et al.* Cloning, characterization, and chromosomal localization of a gene frequently deleted in human liver cancer (DLC-1) homologous to rat RhoGAP. *Cancer research* **58**, 2196-2199 (1998).

89 Wong, C. M., Lee, J. M., Ching, Y. P., Jin, D. Y. & Ng, I. O. Genetic and epigenetic alterations of DLC-1 gene in hepatocellular carcinoma. *Cancer research* **63**, 7646-7651 (2003).

90 Zhou, X., Thorgeirsson, S. S. & Popescu, N. C. Restoration of DLC-1 gene expression induces apoptosis and inhibits both cell growth and tumorigenicity in human hepatocellular carcinoma cells. *Oncogene* **23**, 1308-1313, doi:10.1038/sj.onc.1207246 (2004).

91 Kanai, Y. *et al.* The E-cadherin gene is silenced by CpG methylation in human hepatocellular carcinomas. *International journal of cancer. Journal international du cancer* **71**, 355-359 (1997).

92 Fu, L. *et al.* Down-regulation of tyrosine aminotransferase at a frequently deleted region 16q22 contributes to the pathogenesis of hepatocellular carcinoma. *Hepatology* **51**, 1624-1634, doi:10.1002/hep.23540 (2010).

93 Liu, M. *et al.* Allele-specific imbalance of oxidative stress-induced growth inhibitor 1 associates with progression of hepatocellular carcinoma. *Gastroenterology* **146**, 1084-1096, doi:10.1053/j.gastro.2013.12.041 (2014).

94 Nishida, N. *et al.* Role and mutational heterogeneity of the p53 gene in hepatocellular carcinoma. *Cancer research* **53**, 368-372 (1993).

95 Chen, C. & Wang, G. Mechanisms of hepatocellular carcinoma and challenges and opportunities for molecular targeted therapy. *World journal of hepatology* **7**, 1964-1970, doi:10.4254/wjh.v7.i15.1964 (2015).

96 Zhao, M., He, H. W., Sun, H. X., Ren, K. H. & Shao, R. G. Dual knockdown of N-ras and epiregulin synergistically suppressed the growth of human hepatoma cells. *Biochemical and biophysical research communications* **387**, 239-244, doi:10.1016/j.bbrc.2009.06.128 (2009).

97 Zhang, X. & Ding, H. G. Key role of hepatitis B virus mutation in chronic hepatitis B development to hepatocellular carcinoma. *World journal of hepatology* **7**, 1282-1286, doi:10.4254/wjh.v7.i9.1282 (2015).

98 Jeon, Y. E. *et al.* Histology-directed matrix-assisted laser desorption/ionization analysis reveals tissue origin and p53 status of primary liver cancers. *Pathology international* **61**, 449-455, doi:10.1111/j.1440-1827.2011.02686.x (2011).

99 Boiko, A. D. *et al.* A systematic search for downstream mediators of tumor suppressor function of p53 reveals a major role of BTG2 in suppression of Ras-induced transformation. *Genes & development* **20**, 236-252, doi:10.1101/gad.1372606 (2006).

100 Zhang, Z. *et al.* Aberrant expression of the p53-inducible antiproliferative gene BTG2 in hepatocellular carcinoma is associated with overexpression of the cell cycle-related proteins. *Cell Biochem Biophys* **61**, 83-91, doi:10.1007/s12013-011-9164-x (2011).

101 Bupathi, M., Kaseb, A., Meric-Bernstam, F. & Naing, A. Hepatocellular carcinoma: Where there is unmet need. *Molecular oncology* **9**, 1501-1509, doi:10.1016/j.molonc.2015.06.005 (2015).

102 Scaggiante, B. *et al.* Novel hepatocellular carcinoma molecules with prognostic and therapeutic potentials. *World journal of gastroenterology : WJG* **20**, 1268-1288, doi:10.3748/wjg.v20.i5.1268 (2014).

103 Hanahan, D. & Folkman, J. Patterns and emerging mechanisms of the angiogenic switch during tumorigenesis. *Cell* **86**, 353-364 (1996).

104 Torimura, T. *et al.* Overexpression of angiopoietin-1 and angiopoietin-2 in hepatocellular carcinoma. *Journal of hepatology* **40**, 799-807, doi:10.1016/j.jhep.2004.01.027 (2004).

105 Baiz, D. *et al.* Bortezomib effect on E2F and cyclin family members in human hepatocellular carcinoma cell lines. *World journal of gastroenterology : WJG* **20**, 795-803, doi:10.3748/wjg.v20.i3.795 (2014).

106 Frolov, M. V. & Dyson, N. J. Molecular mechanisms of E2F-dependent activation and pRB-mediated repression. *Journal of cell science* **117**, 2173-2181, doi:10.1242/jcs.01227 (2004).

107 Conner, E. A. *et al.* Dual functions of E2F-1 in a transgenic mouse model of liver carcinogenesis. *Oncogene* **19**, 5054-5062, doi:10.1038/sj.onc.1203885 (2000).

108 Taub, R. Liver regeneration: from myth to mechanism. *Nature reviews. Molecular cell biology* **5**, 836-847, doi:10.1038/nrm1489 (2004).

109 Nelsen, C. J. *et al.* Short term cyclin D1 overexpression induces centrosome amplification, mitotic spindle abnormalities, and aneuploidy. *The Journal of biological chemistry* **280**, 768-776, doi:10.1074/jbc.M407105200 (2005).

110 Liu, H., Dibling, B., Spike, B., Dirlam, A. & Macleod, K. New roles for the RB tumor suppressor protein. *Current opinion in genetics & development* **14**, 55-64, doi:10.1016/j.gde.2003.11.005 (2004).

111 Huber, A. H. & Weis, W. I. The structure of the beta-catenin/E-cadherin complex and the molecular basis of diverse ligand recognition by beta-catenin. *Cell* **105**, 391-402 (2001).

112 Giles, R. H., van Es, J. H. & Clevers, H. Caught up in a Wnt storm: Wnt signaling in cancer. *Biochimica et biophysica acta* **1653**, 1-24 (2003).

113 Calvisi, D. F., Factor, V. M., Loi, R. & Thorgeirsson, S. S. Activation of beta-catenin during hepatocarcinogenesis in transgenic mouse models: relationship to phenotype and tumor grade. *Cancer research* **61**, 2085-2091 (2001).

114 Srisuttee, R. *et al.* Hepatitis B virus X (HBX) protein upregulates beta-catenin in a human hepatic cell line by sequestering SIRT1 deacetylase. *Oncology reports* **28**, 276-282, doi:10.3892/or.2012.1798 (2012).

115 Breuhahn, K., Longerich, T. & Schirmacher, P. Dysregulation of growth factor signaling in human hepatocellular carcinoma. *Oncogene* **25**, 3787-3800, doi:10.1038/sj.onc.1209556 (2006).

116 Galuppo, R., Ramaiah, D., Ponte, O. M. & Gedaly, R. Molecular therapies in hepatocellular carcinoma: what can we target? *Digestive diseases and sciences* **59**, 1688-1697, doi:10.1007/s10620-014-3058-x (2014).

117 Galuppo, R. *et al.* Synergistic inhibition of HCC and liver cancer stem cell proliferation by targeting RAS/RAF/MAPK and WNT/beta-catenin pathways. *Anticancer research* **34**, 1709-1713 (2014).

118 Yothaisong, S. *et al.* Increased activation of PI3K/AKT signaling pathway is associated with cholangiocarcinoma metastasis and PI3K/mTOR inhibition presents a possible therapeutic strategy. *Tumour biology : the journal of the International Society for Oncodevelopmental Biology and Medicine* **34**, 3637-3648, doi:10.1007/s13277-013-0945-2 (2013).

119 Hassan, B., Akcakanat, A., Holder, A. M. & Meric-Bernstam, F. Targeting the PI3-kinase/Akt/mTOR signaling pathway. *Surgical oncology clinics of North America* **22**, 641-664, doi:10.1016/j.soc.2013.06.008 (2013).

120 Peltier, J., O'Neill, A. & Schaffer, D. V. PI3K/Akt and CREB regulate adult neural hippocampal progenitor proliferation and differentiation. *Developmental neurobiology* **67**, 1348-1361, doi:10.1002/dneu.20506 (2007).

121 Rafalski, V. A. & Brunet, A. Energy metabolism in adult neural stem cell fate. *Progress in neurobiology* **93**, 182-203, doi:10.1016/j.pneurobio.2010.10.007 (2011).

122 Grabinski, N. *et al.* Combined targeting of AKT and mTOR synergistically inhibits proliferation of hepatocellular carcinoma cells. *Molecular cancer* **11**, 85, doi:10.1186/1476-4598-11-85 (2012).

123 Naing, A. *et al.* Safety, tolerability, pharmacokinetics and pharmacodynamics of AZD8055 in advanced solid tumours and lymphoma. *British journal of cancer* **107**, 1093-1099, doi:10.1038/bjc.2012.368 (2012).

124 Breunig, C. *et al.* BRaf and MEK inhibitors differentially regulate cell fate and microenvironment in human hepatocellular carcinoma. *Clinical cancer research : an official journal of the American Association for Cancer Research* **20**, 2410-2423, doi:10.1158/1078-0432.CCR-13-1635 (2014).

125 Gupta, S., Takebe, N. & Lorusso, P. Targeting the Hedgehog pathway in cancer. *Therapeutic advances in medical oncology* **2**, 237-250, doi:10.1177/1758834010366430 (2010).

126 Arzumanyan, A. *et al.* Hedgehog signaling blockade delays hepatocarcinogenesis induced by hepatitis B virus X protein. *Cancer research* **72**, 5912-5920, doi:10.1158/0008-5472.CAN-12-2329 (2012).

127 Sicklick, J. K. *et al.* Dysregulation of the Hedgehog pathway in human hepatocarcinogenesis. *Carcinogenesis* **27**, 748-757, doi:10.1093/carcin/bgi292 (2006).

128 Kim, Y. *et al.* Selective down-regulation of glioma-associated oncogene 2 inhibits the proliferation of hepatocellular carcinoma cells. *Cancer research* **67**, 3583-3593, doi:10.1158/0008-5472.CAN-06-3040 (2007).

129 Giannelli, G., Villa, E. & Lahn, M. Transforming growth factor-beta as a therapeutic target in hepatocellular carcinoma. *Cancer research* **74**, 1890-1894, doi:10.1158/0008-5472.CAN-14-0243 (2014).

130 Thiery, J. P. Epithelial-mesenchymal transitions in tumour progression. *Nature reviews. Cancer* **2**, 442-454, doi:10.1038/nrc822 (2002).

131 Heldin, C. H. & Moustakas, A. Role of Smads in TGFbeta signaling. *Cell and tissue research* **347**, 21-36, doi:10.1007/s00441-011-1190-x (2012).

132 Brenner, C., Galluzzi, L., Kepp, O. & Kroemer, G. Decoding cell death signals in liver inflammation. *Journal of hepatology* **59**, 583-594, doi:10.1016/j.jhep.2013.03.033 (2013).

133 Coulouarn, C., Factor, V. M. & Thorgeirsson, S. S. Transforming growth factor-beta gene expression signature in mouse hepatocytes predicts clinical outcome in human cancer. *Hepatology* **47**, 2059-2067, doi:10.1002/hep.22283 (2008).

134 Gressner, O. A. *et al.* Intracrine signalling of activin A in hepatocytes upregulates connective tissue growth factor (CTGF/CCN2) expression. *Liver international : official journal of the International Association for the Study of the Liver* **28**, 1207-1216, doi:10.1111/j.1478-3231.2008.01729.x (2008).

135 Yang, P. *et al.* TGF-beta-miR-34a-CCL22 signaling-induced Treg cell recruitment promotes venous metastases of HBV-positive hepatocellular carcinoma. *Cancer cell* **22**, 291-303, doi:10.1016/j.ccr.2012.07.023 (2012).

136 Wu, K. *et al.* Hepatic transforming growth factor beta gives rise to tumor-initiating cells and promotes liver cancer development. *Hepatology* **56**, 2255-2267, doi:10.1002/hep.26007 (2012).
137 Dituri, F. *et al.* Differential Inhibition of the TGF-beta Signaling Pathway in HCC Cells Using the Small Molecule Inhibitor LY2157299 and the D10 Monoclonal Antibody against TGF-beta Receptor Type II. *PloS one* **8**, e67109, doi:10.1371/journal.pone.0067109 (2013).
138 Mima, K. *et al.* High CD44s expression is associated with the EMT expression profile and intrahepatic dissemination of hepatocellular carcinoma after local ablation therapy. *Journal of hepato-biliary-pancreatic sciences* **20**, 429-434, doi:10.1007/s00534-012-0580-0 (2013).
139 Zheng, L. *et al.* Prognostic significance of AMPK activation and therapeutic effects of metformin in hepatocellular carcinoma. *Clinical cancer research : an official journal of the American Association for Cancer Research* **19**, 5372-5380, doi:10.1158/1078-0432.CCR-13-0203 (2013).
140 Lee, C. W. *et al.* AMPK promotes p53 acetylation via phosphorylation and inactivation of SIRT1 in liver cancer cells. *Cancer research* **72**, 4394-4404, doi:10.1158/0008-5472.CAN-12-0429 (2012).
141 Trojan, J. & Zeuzem, S. Tivantinib in hepatocellular carcinoma. *Expert opinion on investigational drugs* **22**, 141-147, doi:10.1517/13543784.2013.741586 (2013).
142 Santoro, A. *et al.* Tivantinib for second-line treatment of advanced hepatocellular carcinoma: a randomised, placebo-controlled phase 2 study. *The Lancet. Oncology* **14**, 55-63, doi:10.1016/S1470-2045(12)70490-4 (2013).
143 Harding, J. J. & Abou-Alfa, G. K. Systemic therapy for hepatocellular carcinoma. *Chinese clinical oncology* **2**, 37, doi:10.3978/j.issn.2304-3865.2013.07.06 (2013).
144 Bird, A. The essentials of DNA methylation. *Cell* **70**, 5-8 (1992).
145 Lee, S. *et al.* Aberrant CpG island hypermethylation along multistep hepatocarcinogenesis. *The American journal of pathology* **163**, 1371-1378, doi:10.1016/S0002-9440(10)63495-5 (2003).
146 Calvisi, D. F. *et al.* Mechanistic and prognostic significance of aberrant methylation in the molecular pathogenesis of human hepatocellular carcinoma. *The Journal of clinical investigation* **117**, 2713-2722, doi:10.1172/JCI31457 (2007).
147 Vertino, P. M. *et al.* DNMT1 is a component of a multiprotein DNA replication complex. *Cell cycle* **1**, 416-423 (2002).
148 Mizuno, S. *et al.* Expression of DNA methyltransferases DNMT1, 3A, and 3B in normal hematopoiesis and in acute and chronic myelogenous leukemia. *Blood* **97**, 1172-1179 (2001).
149 Oh, B. K. *et al.* DNA methyltransferase expression and DNA methylation in human hepatocellular carcinoma and their clinicopathological correlation. *International journal of molecular medicine* **20**, 65-73 (2007).
150 Wang, G. G., Allis, C. D. & Chi, P. Chromatin remodeling and cancer, Part I: Covalent histone modifications. *Trends in molecular medicine* **13**, 363-372, doi:10.1016/j.molmed.2007.07.003 (2007).
151 Kouzarides, T. Chromatin modifications and their function. *Cell* **128**, 693-705, doi:10.1016/j.cell.2007.02.005 (2007).
152 Chen, Y. *et al.* Lentivirus-mediated RNA interference targeting enhancer of zeste homolog 2 inhibits hepatocellular carcinoma growth through down-regulation of stathmin. *Hepatology* **46**, 200-208, doi:10.1002/hep.21668 (2007).

153 Zheng, X. *et al.* Histone acetyltransferase PCAF up-regulated cell apoptosis in hepatocellular carcinoma via acetylating histone H4 and inactivating AKT signaling. *Molecular cancer* **12**, 96, doi:10.1186/1476-4598-12-96 (2013).
154 Armeanu, S. *et al.* Apoptosis on hepatoma cells but not on primary hepatocytes by histone deacetylase inhibitors valproate and ITF2357. *Journal of hepatology* **42**, 210-217, doi:10.1016/j.jhep.2004.10.020 (2005).
155 Guichard, C. *et al.* Integrated analysis of somatic mutations and focal copy-number changes identifies key genes and pathways in hepatocellular carcinoma. *Nature genetics* **44**, 694-698, doi:10.1038/ng.2256 (2012).
156 Rousseau, B. *et al.* Overexpression and role of the ATPase and putative DNA helicase RuvB-like 2 in human hepatocellular carcinoma. *Hepatology* **46**, 1108-1118, doi:10.1002/hep.21770 (2007).
157 Endo, M. *et al.* Alterations of the SWI/SNF chromatin remodelling subunit-BRG1 and BRM in hepatocellular carcinoma. *Liver international : official journal of the International Association for the Study of the Liver* **33**, 105-117, doi:10.1111/liv.12005 (2013).
158 Chen, L. *et al.* CHD1L promotes hepatocellular carcinoma progression and metastasis in mice and is associated with these processes in human patients. *The Journal of clinical investigation* **120**, 1178-1191, doi:10.1172/JCI40665 (2010).
159 Mercer, T. R., Dinger, M. E. & Mattick, J. S. Long non-coding RNAs: insights into functions. *Nature reviews. Genetics* **10**, 155-159, doi:10.1038/nrg2521 (2009).
160 Guttman, M. & Rinn, J. L. Modular regulatory principles of large non-coding RNAs. *Nature* **482**, 339-346, doi:10.1038/nature10887 (2012).
161 Yang, F. *et al.* Long noncoding RNA high expression in hepatocellular carcinoma facilitates tumor growth through enhancer of zeste homolog 2 in humans. *Hepatology* **54**, 1679-1689, doi:10.1002/hep.24563 (2011).
162 Lai, M. C. *et al.* Long non-coding RNA MALAT-1 overexpression predicts tumor recurrence of hepatocellular carcinoma after liver transplantation. *Medical oncology* **29**, 1810-1816, doi:10.1007/s12032-011-0004-z (2012).
163 Han, K. & Kim, J. H. Transarterial chemoembolization in hepatocellular carcinoma treatment: Barcelona clinic liver cancer staging system. *World journal of gastroenterology : WJG* **21**, 10327-10335, doi:10.3748/wjg.v21.i36.10327 (2015).
164 Liver, E. A. F. T. S. O. T. European Organisation For Research And Treatment Of Cancer. EASL- EORTC clinical practice guidelines: management of hepatocellular carcinoma. *Journal of hepatology* **56**, 1020-1022, doi:10.1016/j.jhep.2011.12.001 (2012).
165 Cucchetti, A. *et al.* Cost-effectiveness of hepatic resection versus percutaneous radiofrequency ablation for early hepatocellular carcinoma. *Journal of hepatology* **59**, 300-307, doi:10.1016/j.jhep.2013.04.009 (2013).
166 Choi, D. *et al.* Percutaneous radiofrequency ablation for early-stage hepatocellular carcinoma as a first-line treatment: long-term results and prognostic factors in a large single-institution series. *European radiology* **17**, 684-692, doi:10.1007/s00330-006-0461-5 (2007).
167 Bruix, J., Sherman, M. & American Association for the Study of Liver, D. Management of hepatocellular carcinoma: an update. *Hepatology* **53**, 1020-1022, doi:10.1002/hep.24199 (2011).
168 N'Kontchou, G. *et al.* Radiofrequency ablation of hepatocellular carcinoma: long-term results and prognostic factors in 235 Western patients with cirrhosis. *Hepatology* **50**, 1475-1483, doi:10.1002/hep.23181 (2009).

169 Sala, M., Forner, A., Varela, M. & Bruix, J. Prognostic prediction in patients with hepatocellular carcinoma. *Seminars in liver disease* **25**, 171-180, doi:10.1055/s-2005-871197 (2005).
170 Forner, A., Reig, M. E., de Lope, C. R. & Bruix, J. Current strategy for staging and treatment: the BCLC update and future prospects. *Seminars in liver disease* **30**, 61-74, doi:10.1055/s-0030-1247133 (2010).
171 Knox, J. J., Cleary, S. P. & Dawson, L. A. Localized and systemic approaches to treating hepatocellular carcinoma. *Journal of clinical oncology : official journal of the American Society of Clinical Oncology* **33**, 1835-1844, doi:10.1200/JCO.2014.60.1153 (2015).
172 Nagahama, H. *et al.* Predictive factors for tumor response to systemic chemotherapy in patients with hepatocellular carcinoma. *Japanese journal of clinical oncology* **27**, 321-324 (1997).
173 Thomas, M. B. *et al.* Systemic therapy for hepatocellular carcinoma: cytotoxic chemotherapy, targeted therapy and immunotherapy. *Annals of surgical oncology* **15**, 1008-1014, doi:10.1245/s10434-007-9705-0 (2008).
174 Llovet, J. M. *et al.* Sorafenib in advanced hepatocellular carcinoma. *The New England journal of medicine* **359**, 378-390, doi:10.1056/NEJMoa0708857 (2008).
175 Cheng, A. L. *et al.* Efficacy and safety of sorafenib in patients in the Asia-Pacific region with advanced hepatocellular carcinoma: a phase III randomised, double-blind, placebo-controlled trial. *The Lancet. Oncology* **10**, 25-34, doi:10.1016/S1470-2045(08)70285-7 (2009).
176 Abou-Alfa, G. K. *et al.* Doxorubicin plus sorafenib vs doxorubicin alone in patients with advanced hepatocellular carcinoma: a randomized trial. *Jama* **304**, 2154-2160, doi:10.1001/jama.2010.1672 (2010).
177 Huynh, H. *et al.* Comparing the efficacy of sunitinib with sorafenib in xenograft models of human hepatocellular carcinoma: mechanistic explanation. *Current cancer drug targets* **11**, 944-953 (2011).
178 Bagi, C. M., Gebhard, D. F. & Andresen, C. J. Antitumor effect of vascular endothelial growth factor inhibitor sunitinib in preclinical models of hepatocellular carcinoma. *European journal of gastroenterology & hepatology* **24**, 563-574, doi:10.1097/MEG.0b013e328350916f (2012).
179 Teramoto, K., Ohshio, Y., Fujita, T., Hanaoka, J. & Kontani, K. Simultaneous activation of T helper function can augment the potency of dendritic cell-based cancer immunotherapy. *Journal of cancer research and clinical oncology* **139**, 861-870, doi:10.1007/s00432-013-1394-4 (2013).
180 Cainap, C. *et al.* Linifanib versus Sorafenib in patients with advanced hepatocellular carcinoma: results of a randomized phase III trial. *Journal of clinical oncology : official journal of the American Society of Clinical Oncology* **33**, 172-179, doi:10.1200/JCO.2013.54.3298 (2015).
181 Gherardi, E., Birchmeier, W., Birchmeier, C. & Vande Woude, G. Targeting MET in cancer: rationale and progress. *Nature reviews. Cancer* **12**, 89-103, doi:10.1038/nrc3205 (2012).
182 Previdi, S., Abbadessa, G., Dalo, F., France, D. S. & Broggini, M. Breast cancer-derived bone metastasis can be effectively reduced through specific c-MET inhibitor tivantinib (ARQ 197) and shRNA c-MET knockdown. *Molecular cancer therapeutics* **11**, 214-223, doi:10.1158/1535-7163.MCT-11-0277 (2012).
183 Hurwitz, H. *et al.* Bevacizumab plus irinotecan, fluorouracil, and leucovorin for metastatic colorectal cancer. *The New England journal of medicine* **350**, 2335-2342, doi:10.1056/NEJMoa032691 (2004).

184 Chou, T. & Finn, R. S. Brivanib: a review of development. *Future oncology* **8**, 1083-1090, doi:10.2217/fon.12.104 (2012).
185 Finn, R. S. *et al.* Phase II, open-label study of brivanib as second-line therapy in patients with advanced hepatocellular carcinoma. *Clinical cancer research : an official journal of the American Association for Cancer Research* **18**, 2090-2098, doi:10.1158/1078-0432.CCR-11-1991 (2012).
186 Llovet, J. M. *et al.* Brivanib in patients with advanced hepatocellular carcinoma who were intolerant to sorafenib or for whom sorafenib failed: results from the randomized phase III BRISK-PS study. *Journal of clinical oncology : official journal of the American Society of Clinical Oncology* **31**, 3509-3516, doi:10.1200/JCO.2012.47.3009 (2013).
187 Verslype, C. Activity of cabozantinib (XL184) in hepatocellular carcinoma: results from a Phase 2 randomized discontinuation trial (RDT). *Journal of Clinical Oncology* **30**, 1 (2012).
188 Zhu, A. X., Kudo M., Assenat E. et al. EVOLVE-1: phase 3 study of everolimus for advanced HCC that progressed during or after sorafenib. *Journal of Clinical Oncology* **32** (2014).
189 Anestopoulos, I. Epigenetic therapy as a novel approach in hepatocellular carcinoma. *Pharmacology & Therapeutics* **145**, 17 (2015).
190 Jones, P. A. & Baylin, S. B. The epigenomics of cancer. *Cell* **128**, 683-692, doi:10.1016/j.cell.2007.01.029 (2007).
191 Claes, B., Buysschaert, I. & Lambrechts, D. Pharmaco-epigenomics: discovering therapeutic approaches and biomarkers for cancer therapy. *Heredity* **105**, 152-160, doi:10.1038/hdy.2010.42 (2010).
192 Sharma, S., Kelly, T. K. & Jones, P. A. Epigenetics in cancer. *Carcinogenesis* **31**, 27-36, doi:10.1093/carcin/bgp220 (2010).
193 Hellebrekers, D. M., Griffioen, A. W. & van Engeland, M. Dual targeting of epigenetic therapy in cancer. *Biochimica et biophysica acta* **1775**, 76-91, doi:10.1016/j.bbcan.2006.07.003 (2007).
194 Mani, S. & Herceg, Z. DNA demethylating agents and epigenetic therapy of cancer. *Advances in genetics* **70**, 327-340, doi:10.1016/B978-0-12-380866-0.60012-5 (2010).
195 Taylor, S. M. & Jones, P. A. Multiple new phenotypes induced in 10T1/2 and 3T3 cells treated with 5-azacytidine. *Cell* **17**, 771-779 (1979).
196 Yang, J. D. & Roberts, L. R. Hepatocellular carcinoma: A global view. *Nature reviews. Gastroenterology & hepatology* **7**, 448-458, doi:10.1038/nrgastro.2010.100 (2010).
197 Yoo, C. B. & Jones, P. A. Epigenetic therapy of cancer: past, present and future. *Nature reviews. Drug discovery* **5**, 37-50, doi:10.1038/nrd1930 (2006).
198 Beumer, J. H. *et al.* Concentrations of the DNA methyltransferase inhibitor 5-fluoro-2'-deoxycytidine (FdCyd) and its cytotoxic metabolites in plasma of patients treated with FdCyd and tetrahydrouridine (THU). *Cancer chemotherapy and pharmacology* **62**, 363-368, doi:10.1007/s00280-007-0603-8 (2008).
199 Juttermann, R., Li, E. & Jaenisch, R. Toxicity of 5-aza-2'-deoxycytidine to mammalian cells is mediated primarily by covalent trapping of DNA methyltransferase rather than DNA demethylation. *Proceedings of the National Academy of Sciences of the United States of America* **91**, 11797-11801 (1994).
200 Gaudet, F. *et al.* Induction of tumors in mice by genomic hypomethylation. *Science* **300**, 489-492, doi:10.1126/science.1083558 (2003).
201 Feinberg, A. P. Cancer epigenetics is no Mickey Mouse. *Cancer cell* **8**, 267-268, doi:10.1016/j.ccr.2005.09.014 (2005).
202 Ghoshal, K. & Bai, S. DNA methyltransferases as targets for cancer therapy. *Drugs of today* **43**, 395-422, doi:10.1358/dot.2007.43.6.1062666 (2007).

203 Venturelli, S. *et al.* Dual antitumour effect of 5-azacytidine by inducing a breakdown of resistance-mediating factors and epigenetic modulation. *Gut* **60**, 156-165, doi:10.1136/gut.2010.208041 (2011).

204 Byun, H. M. *et al.* 2'-Deoxy-N4-[2-(4-nitrophenyl)ethoxycarbonyl]-5-azacytidine: a novel inhibitor of DNA methyltransferase that requires activation by human carboxylesterase 1. *Cancer letters* **266**, 238-248, doi:10.1016/j.canlet.2008.02.069 (2008).

205 Hayashi, M. *et al.* Identification of the A kinase anchor protein 12 (AKAP12) gene as a candidate tumor suppressor of hepatocellular carcinoma. *Journal of surgical oncology* **105**, 381-386, doi:10.1002/jso.22135 (2012).

206 Wong, C. M. *et al.* Tissue factor pathway inhibitor-2 as a frequently silenced tumor suppressor gene in hepatocellular carcinoma. *Hepatology* **45**, 1129-1138, doi:10.1002/hep.21578 (2007).

207 Calvisi, D. F. *et al.* Ubiquitous activation of Ras and Jak/Stat pathways in human HCC. *Gastroenterology* **130**, 1117-1128, doi:10.1053/j.gastro.2006.01.006 (2006).

208 Nakamura, K. *et al.* DNA methyltransferase inhibitor zebularine inhibits human hepatic carcinoma cells proliferation and induces apoptosis. *PloS one* **8**, e54036, doi:10.1371/journal.pone.0054036 (2013).

209 Andersen, J. B. *et al.* An integrated genomic and epigenomic approach predicts therapeutic response to zebularine in human liver cancer. *Science translational medicine* **2**, 54ra77, doi:10.1126/scitranslmed.3001338 (2010).

210 Datta, J. *et al.* A new class of quinoline-based DNA hypomethylating agents reactivates tumor suppressor genes by blocking DNA methyltransferase 1 activity and inducing its degradation. *Cancer research* **69**, 4277-4285, doi:10.1158/0008-5472.CAN-08-3669 (2009).

211 Tada, M. *et al.* Procaine inhibits the proliferation and DNA methylation in human hepatoma cells. *Hepatology international* **1**, 355-364, doi:10.1007/s12072-007-9014-5 (2007).

212 Ambros, V. The functions of animal microRNAs. *Nature* **431**, 350-355, doi:10.1038/nature02871 (2004).

213 Bartel, D. P. MicroRNAs: target recognition and regulatory functions. *Cell* **136**, 215-233, doi:10.1016/j.cell.2009.01.002 (2009).

214 Fabian, M. R., Sonenberg, N. & Filipowicz, W. Regulation of mRNA translation and stability by microRNAs. *Annual review of biochemistry* **79**, 351-379, doi:10.1146/annurev-biochem-060308-103103 (2010).

215 Bartel, D. P. MicroRNAs: genomics, biogenesis, mechanism, and function. *Cell* **116**, 281-297 (2004).

216 Bentwich, I. *et al.* Identification of hundreds of conserved and nonconserved human microRNAs. *Nature genetics* **37**, 766-770, doi:10.1038/ng1590 (2005).

217 Lagos-Quintana, M. *et al.* Identification of tissue-specific microRNAs from mouse. *Current biology : CB* **12**, 735-739 (2002).

218 Friedman, R. C., Farh, K. K., Burge, C. B. & Bartel, D. P. Most mammalian mRNAs are conserved targets of microRNAs. *Genome research* **19**, 92-105, doi:10.1101/gr.082701.108 (2009).

219 Lee, R. C., Feinbaum, R. L. & Ambros, V. The C. elegans heterochronic gene lin-4 encodes small RNAs with antisense complementarity to lin-14. *Cell* **75**, 843-854 (1993).

220 Brennecke, J., Hipfner, D. R., Stark, A., Russell, R. B. & Cohen, S. M. bantam encodes a developmentally regulated microRNA that controls cell proliferation and regulates the proapoptotic gene hid in Drosophila. *Cell* **113**, 25-36 (2003).

221 Chen, C. Z., Li, L., Lodish, H. F. & Bartel, D. P. MicroRNAs modulate hematopoietic lineage differentiation. *Science* **303**, 83-86, doi:10.1126/science.1091903 (2004).
222 Mizuguchi, Y., Takizawa, T., Yoshida, H. & Uchida, E. Dysregulated microRNAs in progression of hepatocellular carcinoma: A systematic review. *Hepatology research : the official journal of the Japan Society of Hepatology*, doi:10.1111/hepr.12606 (2015).
223 Gregory, R. I. *et al.* The Microprocessor complex mediates the genesis of microRNAs. *Nature* **432**, 235-240, doi:10.1038/nature03120 (2004).
224 Hutvagner, G. & Zamore, P. D. A microRNA in a multiple-turnover RNAi enzyme complex. *Science* **297**, 2056-2060, doi:10.1126/science.1073827 (2002).
225 Lee, I. *et al.* New class of microRNA targets containing simultaneous 5'-UTR and 3'-UTR interaction sites. *Genome research* **19**, 1175-1183, doi:10.1101/gr.089367.108 (2009).
226 Corsini, L. R. *et al.* The role of microRNAs in cancer: diagnostic and prognostic biomarkers and targets of therapies. *Expert opinion on therapeutic targets* **16 Suppl 2**, S103-109, doi:10.1517/14728222.2011.650632 (2012).
227 Si, M. L. *et al.* miR-21-mediated tumor growth. *Oncogene* **26**, 2799-2803, doi:10.1038/sj.onc.1210083 (2007).
228 Meng, F. *et al.* MicroRNA-21 regulates expression of the PTEN tumor suppressor gene in human hepatocellular cancer. *Gastroenterology* **133**, 647-658, doi:10.1053/j.gastro.2007.05.022 (2007).
229 Connolly, E. C., Van Doorslaer, K., Rogler, L. E. & Rogler, C. E. Overexpression of miR-21 promotes an in vitro metastatic phenotype by targeting the tumor suppressor RHOB. *Molecular cancer research : MCR* **8**, 691-700, doi:10.1158/1541-7786.MCR-09-0465 (2010).
230 Zhu, Q. *et al.* miR-21 promotes migration and invasion by the miR-21-PDCD4-AP-1 feedback loop in human hepatocellular carcinoma. *Oncology reports* **27**, 1660-1668, doi:10.3892/or.2012.1682 (2012).
231 Bao, L. *et al.* MicroRNA-21 suppresses PTEN and hSulf-1 expression and promotes hepatocellular carcinoma progression through AKT/ERK pathways. *Cancer letters* **337**, 226-236, doi:10.1016/j.canlet.2013.05.007 (2013).
232 Xu, G. *et al.* MicroRNA-21 promotes hepatocellular carcinoma HepG2 cell proliferation through repression of mitogen-activated protein kinase-kinase 3. *BMC cancer* **13**, 469, doi:10.1186/1471-2407-13-469 (2013).
233 Tomimaru, Y. *et al.* MicroRNA-21 induces resistance to the anti-tumour effect of interferon-alpha/5-fluorouracil in hepatocellular carcinoma cells. *British journal of cancer* **103**, 1617-1626, doi:10.1038/sj.bjc.6605958 (2010).
234 Zhu, W. & Xu, B. MicroRNA-21 identified as predictor of cancer outcome: a meta-analysis. *PloS one* **9**, e103373, doi:10.1371/journal.pone.0103373 (2014).
235 Pan, X., Wang, Z. X. & Wang, R. MicroRNA-21: a novel therapeutic target in human cancer. *Cancer biology & therapy* **10**, 1224-1232 (2010).
236 Fornari, F. *et al.* MiR-221 controls CDKN1C/p57 and CDKN1B/p27 expression in human hepatocellular carcinoma. *Oncogene* **27**, 5651-5661, doi:10.1038/onc.2008.178 (2008).
237 Gramantieri, L. *et al.* MicroRNA-221 targets Bmf in hepatocellular carcinoma and correlates with tumor multifocality. *Clinical cancer research : an official journal of the American Association for Cancer Research* **15**, 5073-5081, doi:10.1158/1078-0432.CCR-09-0092 (2009).
238 Fu, X. *et al.* Clinical significance of miR-221 and its inverse correlation with p27Kip(1) in hepatocellular carcinoma. *Molecular biology reports* **38**, 3029-3035, doi:10.1007/s11033-010-9969-5 (2011).

239 Santhekadur, P. K. *et al.* Multifunction protein staphylococcal nuclease domain containing 1 (SND1) promotes tumor angiogenesis in human hepatocellular carcinoma through novel pathway that involves nuclear factor kappaB and miR-221. *The Journal of biological chemistry* **287**, 13952-13958, doi:10.1074/jbc.M111.321646 (2012).
240 Garofalo, M. *et al.* miR-221&222 regulate TRAIL resistance and enhance tumorigenicity through PTEN and TIMP3 downregulation. *Cancer cell* **16**, 498-509, doi:10.1016/j.ccr.2009.10.014 (2009).
241 Pineau, P. *et al.* miR-221 overexpression contributes to liver tumorigenesis. *Proceedings of the National Academy of Sciences of the United States of America* **107**, 264-269, doi:10.1073/pnas.0907904107 (2010).
242 He, X. X. *et al.* Bioinformatics analysis identifies miR-221 as a core regulator in hepatocellular carcinoma and its silencing suppresses tumor properties. *Oncology reports* **32**, 1200-1210, doi:10.3892/or.2014.3306 (2014).
243 Sun, Z. *et al.* MicroRNA-9 enhances migration and invasion through KLF17 in hepatocellular carcinoma. *Molecular oncology* **7**, 884-894, doi:10.1016/j.molonc.2013.04.007 (2013).
244 Tan, H. X. *et al.* MicroRNA-9 reduces cell invasion and E-cadherin secretion in SK-Hep-1 cell. *Medical oncology* **27**, 654-660, doi:10.1007/s12032-009-9264-2 (2010).
245 Cai, L. & Cai, X. Up-regulation of miR-9 expression predicate advanced clinicopathological features and poor prognosis in patients with hepatocellular carcinoma. *Diagnostic pathology* **9**, 1000, doi:10.1186/s13000-014-0228-2 (2014).
246 Wang, Y. *et al.* Profiling microRNA expression in hepatocellular carcinoma reveals microRNA-224 up-regulation and apoptosis inhibitor-5 as a microRNA-224-specific target. *The Journal of biological chemistry* **283**, 13205-13215, doi:10.1074/jbc.M707629200 (2008).
247 Li, Q. *et al.* MicroRNA-224 is upregulated in HepG2 cells and involved in cellular migration and invasion. *Journal of gastroenterology and hepatology* **25**, 164-171, doi:10.1111/j.1440-1746.2009.05971.x (2010).
248 Wang, Y. *et al.* MicroRNA-224 targets SMAD family member 4 to promote cell proliferation and negatively influence patient survival. *PloS one* **8**, e68744, doi:10.1371/journal.pone.0068744 (2013).
249 Yu, L., Zhang, J., Guo, X., Li, Z. & Zhang, P. MicroRNA-224 upregulation and AKT activation synergistically predict poor prognosis in patients with hepatocellular carcinoma. *Cancer epidemiology* **38**, 408-413, doi:10.1016/j.canep.2014.05.001 (2014).
250 Jopling, C. Liver-specific microRNA-122: Biogenesis and function. *RNA biology* **9**, 137-142, doi:10.4161/rna.18827 (2012).
251 Coulouarn, C., Factor, V. M., Andersen, J. B., Durkin, M. E. & Thorgeirsson, S. S. Loss of miR-122 expression in liver cancer correlates with suppression of the hepatic phenotype and gain of metastatic properties. *Oncogene* **28**, 3526-3536, doi:10.1038/onc.2009.211 (2009).
252 Bandiera, S., Pfeffer, S., Baumert, T. F. & Zeisel, M. B. miR-122--a key factor and therapeutic target in liver disease. *Journal of hepatology* **62**, 448-457, doi:10.1016/j.jhep.2014.10.004 (2015).
253 Tsai, W. C. *et al.* MicroRNA-122 plays a critical role in liver homeostasis and hepatocarcinogenesis. *The Journal of clinical investigation* **122**, 2884-2897, doi:10.1172/JCI63455 (2012).
254 Li, X. *et al.* microRNAs: novel players in hepatitis C virus infection. *Clinics and research in hepatology and gastroenterology* **38**, 664-675, doi:10.1016/j.clinre.2014.04.008 (2014).

255 Chen, Y. *et al.* A liver-specific microRNA binds to a highly conserved RNA sequence of hepatitis B virus and negatively regulates viral gene expression and replication. *FASEB journal : official publication of the Federation of American Societies for Experimental Biology* **25**, 4511-4521, doi:10.1096/fj.11-187781 (2011).
256 Fornari, F. *et al.* MiR-122/cyclin G1 interaction modulates p53 activity and affects doxorubicin sensitivity of human hepatocarcinoma cells. *Cancer research* **69**, 5761-5767, doi:10.1158/0008-5472.CAN-08-4797 (2009).
257 Wang, S. C. *et al.* MicroRNA-122 triggers mesenchymal-epithelial transition and suppresses hepatocellular carcinoma cell motility and invasion by targeting RhoA. *PloS one* **9**, e101330, doi:10.1371/journal.pone.0101330 (2014).
258 Tsai, W. C. *et al.* MicroRNA-122, a tumor suppressor microRNA that regulates intrahepatic metastasis of hepatocellular carcinoma. *Hepatology* **49**, 1571-1582, doi:10.1002/hep.22806 (2009).
259 Bai, S. *et al.* MicroRNA-122 inhibits tumorigenic properties of hepatocellular carcinoma cells and sensitizes these cells to sorafenib. *The Journal of biological chemistry* **284**, 32015-32027, doi:10.1074/jbc.M109.016774 (2009).
260 Koberle, V. *et al.* Serum microRNA-1 and microRNA-122 are prognostic markers in patients with hepatocellular carcinoma. *European journal of cancer* **49**, 3442-3449, doi:10.1016/j.ejca.2013.06.002 (2013).
261 Li, N. *et al.* miR-34a inhibits migration and invasion by down-regulation of c-Met expression in human hepatocellular carcinoma cells. *Cancer letters* **275**, 44-53, doi:10.1016/j.canlet.2008.09.035 (2009).
262 Guo, Y. *et al.* MiR-34a inhibits lymphatic metastasis potential of mouse hepatoma cells. *Molecular and cellular biochemistry* **354**, 275-282, doi:10.1007/s11010-011-0827-0 (2011).
263 Lou, W. *et al.* Oncolytic adenovirus co-expressing miRNA-34a and IL-24 induces superior antitumor activity in experimental tumor model. *Journal of molecular medicine* **91**, 715-725, doi:10.1007/s00109-012-0985-x (2013).
264 Cermelli, S., Ruggieri, A., Marrero, J. A., Ioannou, G. N. & Beretta, L. Circulating microRNAs in patients with chronic hepatitis C and non-alcoholic fatty liver disease. *PloS one* **6**, e23937, doi:10.1371/journal.pone.0023937 (2011).
265 Xu, X. *et al.* miR-34a induces cellular senescence via modulation of telomerase activity in human hepatocellular carcinoma by targeting FoxM1/c-Myc pathway. *Oncotarget* **6**, 3988-4004, doi:10.18632/oncotarget.2905 (2015).
266 Su, H. *et al.* MicroRNA-101, down-regulated in hepatocellular carcinoma, promotes apoptosis and suppresses tumorigenicity. *Cancer research* **69**, 1135-1142, doi:10.1158/0008-5472.CAN-08-2886 (2009).
267 Zheng, F. *et al.* Systemic delivery of microRNA-101 potently inhibits hepatocellular carcinoma in vivo by repressing multiple targets. *PLoS genetics* **11**, e1004873, doi:10.1371/journal.pgen.1004873 (2015).
268 Fu, Y. *et al.* Circulating microRNA-101 as a potential biomarker for hepatitis B virus-related hepatocellular carcinoma. *Oncology letters* **6**, 1811-1815, doi:10.3892/ol.2013.1638 (2013).
269 Xu, T. *et al.* MicroRNA-195 suppresses tumorigenicity and regulates G1/S transition of human hepatocellular carcinoma cells. *Hepatology* **50**, 113-121, doi:10.1002/hep.22919 (2009).
270 Bracken, C. P. *et al.* A double-negative feedback loop between ZEB1-SIP1 and the microRNA-200 family regulates epithelial-mesenchymal transition. *Cancer research* **68**, 7846-7854, doi:10.1158/0008-5472.CAN-08-1942 (2008).

271 Oishi, N. *et al.* Transcriptomic profiling reveals hepatic stem-like gene signatures and interplay of miR-200c and epithelial-mesenchymal transition in intrahepatic cholangiocarcinoma. *Hepatology* **56**, 1792-1803, doi:10.1002/hep.25890 (2012).
272 Hung, C. S. *et al.* MicroRNA-200a and -200b mediated hepatocellular carcinoma cell migration through the epithelial to mesenchymal transition markers. *Annals of surgical oncology* **20 Suppl 3**, S360-368, doi:10.1245/s10434-012-2482-4 (2013).
273 Dhayat, S. A. *et al.* The microRNA-200 family--a potential diagnostic marker in hepatocellular carcinoma? *Journal of surgical oncology* **110**, 430-438, doi:10.1002/jso.23668 (2014).
274 Wong, C. M. *et al.* MiR-200b/200c/429 subfamily negatively regulates Rho/ROCK signaling pathway to suppress hepatocellular carcinoma metastasis. *Oncotarget* **6**, 13658-13670, doi:10.18632/oncotarget.3700 (2015).
275 Lin, L. *et al.* microRNA-141 inhibits cell proliferation and invasion and promotes apoptosis by targeting hepatocyte nuclear factor-3beta in hepatocellular carcinoma cells. *BMC cancer* **14**, 879, doi:10.1186/1471-2407-14-879 (2014).
276 Shimizu, S. *et al.* The let-7 family of microRNAs inhibits Bcl-xL expression and potentiates sorafenib-induced apoptosis in human hepatocellular carcinoma. *Journal of hepatology* **52**, 698-704, doi:10.1016/j.jhep.2009.12.024 (2010).
277 Wong, C. C. *et al.* The microRNA miR-139 suppresses metastasis and progression of hepatocellular carcinoma by down-regulating Rho-kinase 2. *Gastroenterology* **140**, 322-331, doi:10.1053/j.gastro.2010.10.006 (2011).
278 Huang, D. *et al.* Rock2 promotes the invasion and metastasis of hepatocellular carcinoma by modifying MMP2 ubiquitination and degradation. *Biochemical and biophysical research communications* **453**, 49-56, doi:10.1016/j.bbrc.2014.09.061 (2014).
279 Wang, B. *et al.* Expression and significance of MMP2 and HIF-1alpha in hepatocellular carcinoma. *Oncology letters* **8**, 539-546, doi:10.3892/ol.2014.2189 (2014).
280 Zou, F. *et al.* Targeted deletion of miR-139-5p activates MAPK, NF-kappaB and STAT3 signaling and promotes intestinal inflammation and colorectal cancer. *FEBS J*, doi:10.1111/febs.13678 (2016).
281 Sun, C. *et al.* Hsa-miR-139-5p inhibits proliferation and causes apoptosis associated with down-regulation of c-Met. *Oncotarget* **6**, 39756-39792, doi:10.18632/oncotarget.5476 (2015).
282 Rothschild, M. A., Oratz, M. & Schreiber, S. S. Albumin synthesis (second of two parts). *The New England journal of medicine* **286**, 816-821, doi:10.1056/NEJM197204132861505 (1972).
283 Fujise, K. *et al.* Integration of hepatitis B virus DNA into cells of six established human hepatocellular carcinoma cell lines. *Hepato-gastroenterology* **37**, 457-460 (1990).
284 Grassi, G. *et al.* The expression levels of the translational factors eEF1A 1/2 correlate with cell growth but not apoptosis in hepatocellular carcinoma cell lines with different differentiation grade. *Biochimie* **89**, 1544-1552, doi:10.1016/j.biochi.2007.07.007 (2007).
285 Schippers, I. J. *et al.* Immortalized human hepatocytes as a tool for the study of hepatocytic (de-)differentiation. *Cell biology and toxicology* **13**, 375-386 (1997).
286 Giobbe, G. G. *et al.* Functional differentiation of human pluripotent stem cells on a chip. *Nature methods* **12**, 637-640, doi:10.1038/nmeth.3411 (2015).
287 Dalby, B. *et al.* Advanced transfection with Lipofectamine 2000 reagent: primary neurons, siRNA, and high-throughput applications. *Methods* **33**, 95-103, doi:10.1016/j.ymeth.2003.11.023 (2004).

288 Tost, J. *et al.* Methylation of specific CpG sites in the P2 promoter of parathyroid hormone-related protein determines the invasive potential of breast cancer cell lines. *Epigenetics* **6**, 1035-1046, doi:10.4161/epi.6.8.16077 (2011).
289 Festuccia, C. *et al.* Azacitidine improves antitumor effects of docetaxel and cisplatin in aggressive prostate cancer models. *Endocr Relat Cancer* **16**, 401-413, doi:10.1677/ERC-08-0130 (2009).
290 Manero-Garcia, G. Phase I Study of Oral Azacitidine in Myelodysplastic Syndromes, Chronic Myelomonocytic Leukemia, and Acute Myeloid Leukemia. *Journal of Clinical Oncology* **29**, 7 (2011).
291 Olson, J. S. C. Assay for Determination of Protein Concentration. *Current Protocols in Protein Science* (2007).
292 Mahmood, T. & Yang, P. C. Western blot: technique, theory, and trouble shooting. *North American journal of medical sciences* **4**, 429-434, doi:10.4103/1947-2714.100998 (2012).
293 Laemmli, U. K. Cleavage of structural proteins during the assembly of the head of bacteriophage T4. *Nature* **227**, 680-685 (1970).
294 Wilkesman, J. & Kurz, L. Protease analysis by zymography: a review on techniques and patents. *Recent patents on biotechnology* **3**, 175-184 (2009).
295 Liang, C. C., Park, A. Y. & Guan, J. L. In vitro scratch assay: a convenient and inexpensive method for analysis of cell migration in vitro. *Nature protocols* **2**, 329-333, doi:10.1038/nprot.2007.30 (2007).
296 Spessotto, P., Giacomello, E. & Perri, R. Improving fluorescence-based assays for the in vitro analysis of cell adhesion and migration. *Molecular biotechnology* **20**, 285-304 (2002).
297 Pfaffl, M. W., Tichopad, A., Prgomet, C. & Neuvians, T. P. Determination of stable housekeeping genes, differentially regulated target genes and sample integrity: BestKeeper--Excel-based tool using pair-wise correlations. *Biotechnology letters* **26**, 509-515 (2004).
298 Venturelli, S. *et al.* Epigenetic combination therapy as a tumor-selective treatment approach for hepatocellular carcinoma. *Cancer* **109**, 2132-2141, doi:10.1002/cncr.22652 (2007).
299 Kaminskas, E., Farrell, A. T., Wang, Y. C., Sridhara, R. & Pazdur, R. FDA drug approval summary: azacitidine (5-azacytidine, Vidaza) for injectable suspension. *Oncologist* **10**, 176-182, doi:10.1634/theoncologist.10-3-176 (2005).
300 Dekens, M. P. *et al.* Light regulates the cell cycle in zebrafish. *Current biology : CB* **13**, 2051-2057 (2003).
301 Soldani, C. *et al.* Poly(ADP-ribose) polymerase cleavage during apoptosis: when and where? *Exp Cell Res* **269**, 193-201, doi:10.1006/excr.2001.5293 (2001).
302 Chipuk, J. E. *et al.* Direct activation of Bax by p53 mediates mitochondrial membrane permeabilization and apoptosis. *Science* **303**, 1010-1014, doi:10.1126/science.1092734 (2004).
303 Kang, S. G. *et al.* Mechanism of growth inhibitory effect of Mitomycin-C on cultured human retinal pigment epithelial cells: apoptosis and cell cycle arrest. *Curr Eye Res* **22**, 174-181 (2001).
304 Gunning, P. W., Ghoshdastider, U., Whitaker, S., Popp, D. & Robinson, R. C. The evolution of compositionally and functionally distinct actin filaments. *Journal of cell science* **128**, 2009-2019, doi:10.1242/jcs.165563 (2015).
305 Morse, D. L., Gray, H., Payne, C. M. & Gillies, R. J. Docetaxel induces cell death through mitotic catastrophe in human breast cancer cells. *Molecular cancer therapeutics* **4**, 1495-1504, doi:10.1158/1535-7163.MCT-05-0130 (2005).

306 Kubara, P. M. *et al.* Human cells enter mitosis with damaged DNA after treatment with pharmacological concentrations of genotoxic agents. *Biochem J* **446**, 373-381, doi:10.1042/BJ20120385 (2012).
307 Khatri, P., Draghici, S., Ostermeier, G. C. & Krawetz, S. A. Profiling gene expression using onto-express. *Genomics* **79**, 266-270, doi:10.1006/geno.2002.6698 (2002).
308 Draghici, S. *et al.* A systems biology approach for pathway level analysis. *Genome research* **17**, 1537-1545, doi:10.1101/gr.6202607 (2007).
309 Attwooll, C., Lazzerini Denchi, E. & Helin, K. The E2F family: specific functions and overlapping interests. *EMBO J* **23**, 4709-4716, doi:10.1038/sj.emboj.7600481 (2004).
310 Chiu, R. *et al.* The c-Fos protein interacts with c-Jun/AP-1 to stimulate transcription of AP-1 responsive genes. *Cell* **54**, 541-552 (1988).
311 Han, S., Khuri, F. R. & Roman, J. Fibronectin stimulates non-small cell lung carcinoma cell growth through activation of Akt/mammalian target of rapamycin/S6 kinase and inactivation of LKB1/AMP-activated protein kinase signal pathways. *Cancer research* **66**, 315-323, doi:10.1158/0008-5472.CAN-05-2367 (2006).
312 Janik, M. E., Litynska, A. & Vereecken, P. Cell migration-the role of integrin glycosylation. *Biochimica et biophysica acta* **1800**, 545-555, doi:10.1016/j.bbagen.2010.03.013 (2010).
313 Roomi, M. W., Monterrey, J. C., Kalinovsky, T., Rath, M. & Niedzwiecki, A. Patterns of MMP-2 and MMP-9 expression in human cancer cell lines. *Oncology reports* **21**, 1323-1333 (2009).
314 Stetler-Stevenson, W. G. The role of matrix metalloproteinases in tumor invasion, metastasis, and angiogenesis. *Surgical oncology clinics of North America* **10**, 383-392, x (2001).
315 Gu, P. *et al.* Frequent loss of TIMP-3 expression in progression of esophageal and gastric adenocarcinomas. *Neoplasia* **10**, 563-572 (2008).
316 Hai, T., Wolfgang, C. D., Marsee, D. K., Allen, A. E. & Sivaprasad, U. ATF3 and stress responses. *Gene Expr* **7**, 321-335 (1999).
317 Yuan, X. *et al.* ATF3 suppresses metastasis of bladder cancer by regulating gelsolin-mediated remodeling of the actin cytoskeleton. *Cancer research* **73**, 3625-3637, doi:10.1158/0008-5472.CAN-12-3879 (2013).
318 Xie, J. J. *et al.* ATF3 functions as a novel tumor suppressor with prognostic significance in esophageal squamous cell carcinoma. *Oncotarget* **5**, 8569-8582, doi:10.18632/oncotarget.2322 (2014).
319 Chen, Y. *et al.* Piperlongumine selectively kills hepatocellular carcinoma cells and preferentially inhibits their invasion via ROS-ER-MAPKs-CHOP. *Oncotarget* **6**, 6406-6421, doi:10.18632/oncotarget.3444 (2015).
320 Zhang, H. D. *et al.* MiR-139-5p inhibits the biological function of breast cancer cells by targeting Notch1 and mediates chemosensitivity to docetaxel. *Biochemical and biophysical research communications* **465**, 702-713, doi:10.1016/j.bbrc.2015.08.053 (2015).
321 Qiu, G., Lin, Y., Zhang, H. & Wu, D. miR-139-5p inhibits epithelial-mesenchymal transition, migration and invasion of hepatocellular carcinoma cells by targeting ZEB1 and ZEB2. *Biochemical and biophysical research communications* **463**, 315-321, doi:10.1016/j.bbrc.2015.05.062 (2015).
322 Shen, K. *et al.* Post-transcriptional regulation of the tumor suppressor miR-139-5p and a network of miR-139-5p-mediated mRNA interactions in colorectal cancer. *FEBS J* **281**, 3609-3624, doi:10.1111/febs.12880 (2014).

323 Wong, C. C., Wong, C. M., Tung, E. K., Man, K. & Ng, I. O. Rho-kinase 2 is frequently overexpressed in hepatocellular carcinoma and involved in tumor invasion. *Hepatology* **49**, 1583-1594, doi:10.1002/hep.22836 (2009).
324 Schofield, A. V. & Bernard, O. Rho-associated coiled-coil kinase (ROCK) signaling and disease. *Crit Rev Biochem Mol Biol* **48**, 301-316, doi:10.3109/10409238.2013.786671 (2013).
325 Newby, A. C. Matrix metalloproteinases regulate migration, proliferation, and death of vascular smooth muscle cells by degrading matrix and non-matrix substrates. *Cardiovasc Res* **69**, 614-624, doi:10.1016/j.cardiores.2005.08.002 (2006).
326 Gao, W. *et al.* Variable DNA methylation patterns associated with progression of disease in hepatocellular carcinomas. *Carcinogenesis* **29**, 1901-1910, doi:10.1093/carcin/bgn170 (2008).
327 Mc Gee, M. M. Targeting the Mitotic Catastrophe Signaling Pathway in Cancer. *Mediators Inflamm* **2015**, 146282, doi:10.1155/2015/146282 (2015).
328 Vakifahmetoglu, H., Olsson, M. & Zhivotovsky, B. Death through a tragedy: mitotic catastrophe. *Cell Death Differ* **15**, 1153-1162, doi:10.1038/cdd.2008.47 (2008).
329 Bucher, N. & Britten, C. D. G2 checkpoint abrogation and checkpoint kinase-1 targeting in the treatment of cancer. *British journal of cancer* **98**, 523-528, doi:10.1038/sj.bjc.6604208 (2008).
330 Boutros, R., Dozier, C. & Ducommun, B. The when and wheres of CDC25 phosphatases. *Curr Opin Cell Biol* **18**, 185-191, doi:10.1016/j.ceb.2006.02.003 (2006).
331 Farra, R. *et al.* Impairment of the Pin1/E2F1 axis in the anti-proliferative effect of bortezomib in hepatocellular carcinoma cells. *Biochimie* **112**, 85-95, doi:10.1016/j.biochi.2015.02.015 (2015).
332 Herskowitz, J. H. *et al.* Pharmacologic inhibition of ROCK2 suppresses amyloid-beta production in an Alzheimer's disease mouse model. *J Neurosci* **33**, 19086-19098, doi:10.1523/JNEUROSCI.2508-13.2013 (2013).
333 Sieghart, W. *et al.* Erlotinib and sorafenib in an orthotopic rat model of hepatocellular carcinoma. *Journal of hepatology* **57**, 592-599, doi:10.1016/j.jhep.2012.04.034 (2012).